ABSTRACT

Title of Dissertation: MODELING AND MONITORING PATHOGEN TRANSPORT THROUGH VEGETATED FILTER STRIPS

Gholamreza Moosapour Roodsari, Doctor of Philosophy, 2004

Dissertation directed by: Professor Adel Shirmohammadi
Department of Biological Resources Engineering

Contamination of natural waters by microorganisms directly affects public health. Field application of manure can potentially result in surface and groundwater contamination. The objective of this study was to observe and quantify the effects of vegetated filter strips (VFS) on surface and subsurface transport of fecal oviform (FC) surrogates for bacterial pathogens released from a surface - applied bovine/swine manure.

The study included a field-based lysimeter equipped with multi-sensor moisture probes to monitor real-time water content through the soil profile, and with other proper instrumentation to monitor and quantify the spatial and temporal release

rates of pathogenic bacteria. Another component of this study involved development and testing of a computer model to predict the surface and subsurface transport of FC.

Results showed that bare plots offered no resistance to surface flow, thus FC were detected in runoff at 600 cm from the ridge of the lysimeter within 10 minutes of the rainfall initiation. Results from vegetated plots showed that vegetation substantially attenuated surface flow of water as compared to bare plots. Unlike the bare soil, the results showed that the vegetated soil surface created a much less uniform transport pattern for FC. Vegetation changed transport patterns and levels of FC concentrations much more significantly than soil texture did.

Results showed that *E.coli* and *Salmonella cholerasuis* behaved similarly and resulted in similar transport patterns in both bare plots. Results also showed that both organisms demonstrated a two-stage exponential release rate with a fast release rate in the first 10 minutes of the rainfall simulation.

A one-dimensional convective-dispersive equation using the continuity equation and the Manning's equation were used in MODCHOI model (a modified version of KORMIL2) to predict the surface transport of FC. To simulate the vertical movement of FC, a one-dimensional kinematic wave model was developed and used. Green and Ampt, Philip, and Schmid infiltration models were also applied to the vertical water flow movement. The models simulated the spatial and the temporal distribution of FC in runoff assuming an exponential release of FC from the manure. Simulation results satisfactorily modeled both flow and FC.

MODELING AND MONITORING PATHOGEN TRANSPORT THROUGH VEGETATED FILTER STRIPS

by

Gholamreza Moosapour Roodsari

Dissertation submitted to the Faculty of the Graduate School of the
University of Maryland, College Park in partial fulfillment
Of the requirements for the degree of
Doctor of Philosophy
2004

Advisory Committee:

Professor Adel Shirmohammadi, Chair/Advisor
Associate Professor Kaye L. Brubaker
Associate Professor Huber J. Montas
Daniel Shelton Microbiologist, Ph.D.
Professor Fredrick W. Wheaton

DEDICATION

to all children, especially those who are the victims of
poverty, exploitation, and violence;
our peaceful and prosperous tomorrows depend upon their
glorious todays.

AKNOWLEDGMENT

The author expresses his sincere appreciation to Dr. Adel Shirmohammadi, Professor, Department of Biological Resources Engineering, University of Maryland, College Park, Maryland for his continuous advice, encouragement, and instruction throughout this study. His knowledge, dedication, and kind humbleness are admired. The author also expresses his special gratitude to Dr. Daniel Shelton, Microbiologist, and Dr. Yakov Pachepsky, Hydrologist, Environmental Microbial Safety Laboratory, USDA/ARS, Dr. Ali Sadeghi, And Dr. Jim Starr Soil Scientists, Environmental Quality Laboratory, USDA/ARS, Beltsville, Maryland for their continuous involvement, advise and financial support during this study.

The author also would like to thank all of his committee members, Dr. Fredrick Wheaton and Dr. Hubert Montas, Department of Biological Resources Engineering and Dr. Kaye Brubaker, Department of Civil and Environmental Engineering, for their kind advice, suggestions, and support.

The author wishes to give special thanks to his wife, Roya, and his daughter Sakineh, for their love and encouragement during this endeavor. Without doubt, appreciation of his wife's role and inspiration is beyond the ability of the author to express.

Many thanks to Fatima Cardoso, graduate student at the University of Maryland, for her sincere and dedicated work during this study. The author wishes to express his gratitude to Valerie McPhatter, Laura Weltz, technicians at the Environmental Microbial Safety Laboratory, USDA/ARS, Beltsville, Maryland, and to Kerry Sefton, and Peter Downey technicians at the Environmental Quality

Laboratory, USDA/ARS, Beltsville, Maryland for their dedicated help during this study.

The author also wishes to thank his graduate fellows at the Biological Resources Engineering: Abby Vogel for her helpful editorial comments, Dr. Tzyy-Woei Chu, Aisha Sexton, Pouyan Nejadhashemi, and Kouroush Sadeghzadeh for their sincere advice, support and help.

Finally, the author expresses his sincere gratitude to his mother and his late father for the love and dedication, and for the inspiration they have provided.

TABLE OF CONTENTS

LIST OF TABLES

LIST OF FIGURES

LIST OF SYMBOLS

A	area (L^2)
A_t	total cross sectional area of flowing water (L^2)
An	net flow area (L^2)
B_{att}	rate of microbial attachment mass per unit volume per unit time ($ML^{-3}T^{-1}$)
B_{dec}	rate of microbial decay per unit volume per unit time ($ML^{-3}T^{-1}$)
B_{det}	rate of microbial detachment per unit volume per unit time ($ML^{-3}T^{-1}$)
B_g	rate of microbial growth mass per unit volume per unit time ($ML^{-3}T^{-1}$)
C	concentration of bacteria (ML^{-3})
$\bar{C}$	volumetric concentration (ML^{-3})
d_{ave}	average diameter of grass stalks (L)
D	dispersion coefficient (L^2T^{-1})
C^a	concentration of bacteria in attached phase (MM^{-1})
$C^a{}_m$	maximum mass of bacteria retained by a unit mass of particles (MM^{-1})
D	combination of diffusion, hydrodynamic dispersion, and random motility coefficient (L^2T^{-1})
D_d	diffusion coefficient (L^2T^{-1})
D_h	hydrodynamic dispersion coefficient (L^2T^{-1})
D_t	random motility coefficient (L^2T^{-1})
E	total evaporation (L)
f_t	total lateral outflow ($L^3T^{-1}L^{-1}$)
F	total infiltration (L)
h	empirical constant

I	total interception (L)
J_d	combination of dispersion, diffusion, and random motility flux ($ML^{-2}T^{-1}$)
J_v	advective mass flux of microorganisms ($ML^{-2}T^{-1}$)
J_w	volume of flowing water per unit area per unit time ($L^3L^{-2}T^{-1}$)
J_x	chemotactic flux of microorganisms ($ML^{-2}T^{-1}$)
K_x	chemotactic coefficient
K_s	concentration of limiting substrate at which the specific growth rate of bacteria is half the maximum value (growth saturation constant), ML^{-3}
K_d	distribution coefficient, ratio between adsorbed chemical concentration and dissolved (L^3M^{-1})
K_a	attachment coefficient
K_d	detachment coefficient (T^{-1})
m	mass (M)
N	total population of microorganism
NG_{ave}	average number of grass stalks per unit width
P	total precipitation (L)
Q	runoff rate (L^3T^{-1})
q	soil water flux ($L^3L^{-2}T^{-1}$)
Q_t	total discharge rate (L^3T^{-1})
q_t	total lateral inflow (L^3TL^{-1})
R_{gs}	growth rate of bacteria in deposited state ($ML^{-3}T^{-1}$)
R_{ds}	decay rate of bacteria in deposited state ($ML^{-3}T^{-1}$)
R_a	rate of attachment of bacteria ($ML^{-3}T^{-1}$)

R_{gw} microbial growth rate in water phase ($ML^{-3}T^{-1}$)

R hydraulic radius (L)

R_y rate of detachment of bacteria ($ML^{-3}T^{-1}$)

R^a_g bacteria growth rate in attachment phase ($ML^{-3}T^{-1}$)

R^a_d bacteria decay rate in attachment phase ($ML^{-3}T^{-1}$)

R_f funnel runoff rate (LT^{-1})

R total measured runoff (L)

Rg runoff rate at the gutter (LT^{-1})

R_{gutter} gutter runoff rates (L^3T^{-1})

s bed slope

S concentration of adsorbed fraction, mass per gram of soil mass (MM^{-1})

S_s mean media spacing (L)

t time (T)

T sampling time interval (T)

U average flow velocity (LT^{-1})

V_w average water velocity (LT^{-1})

Vx active chemotactic velocity of bacteria (LT^{-1})

V volume (L^3)

V_{1-9} funnels total runoff volume at each time interval (L^3)

Y flow depth (L)

Z soil depth (L)

μ specific growth rate (T^{-1})

μ constant of entrapment-entrainment (T^{-1})

μ_m maximum specific growth rate (T^{-1})

α empirical constant

β empirical constant

γ specific growth rate of bacteria (negative value indicates an exponential die-off) (T^{-1})

σ volume of deposited bacteria per unit volume of porous medium (L^3L^{-3})

ρ density of particles (ML^{-3})

τ tortuosity

θ volumetric water content (L^3L^{-3})

ρ_b bulk density (ML^{-3})

ρ_{bac} mass of microorganisms per unit volume of biomass (ML^{-3})

CHAPTER I. INTRODUCTION

There is insufficient data in the United States to consistently characterize the biological aspect of water quality on a national scale. In 1997, the United States Geological Survey (USGS) added microbial analysis to its " National Water Quality Assessment (NAWQA)" program. The NAWQA program focuses on microbiological quality over large representative areas of the U.S., covers multiple hydrological systems and includes both natural and human factors (Hirsch et al., 1988). The U.S. Environmental Protection Agency (EPA) recommended that *Escherichia coli* (*E.coli*) be considered as the bio-indicator for water quality purposes (USEPA, 1994). Total fecal coliforms (FC) and *E.coli* are the most common water quality bio- indicators used in the United States.

A substantial body of literature exists describing infiltration / leaching of microorganisms through soils and runoff to surface waters. Early studies on subsurface bacterial transport from septic effluents reviewed by Hagedorn (1981) and Bitton and Harvey (1992) indicate that bacterial transport from a few meters to 830 meters depends on soil texture (sand vs. gravel), water content (saturated vs. unsaturated), and time. Recent laboratory-scale studies have focused on elucidating soil parameters affecting leaching. These studies indicate that the predominant factors affecting leaching in tilled soils are soil structure/texture and porosity/bulk density in conjunction with bacterial size (Gannon *et al.*, 1991a, 1991b; Huysman and Veerstracte, 1993; Tan *et al.*, 1991); while in no-tilled soils, the predominant factors are distribution and continuity of macropores (preferential flow pathways) in conjunction with initial water content (McMurry *et al.*, 1998; Paterson *et al.*, 1992).

In general, higher leaching rates are observed in no-tilled than tilled soils (Smith *et al.*, 1985; Van Elsa's *et al.*, 1991). Limited research suggests that parasites (i.e. *Cryptosporidium parvum*) leach more slowly through soils than bacteria (Mawdsley et al., 1996a, 1996b). Still, quantitative relationships have yet to be established describing rates or extent of pathogen leaching on the field or watershed scale.

Previous studies that evaluated the use of vegetated filter strips (VFS) for reducing sediment and nutrient transport may be relevant for pathogens. Wilson (1967) used an empirical study to evaluate the effects of Bermuda grass on sediment transport. His results showed that maximum percentages of sand, silt, and clay were trapped at 3, 15, and 122 m distance from the applied manure area, respectively. Li and Shen (1973) evaluated the effects of tall vegetation on sediment transport on a watershed scale. Based on their findings, it was recommended that tall vegetation is an effective media to reduce sediment yield by reducing surface runoff, increasing infiltration, and protecting the soil surface from detachment/deterioration as a result of direct rainfall impact. Kao and Barfield (1978) used artificial filter strips to develop an equation of flow by employing the momentum balance principle. They concluded that the filter media drag resistance was the dominant force in retarding the surface runoff. Haggard et al. (2002) investigated the effects of soil texture, slope, grazing management, and pasture renovation on surface runoff from small plots using a rainfall simulator. Their results showed that pasture renovation substantially increased time to runoff generation, reduced nutrient loss from land applied with animal manure, and alleviated water-quality concerns on agricultural lands. Chaubey

et al. (1994) observed improvement of ammonia and phosphorous removal from swine lagoon effluent with increased VFS with lengths up to nine meters.

Bovine manure has been documented to contain various pathogenic microorganisms (Elder et al., 2000; Hancock et al., 1998; Porter et al., 1997). Field application of manure can potentially result in surface and groundwater contamination. Consequently, proper manure management practices are needed to prevent or minimize deterioration of water quality from manure-born pathogens. Chandler et al. (1981) studied the distribution and survival of bacteria indicator organisms on land used for the disposal of swine effluent under a range of management, climatic, and soil conditions. They studied the effect of soil type on the persistence of FC at several farms with different soil types. Also, vertical transport of FC into the subsoil was investigated on several sites irrigated with swine effluent. The results indicated that well separated applications of manure provided an efficient method to decrease FC release from the manure application areas. Their results further indicated that the topsoil (up to a three cm depth) provided a more suitable environment for FC persistence than pasture or subsoil.

Walker et al. (1990) suggested that grass filter strips alone would not reduce the concentration of microorganisms enough to meet water quality requirement, however, no field data were available for validation of their predictions. The majority of published findings support, to various degrees, the role of filter strips in removing pathogens from overland flow (Coyne et al., 1995; Crane et al., 1983). Moore et al. (1988) recommended that effective VFS should be at least three meters wide and have a slope of 0 to15%. Conflicting results on the effectiveness of vegetative filters

on removing bacteria (Srivastava et al., 1996; Hunt et al., 1979; Dickey and Vanderholm, 1981) indicate that surface conditions (e.g. soil type and types of vegetation), manure application technology, as well as rainfall characteristics may affect the efficiency of filter strips. Schelinger and Clausen (1992) noticed a 30% decrease in bacteria concentrations from a dairy manure detection pond after transport through a VFS. Lim (1997) found that all fecal coliforms were removed within the first 6.1 m of VFS used to treat runoff from a simulated pasture.

Computer simulation models have become very useful in predicting chemical pollutant transport from major agricultural lands (Addiscott et al., 1986; Barraclough et al., 1989; Bergstrom et al., 1991; Jarvis et al., 1991). The application of these models varies significantly according to their objectives. Among these models are PRZM (Carsel et al., 1984), CREAMS (Knisel et al., 1980), GLEAMS (Leonard et al., 1987, Knisel et al., 1993), HSPF (Doingian et al., 1983), ANSWERS (Beasley and Huggins, 1981), MACRO (Jarvis et al., 1995), and SLIM (Addiscott and Wagenet, 1986, Addiscott and Whitemore, 1991). Shirmohammadi et al. (2001) provide a detailed discussion on different types of hydrologic and water quality models.

Although many models have been developed to assess the transport of chemical pollutants, modeling of microorganisms in surface and subsurface flow is still in the early stages. Researchers have conducted numerous laboratory scale experiments to quantify fecal coliform leaching through the soil column. Similar experiments were also conducted independently for surface transport of fecal coliforms in the laboratory. In both cases, the combination of surface and subsurface

transport was not coupled to evaluate the effect of infiltration on the overland transport of microorganisms.

The objectives of this study were to: 1) observe and quantify the effect of vegetated filter strips on surface runoff, infiltration, and vertical transport of FC released from surface-applied bovine manure; 2) provide guidelines regarding the design of vegetated filter strips to prevent pathogen contamination of surface waters; and 3) devise a mathematical model capable of predicting the overland transport of fecal coliforms.

References

Addiscott, T.M., and R.J. Wagenet. 1986. Concepts of solute leaching in soils: A review of modeling approaches. J. Soil Sci. 36:411-424.

Addiscott, T.M., and A.P. Whitemore, 1991. Simulation of solute leaching in soils of differing permeabilities. Soil Use Manag. 7, 97-102.

Barraclough, P.B., H. Kuhlmann, and A.H. Weir. 1989. The effects of prolonged drought and nitrogen fertilizer on root and shoot growth and water uptake by winter wheat. Journal of Agronomy and Crop Science 163, 352-360.

Beasley, D.B. and L.F. Huggins. 1981. A real Nonpoint Source Watershed Environment Response Simulation (ANSWERS). User Manual. EPA-905/9-82-001. U.S. EPA, Region V. Chicago, IL.

Bergstrom, L., A. McGibbon, S. Day, and M. Snel. 1991. Leaching potential and decomposition of clopyralid in Swedish soils under field conditions. Environ. Toxicol. Chem. 10:563–571.

Bitton, G., and R.W. Harvey, (1992) Transport of pathogens through soils and aquifers. In: Mitchell R (Ed) Environmental Microbiology (pp-103-124). Wiley-Liss, New York.

Carsel, R.F., C.N. Smith, L.A. Mulkey, J.D. Dean and P. Jowise. 1984. Users Manual for the Pesticide Root Zone Model (PRZM) Release 1. EPA-600/3-84-109. U.S. EPA, Athens, GA.

Chandler, D.S., J. Farran and J.A. Craven. 1981. Persistence and distribution of pollution indicator bacteria on land used for disposal of piggery effluent. Applied and Environmental Microbiology 42:453-460.

Chaubey, I., D.R. Edwards, T.C. Daniel, P.A. Moore, Jr. and D.J. Nichols. 1994. Effectiveness of vegetative filter strips in retaining surface-applied swine manure constituents. Transactions of the ASAE. 37(3): 845-850.

Coyne, M.S., R.A. Gilfillen, R.W. Rhodes, and R.L. Blevins. 1995. Soil and fecal coliform trapping by grass filter strips during simulated rain. J. Soil and Water Cons. 50(4): 405-408.

Crane, S.R., J.A. Moore, M.E. Grismer, and J.R. Miner. 1983. Bacterial pollution from agricultural sources: a review. Transactions of the ASAE. 26(3): 858-866.

Dickey, E. C. and D. H. Vanderholm. 1981. Vegetative filter treatment of livestock feedlot runoff. J. Envir. Qual., 10:279-284.

Donigian, A.S. Jr., Baker, D.A. Haith and M.F. Walter. 1983. HSPF Parameter Adjustments to Evaluate the Effects of Agricultural Best Management Practices, EPA Contract No. 68-03-2895, U.S. EPA Environmental Research Laboratory, Athens, GA, (PB-83-247171).

Elder, R.O., J.L. Keen. G.R. Siragusa, G.A. Barkocy-Gallagher, M. Koohmaraie, and W.W. Laegreid. 2000. Correlation of enterohemorrhagic Escherichia coli O157 prevalence in feces, hides, and carcasses of beef cattle during processing. Proc. Natl. Acad. Sci. USA 97:2999-3003.

Gannon, J.T., V.B. Manilal and M. Alexander. 1991a. Relationship between cell surface properties and transport of bacteria through soil. Appl. Environ. Microbiol. 57(1): 190-193.

Gannon, J.T., U. Mingelgrin, M. Alexander and R.T. Wagnet, 1991b. Bacteria transport through homogeneous soil. Soil Biol. Biochem. 23(12): 1155-1160

Hagedorn, C., 1981. Transport and fate : Bacteria pathogens in groundwater. Pro. Con. On microbial health considerations of soil disposal of domestic wastewaters, Norman, Okla., pp. 84 -102.

Haggard, B.E., P.A. Moor, P.B. Delaune, D.R. Smith, S. Formica, P.J. Kleinman, amd T.C. Daniel, 2002. Effect of slope, grazing and aeration on pasture hydrology. Transactions of the ASAE., paper number 022156, presented at ASAE Annual International Meeting at Chicago, July 28- July 31.

Hancock, D.D., T.E. Besser, D.H. Rice, E.D. Ebel, D.E. Herriott, and L.V. Carpenter. 1998. Multiple sources of Escherichia coli O157 in feedlots and dairy farms in the Northwestern USA. Prev. Vet. Med. 35:11-19.

Hirsch, R.M., W.M. Alley, and W.G. Wilber. 1988. Concepts for a National-Water Quality Assessment Program. U.S. Geol. Surv. Circ. 1021.

Hunt, P.G., R.E. Peters, T.C. Sturgis, and C.R. Lee. 1979. Reliability problems with indicator organisms for monitoring overland flow treated wastewater effluent. J. Environ. Qual. 8(3): 301-304.

Huysman, F., and W. Verstraete, 1993. Water-facilitated transport of bacteria in unsaturated soil columns: Influence of inoculation and irrigation methods. Soil Biol. Biochem. 25: 91-97.

Jarvis, N.J., L. Bergström, and P.E. Dik, 1991. Modeling water and solute movement in macroporous soil. II. Chloride leaching under non-steady flow. Journal of Soil Science 42, 71-81.

Jarvis, N.J., L.F. Bergstrom, and C.D. Brown. 1995. Pesticiae leaching model and their use for management purposes. In: T.R. Robert and P.C. Kearney (ed.), Environmental Behavior of Agrochemicals, 185.

Kao, T. Y. and B.J. Barfield. 1978. Prediction of flow hydraulics for vegetated channels, Transaction of ASAE. 22:489-494.

Knisel, W.G. 1980. CREAMS: a field scale model for Chemicals, Runoff, and Erosion for Agricultural Management Sysytems. USDA Cnservation Research Report No. 26.640 pp.

Knisel, W.G., F.M. Davis, R.A. Leonard, 1993. GLEAMS version 2.10. Part I: Nutrient Component Documentation. USDA-ARS, Coastel Plain. Experiment Station. Southeast Watershed Research Laboratory. Tifton, Georgia, 31793. 81 p.

Leonard, R.A., W.G. Knisel, and D.A. Still. 1987. GLEAMS: Groundwater Loading Effects of Agricultural Management Systems. Trans. ASAE 30: 14031418.

Li, R. M. and H. W. Shen. 1973. Effect of total vegetation on flow and sediment, J. Hyd. Div., Proceeding of ASCE, Vol. 99 (HY5) 793-814.

Lim, T.T., D.R. Edwards, S.R. Workman, and B.T. Larson, 1997. Vegetated filter strip length effects on quality of runoff from grazed pastures. Transactions of the ASAE, 41 (5).

Mawdsley, J.L., A.E. Brooks, and R.J. Merry. 1996a. Movement of the protozoan pathogen Cryptosporidium parvum through three contrasting soil types. Biol. Fertil. Soils. 21: 30-36.

Mawdsley, J.L., A.E. Brooks, R.J. Merry, and B.F. Pain. 1996b. Use of a novel soil-tilting table to demonstrate the horizontal and vertical movement of the protozoan pathogen Cryptosporidium parvum in soil. Biol. Fertil. Soils. 23: 215-220.

McMurry, S.W., M.S. Coyne, and E. Perfect. 1998. Fecal coliform transport through intact soil blocks amended with poultry manure. J. Environ. Qual. 27: 86-92.

Moore, J.A., J.D. Smyth, E.S. Baker, and J.R. Miner. 1988. Evaluating coliform concentrations in runoff from various animal waste management systems. Special Report 817: Agricultural Experiment Stations, Oregon State University, Corvallis, Oregano.

Paterson, E., J.S. Kemp, S.M. Gammack, E. Fitz Patrick, C. Adisl, S. Malcom, C.E. Mullins, and K. Killham. 1992. Leaching of genetically modified pseudomonas fluorescents through intact soil microcosms: influence of soil type. Biol. Fertil. Soils. 15: 308-314.

Porter, J., K. Moobs, C.A. Hart, J.R. Saunders, R.W. Pickup, and C. Edwards. 1997. Detection, distribution and probable fate of Escherichia coli O157 from asymptomatic cattle on a dairy farm. J. Appl. Microbio. 83:297-306.

Schellinger, G.R., and J.C. Clausen. 1992. Vegetated filter treatment of dairy barnyard runoff in cold regions. J. Environ. Qual. 21:40-45.

Shirmohammadi, A., H.J. Montas, L.F. Bergstrom, and W.G. Knisel. 2001. Water Quality Models. In: Agricultural Nonpoint Source Pollution-Watershed Management and Hydrology: Ritter. W.F. and A. Shirmohammadi, (eds.); Lewis Publishers Washington, D.C., pp. 233-256.

Smith, M.S., Thomas, G.W., White, R.E., Ritonga, D. 1985. Transport of *Escherichia coli* through intact and disturbed soil columns. J. Environ. Qual. 14:87-91.

Srivastava, P., D.R. Edwards, T.C. Daniel, P.A. Moore, and T.A. Costello. 1996. Performance of vegetative filter strips with varying pollutant sources and filter strip length. Transactions of the ASAE 39(6): 2231-2239.

Tan, Y., Bond, W.J., Rovira, A.D. Brisbane, P.G., and Griffin, D.M. 1991. Movement through soil of a biological control agent, Pseudomonas fluorescences. Soil Biol. Biochem. 23: 821-825.

USEPA, 1994. National Water Quality Inventory: Report to Congress, USEPA, office of Water, Washington, D.C.

Van Elsa's, J.D., J.T. Trevors, and L.S. Van Overbeek. 1991. Influence of soil properties on the vertical movement of genetically –marked pseudomonas fluorescents through large soil microorganisms. Biol. Fertil. Soils.10: 249-255.

Walker, S.E., S. Mostaghimi, T.A. Dillaha, and F.E. Woeste. 1990. Modeling animal waste management practices: Impacts on bacteria levels in runoff from agricultural lands. Trans. of the ASAE 33(3): 807-817.

Wilson, L.G. 1967. Sediment removal from flood water, Transaction of ASAE, 10 (1): 35 -37

CHAPTER II. EXPERIMENTAL ASSESSMENT OF PATHOGEN TRANSPORT WITH AND WITHOUT VEGETATED FILTER STRIPS

2.1 Abstract

The land application of manure is frequently recommended to recycle organic matter and nutrients in soil thereby enhancing soil quality and crop productivity. However, contaminated manure may pose a human health risk if contaminants reach potable or recreational water bodies. The objective of this study was to observe and quantify the effects of vegetated filter strips (VFS) on surface and subsurface transport of fecal coliform (FC) surrogates for bacterial pathogens released from surface-applied bovine/swine manure. A two-sided lysimeter with 20% slope on both sides was instrumented to monitor the surface and vertical transport of FC. Soil on one side of the lysimeter was sandy loam, while on the other side it was clay loam. Each side of the lysimeter was divided into two sub-plots (each 6.0 m x 6.4 m), one with grass and the other with bare soil. Plots were instrumented to collect runoff samples along the six meter long slope at three equidistant transects. Samples of runoff were also collected in a gutter at the edge of each plot. All plots were equipped with multi-sensor moisture probes to monitor the real-time water content throughout the soil profile. Bovine manure was applied at the top of the slope of each plot in one-foot wide strips. Rainfall was simulated at 61 mm/hr using a portable rainfall simulator. The surface flow was measured and sampled at five minute intervals at three different transects and in the gutter located at the bottom edge of each plot. Twenty four hours after each simulation, soil samples were taken at incremental depths (0-50 cm). Runoff and soil samples were analyzed for FC.

Results indicated that vegetated filter strips retarded water flow, thus reducing both surface runoff and FC transport. Results also indicated that while 100% of the initial bacterial population could be lost to runoff on bare plots, only 1% of the initial population was lost on vegetative plots. The FC concentrations in runoff decreased with distance along the slope from the point of application. Results showed that bare plots offered no resistance to surface flow, thus FC were detected in runoff at the gutter within ten minutes of the rainfall initiation. This study concluded that even for drastic slopes (i.e. 20%), vegetated filter strips virtually stopped surface transport of FC by facilitating rapid infiltration.

2.2. Introduction

Water quality deterioration associated with non-point source (NPS) pollution has been a great concern for a few decades. Evidence indicates that animal agriculture is a major source although there are multiple environmental sources of pathogenic organisms including humans, companion animals, and wildlife. Land application of manure is recommended to recycle nutrients and organic matter and to enhance soil quality and crop productivity. However, contaminated manure may pose a public health threat if pathogens are transported to potable and recreational waters.

A review of available information indicates that agriculture is the major contributor of NPS pollution to both the surface and groundwater (USEPA, 1994). Effluent disposal areas of farms with high animal densities normally contain large quantities of FC. The risk associated with surface water contamination by manure is, in part, a function of manure volume, site topography, hydrology, and proximity to surface waters. Large, confined animal feeding operations (CAFOs) generate

substantial volumes of animal manure, normally held or applied within a relatively small area. High rates of land-applied manure, particularly where rates exceed soil assimilative capacity, increase the risks for surface and groundwater contamination. These risks may be offset by low rainfall, dryness, minimal land slope, relative isolation of the animal population, and methods of composting, storing, and spreading manure. Pathogens applied or deposited onto soil surfaces may infiltrate into the soil profile or, alternatively, may runoff to surface waters. Because both processes can occur simultaneously, a thorough understanding of the controlling factors is critical in predicting which process will predominate. Knowledge of redistribution and persistence of FC on agricultural land is therefore important in the assessment of any potential contamination of runoff emanating from these areas.

One of the more promising management practices for controlling NPS pollution is to direct the flow of contaminants through a vegetated filter strip. VFS appear to work very efficiently and economically in reducing overland flow of contaminants. They have the potential for removing nutrients and pathogenic organisms when carefully designed and maintained. VFS provide an opportunity for runoff and pollutants to infiltrate into the soil profile. They enhance filtration of suspended sediment by vegetation through settlement, adsorption of chemicals and pathogens to soil and plant surfaces, and enhance uptake of soluble pollutants by plants (Fajardo et al., 2001).

2.3. Literature Review

The literature review is divided into three different subject areas: morphology of microorganisms, physiological and hydrological effects of hill slope on microbial transport, and microorganisms transport processes and fate.

2.3.1. Morphology of Microorganisms

Understanding the morphology of the microorganisms is very important in assessing their environmental fate. The following sections provide some understanding on definition, size, density, and surface conditions of FC, *E.coli*, and *Salmonella cholerasuis.*

2. 3.1.1. Definition, Size, Density, and Surface Conditions

Bacteria are microscopic unicellular organisms, typically spherical, rod, spiral or threadlike in shape, often clumped into colonies. Some bacteria cause disease, while others perform an essential role in nature by recycling materials; for example, by decomposing organic matter into a form available for reuse by plants. Soil contains five major groups of microorganisms (Alexander, 1977). Based on their oxygen environment, they may be aerobic or anaerobic. Bacteria can also be grouped according to their reaction with Gram's stain, which depends upon to their cell wall components. Bacteria which retain stain are referred to as Gram-positive, and those that do not retain stain are termed Gram-negative.

Pathogenic bacteria are those bacteria that originate from fecal contamination, known collectively as enteric. Sources of contamination can be classified as point or non-point sources. Contamination from point sources may be well controlled by good

management practices. The primary sources of point source pathogenic fecal contamination are wastewater treatment centers and effluent reuse. Failure to eliminate pathogenic organisms prior to their entry into the drinking water may cause serious health problems (Tate et al., 1990).

Much of the previous research ignores the importance of soil surface roughness on bacteria transport. In a flowing system, bacteria deposited in the micro-crevices of a soil surface possessing undulations may not be resuspended and carried away. On the other hand, organisms deposited on the elevated spots of the soil surface may be re-suspended and transported with subsequent runoff events. Consequently on surfaces with frequent micro-crevices, there would be a greater chance for organisms to adhere and colonize, thus reducing their transport. Figure 2.1 shows organisms trapped in a soil surface containing micro-crevices.

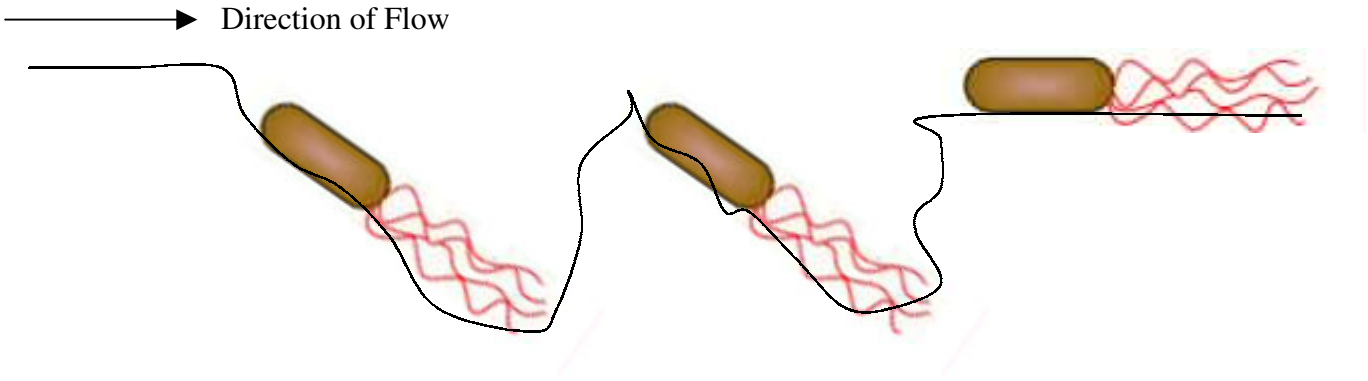

Figure. 2.1 Organisms trapped in micro-crevices

2. 3.1.2. Fecal Coliform (FC)

The traditional definition of total coliforms is aerobic and facultative anaerobic, rod-shaped gram-negative organisms that ferment lactose acid and produce gas within 24-48 hours at 35 degrees Celsius (Dutka et al., 1974). The persistence of these bacteria in water bodies is very similar to that of waterborne bacteria (Payment et al., 1991). Fecal coliforms are more definitive indicators of total coliforms and they are often used as indicators of the sanitary quality of the water. FC are present in the intestine or feces of warm-blooded animals, and have been found to have excellent correlation with fecal contamination from warm-blooded animals (Pourcher et al., 1991). In the laboratory they are defined as all organisms that produce blue colonies within 24 hours when incubated at 44.5 ± 0.2° C on M-FC medium (nutrient medium for bacterial growth, Toranzos and McFeters, 1997). The concentration of FC is expressed as the number of colonies per 100 mL of sample.

2. 3.1. 3. *E.coli*

E.coli are classified as enteric bacteria of the enterobacteriaceae family and are shown in Figure 2.1a. They are facultatively anaerobic and are able to ferment sugars by production of acid and gas. E.coli has been characterized to be a more specific indicator of fecal contamination in water bodies than fecal coliforms (Dufour, 1977), and has recently been incorporated into U.S. drinking water regulations as a specific indicator of fecal contamination. The approximate length of E.coli is 3 μ m, the mass of most enteric bacteria is 10^{-12} g, and their total concentration in one gram of soil typically varies between 10^6 and 10^9 bacteria (Wood, 1989).

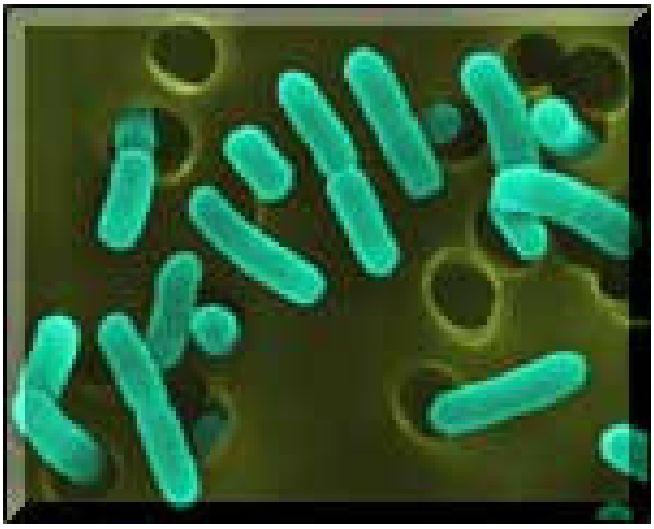

Figure. 2.1a E.*coli*

2.3.1.4. *Salmonella cholerasuis*

Salmonella cholerasuis causes one of the most common intestinal infections in the U.S. *Salmonella cholerasuis* can be found in the intestinal tracts of numerous infected domestic and wild animals. Therefore, the contamination of water from animal feces also poses a human health risk. Previous studies have indicated that a population of *Salmonella cholerasuis* may reach its half-life in approximately 2.5 hours in well water at 20 °C (McFfeters et al., 1974). More recent studies indicate that enteric bacteria such as *Salmonella cholerasuis* can survive for many months after entering the dormant state (viable but not culturable), and still be infectious (Walch and Colwell, 1994). The size, density, and the shape of *Salmonella cholerasuis* are very similar to *E.coli* (Figure 2.1b).

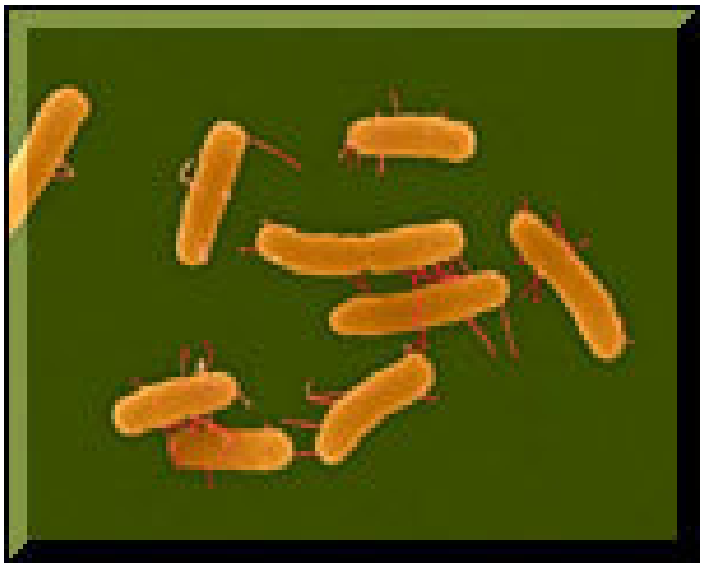

Figure. 2.1b *Salmonella cholerasuis*

2.3.2. Population Growth and Decay Function

A microbial population may increase, stay constant, or decrease during the course of an experiment depending upon the environmental conditions of the experimental site. Although bacteria are capable of utilizing many substrates simultaneously, a single substrate can control the growth of bacteria. The relationship between specific growth rate and substrate concentration was lately categorized as structured and unstructured (Tan et al., 1994). The structured relationship emphasizes the internal complexity of microorganisms, and the unstructured ignores the inside structural effects on microbial activities and relies on surface structures of microorganisms (Tan et al., 1994).

The most widely used single substrate unstructured bacteria growth rate model was introduced by Monod in 1942. The general form of Monod's equation is as follows:

$$\mu = \frac{\mu_m \quad S}{K_s + S} \tag{1}$$

where μ is the specific growth rate, μ_m is the maximum specific growth rate, S is the concentration of substrate, and K_s is the concentration of limiting substrate at which the specific growth rate of bacteria is half the maximum value.

Tan et al. (1994) developed a mathematical model using a statistical mechanical method to describe all types of bacteria growth dependent on a unique substrate. Tan and Bond (1995), and Corapcioglu and Haridas (1984) recommended a specific bacteria growth model in a water and attachment biomass phase, respectively, using Monod's equation. These equations take the form:

$$R_{gw} = \frac{\mu_m \quad S}{K_s + S} \theta C \tag{2a}$$

$$R_{ga} = \frac{\mu_m \quad S}{K_s + S} \rho_{bac} \sigma \tag{2b}$$

where θ is the water filled porosity, C is the concentration of bacteria in the water phase (mass of microbial cells per unit volume of water), R_{gw}, and R_{ga} are the microbial growth rate in the water and attached phase ($ML^{-3}T^{-1}$), respectively, S is the substrate concentration in water phase (ML^{-3}), ρ_{bac} is the mass of microorganisms per unit volume of biomass (ML^{-3}), and σ is the volume of microorganisms per unit volume of porous medium (L^3L^{-3}).

Previous research attempted to quantify the microbial growth rate on surfaces (Brock, 1971). Brock's results indicated that microorganisms have an exponential

growth rate, and consequently, the use of an exponential growth equation was used for microbial surface colonization in his study.

Reproduction (birth) and decomposing (death) functions of bacteria can be shown by the following equations:

$$\text{Births} = \alpha \, \text{N} \, \Delta t$$

$$\text{Death} = \beta \, \text{N} \, \Delta t$$

where, N is total population, and α and β are constants. Any increase in population ΔN, for a corresponding time interval, Δt, may be given as:

$$\Delta N = \alpha \, \text{N} \, \Delta t - \beta \, \text{N} \, \Delta t$$

$$= (\alpha - \beta) N \Delta t$$

$$= \gamma \, N \Delta t$$

By dividing both sides of the above equation by Δt, and taking the time limit as Δt approaches zero, the following is obtained:

$$\underset{\Delta t \to 0}{\text{Limit}} \frac{\Delta N}{\Delta t} = \frac{dN}{dt} \gamma \, \text{N}$$

Integrating both sides of the above equation and applying the initial condition, the general growth and decay function may be achieved as shown in Equation 3.

$$\int \frac{dN}{N} = \int \gamma \, \text{dt}$$

$$\ln \text{N} = \gamma \, \text{t} + \text{C}$$

by applying the initial condition as $N=N_0$ at t = 0, then

$$\ln N_0 = 0 + C$$
$$C = \ln N_0$$

Therefore,

$$\ln N = \gamma t + \ln N_0$$

or,

$$N = N_o e^{\gamma t} \qquad (3)$$

where γ is the specific growth rate (h^{-1}), and t is time (h). For microbial decay, γ is negative indicating an exponential microbial die-off. The two main factors which determine the potential for microbial contamination of groundwater are survival and the transport rate of the organisms.

2.3.3. Factors Affecting Growth and Survival

The growth and survival of microorganisms obviously affect their transport in the environment. Previous studies from Gerba et al. (1975), Crane and Moore (1984), and Yates and Yates (1988), indicate a bacterial survival period of several weeks to a few months. Therefore, distance that bacteria can travel could be highly dependent on survival within that environment.

There are various pathogenic (harmful) microorganisms in the soil. The survival of these organisms depends on a multitude of hydro-environmental factors. Many studies have been conducted to investigate survival of these organisms from potential sources such as animal droppings, manure application area, sewage and sludge, and the tissues of diseased plants (Lance et al., 1982; Loehr, 1979; Schaub and Sorber, 1977; Pettygrove and Asano, 1985; Reed et al., 1980). Pathogenic

bacteria may survive in soil for a period of a few hours to several months, depending on the soil type, soil pH level, soil temperature, moisture content, sunlight, and precipitation. In general, enteric bacteria persist in soil for two to three months; however, under favorable conditions, pathogenic bacteria may also multiply (Loehr, 1979).

Soil organic matter can provide substrates and nutrients to microorganisms. However, toxic organic matter such as antibiotics can harm and decrease the population of microorganisms. An increase in temperature will also cause higher soil biological activity and therefore, higher bacteria population density. The survival time is usually less in sandy soil than in clay soil (Loehr, 1979). Under high moisture conditions in sandy soils, bacteria are more mobile than in clay soil. In clayish soil, bacteria can be effectively filtered out by one to two meters of soil depth. Bacteria can easily be adsorbed on the soil particles in fine-textured soils, but they are removed through filtration in sandy soils (Lance and Gerba, 1984).

2.3.4. Factors Affecting Transport of Microorganisms

The transport of microorganisms is affected by the chemical and physical properties of the soil and water, the surface characteristics of the organisms, and the hydrological conditions of the area (Teutsch et al., 1991; Abu-Ashour, 1998). The transport of microorganisms is also affected by the available pore spaces that are not occupied by other organisms within the soil media (Teutsch et al., 1991; Abu Ashour, 1998).

2.4. Physiological and Hydrological Effects of Hill Slope on Microbial Transport

The relevant studies on hill slope hydrology may be categorized into three different groups: significance of vegetated filter strips (VFS) on microbial transport, significance of slope on runoff, and significance of preferential flow on contaminant transport.

2.4.1. Significance of Vegetated Filter Strip (VFS) on Microbial Transport

Water quality concerns associated with non-point source (NPS) pollution has recently become a great concern to most environmentalists. Recent evidence indicates that there are multiple environmental sources of pathogenic organisms including humans, companion animals, wildlife, and farm animals. Land application of manure is recommended to recycle nutrients and organic matter and to enhance soil quality and crop productivity. However, contaminated manure may pose a public health threat if pathogens are transported to potable and recreational water sources.

The transport of surface–applied bovine manure through soils into ground water has become a major concern to environmentalists and the general public. A review of available information indicates that agricultural lands are the major contributor of non- point source pollution in both surface and ground water (USEPA, 1994). Effluent disposal areas of farms with high animal densities normally contain large quantities of fecal coliforms. The risk associated with surface water contamination by manure is, in part, a function of manure volume, site hydrology, and proximity to surface water. Large, confined animal feeding operations (CAFOs) generate a substantial volume of animal manure that is normally held or applied within a relatively small area. High rates of land-applied manure, particularly where

rates exceed soil assimilative capacity, increase the risk for surface or ground water contamination. Risk may be offset by low rainfall, dryness, minimal land slope, relative isolation of the animal population, and methods of composting, storing, and spreading manure. Pathogens applied or deposited onto soil surfaces may infiltrate into the soil profile or, alternatively, may run off to surface waters. Since both processes can occur simultaneously, a thorough understanding of the controlling factors is critical in predicting which process will predominate. Knowledge of redistribution and persistency of fecal coliforms on most agricultural lands is, therefore, important in the assessment of any potential contaminant runoff.

One of the more promising management practices for controlling NPS pollution is to direct the flow of contaminants through a vegetated filter strip. A VFS appears to be an efficient and economical best management practice (BMP) in reducing overland flow of contaminants. A VFS provides an opportunity for runoff and pollutants to infiltrate into the soil profile. It enhances vegetative filtration of suspended sediment, provides adsorption on soil and plant surfaces, and enhances absorption of soluble pollutants by plants (Fajardo et al., 2001). Non-point source overland flow contamination often results from both infected animals defecating directly into the streams and from other sources of water such as surface runoff and subsurface drains of an applied manure area.

Substantial research has been conducted regarding both leaching/infiltration of microorganisms through soils and runoff to surface waters. Early studies on subsurface bacterial transport from septic effluents reviewed by Hagedorn et al. (1981) and Bitton and Harvey (1992) indicated that bacteria transport from a few

meters to 830 meters depends on soil texture (sand vs. gravel), water content (saturated vs. unsaturated), and time. Recently, laboratory-scale studies have focused on elucidating soil parameters affecting leaching. These studies have shown that the predominant factors affecting leaching in tilled soils are soil structure/texture and porosity/bulk density in conjunction with bacterial size (Gannon *et al.*, 1991a, 1991b; Huysman and Verstracte, 1993; Tan *et al.*, 1991); while in no-till soils, the predominant factors are distribution and continuity of macropores (preferential flow pathways) in conjunction with initial water content (McMurry *et al.*, 1998; Paterson *et al.*, 1992). In general, observed leaching rates are higher in no-till than tilled soils (Smith *et al.*, 1985; Van Elsa's *et al.*, 1991). Limited research suggests that parasites (i.e. *Cryptosporidium parvum*) leach more slowly through soils than bacteria (Mawdsley et al., 1996a, 1996b). Still, quantitative relationships have yet to be established describing rates or extent of pathogen leaching at the field or watershed scale.

Wilson (1967) used an empirical study to evaluate the effects of Bermuda grass on sediment transport. His results showed that maximum percentages of sand, silt, and clay were trapped at distances of 3, 15, and 122 m from the manure application area, respectively. Li and Shen (1973) evaluated the effects of tall vegetation on sediment transport on a watershed scale. Based on their findings, they recommended that tall vegetation is an effective media to reduce sediment yield by reducing surface runoff, increasing infiltration, and protecting the soil surface from detachment/deterioration as a result of direct rainfall impact. Kao and Barfield (1978) used artificial filter strips to develop an equation of flow by employing the

momentum balance principle. They concluded that the filter media drag resistance was the dominant force in retarding the surface runoff. Haggard et al. (2002) investigated the effects of slope, grazing management, and pasture renovation on surface runoff from small plots using a rainfall simulator. Their results showed that pasture renovation increased time to runoff and substantially reduced nutrient loss from land-applied animal manure and alleviated water-quality concerns in agricultural lands.

Studies addressing runoff of bacteria to surface waters have been reviewed by Baxter, Potter and Gilliland (1988), Khaleel *et al.* (1980), and Patni *et al.* (1985). Their studies showed that major factors controlling bacteria concentrations in runoff are manure management practices, wildlife activity, channel/bank storage, microbial mortality, and watershed hydrology. However, due to the complexity of interactions and nonlinear effects, few quantitative relationships have been established between the various factors. For example, a previous study reported the absence of a significant correlation between fecal coliform concentration in surface water and the presence of beef or dairy operations (Pasquarell et al., 1995). Similar results have also been reported for karst aquifers (Pasquarell and Boyer, 1995). This could be due to effective livestock/manure management practices, hydrological characteristics that do not favor transport, high microbial mortality rates, high background concentrations from wildlife, or a combination of the above reasons. In particular, very few studies have addressed the role of fecal coliform/pathogen contributions from wildlife (Atwill *et al.*, 1997). Similarly, studies suggest that stream/river banks and channels may serve as reservoirs for fecal coliform and that increased concentrations observed

during storm events are due to microbial re-suspension during periods of turbulent flow (McDonald *et al.*, 1982).

Bovine manure has been documented to contain various pathogenic microorganisms (Reddy et al., 1981). Field application of manure can potentially result in surface and groundwater contamination. Consequently, proper manure management practices are needed to prevent or minimize the deterioration of water quality from manure-born pathogens. Chandler et al. (1981) studied the distribution and survival of bacteria indicator organisms on land used for the disposal of swine effluent under a range of management, climate, and soil conditions. They studied the effect of soil type on the persistence of FC at several farms with different soil types. Also, vertical transport of FC into the subsoil was investigated on several irrigated sites with swine effluent. The results indicated that well divided applications of manure to the land can provide a relatively better and more efficient method to decrease the release of FC from manure application areas. Their results further indicated that the topsoil (up to a three centimeter depth) was found to provide a more suitable environment for FC persistence than pasture or subsoil.

Walker et al. (1990) suggested that grass filter strips alone would not reduce the concentration of microorganisms enough to meet the water quality requirement, but they indicated that no field data was available for validation of their predictions. The majority of published findings however, support, to various degrees, the role of filter strips in removing pathogens from overland flow (Coyne et al., 1995; Crane et al., 1983). Moore et al. (1988) recommended that effective vegetative filter strips should be at least three meters wide and have a slope of 0 to15%. Conflicting results

on the effectiveness of vegetative filters on removing bacteria (Srivastava et al., 1996; Hunt et al., 1979; Dickey and Vanderholm, 1981) indicate that surface conditions (e.g. soil type and types of vegetation), manure application technology, and rainfall characteristics may affect the efficiency of filter strips. Chaubey et al. (1994) observed improvement on ammonia and phosphorus removal from swine lagoon effluent with increased VFS with lengths of up to nine meters. Schelinger and Clausen (1992) noticed a 30% decrease in bacteria concentrations from a dairy manure detection pond after transport through a VFS. Lim (1997) found that all fecal coliforms were removed within the first 6.1 meters of VFS use to treat runoff from a simulated pasture.

Transport and fate of microorganisms have been well documented in soil columns (Bitton et al., 1979; Huysman et al., 1993). Soil column studies have shown that soil drying prevented the release of sorbed microbes after a rainfall application (Lance et al., 1976). Precipitation lowers the ionic strength of soil pore water, and preferential flow paths created by wormholes and plant roots promote microbial transport by allowing percolating water through the soil profile (Madsen et al., 1982; Zyman et al., 1988; Trevors, 1990). The experiments performed by Miller et al. (1965) indicated that solute displacement behavior depends on the method of water application. Using larger application rates often results in rapid water movement through the larger pores in the soil profile, bypassing the pollutant contained in the smaller pores. On the other hand, low application rates of water provide low infiltration rates, thus resulting in uniform flow through the soil profile (piston flow) and displacement of more pollutants. The degree of water saturation is also

considered to be a major factor in transporting pollutants through the soil profile. Bacteria are transported over much greater depths in a saturated soil matrix, and the lack of movement and survival of bacteria in soil is associated with unsaturated conditions of the soil (Bitton and Harvey, 1992).

If the environment is favorable, the adsorbed organisms grow and replicate, resulting in multiple patches of colonies that eventually become a continuous biofilm (Characklis and Marshall, 1990). However, significant biofilm accumulation changes the soil micropore geometry resulting in reduced soil permeability and porosity (Taylor et al., 1990a; Cunningham et al., 1991) and increased hydrodynamic dispersivity (Taylor and Jaffe, 1990b).

A study by Gerba et al. (1975) indicated the movement of coliform bacteria through different soil medias for distances ranging from 1 to 450 m. Hagedorn (1981) showed that bacterial contaminated groundwater traveled laterally 1 to 830 m through soil on various field experiments. Although some authors have concluded the transport of microbial contaminant negligible for granular filters and soil-microbial mass systems (Wollum and Cassel, 1978; Sykes et al., 1982), many other investigators have found the movement of bacteria very significant and recommended the use of microorganisms as a tracer indicator.

As reported by various researchers in the literature, changes in soil oxygen content, dissolved cementing agents, secretion of extracellular substances by bacteria (McCarthy and Zachara, 1989), replacement of saline water by fresh water, and even groundwater pumping can mobilize colloids in groundwater aquifers.

In general, the microbial transport equation in porous media is based on the continuity or mass balance equation. This indicates that the rate of change of the total biomass in a control volume of a soil media is equal to the difference between mass inflow rate and mass outflow rate, plus the rate of change due to population growth and decay of the microorganisms (Tan et al., 1992).

2.4. 2. Significance of Slope on Runoff

Slope significantly affects the total surface runoff. Dunne and Black (1970) concluded that the theory of saturation excess runoff presented by Horton in 1933 did not occur in some watersheds. Haggard et al. (2002) studied the effects of slope, grazing, and aeration on pasture hydrology and concluded that the measured runoff volume increased logarithmically with increasing slope of 1 to 28%.

Studies performed by Nassif and Wilson (1975) indicated that rainfall intensity, slope, soil cover, and soil type affect infiltration. They conducted an experiment and measured the infiltration rate on bare and grassed loam plots using 15-minute rainstorms on different slopes. Their results indicated that increasing the slope by 20% would result in a substantial reduction in infiltration. Reduction in infiltration by increasing the slope was estimated to be around 87% for bare soil and 54% for grassed soil after 15 minutes of rainfall. Further, the results indicated that soil surface cover (grass) will attenuate the surface runoff by 33% in comparison to the bare soil, thus allowing more water to infiltrate into the soil.

Data from Nassif and Wilson (1975) used to develop a relationship between infiltration and the land slope is shown in Figure 2.2.

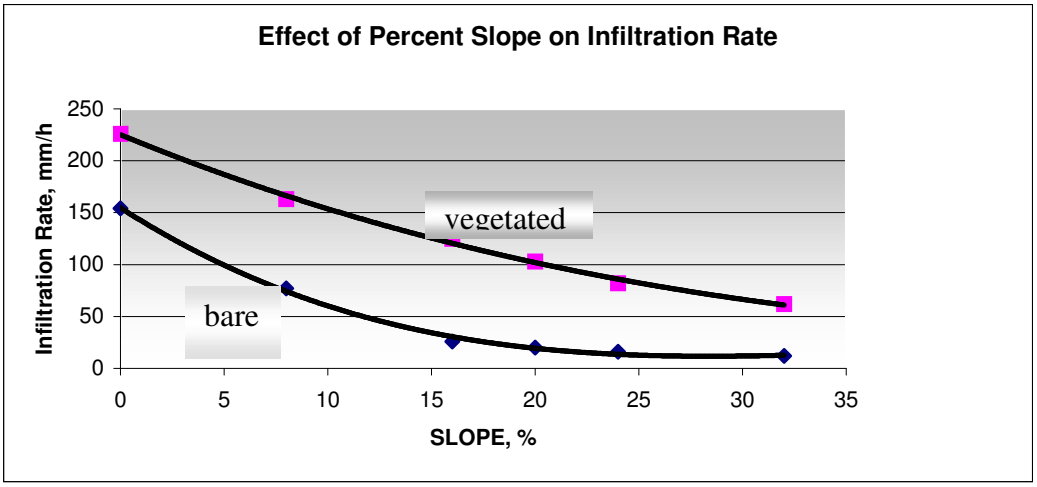

Figure 2.2. The effect of percent slope (X-axis) on infiltration rate (Y-axis), (Nassif and Wilson, 1975)

The cubic polynomial best fit for both bare and grassed soils are shown as follows (Nassif and Wilson, 1975):

$Y = -0.0034X^3 + 0.370X^2 - 12.813X + 154.7$ $R^2 = 0.99$ bare

$Y = -.0006x^3 + 0.1158x^2 - 8.2363x + 225.15$ $R^2 = 0.99$ vegetated

where X is the slope in %, and Y is the infiltration rate in mm/h.

R^2 values for both bare and grassed soils indicate that there exists a strong correlation between slope and infiltration rate. Relationships such as the one shown in Figure. 2.2 indicate the importance of incorporating slope effect in infiltration models.

2.4. 3. Significance of Preferential Flow on Contaminant Transport

A preferential flow path is described as a pathway of preferred flow that has a lower bulk density than the surrounding soil matrix; thus it offers less resistance to flow under specific field conditions and results in bypass flow (Tindall and Vencill,

1995). The macropores are defined as large cracks, wormholes, fauna tunnels, and channels created from decayed roots, with a size range of $> 1000\ \mu$m (Luxmoore, 1981). Soil macropores have been recognized as significant pathways for water and solute transport through the soil matrix (Germann and Beven, 1985). The complex function of macropores raises different problems in understanding the dynamics of flow through soil profiles. Where soils are heterogeneous, porous-media models such as Richard's equation should not be applied. Physical laws for heterogeneities have not been established although properties of macropores on a field scale have been studied (Mosley, 1979; Kitahara, 1993; Tsuboyama et al., 1994; Williams et al., 2003).

Andreini and Steenhuis (1990) conducted experiments on undisturbed soil columns by applying dye and bromide tracers to evaluate the preferential flow in conventional and conservation tillage soil profiles under no ponding conditions. Results indicated that in the no-tilled soil column, almost the entire depth of the soil profile was short-circuited by preferential flow. Rice et al. (1991) also conducted experiments on different soils using sprinkler and flood irrigation methods. They concluded that velocities of the contaminant flow were 1.5 to 2.5 times larger than the velocities obtained directly from the water mass balance and piston flow methods due to the preferential flow contribution.

The topographic condition of the land creates uneven flow patterns and often accelerated flow on some parts of the flow area relative to the rest of the watershed. In a small-scale case, this phenomenon orchestrates increased variability along the

flow surface area; therefore, surface preferential flow takes over in higher elevation areas.

The author has conducted topographic evaluation studies of the entire lysimeter to assess the variability of surface flow contaminant transport in each site in this study.

2.5. Processes Affecting Transport and Fate of Bacteria

Different processes determine the transport of microorganisms. The water flowing through the soil media primarily controls movement of microorganisms. This transport mechanism is considered to be the major transport mechanism for microbial transport and is referred to as the advection process. Hydrodynamic dispersion of the bacterial contaminant in the liquid phase occurs during the advection process in the soil media. When microorganisms move from one place to another within a soil media, they are highly subjected to physico-chemical forces, which usually cause the organisms to be retarded relative to the flowing water (Tan and Bond, 1992). Although a number of existing soil–microbial interaction studies have established relationships between soil material and microbial movement, many are limited by the use of repacked soil cores (Isensee and Sadeghi, 1999), and topsoil (Gagliardi and Karns, 2000).

Studies on mechanisms of bacteria retention are well documented by Butler (1954), Bitton. et al. (1974), Corapcioglu and Haridas (1984), Gerba and Bitton (1984), and McDowell-Boyer et al., (1986). Bacterial mobility under unsaturated soil conditions plays an important role in the dispersal of pathogenic microorganisms and enhancing biorestoration of contaminated soil. Studies by Kei et al. (2002) on bacteria

retention under an unsaturated flow condition indicated that bacterial accumulation was predominately at the soil surface and decreased with depth.

Microorganisms are also subjected to decay and growth depending upon the soil geo-chemical conditions and availability of substrates. Places where attachment of organisms is high, soil porosity will be lower resulting in less bacterial transport. The ability to survive and transport is also affected by the size, shape, and the surface structure of the organisms. Taylor and Jaffe (1990a) did explicitly consider changes in water-filled porosity, permeability, and the dispersion coefficient caused by bacteria attachment and their effect on microbial transport through the soil media.

2.5.1. Advection

Advection is one of the fundamental transport mechanisms that can carry the contaminant with the fluid flow. It is the downstream transport of contaminant at the mean flow velocity. Microorganisms may be carried at approximately the same average velocity as that of the flowing water. Often, it is quite hard to control the flow for evaluation of pollutant transport, especially under turbulent flow conditions. Cases where the flow is laminar, flow evaluation is better and pollutant transport can be controlled easily.

Flowing water in soil often carries dissolved contaminants or suspended colloidal material including clay particles and bacteria. Parke et al. (1986) showed that water flow caused pseudomonads to move faster and over a relatively long distance in soil media. Tan et al. (1992) showed that the mass flux of bacteria carried

with the flow of water within the soil medium is proportional to the concentration of bacteria in solution. This can be shown as:

$$J_v = J_w\, C = v_w\, \theta\, C \qquad (4)$$

where J_v is the advective mass flux of microorganisms (mass of organisms/unit cross sectional area of soil/time), J_w is the volume of flowing water through a unit cross-sectional area of soil per unit time, C is the bacteria concentration (mass per unit volume per unit time), v_w is the average water velocity in the soil media, and θ is the volumetric water content of the soil.

2. 5. 2. Chemotaxis

The ability of cells to respond to concentration gradients of attractants (often nutrients) or to repel toxins by employing temporal sensing mechanisms is referred to as chemotaxis and has been extensively studied by Adler (1969), Berg and Brown (1972), and Dahlquist et al. (1972). Movement toward the source (such as growth substrates) is referred to as positive chemotaxis (attractants) and it happens when the pollutant source is of some benefit. Movement away from pollutant sources is often referred to as negative chemotaxis (repellent), and it usually happens when the source is harmful.

Keller and Segel (1971) stated that even a cell might not be able to respond to any movement due to the concentration gradient. An average cell flux proportional to the macroscopic substrate gradient can be determined based on the cell

characteristics. The resulting macroscopic flux due to chemotactic movement is expressed as:

$$J_x = \theta \; v_x \; C \tag{5}$$

where J_x is the chemotactic flux (Corapcioglue and Haridas, 1984), θ is the water content, C is the concentration of bacteria, and v_x is the average chemotactic velocity of the bacteria and is expressed as:

$$v_x = \frac{k_x}{S} \nabla S \tag{6}$$

where k_x is the chemotactic coefficient, and S is the concentration of an attractant or substrate, and ∇S is the gradient of the subsurface concentration (e.g. in 1-D flow, $\nabla S = \frac{ds}{dx}$). Corapcioglu and Haridas (1985) studied the theoretical transport and fate of microorganisms in porous media. They studied various transport processes including convection, dispersion, chemotaxis, tumbling, and growth and decay of the bacteria. Their theoretical summary of the rate of immobile or attached biomass phase is shown in Equation 7.

$$\frac{\partial \rho_b \sigma}{\partial t} = R_a - R_d + R_{gs} - R_{ds} \tag{7}$$

where, R_a and R_d are the rates of microbial attachment and attachment , and R_{gs} and R_{ds} are the growth and decay terms in the deposited state, respectively, σ is the volume of deposited bacteria per unit volume of porous medium, and ρ_b is the density of bacteria in grams per unit volume of bacteria.

Due to the extreme difficulty in measurement procedures, the chemotactic movements of bacteria for experiments of all four plots were completely ignored in this study. However, to study the transport of bacteria in porous media, there is a need to quantify the contribution of chemotactic movement of bacteria.

2.5. 3. Attachment and Detachment

2.5.3. 1. Adsorption

Adsorption is the attraction between soil particles and microorganisms. Various studies on adsorption of bacteria and viruses on solid surfaces have been documented by Daniels (1972, 1980), Marshall (1976, 1980), Hendricks et al. (1979), Vilker and Burge (1980), and Gerba and Bitton (1984). Brownian motion, active movement of motile bacteria, and fluid flow bring bacteria and viruses to the vicinity of the surfaces of soil particles where they can be attracted or repelled by the forces such as physical adsorption (caused by van der Waals forces), chemical adsorption (resulting from chemical reactions), and physico-chemical adsorption (ionic exchange, electrostatic interaction of charged sites at the surface) (Tan et al., 1991; Corapcioglu and Haridas, 1984).

Herzig et al. (1970) showed that for particles of diameter greater that 0.1 μ m, the van der Waals forces overcome the random movement of Brownian motion, but for particles of smaller diameter it is the contrary. In the soil profile, adsorption is also considered to be a factor in the removal of bacteria by soil. Gerba et al. (1975) and Weaver (1981) found that adsorption plays an important role in the removal of bacteria in soils that contain clay.

2.5.3.2. Sedimentation

When the density of suspended particles is greater than the density of the fluid, particles may settle by gravity. Sedimentation of microorganisms could happen when the organisms are moving vertically through the soil profile or by retention. Smith et al. (1985) and Gannon et al. (1991b) noted that for bacteria, sedimentation is not significant. Their findings seem reasonable because the density of bacteria is usually in the range of 1.0 – 1.1 g/cm^3, which is very close to the density of water (Matthess and Pekdeger, 1981; Corapcioglu and Haridas, 1984; Characklis, 1990). Practically, it is highly unlikely that sedimentation ever happens for bacteria.

2. 5. 3. 3. Interception

The interception of microorganisms occurs when the suspended organisms collide with the surfaces of suspended soil particles in both surface and subsurface flow environments. O'Mel ia and Stumm (1967) noted that interception contributed to retention of suspended microorganisms in soil. A study conducted by Yao et al. (1971) concluded that interception is not a significant process for the retention of bacteria with an average diameter range of 0.2-7 μ m and for viruses with a diameter range of 0.01- 0.5 μ m.

2. 5. 3. 4. Straining

Straining occurs when a suspended particle being carried through a porous medium is larger than the size of the pore space. It is sometimes considered to be the main transport mechanism causing the retardation of larger bacteria in porous media (Gerba and Bitton, 1984; Smith et al., 1985). Wherever the bacteria attachment to

suspended particles increases, bacteria are more susceptible to straining and the degree of straining increases based on the extent of bacteria coagulation.

For quantitative purposes, straining was included as part of the total retention and attachment process as an input for prediction of fecal coliforms throughout the simulation in our studies.

2. 6. General Equations on Microbial Transport

Advection -dispersion equations are the dominant equations in most contaminant transport studies. The detailed theories in microbial transport are discussed in the modeling chapter.

2.7. Materials and Methods

2.7.1. Experimental Set-up

2.7.1.1. Geographic Location

The experimental site was located at the Patuxent Wildlife Research Refuge (U.S. Fish and Wildlife Services), in Beltsville, Maryland. An orthographic map of the lysimeter site is presented in Figure 2.3.

2.7.1. 2. Schematic and Dimensions of the Lysimeter

A two-sided lysimeter (12.7 m wide by 21.5 m long) with 20% slope on both sides was instrumented to monitor the surface and vertical transport of FC, *E.coli*, and *Salmonella cholerasuis* (Figure. 2.4). Soil on one side was sandy loam; while the other

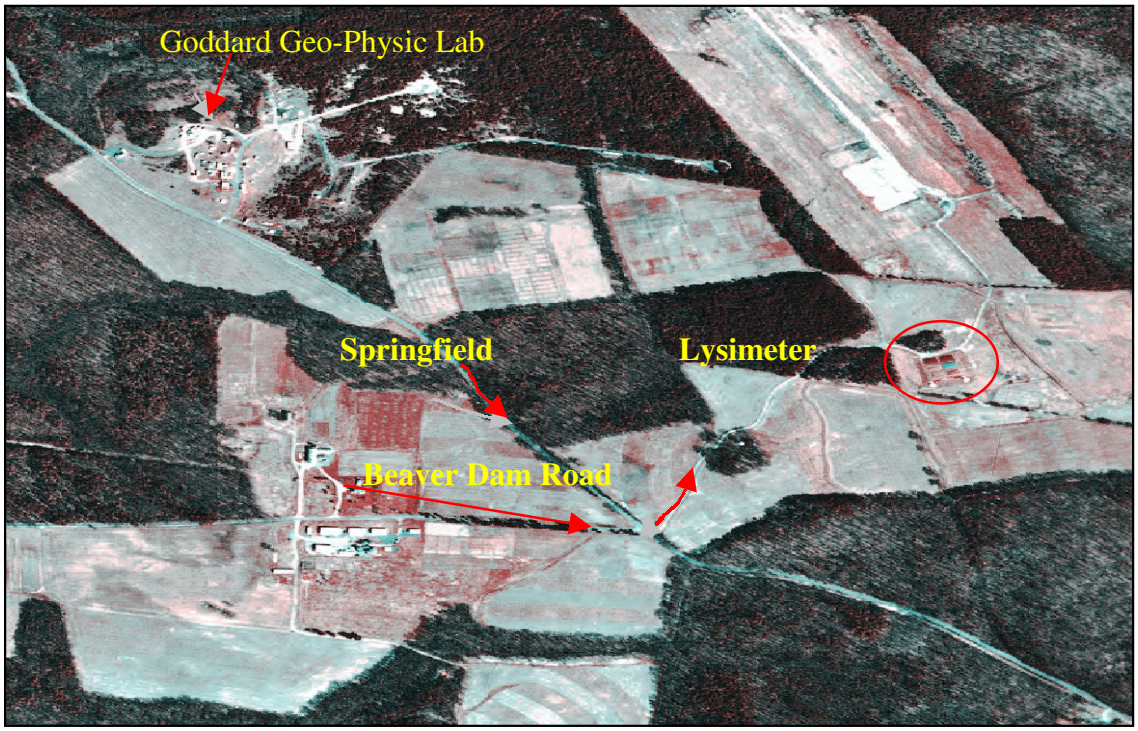

Figure 2.3 Orthographic image of the lysimeter site (approximate scale is 1mm = 7.5 m)

side was clay loam to provide different soil textures. Both sides had a gravel layer below 60 cm of soil. The lysimeter was lined with heavy-gauge vinyl plastic to prevent loss of contaminants. The average depth (gutter to liner) was approximately 3 m. Figure 2.4 shows the detailed schematic of the research site. Deep sampling pits were also constructed just outside the lysimeter to collect the surface runoff.

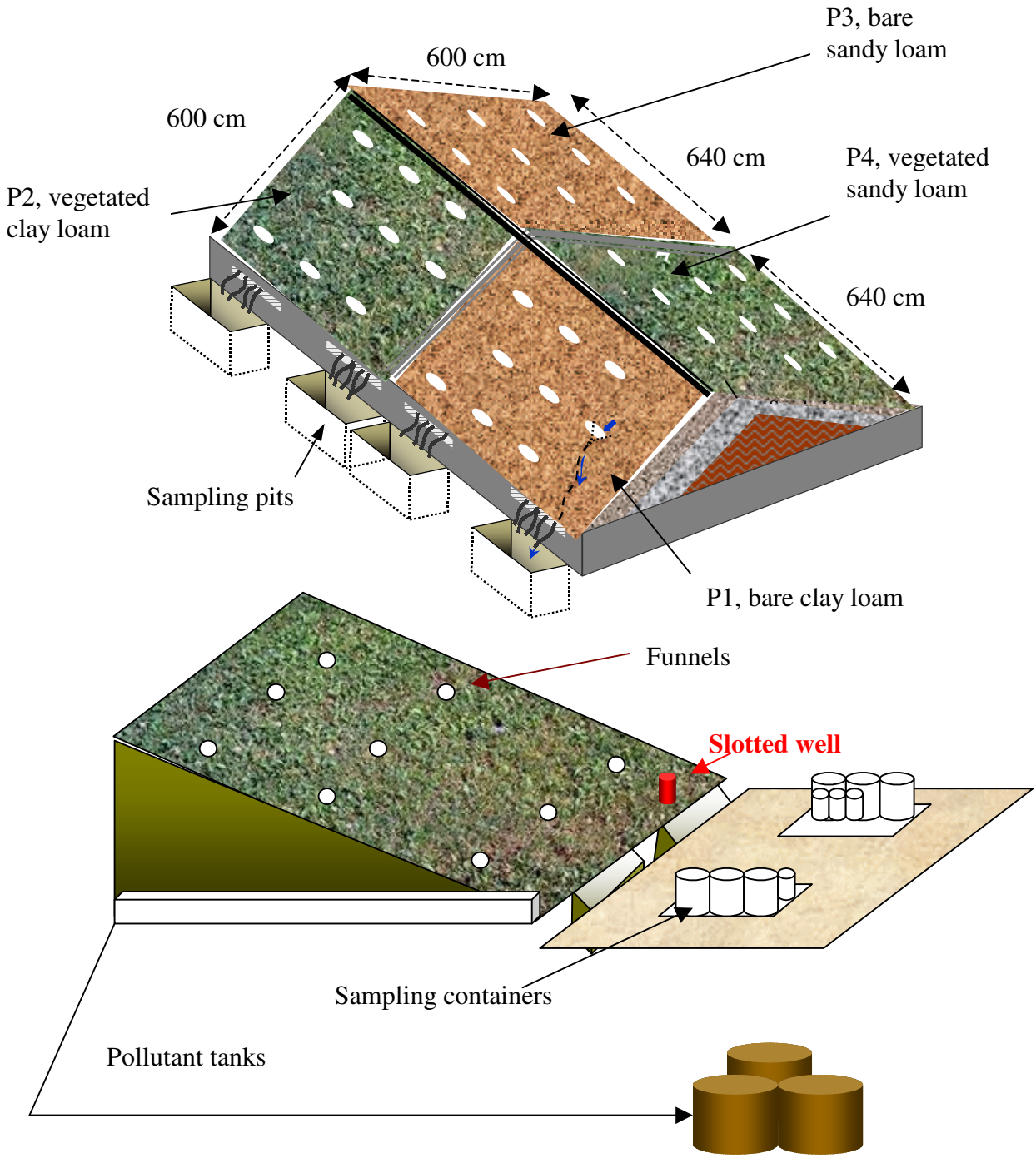

Figure 2.4. Schematic of the lysimeter with four sub-plots, with the bare and the vegetated sides included sampling containers and wastewater tanks. Funnels are at distances of 95 cm, 285 cm, and 490 cm from the ridge of the plot, respectively.

2.7.1.3. Automated soil moisture probes

To continuously and systematically monitor the variation in soil water content, a technique was required to collect real time data during each experiment. The recent development of Time Domain Reflectometry (TDR) techniques and the design of different advanced automated systems for collecting continuous data (Van Wesenbeek and Kachanoski, 1988; Baker and Allmaras, 1990; Heimovaara and Bouten, 1990; Herkelrath et al., 1991) have substantially improved the study of soil water movement.

Series of multisensor capacitance probes have been recently shown to enhance the accuracy in soil moisture measurements. Scientists have recently tested these new capacitance probes under both laboratory and field conditions (Starr and Paltineanu, 1998; Paltineanu and Starr, 1997) and the probes have been exclusively used in Australia since 1991 for irrigation scheduling (Buss, 1993).

The Environ-SCAN soil monitoring system (Sentek Pty, Ltd., Kent Town, South Australia[1]) was used in this research. Four probes with five capacitance sensors each, centered at 10 (5-15), 20 (15-25), 30 (25-35), 40 (35-45), and 50 (45-55) cm depths were placed in each subplot and were connected to a data logging station outside the plot through a cable as shown in Figure 2.5 to continuously record real-time soil volumetric water contents. An internal power supply charged by a solar panel was also provided for operating the system. The data logger was programmed in two and ten minutes intervals to record soil volumetric water content during each experiment.

[1] http://www.sentek.com.au/products/enviroscan.asp? lang=en

To make sure that the connecting tubes between the probes and data-logging station were not blocking the surface runoff, the cables were lifted up and positioned in the direction of flow.

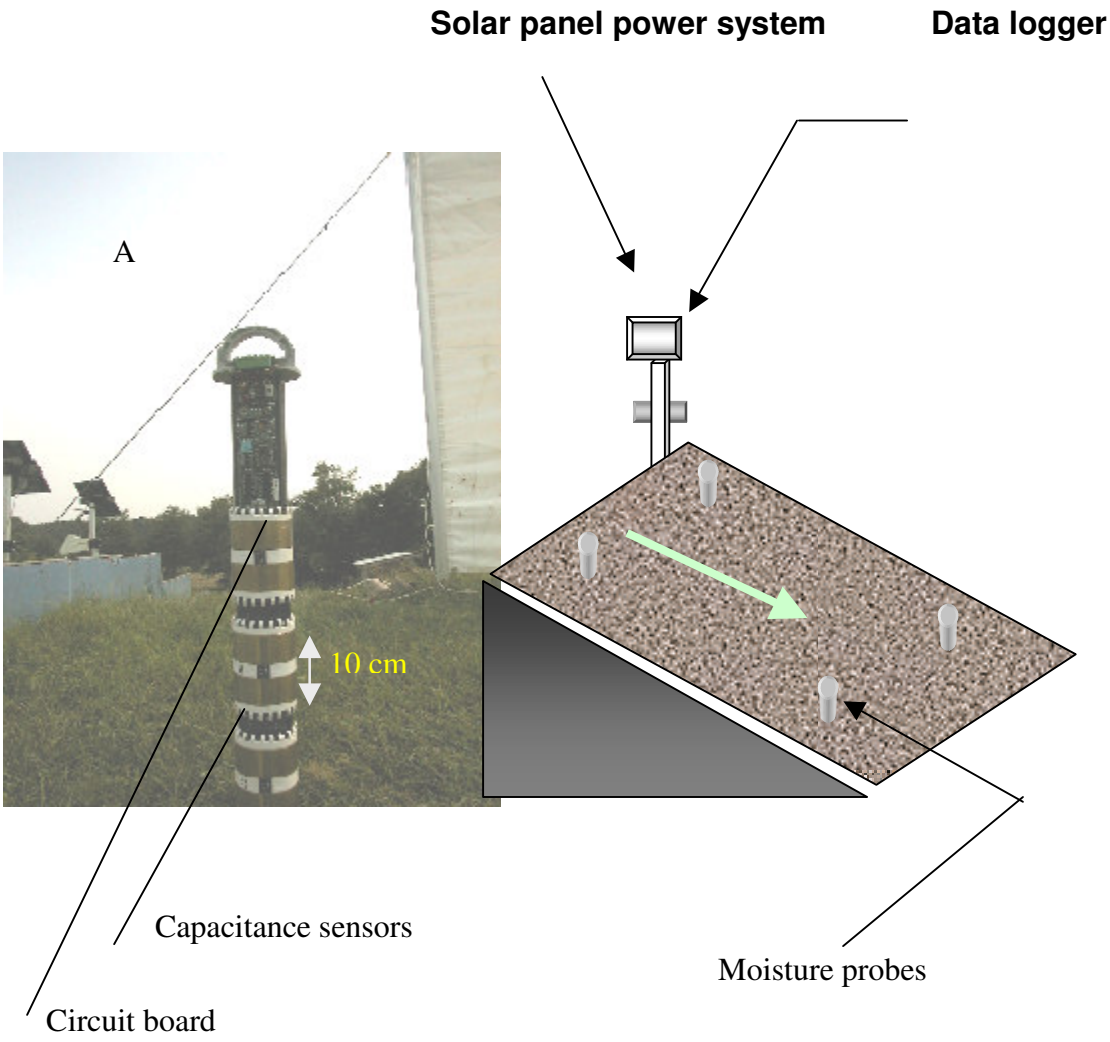

Figure 2.5. Multisensor capacitance probes shown in one subplot with connecting tubes (A) and data-logging station accompanied by a power supply with solar panels (B)

2.7.1. 4. Slotted well

To assess any potential movement of bacteria into the groundwater table, a PVC pipe five centimeters in diameter and seventy centimeters in length was placed vertically at the lower portion of each sub-plot (Figure 2.6). The first fifteen centimeters of the soil depth at the top was replaced with bentonite to prevent any possible subsurface flow into the well through that region. The well controlled subsurface flow from 15 to 70 cm depth. Also the slotted wells were elevated five centimeters from the soil surface to prevent any overland flow of microbial contaminant into the slotted well. The idea of placing the slotted well was to allow the subsurface contaminant to pass through the slotted areas, indicating the subsurface transport of microbial contaminant if there should be any such transport. The slotted wells were capped, maintained well and continuously monitored throughout the entire season.

During each experiment, the slotted well was completely capped to prevent any synthetically generated rain from the rainfall simulator. At the end of every experiment, a water sample was taken from the well for further analysis of microbial contamination.

2.7.1.5. Funnels and mini flumes

To collect the spatial and temporal overland flow runoff, 12.7 cm diameter stainless steel funnels were placed on each subplot at distances of 95, 285, and 490 cm from the ridge of the plot in staggered order. Rectangular stainless steel mini flumes with a width equal to the diameter of the funnels were made in the machine shop and were placed on the upper portion of each funnel to direct flow into the

funnel, and prevent erosion and leaching. Tygon 2275 tubing was used to direct surface runoff from the funnels to the sampling pits outside the lysimeter. To prevent any possible diversion of surface runoff, the tubing was buried approximately 10 centimeters below the soil surface.

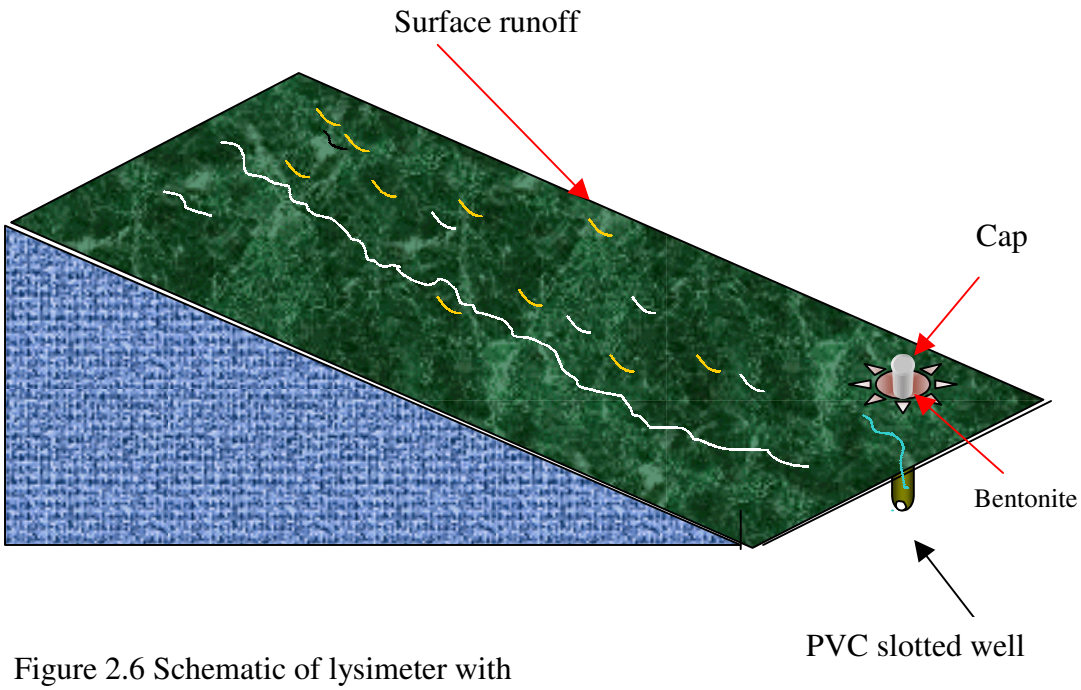

Figure 2.6 Schematic of lysimeter with

2.7.1.6. Rainfall Simulator and Water Pump

To produce a wide range of rainfall intensities, a large-scale mobile rainfall simulator was built at the USDA/ARS machine shop in Beltsville, Maryland. The rainfall simulator was made of 2.4 cm (one inch) pipe with four adjustable nozzles. Depending upon the plot orientation, the nozzles could be rotated and positioned perpendicular to the ground and move horizontally to cover an appropriate surface area. Each nozzle was connected to a single pressure gauge, to regulate the flow for

the desired intensity. A pump was also provided to pump water from two 2000 L (500 gallons) tanks placed in vicinity of the lysimeter. The water source was a local water well located 61 m (200 ft.) away from the lysimeter.

The elevation of nozzles relative to the ground surface was also adjustable by a pulley arrangement to simulate synthetic rain with different degrees of impact. The elevation of nozzles to the ground surface was set to 3.4 m (11 ft) to maintain the same terminal velocity for the raindrops as that of natural rain (Miller, 1987; McKensie, 1985).

2.7.1.7 Plot Partitioning

In order to compare the effect of vegetated surface versus bare soil on microbial transport, the plots on each side of the lysimeter were divided into two equal sub-plots with a buffer in between to ease the sampling process. The size of each sub-plot was 600 cm (in the flow direction) by 640 cm in width. An aluminum barrier was placed along the sides of each sub-plot in the direction of flow to prevent any potential loss of surface runoff from the sub-plot (Figure 2.7). These barriers prevented water loss and allowed a better mass balance to be calculated.

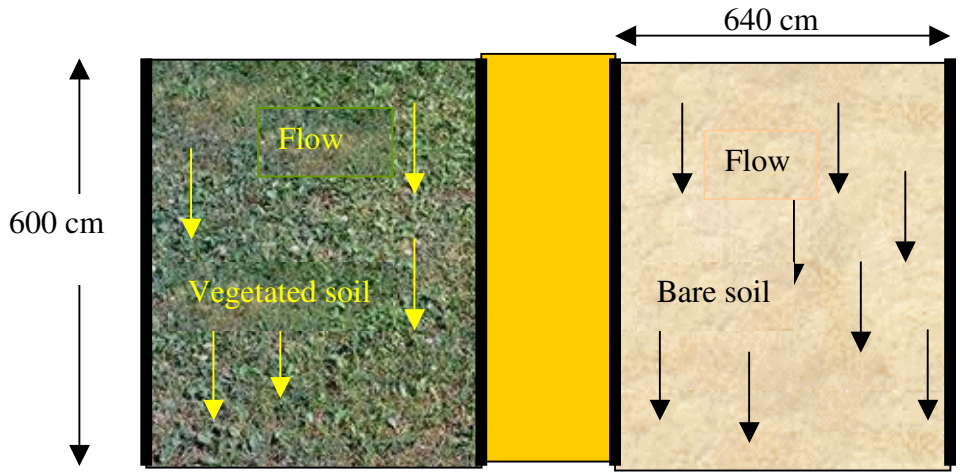

Figure 2.7 Plan view of the sub-plots partitioning

2.7.1.8 Windshield Assembly

To prevent any possible disturbances from wind on the synthetic rain pattern from the rainfall simulator, the two most critical wind directions were identified and completely blocked by a tall sail shield (Figure 2.8). The sail was very resistant to wind and was manufactured specifically for large sailing yachts. The sail shield was tailored and placed vertically in sailing masts extending 60 cm above the rainfall simulator, positioned on the corner of each sub-plot. The aluminum masts prevented winds from disrupting the rainfall simulator pattern. The windshield improved the uniformity coefficient of rainfall significantly and helped to conduct a better experiment.

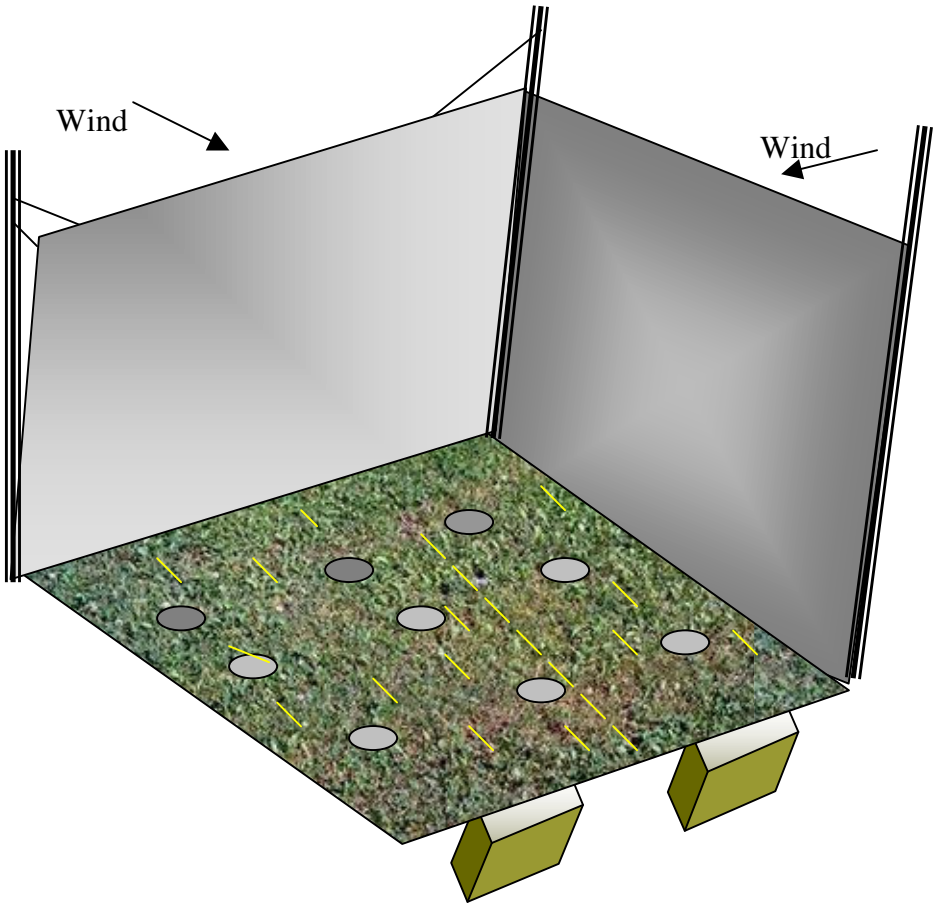

Figure 2.8 Schematic of the field windshield, constructed to achieve a uniform rain distribution over each sub-plot during the experiments

2.7.1. 9 Pollutant Containment Tanks

To collect and route the bio-contaminant from both surface runoff and subsurface flow, the entire site has to be well protected from any possible leaching of contaminants. For this purpose, the lysimeter was lined with a thick vinyl liner located 70 cm below the soil surface. The lining prevented any contaminant leaching to the groundwater source. A 15 cm (six inch) diameter PVC pipe was located at the end of the gutter, where it collected the entire microbe-laden overland flow. This pipe

conveyed the runoff to a 2000L (500 gallon) tank. This collection system contained the contaminated runoff within the closed system. Figure 2.9 shows the 2000 L pollutant tanks. The collected pollutant water was maintained in the tanks until they were scheduled for treatment after the final experiment was completed.

Figure 2.9 Pollutant tanks for collecting all microbial runoff

2.8 Hydrological Characterization and Equipment Calibration

2.8.1 Determination of Rainfall Intensity and the Uniformity Coefficient

To generate synthetic rainfall for the experiments, a realistic rate of precipitation was chosen using hydrological data from the U. S. National Climatic Data Center (NCDC) for a one-hour rainfall duration and a return period of ten years. That rate, approximated 6.1 cm/h, was used throughout all of the experiments. The

Christiansen equation was used to calculate the uniformity coefficient (see Appendix C). The uniformity coefficient of the synthetic rainfall was found to be approximately 90%. This was above the recommended 80%, from most researchers (Zoldoske, 2003).

2.8.2 Calibration of V-notched Weir

A v-notched weir was placed at the end of the gutter to measure the total surface runoff from each subplot. Series of runoffs were collected by a bucket at the outlet and were compared with the direct readings at the weir. Visual observation of the weir flow (Figure 2.10) showed the result of v-notched weir readings were in reasonable agreement to the measured runoff obtained by the bucket.

2.9. Site Physical Characterization

2.9.1. Soil Textural Analysis

To evaluate the soil in the research site, four locations in each plot were considered for texture analysis. Differential soil samples at the top and bottom of each sub-plot were taken into the laboratory for analysis. Those samples were at 0-10, 10-20, 20-30, 30-40, 40-50, 50-60, 60-70, and 70-80 cm depths. The soil was verified as clay loam for plots 1 and 2, and sandy loam for plots 3 and 4 (detailed procedures and table of results are presented in Appendix D).

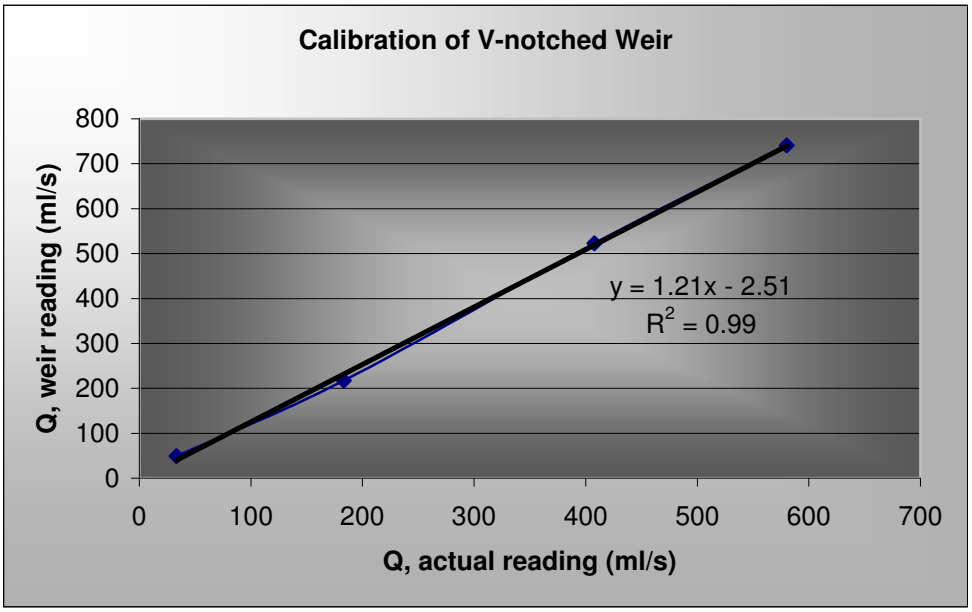

Figure 2.10. Measured overland flow runoff using v-notched weir versus flow measured by a bucket

2.9. 2. Soil Water Characteristics

The soil water characteristic curve describes the soil's ability to store and release water. A nonlinear relationship exists between soil water content and the soil matric potential. The models most frequently used to describe the relationship between soil water content and soil matric potential are those proposed by Brooks and Corey (1964), Campbell (1974), and Van Genuchten (1980). Research indicates that soil texture predominately determines the water-holding capacity. In general, the higher the percent of clay and silt particles, the higher the water holding capacity. The small particles have a much larger surface area per unit volume than the larger particles. Therefore, a larger surface area allows the soil to hold a greater quantity of water.

For the sandy loam plots, samples for determining water retention were collected from four locations. Two locations at the top and two locations at the

bottom on the left and on the right side of the lysimeter were selected. At each designated point, four samples were taken, one each at 0-10, 10-20, 20-30, and 30-40 cm. On the clay loam side, the same procedures were followed except an extra soil sample was taken at 40 - 50 cm depth. Figure 2.11 shows the soil water characteristic curves for the four subplots.

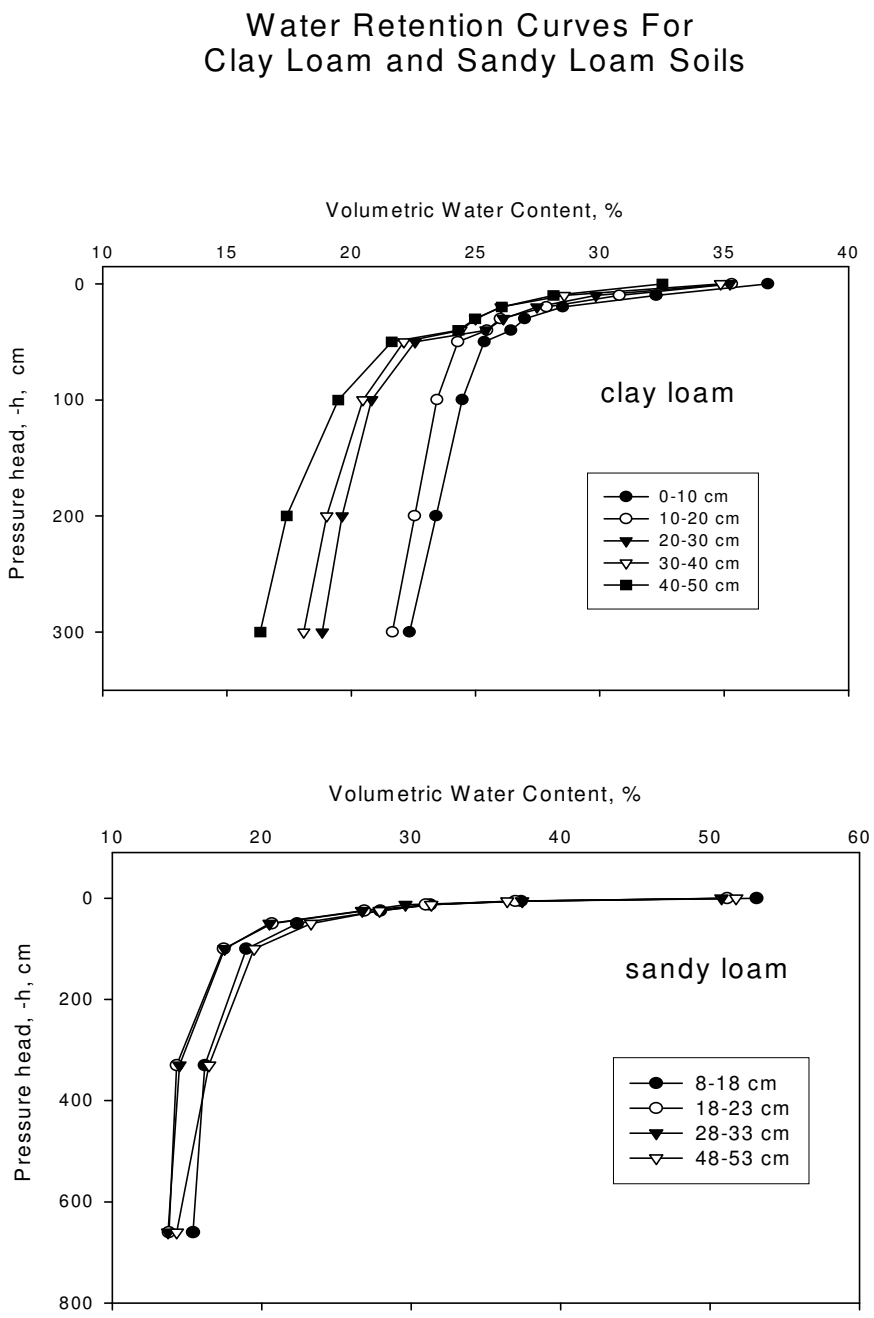

Figure 2.11 Soil water characteristics for clay loam and sandy loam

2.9. 3. Soil Organic Matter

Organic matter is the vast array of carbon compounds in soil. Originally created by plants, microbes, and other organisms, these compounds play a variety of roles in nutrient, water, and biological cycles. Organic matter is especially important in providing nitrogen, phosphorus, sulfur, and iron.

Because soil organic matter has an impact on microbial activities, growth and decay rates, a series of samples from both clay loam and sandy loam soils were taken and delivered to the University of Maryland's Soil Testing Laboratory to evaluate the soil organic matter.

2.10. Experimental Procedures

Bovine and swine manure were used to conduct experiments on FC, *E.coli* and *Salmonella cholerasuis* at the lysimeter two different years (2001and 2002). Sampling procedures of these two experiments (bovine manure for FC, and swine manure for *E.coli* and *Salmonella cholerasuis* were quite different, but most of the laboratory procedures were the same. The experimental procedures contained the pre-simulation laboratory procedure, field experimental procedures, post-simulation laboratory procedures, and the laboratory procedures for sorption.

2.10.1. Pre-Simulation Laboratory Procedures

The pre-simulation processes were required prior to each experiment. These processes included the inoculation of both *E.coli* and *Salmonella cholerasuis* in the manure mix as well as preparation of plates for the incubation of organisms.

2.10.1.1. Plate Preparation

Forty-eight hours prior to the experiments, 58 grams of Brilliant Green Agar was mixed in 1 liter of distilled water, autoclaved for 15 minutes at 121 $^{\circ}$ C, and used to prepare 60 plates for *Salmonella cholerasuis* concentration analysis. This procedure was repeated to make 250 plates. Approximately 400 Mac Conkey plates purchased from Northeast Laboratory Services in Waterville, Maine were prepared to analyze the concentrations of *E.coli* and FC.

2.10.1.2. *E.coli* and *Salmonella cholerasuis* Cultures (Swine Manure Experiments)

Minimal Lactose Broth (MLB) and Mannitol Tetrathionate Broth (MTB) were prepared to culture *E.coli* and *Salmonella cholerasuis*, respectively. A single colony of *E.coli* isolated from pig feces, and *Salmonella cholerasuis* purchased from the American Type Culture Collection (ATCC, Manassas, VA) were transferred to 10 mL of MLB and MTB, respectively, and incubated for 18 hours at *37* $^{\circ}$ C. The incubated MLB and MTB (the inoculums) were then added to 500 mL of each of the original MLB and MTB and were incubated again for 18 hours at 37 $^{\circ}$ C.

2.10.1.3. *E. coli* Inoculation (Swine Manure Experiments)

In the early morning on the day of each experiment, 200 mL of the prepared Minimal Lactose Broth (MLB) was inoculated into 21 liters of pig manure (bringing the approximate population of *E.coli* in pig manure to 1,000,000 per mL) and was thoroughly mixed. Then, the sample of this inoculated manure was taken right before the experiment for the determination of the initial *E.coli* concentration.

2.10.1.4. *Salmonella cholerasuis* Inoculation (Swine Manure Experiments)

One hundred milliliters of Mannitol Tetrathionate Broth (MTB) was inoculated at the same time in the same manure slurry and was thoroughly mixed. Then, the sample of this inoculated manure was taken right before the experiment for the determination of the initial concentration of *Salmonella cholerasuis.*

2.10.2. Bromide Tracer

Bromide has been used extensively to trace water movement through soil within several feet of the ground surface or through sediments in the subsurface (Jabro, J.D., 1991; Iqbal et al., 1996; Steenhuis et al., 1990). To evaluate the transport behavior of the soil in the lysimeter, a bromide tracer was used in all of the experiments. Three grams of potassium bromide in every liter of water makes a concentration of 2000 ppm (K=39 g, Br = 80 g, KBr =119 g makes 80/119 *3 = 2 g of bromide in every liter of water). Therefore, 60 grams of KBr was added to 20 liters of manure slurry to maintain a 2000 ppm concentration of bromide.

2.10.3. Source of Manure

The bovine manure used in our studies was fresh manure taken directly from the USDA/ARS research facility dairy barn in Beltsville, Maryland. This manure was from milk cows and contained 10% solids consisting of microbial biomass (undigested) and bedding materials. Because the deeper portion of the manure mix in the barn was more aged relative to the top portion of the accumulated manure, age consistency was considered while taking manure for different experiments.

For *Salmonella cholerasuis* and *E.coli* experiments, swine manure (pig manure) was provided from a pig lagoon located in Germantown, Maryland that belonged to Dr. Hartsock, a faculty member of the University of Maryland at College Park.

2.10.4. Bovine Manure Mix Preparation

A few days prior to the experiments, enough bovine manure was collected from the USDA/ARS research facility dairy barn located in Beltsville, Maryland. Samples of the manure were taken for determining solid-liquid ratios. Approximately a solid-liquid ratio of 10% was maintained throughout the experiments as was recommended by Ohio State University. Twenty liters of this manure were applied on a 30 cm x 640 cm application area.

2.10.5. Swine Manure Mix Preparation

Approximately 25 gallons of swine manure was taken to conduct the experiment. The swine manure was aged one to two years relative to the bovine manure that was used the previous year to conduct experiments on *FC*. The swine manure relative to the bovine manure was more watery with no solid materials however, it was adjusted to maintain a 4% solid content as this was recommended by most local and state agencies throughout the experiments (Ohio State University). This made the application of swine manure much more difficult on the 20% slope than the bovine manure.

2.10.6. Estimation of Bacteria Initial Population

Prior to the experiments and right before applying manure on the application areas, 100 mL of manure slurry samples were taken and transported immediately to the laboratory for determination of initial microbial concentrations. Manure samples were thoroughly mixed, diluted 1:10 with distilled water, and centrifuged at 100xg in 12-mL conic tubes for ten minutes.

For FC and *E.coli* initialconcentrations, 50 µLsub -samples of the supernatant in two replications were placed onto MacConkey Agar using a Spiral Biotech Autoplater 4000 (Spiral Biotech, Bethesda, Maryland). Plates were incubated at 44.5º C for 18 hours. A Synoptic Limited Protocol Colony Counter was used to count FC in colony forming units (CFU) in each plate.

Also, 50 µLsub -samples were replicated twice and plated on Brilliant Green Agar using the Spiral Biotech Autoplater 4000 for *Salmonella cholerasuis* counts. Plates were incubated at 37 º C for 18 hours. *E.coli* and *Salmonella cholerasuis* counts were obtained using a Q-Count computer. Random plates were also counted by sight to compare with the Q-Count.

2.10.7. Field Experimental Procedures

2.10.7.1. Application of Bovine Manure on the Plots

Bovine manure slurry was applied very uniformly on a 30 cm strip right on the top of each subplot (Figure 2.12) around 6: 30 PM on the evening before the day of rainfall simulation. To prevent immediate runoff from the manure application area on the 20% sloped lysimeter, aluminum barriers were placed in the lower portion of

the manure application area. Those barriers were removed immediately once the rainfall simulator was turned on.

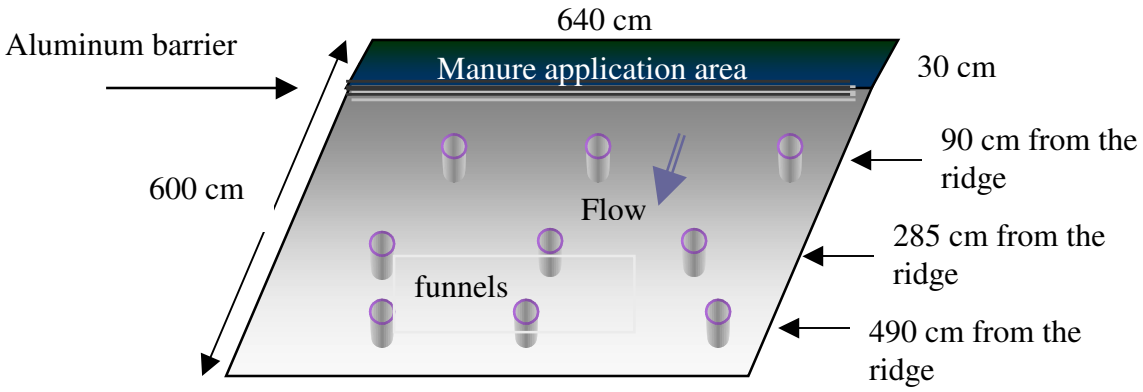

Figure 2.12. Layout of a subplot with manure application area, and the locations of the funnels.

2.10.7.2. Application of Swine Manure on the Plots

For the swine manure experiments, the same procedures were followed as in the bovine manure experiments. Because the swine manure was more liquid than the bovine manure, it was applied in the early morning on the day of the experiments right before the simulation. This was necessary to prevent immediate runoff on the 20 % slope.

2.10.7.3. Soil Temperature and Ambient Temperature

The ambient temperature at the lysimeter site and the soil temperature at eight centimeters depth for five different locations were recorded prior to each simulation. These temperatures were necessary to evaluate the effects of both ambient and soil temperatures on the population dynamics of bacteria. Soil samples were also taken at

20 cm depth to compare the initial water contents of each subplot with the readings of the automated moisture probes.

2.10.7.4. Simulation of Rainfall

The rainfall simulator was already calibrated and was ready to begin the simulation (Figure 2.13). Two 2000 L water tanks were filled with water free of bacteria and were used to provide water for the rainfall simulator. The power generator and the pump were turned on to initiate the rainfall simulation. The main valve was completely opened and the pressure gage for each nozzle was set to 20 PSI to maintain an intensity of 6.1 cm/hr. The nozzles and the pressure gages were continuously monitored throughout the simulation for any possible variation in rainfall. The duration of a rainfall event was 55 minutes for the bare plots, 90 minutes for the vegetated clay loam, and 120 minutes for the vegetated sandy loam (longer duration for vegetated plots were necessary to observe runoff). A crew of seven people were involved for sampling in each simulation.

Figure 2.13. Rainfall simulator used to generate rain for experiments

2.10.7.5. Field Sampling Procedures

Because of the difficulties in dealing with swine manure, different sampling procedures were imposed for that specific experiment. Sampling procedures are presented in two different sections**.**

2.10.7.5.1. Runoff Sampling (Bovine Manure Experiments)

Runoff was collected at five-minute interval for bare and vegetated clay loam, and bare sandy loam, and at ten-minute interval for vegetated sandy loam at every funnel and at the gutter by a v-notch weir. Runoff from each funnel was collected into sampling jars. Each set of three funnels was located at 95, 285, and at 490 cm from the ridge of the plot (Fig. 2.12). After each simulation, collected runoff from each funnel was measured. Water samples from each of the funnel and the gutter were

thoroughly mixed separately and 50-mL sub-samples were taken immediately to the laboratory for microbiological analysis. To avoid cross contamination, all measuring devices were completely rinsed with clean water before measuring the next collected runoff.

To prevent potential overflow of any funnel, sampling intervals were adjusted to a shorter time without disturbing the simulation procedures. Runoff from the plots was continually measured at the gutter after the simulation was over.

2.10.7.5.2. Soil Sampling

The day after the simulations, soil samples were also taken at incremental depths from the areas adjacent to each funnel and in the manure application area within 30 cm of the soil depth in the vegetated clay loam and bare sandy loam, and within 60 cm of the soil depth in the vegetated sandy loam using a 2.54 cm ID core sampler. The remaining manure residue was collected from the application area in bare plots for determining the remaining FC population. Caution was taken in the soil sampling to prevent cross contamination of FCs. No soil samples were taken for swine manure experiments.

2.10.7.5.3. Runoff Sampling (Swine Manure Experiments)

Sampling surface runoffs for swine manure was quite different than for the bovine manure experiments. The sampling time for the two bare plots was every two-minute for the first ten minutes of simulation, and thereafter every ten-minute until the rainfall simulator was turned off. This strategy was necessary on the bare plots

because the release rate of both *E.coli* and *Salmonella cholerasuis* from a manure of 4 % solid-liquid was expected to be very crucial in the early minutes of simulation. For the two vegetated plots, samples were taken every ten-minute.

2.10.8. Post Simulation Laboratory Analytical Procedures

2.10.8.1. Processing of Runoff Samples

Runoff samples were thoroughly mixed and were centrifuged at 100xg in 12-mL conic tubes for ten minutes. Two replicated 50 µL sub -samples of the supernatant were placed onto Mac Conkey agar using a Spiral Bio-Tech autoplater. FC and *E.coli* plates were incubated at 44.5° C for 18 hours. Plates for Salmonella cholerasuis were incubated at 37 ° C for 18 hours.

2.10.8.2. Processing of Soil Samples

Soil samples were diluted 1:10 with distilled water, dispersed for two minutes in a high-speed blender, and then processed as described above for runoff samples. This dilution was necessary to prevent clogging of the spiral platter inlet tubing.

2.10.8.3. Plate Counting Procedures

Figure 2.14 The LCD (Monitor) from Q-counter used to count E.coli and *Salmonella cholerasuis*

2.10.8.3.1. Fecal Coliform

Runoff samples were centrifuged at 100xg in 12-mL conic tubes for ten minutes. Tworeplicated50 µLsub -samples of the supernatant were placed onto Mac Conkey agar using a Spiral Biotech Autoplater. Plates were incubated at 44.5º C for 18 hours. A Synoptic Limited Protocol Colony Counter was used to count FC in colony forming units (CFU) in each plate. Soil samples were diluted 1:10 with distilled water, dispersed for two minutes at high-speed in a blender, and then were

processed as described above for runoff samples. This was necessary to prevent clogging of the spiral plater inlet tubing.

2.10.8.3.2. *E.coli*

As was explained in the previous section, the Q-counter (Figure. 2.14) was used to count the *E.coli* populations. *E.coli* colonies were found to be reddish, convex, and approximately two millimeters in diameter. *E.coli* counting for both bare and vegetated plots was successful and plates exhibited little interference from indigenous bacteria. Since the counter was extremely sensitive to lights and sample plate movement, extensive caution was taken during the counting procedures. Whenever the colony count seemed unreasonable, the plates were manually counted.

2.10.8.3.3. *Salmonella cholerasuis*

Significant differences in colony morphology were observed between bare and vegetated plots. Salmonella cholerasuis colonies were found to be raised, purple in color, shiny at the center, and approximately two millimeters in diameter. However, in the vegetated plots, colony sizes were much larger and the colors were greenish. In the bare plots, counting processes for *Salmonella cholerasuis* were exactly the same as the *E.coli* counting processes. Substantial interferences from indigenous bacteria were observed in the *Salmonella cholerasuis* colonies of the vegetated plots. Because of these terminal difficulties in counting *Salmonella cholerasuis* in vegetated plots, other available methods (BBL Enterotube II and Microscopy) were employed to differentiate *Salmonella cholerasuis* from indigenous organisms. Colonies of *Salmonella cholerasuis* suppressed by other organisms from

the vegetated plots are shown by the Q-counter in Figure 2.15. The figure indicates the interference of indigenous bacteria on *Salmonella cholerasuis* plates and shows how it was not possible to count *Salmonella cholerasuis* even manually.

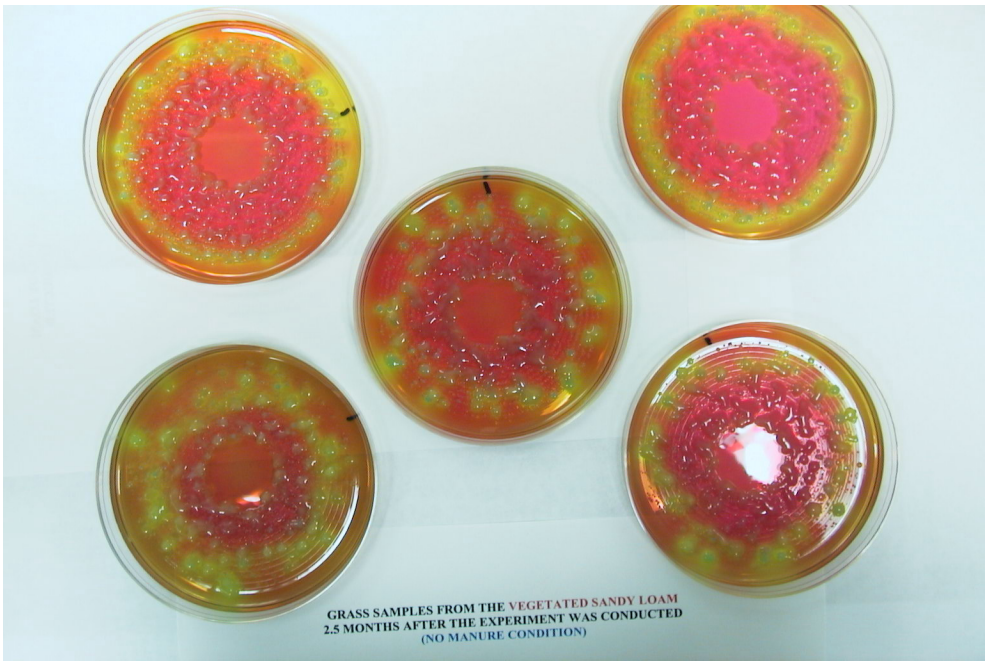

Figure 2.15 Interference of indigenous bacteria on *Salmonella cholerasuis* in vegetated plots

A. BBL Enterotube II

The BBL Enterotubes II (Figure 2.16) were used to clarify the *S.cholerasuis* populations. A well-isolated colony was taken from the *S.cholerasuis* plates by the sharp tip of a wire on the Enterotube, and was pulled from the other end through all twelve compartments. The portion of the wire remaining in the tube maintained anaerobic conditions necessary for tube fermentation of glucose and production of gas. Tubes were incubated at 37 $^{\circ}$C for a period of 18 hours.

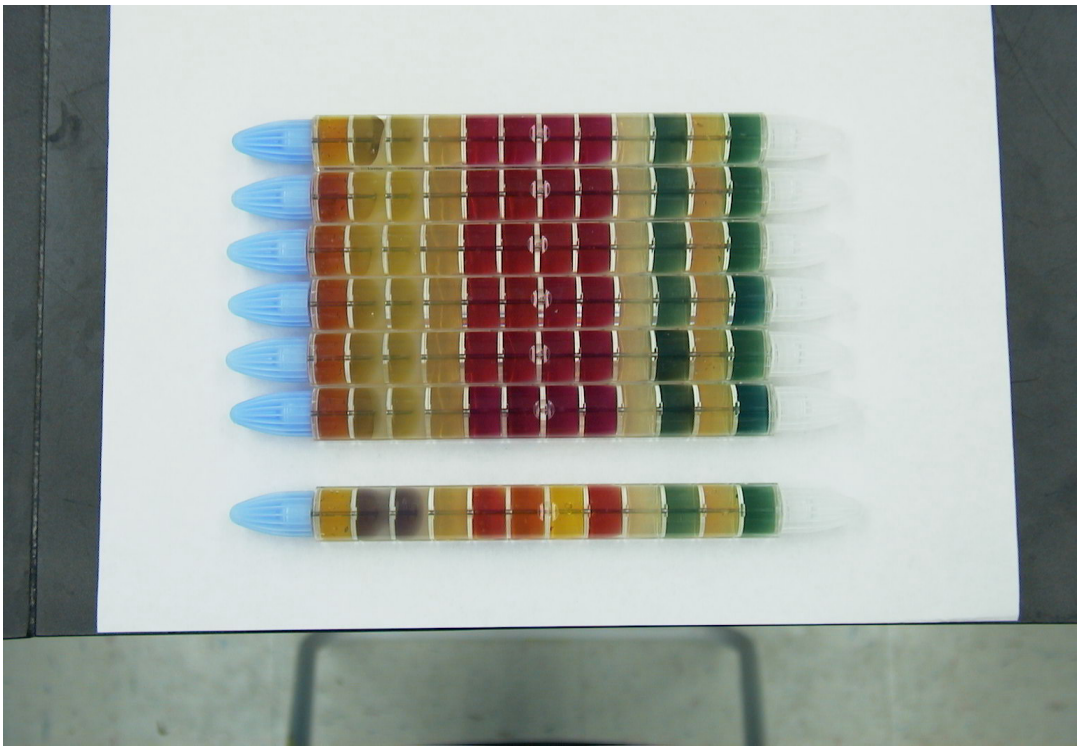

Figure 2.16 BBL Enterotube II used to verify *Salmonella cholerasuis* in vegetated plots

Since the results of the Enterotubes showed no indication of *Salmonella cholerasuis*, the population of *Salmonella cholerasuis* on the vegetated plots was not determined.

B. Microscopy

A single colony from an incubated plate of a vegetated plot, and a single colony from a plated *Salmonella cholerasuis* culture were transferred onto a microscopy slide. Sterile water was added to ease the process. A differential Interference Contrast Microscopy at 1000 X was used to view the organisms. Pictures of both samples in three replications were taken and compared. There was no sign of *Salmonella cholerasuis* in the colony that was removed from the vegetated soil plate.

2.10.8.4. Laboratory Procedures for Bromide Concentrations

Bromide concentrations for both runoff and soil samples were determined by a bromide electrode device.

2.10.8.4.1. Bromide in Runoff Samples

One thousand ppm of NaBr solution was prepared according to the available laboratory procedures (Orion cat. # 940011). Ten milliliters of 1000 ppm solution was added to 100 milliliters of distilled water to make 100ppm NaBr solution. Ten milliliters of 100 ppm solution was added to 100 milliliters of distilled water to make 10 ppm standard solution. Ten milliliters of 10 ppm solution was added to 100 milliliters of distilled water to make 1ppm standard solution. Ten milliliters of 1ppm standard solution then was added to 100 milliliters of distilled water to make 0.1ppm standard solution.

Five milliliters of each standard solution was added to 0.1 mL of ionic strength adjuster into five-milliliter disposable beakers to expedite the probe reading processes.

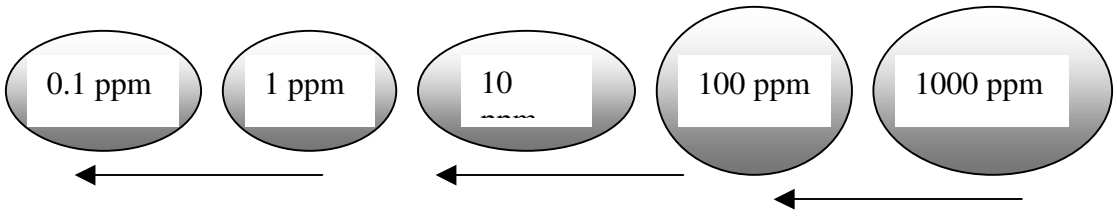

Figure 2.17 Serial dilution preparations for Br concentrations

These procedures were necessary to create a calibration curve by plotting millivolt (mV) values (probe readings) on the linear axis (y-axis) and the standard concentration values on the logarithmic axis (x-axis).

Five milliliters of each runoff sample then was mixed with 0.1 mL of ionic strength adjuster for determining the bromide concentrations using a bromide Electrode Model-525 manufactured by Thermo Orion according to the provided procedures in the Orion catalog (Thermal Orion, USA). Bromide concentrations were determined using the calibration curve described above (voltage readings vs. concentration).

2.10.8.4.2 Bromide in the Soil Samples

To obtain the standard curve for the soil samples, ten grams of soil was added to 100 mL of distilled water. The solution was vortexed and centrifuged for ten minutes at 750 RPM before reading. The same procedures as for runoff samples were followed to determine the soil bromide concentrations.

2.10.8.5 Sorption

A series of experiments were conducted to evaluate the percentage of FC attachments to the soil particles. These experiments were conducted inside the laboratory under static and dynamic conditions for FC. Details of experiments on sorption are presented in Appendix H.

2.10.8.5.1. Static (standing water sample) Conditions

The manure was diluted by a 1:100 ratio. In three separate tubes, one milliliter of diluted manure solution was spiked into 12 mL of water/runoff sample (water was used as a control). Two replicated 50 µL sub -samples of the supernatant were placed onto Mac Conkey agar using a Spiral Biotech Autoplater. All samples were vortexed and centrifuged (as previously mentioned) and plated after 0, 2, 4, and 6 hours. Plates

were incubated at 44.5º C for 18 hours. A Synoptic Limited Protocol Colony Counter was used to count FC in colony forming units (CFU) in each plate.

2.10.8.5. 2. Dynamic (shaking water sample) Conditions

To quantify the percentage of FC adsorption under dynamic conditions, one milliliter of manure was added to 12 mL of runoff samples in six separate tubes. All the samples were shaken by a shaker under 200-RPM for two, four, or six hours. After two hours of shaking, two tubes were removed, centrifuged, plated in two replications, and incubated again at 44.5º C for 18 hours. The same procedures were followed after four, and six hours of shaking the samples. A Synoptic Limited Protocol Colony Counter was used to count FC in colony forming units (CFU) in each plate.

2.11. Data Analysis Methods

At each automated moisture probe, volumetric water content was continuously measured at 10, 20, 30, and 40 cm of soil depth. The water content at each designated depth was averaged and integrated over the entire 40 cm depth of soil profile.
The total runoff from the funnels and the gutter for each plot were calculated using Equations 8, and 9, respectively, as;

$$R_F = \frac{\Sigma\,(V1 \cdots V9}{Area \times T} * 10\,\frac{mm}{cm} \qquad (8)$$

$$R_G = (R_{gutter} \times \frac{3780}{(24 \times 60)(Area)}) \times 10 \frac{mm}{cm} \quad (9)$$

where R_F is the funnels total runoff rates in mm/min at every time step, V1…V9 are the total runoff volumes at each time step (mL), Area is the area of each plot and is equal to $600 \times 640\,cm^2$, T is the time step in minutes, R_G is the gutter runoff rate in mm/min, and R_{gutter} is the gutter runoff in gpd at each time interval. The infiltration of water on each plot was measured based on a simple mass balance equation as shown in Equation 10.

$$F = P\text{-}R\text{-}E\text{-}I \quad (10)$$

where,

F= Total infiltration, cm

P= Total precipitation, cm

R= Total measured runoff at the gutter during the experiment, cm

E= Total evaporation, cm

I= Total interception either by depression or by surface cover, cm

The means of volumetric runoff, bromide and bacteria concentrations were calculated from three replications at each row in every experiment. Arithmetic, geometric, and volumetric concentrations were calculated. The volumetric concentrations for each row (x = 95, 285, and 490 cm distances from the ridge) were determined using Equation 11.

$$\overline{C} = \frac{C_1V_1 + C_2V_2 + C_3V_3}{V_T} \quad (11)$$

where $\overline{C}$ is the volumetric concentrations at distance X from the manure application area; C1, C2,and C3 are the FC concentrations; and V1, V2, and V3 are the volumes of runoff at Funnels 1, 2, and 3, respectively; and V_T is the total runoff through the funnels at each row.

Statistical analysis was accomplished by using Percent Error, Root Mean Square Error (RMSE), and the two-tailed Student's t -test of measured and simulated infiltrations. Percent error indicates how accurate the simulated values are in comparison to the measured values. The RMSE has been widely used by researchers as a criterion for evaluating hydrologic models (Ma et al., 1998; Zacharias and Heatwole, 1994). The equations are as follows:

$$\text{Percent Error} = \frac{|Simulated - Measured|}{Measured} \times 100 \quad (12)$$

$$\text{RMSE} = \sqrt{\frac{\sum_{1}^{n}(P-M)^2}{n}} \quad (13)$$

where P is the predicted value, M is the measured value, and n is the number of observations. The t-test was calculated by:

$$t = \frac{\bar{x} - \mu}{s/\sqrt{n}} \tag{14}$$

where $\bar{x}$ is the mean of measured data, μ is the mean of the simulated data, s is the standard deviation of the measured data, and n is the number of samples.

An analysis of variance (ANOVA) was used to determine whether the average concentrations of FC on each row, and the total populations of FC on each plot were significantly different under different treatments. The level of significance, α, was set at 0.05 to test whether the predicted means would fall within the 95% confidence interval of the observed mean. The standard error of the fraction of FC in runoff s_f was computed as:

$$s_f = f\sqrt{\frac{(s_Q)^2}{Q} + \frac{(s_{p-r})^2}{p-r}} = f\sqrt{\frac{\left(\frac{q}{a}\frac{s_a}{a}\right)^2}{\frac{q}{a}} + \frac{(s_p)^2 + (s_r)^2}{p-r}} = f\sqrt{Q\left(\frac{s_a}{a}\right)^2 + \frac{(s_p)^2 + (s_r)^2}{p-r}} \tag{15}$$

where $f = Q/(p-r)$ is the fraction of FC in runoff, p is the average count of FC before the simulation, r is the average count of FC remained at the surface of the application area, q is the average count of FC in runoff, Q is the average adjusted count of bacteria, $Q=q/a$, a is the average extraction efficiency, and s denotes the standard error of the value in the subscript. The coefficient of extraction efficiency was

obtained in the laboratory. This was necessary to find out the percentage of FC participated in runoff after being adsorbed to the sediment particles.

In our case:

q = count of bacteria in runoff in billions

Q=q/a, adjusted count of bacteria in billions

a = 0.75 for plots 1 and 2, a = 0.70 for plots 3 and 4

p = count of bacteria before experiment

r = count of bacteria after experiment

2.12. Results and Discussions

2.12.1 Total Runoff of FC (Bovine Manure Experiments)

The hydrographs in Figure 2.18 indicate that in both bare clay loam and bare sandy loam plots, runoff started much earlier as compared to the vegetated plots, with both showing a very sharp rise in runoff during the early stages of simulation. Results also indicated that on the bare clay loam plot, after a sharp rise within the first ten minutes, the runoff gradually increased until the rainfall simulator was turned off. On the bare sandy loam, however, runoff remained at a constant rate after a sharp rise during the first 15 minutes of the simulation. Surface sealing developed rather quickly on the bare clay loam soil, causing the increase in runoff rate.

The very flat hydrograph on the vegetated sandy loam plot also indicated the importance of soil texture in runoff and infiltration on the vegetated surfaces. Results from both vegetated plots show that vegetation drastically attenuated the surface flow of water (less runoff). It will be shown that the reduced runoff on vegetated plots

decreased the surface transport of FC, while increasing its vertical transport because of increased infiltration.

Figures 2.19-2.22 indicate the water balance components with calculated infiltration based on a simple mass balance equation in all sub plots. The results show that for a total of 6.1 cm of rainfall in 60 minutes of rainfall simulation, a total of 0.5 cm and 2.2 cm of water was infiltrated in the bare clay loam and in the bare sandy loam (Figures 2.19 and 2.21), and 4.6 cm, and 6.0 cm in the vegetated clay loam and vegetated sandy loam, respectively (Figures 2.20 and 2.22). Results from the bare soils were not expected to exhibit higher measured increments in water content in 0-40 cm depth of soil than the total infiltrated water (Figures 2.19 and 2.21) as compared to those of the vegetated soil (Figures 2.20 and 2.22). However, it seems that the loss of the automated moisture probe's surface contact with the soil particles in the bare soils may have played an important role as a potential pathway for macropore flow resulting in much higher readings in volumetric water content by the automated moisture probes. On the other hand, vegetated soils were less susceptible to surface cracking, and therefore, resulted in more reasonable probe readings with smaller standard errors (Figures 2.20 and 2.22). Results showed that infiltration in both vegetated soils continued even the automated moisture probes did show relatively stable condition after fifty five minutes of rainfall simulation (Figures 2.22, and 2.24). Possible cause may have been attributed to the fact that soil within the proximity of the moisture probes have reached saturation earlier therefore, did not show any more change in water content while water was continuously percolating.

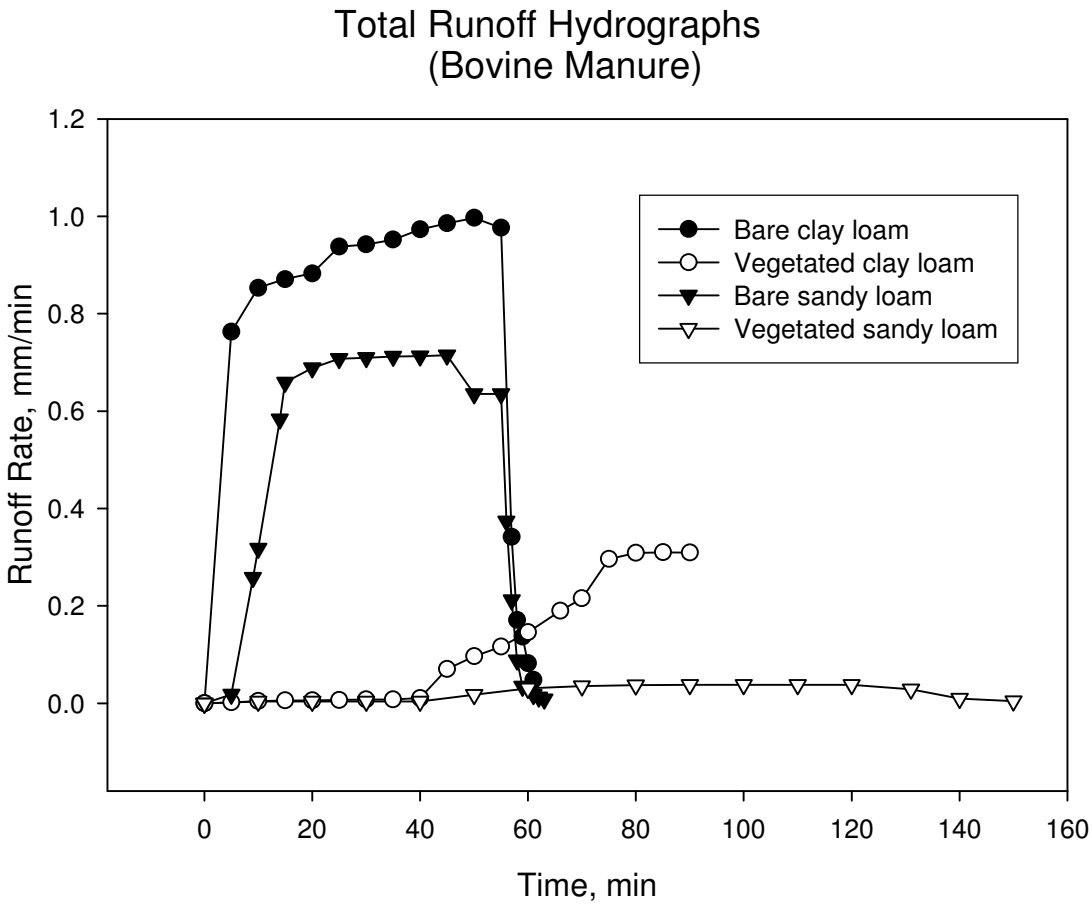

Figure 2.18. Runoff hydrographs on both bare clay and sandy loam, and both vegetated clay and vegetated sandy loams for FC experiments (bovine manure)

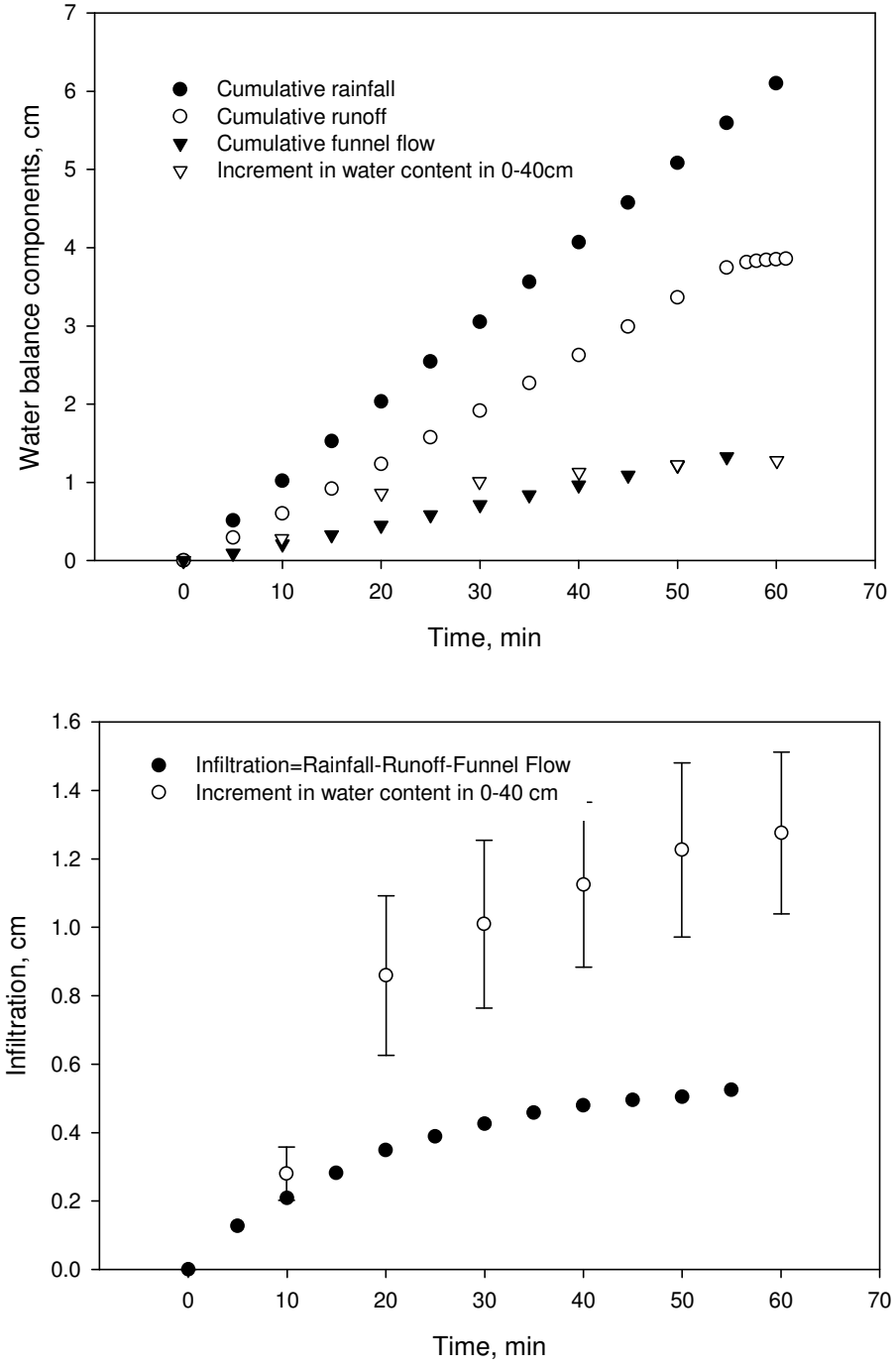

Figure 2.19. Cumulative rain, cumulative runoff at gutter, total runoff through funnels, and infiltration for bare clay loam (plot 1) in cm

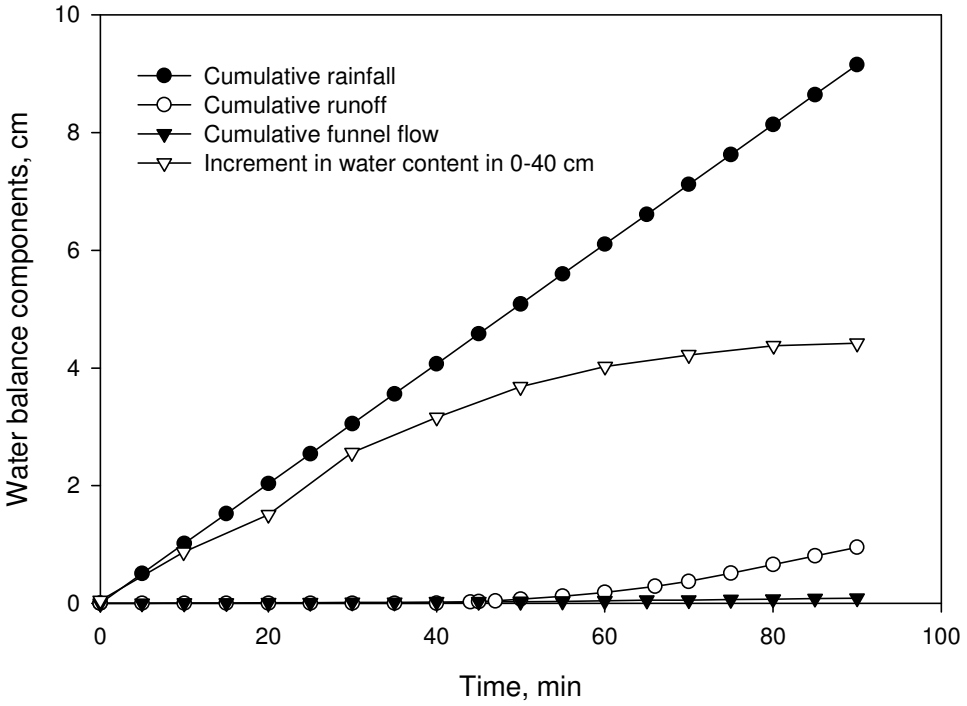

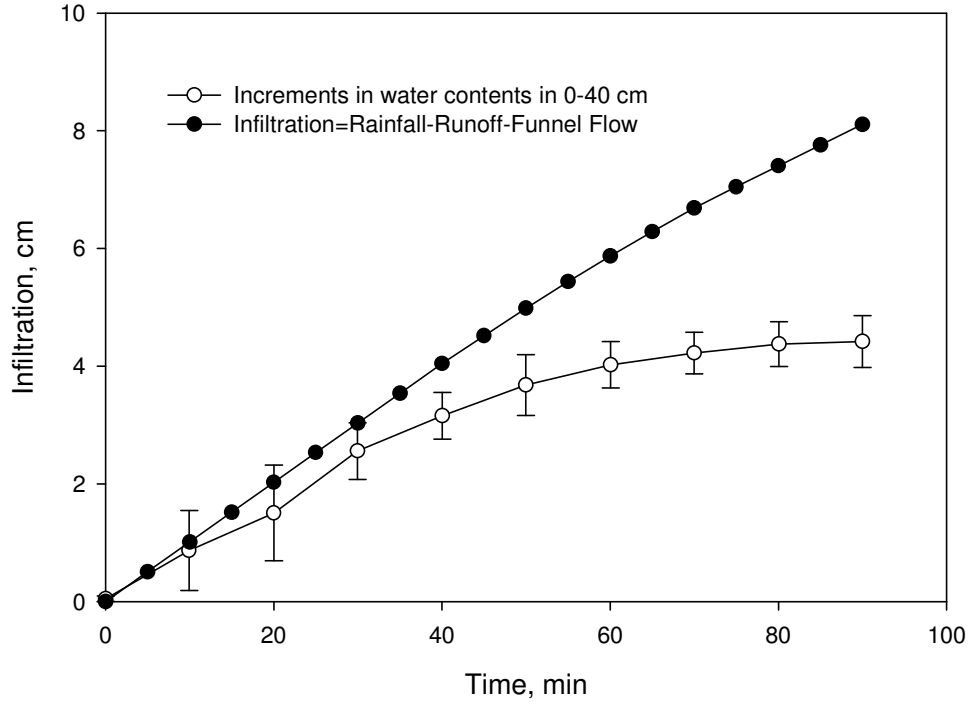

Figure 2.20 Total rain, total runoff at gutter, total runoff through funnels, and infiltration for vegetated clay loam (plot 2)

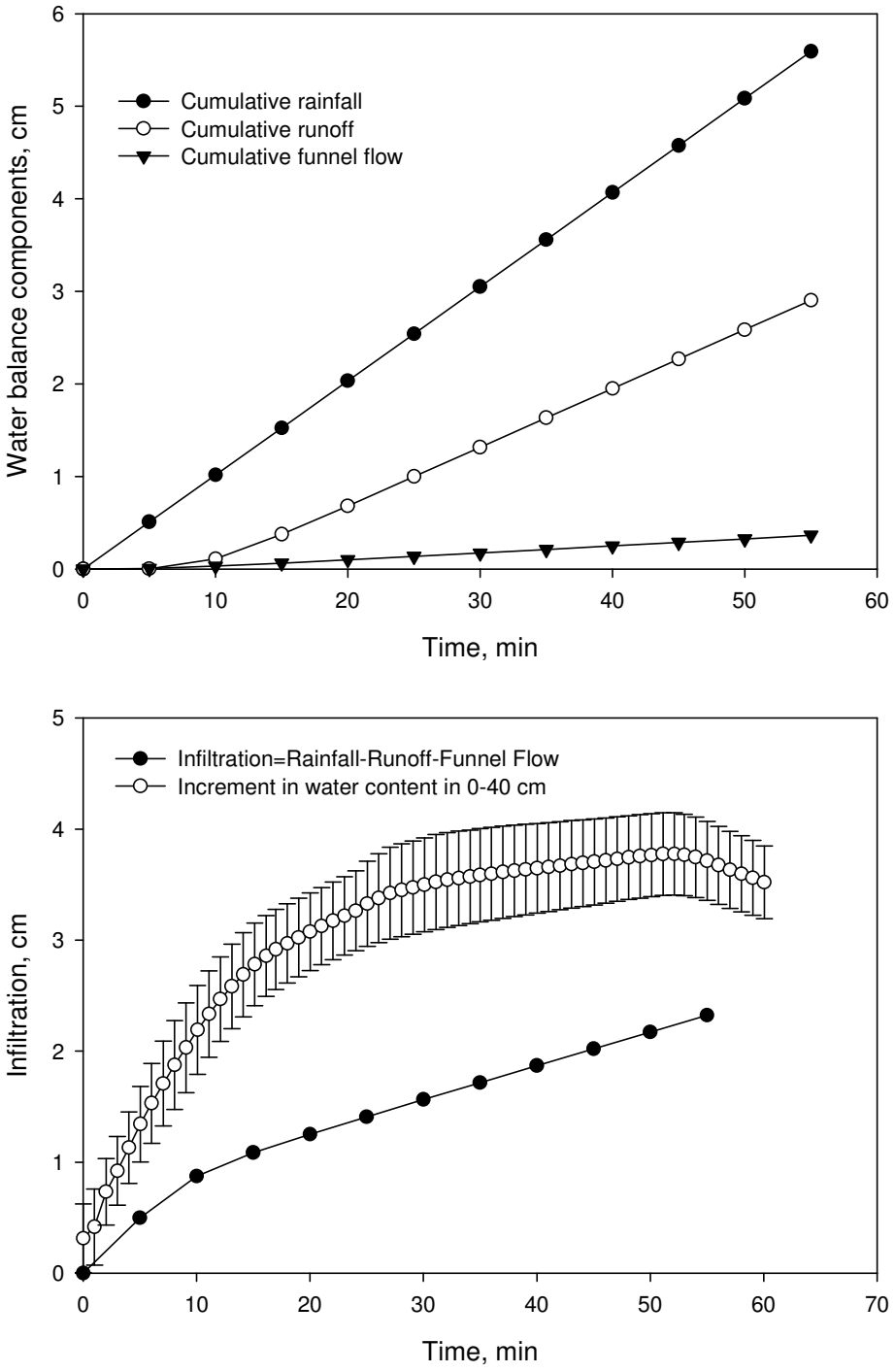

Figure2.21. Total rain, total runoff at gutter, total runoff through funnels, and infiltration for bare sandy loam (plot 3)

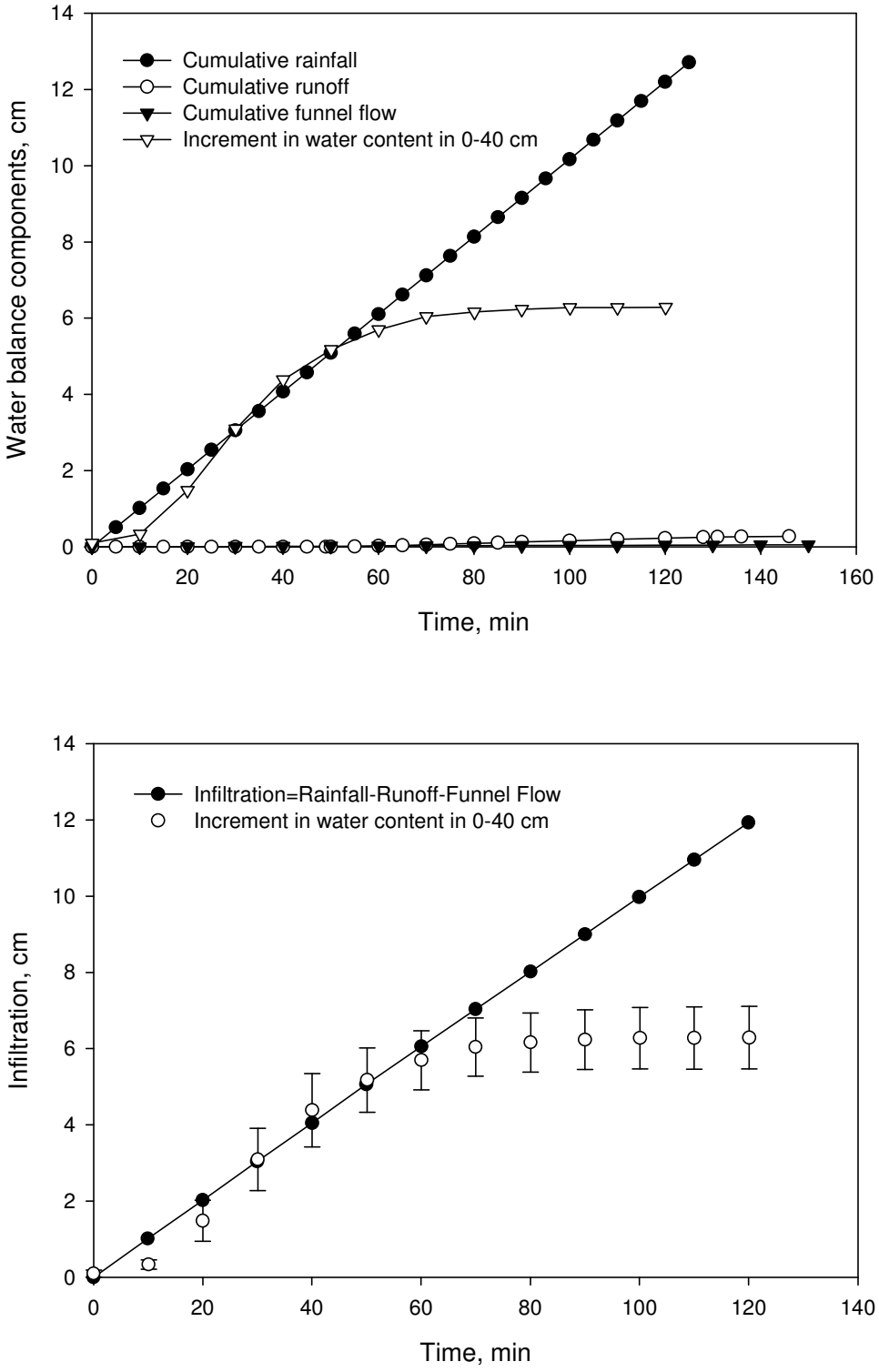

Figure 2.22. Total rain, total runoff at gutter, total runoff through funnels, and infiltration for vegetated sandy loam (plot 4)

Unlike the vegetated soil, bare soils initiated much earlier surface runoff and contributed more over land flow, thus indicating the significance of the vegetated filter strip in attenuation of the surface runoff. The results also showed that the soil profile was saturated after the first 40-60 minutes of simulation and the water contents remained relatively constant after a sharp rise during the first 40-60 minutes of simulation in the vegetated soil plots (Figures 2.20 and 2.22).

2.12. 2 Total Runoff of *E. coli* and *Salmonella cholerasuis* (Swine Manure Experiments)

The results of runoff rates for swine manure experiments are presented in Figure 2.23. The hydrographs indicate that in the bare clay loam (Plot 1), runoff maintained constant after a very sharp rise during the first eight minutes of the simulation. Both gutter and funnels verified the constant runoff rates after the first eight minutes of simulation. The hydrograph results for vegetated clay loam (Plot 2) in Figure 2.23 indicate that runoff started after forty minutes of simulation and after a sharp rise for the next ten minutes, it gradually increased until the rainfall simulator was turned off. Results indicated the effect of vegetation in attenuation of surface runoff.

On the bare sandy loam (Plot 3), the hydrograph results (Figure 2.23) indicate a sharp rise in runoff rate within the first 25 minutes of simulation and then a relatively constant rate until the end of the simulation. Surface channelization on this plot may have caused the early constant runoff through the funnels. The results also indicate that in the vegetated sandy loam, runoff initiation was delayed up to forty minutes followed by a sharp rise for the next ten minutes, and slightly increased for

the remaining of the rainfall simulation (Figure 2.23). It seems that vegetation coupled with a non-structured soil texture (sandy loam) retarded most of the runoff.

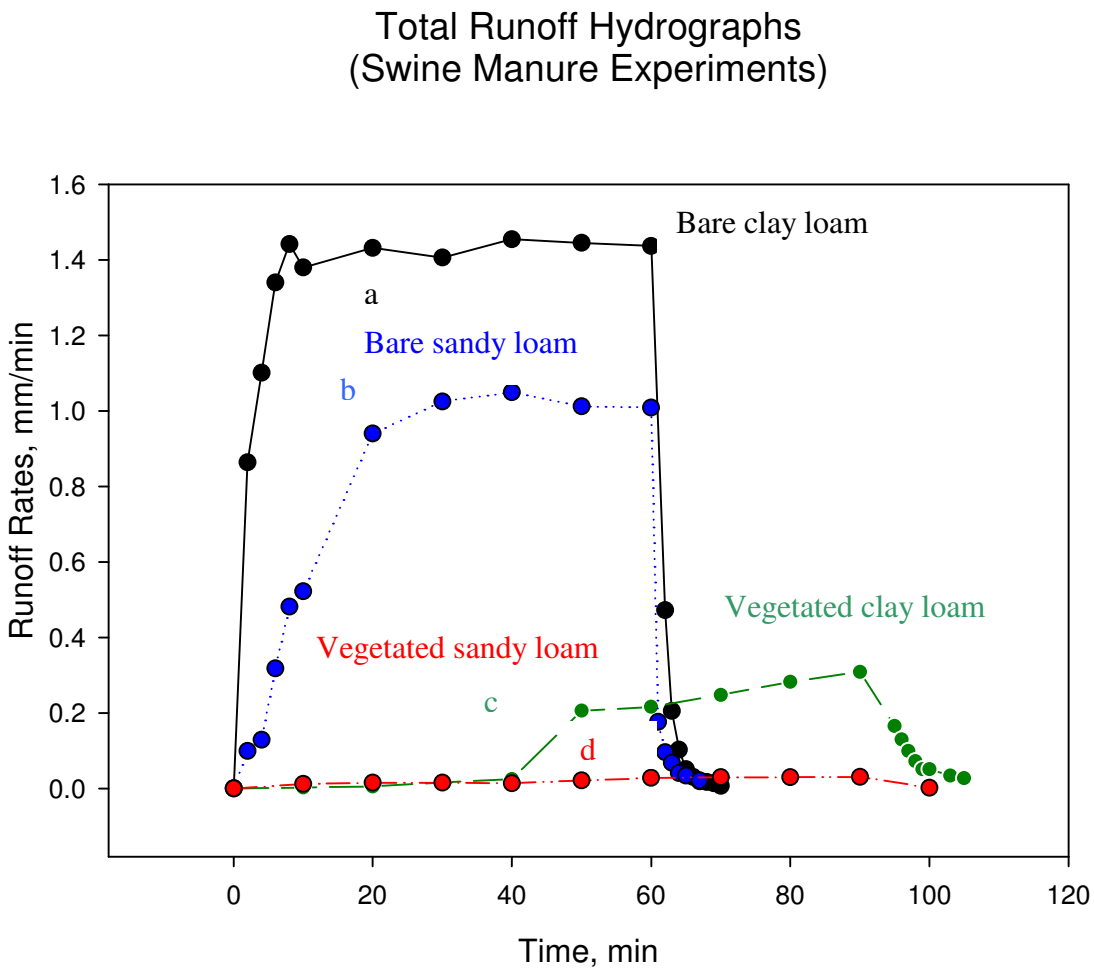

Figure 2.23. Total runoff hydrographs for swine manure experiments: (a) bare clay loam (plot1), (b) bare sandy loam (plot3), (c) vegetated clay loam (plot2), (d) vegetated sandy loam (plot4)

The average suction ahead of the wetting front S_{av} for both clay and sandy loams were calculated using Soil Water Characteristics Curves (Figure 2.24). These values were calculated based on Brooks and Corey (1964) and were 31 and 18 cm for clay and sandy loams, respectively (detailed calculation procedures are shown in Appendix E). These values were needed as the initial values to simulate infiltration using the Green and Ampt model and were later modified to best fit the measured infiltration.

2.12. 3. Bromide Concentrations in Bare Clay Loam (plot 1)

The purpose of using bromide as a tracer in this study was to find the similarity between its transport to that of the FC. The results of bromide concentrations (Figure 2.24) indicated that the bromide concentrations were very low after the first five minutes of simulation at 95 cm, 490 cm, and 600 cm distances from the ridge of the plot. The concentrations at 490 cm and 600 cm distances from the ridge of the plot stayed very low during the entire duration of the rainfall simulation. However, the concentration at a distance of 285 cm from the ridge of the plot appeared to be relatively high after the first five minutes of simulation, sharply dropped for the next fifteen minutes, and gradually decreased for the rest of the rainfall simulation. The possible reason for the high bromide concentration early in the simulation at 285 cm distance may have been attributed to the surface channelization. Figure 2.25 shows the topographic map of all subplots indicating the role of micro elevation and surface channelization in a non-uniform distribution of surface runoff. Results also show that the bromide concentration at a distance of 95 cm from the ridge also had a sharp drop after a sharp rise in the first ten minutes and

gradually decreased for the rest of the duration. The patterns of concentrations for bromide also indicated a two-stage exponential release rate with fast release rate from 10 to 20 minutes of simulation at 95 cm and from 5 to 20 minutes of simulation at 285 cm distances from the ridge of the plot followed by a slow release rate after 20 minutes of simulation in the bare clay loam (Figures 2.24).

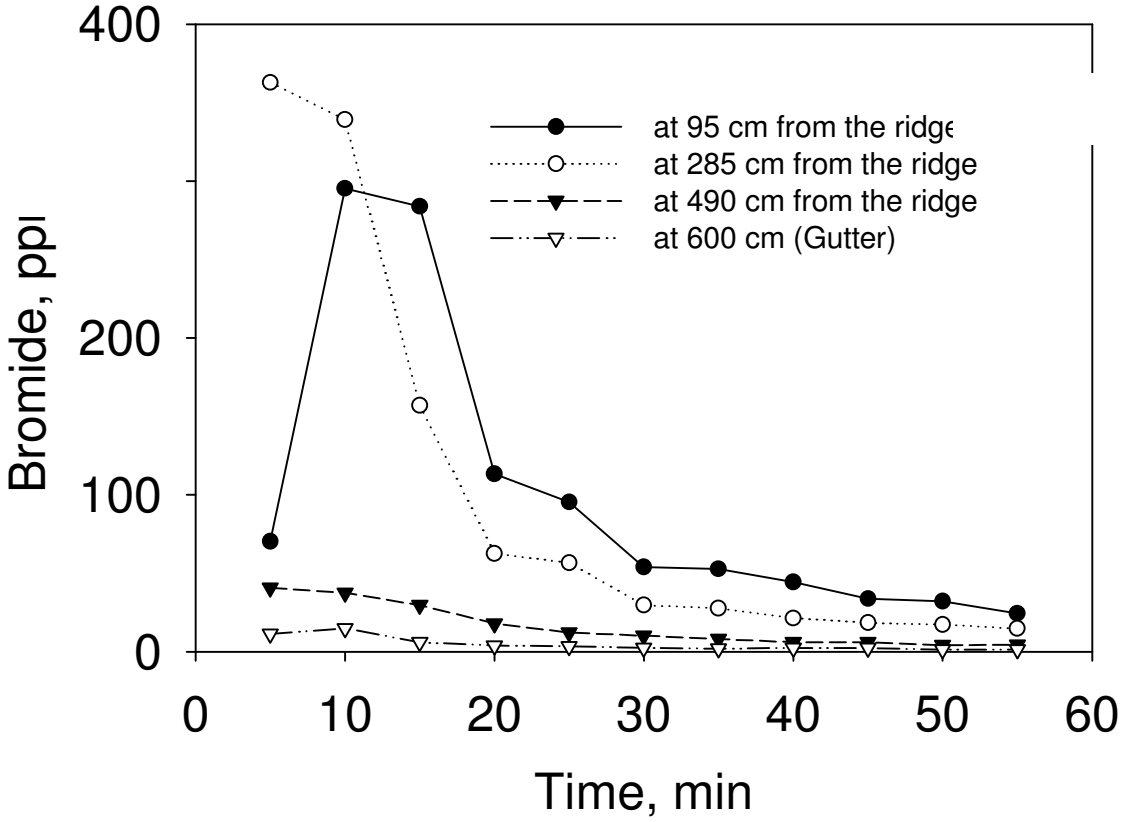

Figure 2.24. Bromide concentrations of surface runoff samples at the top row (95 cm), middle row (285 cm), bottom row (490 cm), and at the gutter (600 cm) from the ridge for bare clay loam (Plot 1)

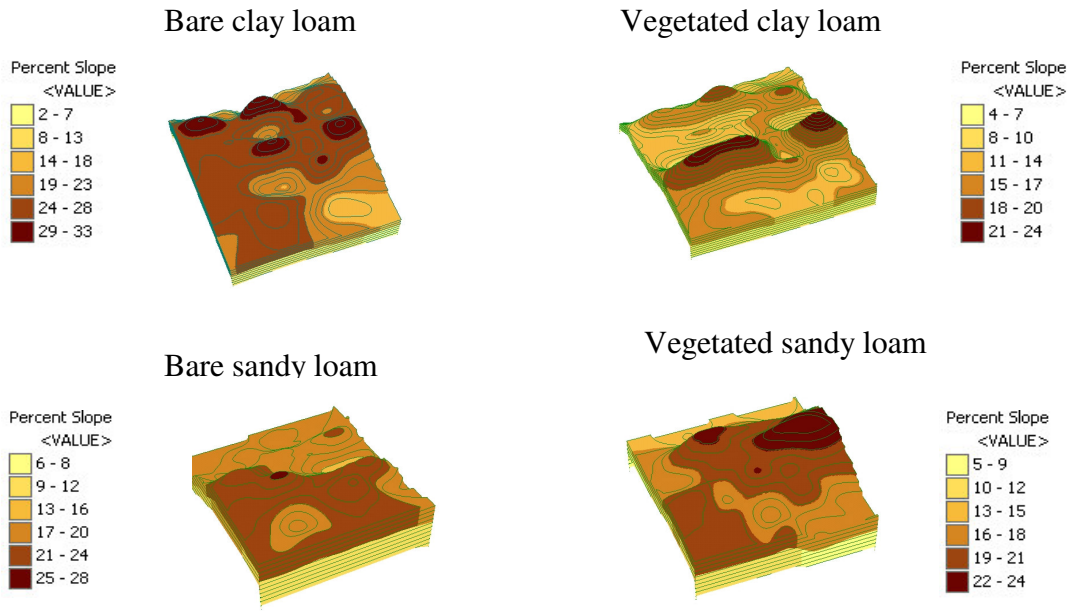

Figure 2.25. Topographic maps generated by ARCGIS indicating the surface channelization and micro crevices.

2.12.4. Bromide Concentrations for Vegetated Clay Loam (plot 2)

The results of bromide concentrations in runoff are presented in Figure 2.26. Results indicate that only at the 95 cm distance (top row) away from the ridge of the plot (near to the source), bromide concentrations decreased exponentially with respect to time after a relatively sharp rise within the first ten minutes of rainfall simulation. Runoff attenuation within the first forty minutes of rainfall simulation in vegetated clay loam (Figure 2.18) promoted vertical transport of bromide into the soil profile by the infiltrated water. Therefore, no bromide concentration was observed at 285, 490, and at 600 cm distances from the ridge of the plot (Figure 2.26).

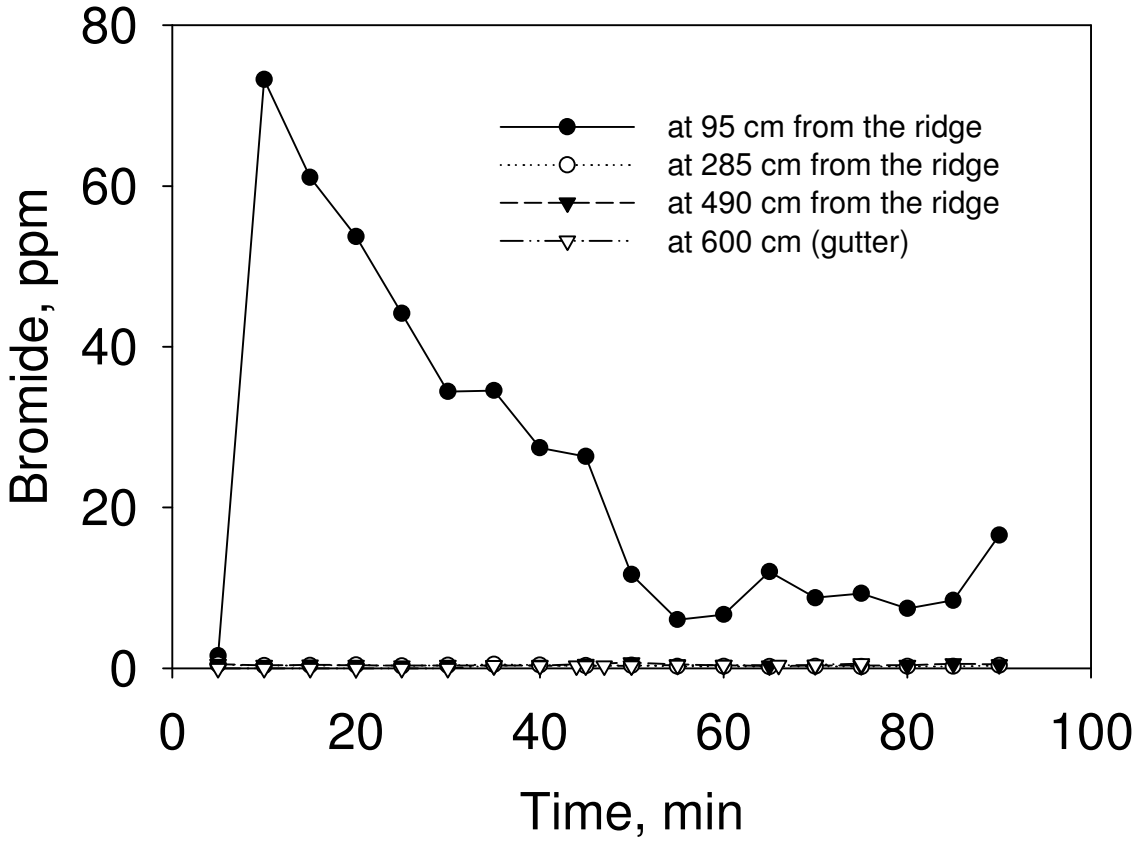

Figure 2.26 Bromide concentrations of runoff samples at the top row (95 cm), middle row (285 cm), bottom row (490 cm), and at the gutter (600 cm) distances from the ridge for the vegetated clay loam (Plot 2)

2.12. 5. Bromide Concentrations in Bare Sandy Loam (plot 3)

The results of bromide concentrations in runoff for bare sandy loam (plot 3) are presented in Figure 2.27. Results indicate that in the bare sandy loam plot, only at 95 cm distance from the application area did bromide concentrations exponentially decrease with respect to time. It seems that bromide concentrations had a slow release after a fast concentration release rate during the early minutes of simulation. Because sandy loam is a non-structured soil with high conductance (relatively high hydraulic

conductivity) capacity, more bromide infiltrated into the soil profile before reaching the gutter at 600 cm distance from the application area (Figure 2.27).

2.12.6. Bromide Concentrations in Vegetated Sandy Loam (plot 4)

The results of bromide concentrations in runoff for plot 4 are presented in Figure 2.28. Results indicate that only at the 95 cm distance from the application area did the bromide concentration exhibit a decreasing exponential release rate from the manure application area at the early simulation and maintained a relatively constant rate after 40 minutes of simulation. However, the results of runoff on the vegetated sandy loam (Figure 2.18) indicated that the runoff was attenuated for the first 60 minutes of rainfall simulation by the soil surface vegetation therefore, allowing bromide to transport vertically with the infiltrated water.

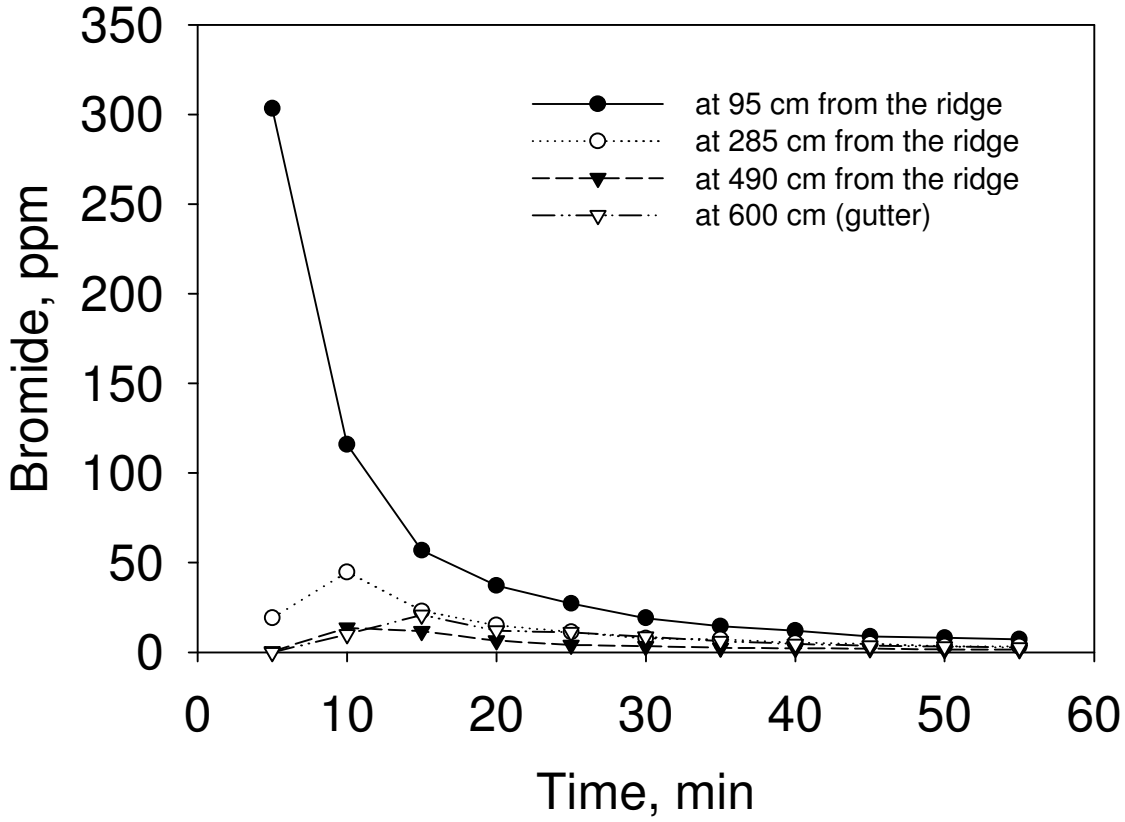

Figure 2.27. Bromide concentrations of runoff samples at the top row (95 cm), middle row (285 cm), bottom row (490 cm), and at the gutter (600 cm) distances from the ridge, bare sandy loam (plot 3)

It seemed that the combination of soil surface vegetation and the soil texture have substantially retarded the surface runoff (Figure 2.18); thus, bromide concentration in runoff substantially decreased in vegetated sandy loam by 95% at 95 cm distance from the ridge of the plot (from 120 to 5.5 ppm), and by 98% at 285 cm distance from the ridge (from 45 to 1 ppm) within the first ten minutes of rainfall simulation as they were compared to those of the bare sandy loam, plot3 (Figure 2.27).

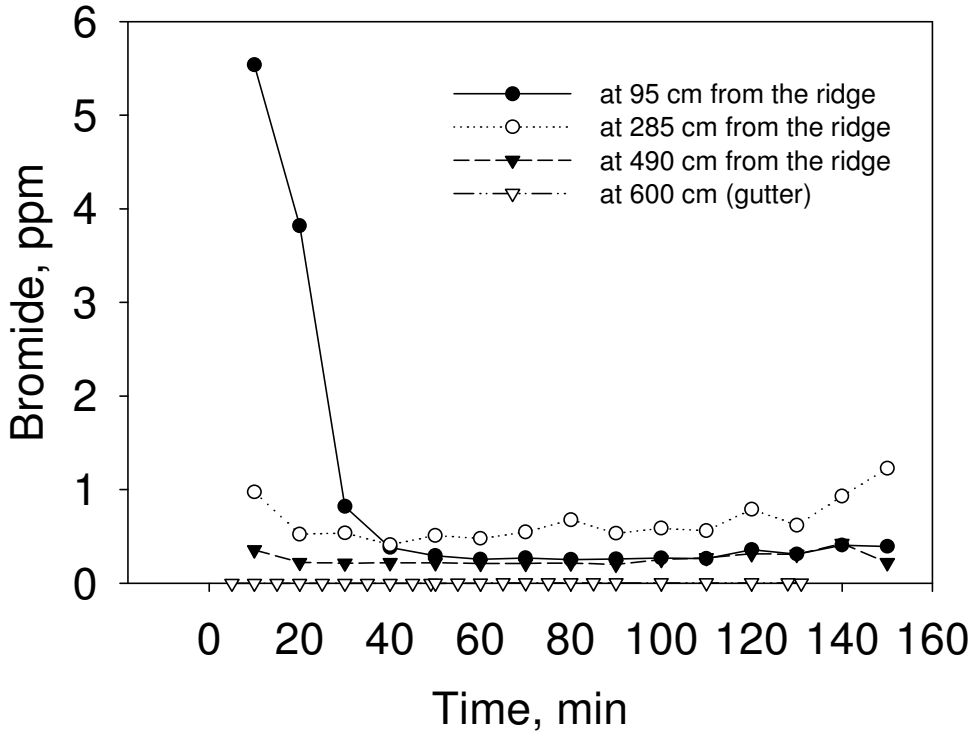

Figure 2.28. Bromide concentrations of runoff samples at the top row (95 cm), middle row (285 cm), bottom row (490 cm), and at the gutter (600 cm) distances from the ridge for vegetated sandy loam (plot 4)

2.12.7. FC Concentrations

The results of FC concentrations in surface runoff are shown in Figure 2.29. Concentrations of FC in runoff decreased with time at various distances from the source of manure application on both bare clay loam (Figure 2.29a) and bare sandy loam plots (Figure 2.29b). Because infiltration played a secondary role in the FC transport on bare surfaces, the decrease in FC concentrations with time reflects primarily the kinetics of FC release from the manure, while the rate of change in FC concentration with respect to distance reflects the dilution and possible settlement.

Maximum FC concentrations in runoff decreased with the distance from the source of manure application.

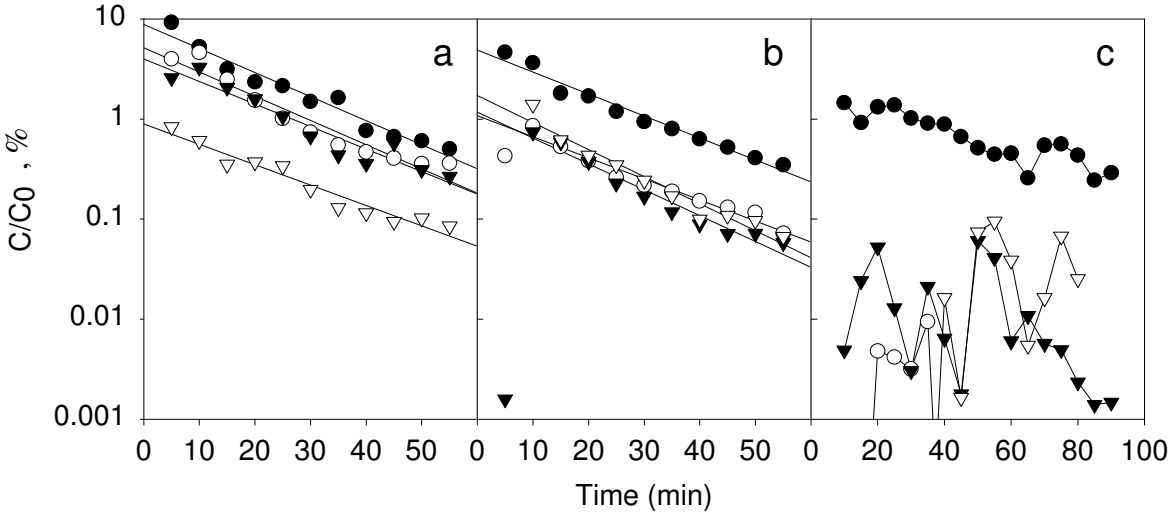

Figure 2.29. Relative concentrations of fecal coliform in runoff; a - bare clay loam, b - bare sandy loam, c - vegetated clay loam; ● - 95 cm, ○ - 285 cm, ▼- 490 cm,▽ - 600 cm from the ridge. Not enough surface runoff samples to process for FC concentration in the vegetated sandy loam.

A comparison of Figures 2.29a and 2.29b showed that the pattern of decrease was affected by soil texture. On the bare clay loam plot, concentrations of FC at 95, 285, and 485 cm distances from the edge of the manure application area were similar and substantially higher than the FC concentration at 600 cm distance. On the contrary, for the bare sandy loam plot, FC concentrations were similar at 285, 485, and 600 cm distances from the top edge of the manure application area, and less than the concentrations at a distance of 95 cm.

Unlike the bare soil, vegetated soil surfaces created a much less uniform FC transport pattern due to the channelization effect of vegetation (Figure 2.29c). Only at the 95 cm distance from the top edge of the manure application area, did the FC

concentration show a steady decrease with respect to time. Infiltration and drainage can transport large amounts of enteric pathogens from manure (Evans and Owens, 1972), thus reducing their availability on the soil surface. Vegetation changed transport patterns and levels of FC concentrations much more significantly than soil texture (Figures 2.30a,b and 2.31a,b). Results indicated that vegetation significantly attenuated the surface transport of FC in both clay and sandy loam plots (Figures 2.30 and 2.31). Results also indicated that the combined effect of vegetation (grass filters) and coarse soil texture on FC transport was the highest (Figures 2.30b and 2.31b). Such a significant FC attenuation effect could be attributed to the fact that vegetated filters retard the flow and promote infiltration, especially in coarse textured sandy loam soil. Also, vegetation retards the runoff and causes settlement of particulates and particulate bound constituents such as FC.

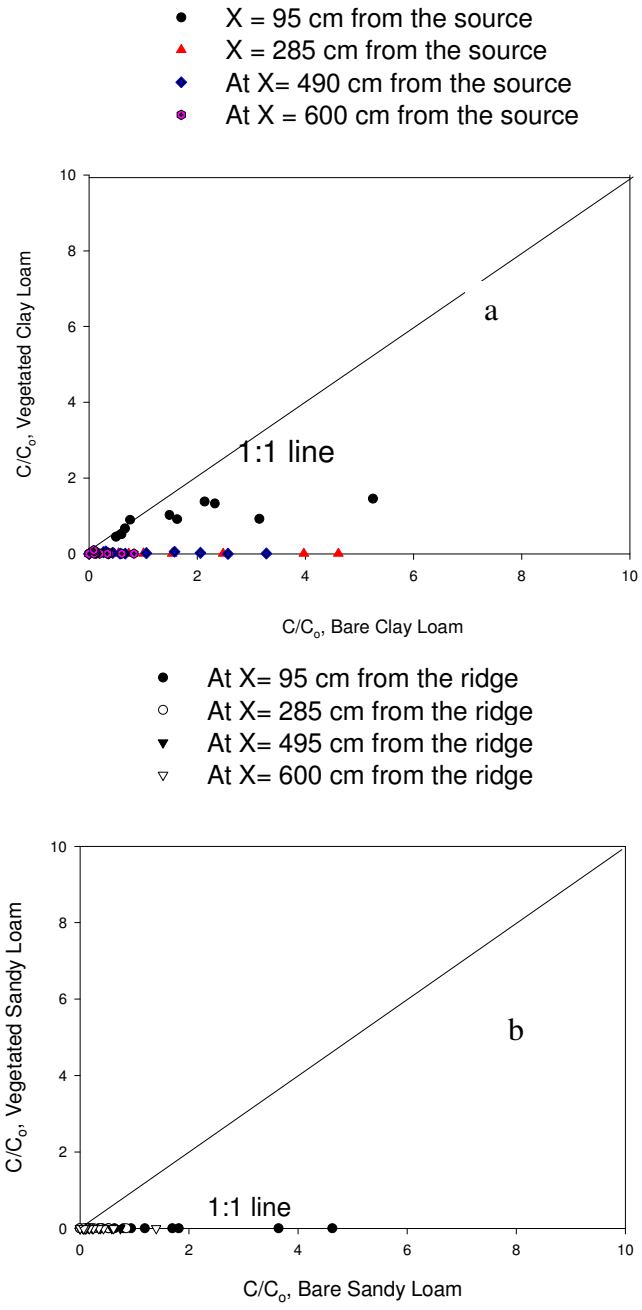

Figure 2.30. Comparison of the relative concentrations of FC between bare and vegetated plots (effects of soil surface condition)

Comparison of FC Concentration Ratios(C/C0) in Runoff (Effect of Soil Texture)

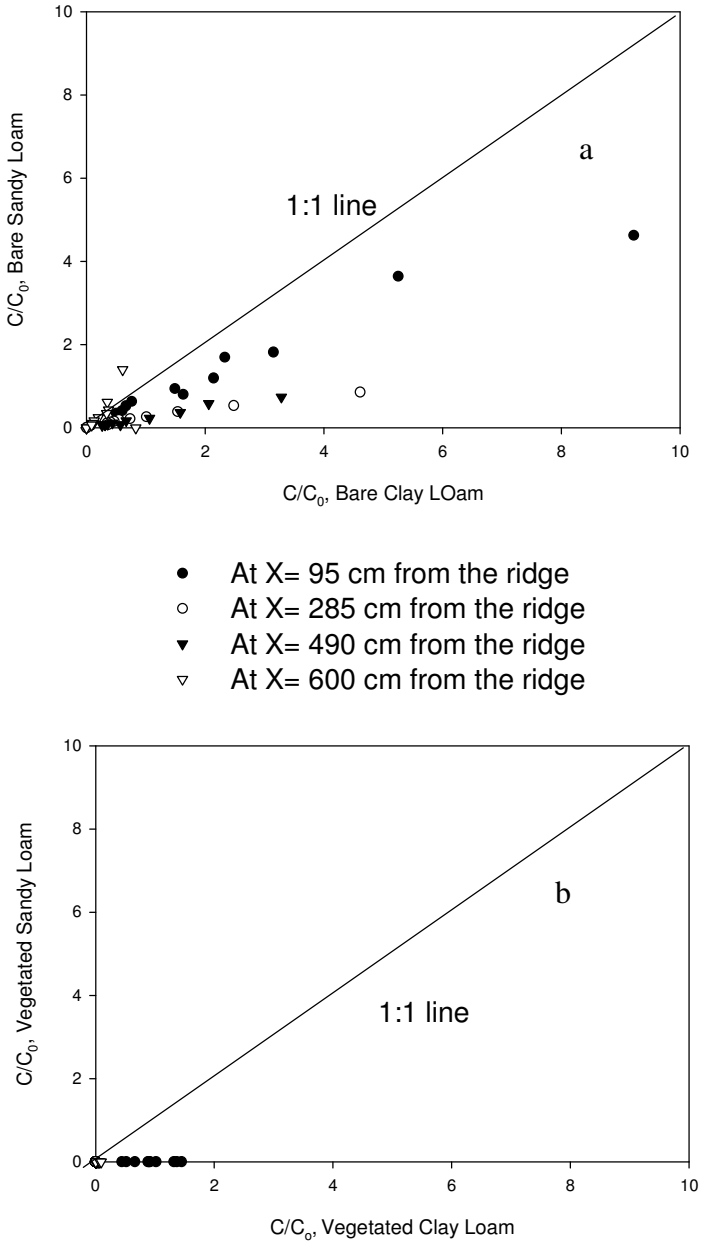

Figure 2.31. Comparison of the relative concentrations of FC between the two bare and the two vegetated plots (effects of soil texture)

FC levels in soil decreased with soil depth in all plots regardless of the soil texture and surface cover (Figure 2.32). The exponential decrease with depth at 95 cm distance from the ridge was similar to what was observed by Fleming et al. (1990). At longer distances, FC concentrations decreased faster in the top layer of the soil profile and exhibited a much slower decrease in the bottom layers of the soil profile. FC moved to a deeper depth in the soil profile on vegetated sandy loam soil (Figure 2.32c) than in the vegetated clay loam soil (Figure 2.32a). Soil texture seemed to play an important role for vertical transport of FC. Vegetation promoted vertical FC transport close to the source, but did not seem to have much effect at distances away from the source of manure application. This may be due to the fact that very little FC was transported far away from the source via surface runoff (Figure 2.29c). The same FC contents were also found at a 30 cm depth in the vegetated sandy loam soil (Figure 2.32c) and at a 10 cm depth in the vegetated clay loam soil (Figure 2.32a) from the samples taken at a 95 cm distance from the line of manure application. No significant FC contents were found at larger distances from the source of application in the vegetated sandy loam; because of grater infiltration most of the FC was transported vertically at the top of the plot near the manure application area.

The average pH and the average soil organic matter were found to be 5.85 $\pm$ 0.6 and 2.73 for clay loam, 6.16$\pm$ 0.33, and 1.72 for sandy loam, respectively. The results of pH and % organic matter indicated no critical condition for bioactivity within the soil profile.

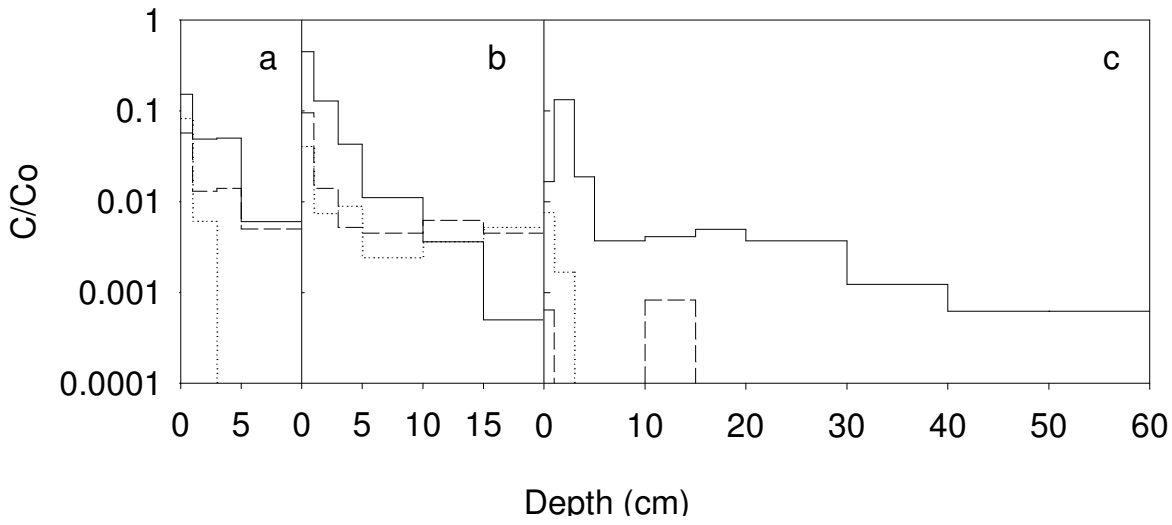

Figure 2.32. Relative contents of fecal coliform in soil; a - vegetated clay loam, b - bare sandy loam, c - vegetated sandy loam; _____ - 95 cm, - - - - 285 cm, ……. - 490 cm from the ridge. Data for bare clay loam are not shown because fecal coliform was not detected below the top cm.

The results of bromide concentrations from the bare sandy loam showed that water movement was very smooth with less disturbance (Figure 2.33). Results of bromide concentration on vegetated sandy loam (Figure 2.34) indicated that bromide was completely flushed out and infiltrated into the soil profile at the manure application area. Very small concentrations were measured in the soil profiles at the 95 cm distance from the top edge of the manure application area. These results reflected the significant effects of the non-structured sandy loam soil as it was coupled with the soil surface vegetation to attenuate the surface runoff and promote infiltration.

FC and Br concentrations for bare clay loam, vegetated clay loam, and bare sandy loam were also compared and presented in Figures 2.35-2.37. The results indicated that on both bare plots, FC and Br had very similar transport patterns at

distances of 95, 285, 490, and 600 cm from the edge of the manure application area. The slight difference in concentration of FC may have been due to the attachment to the soil particles.

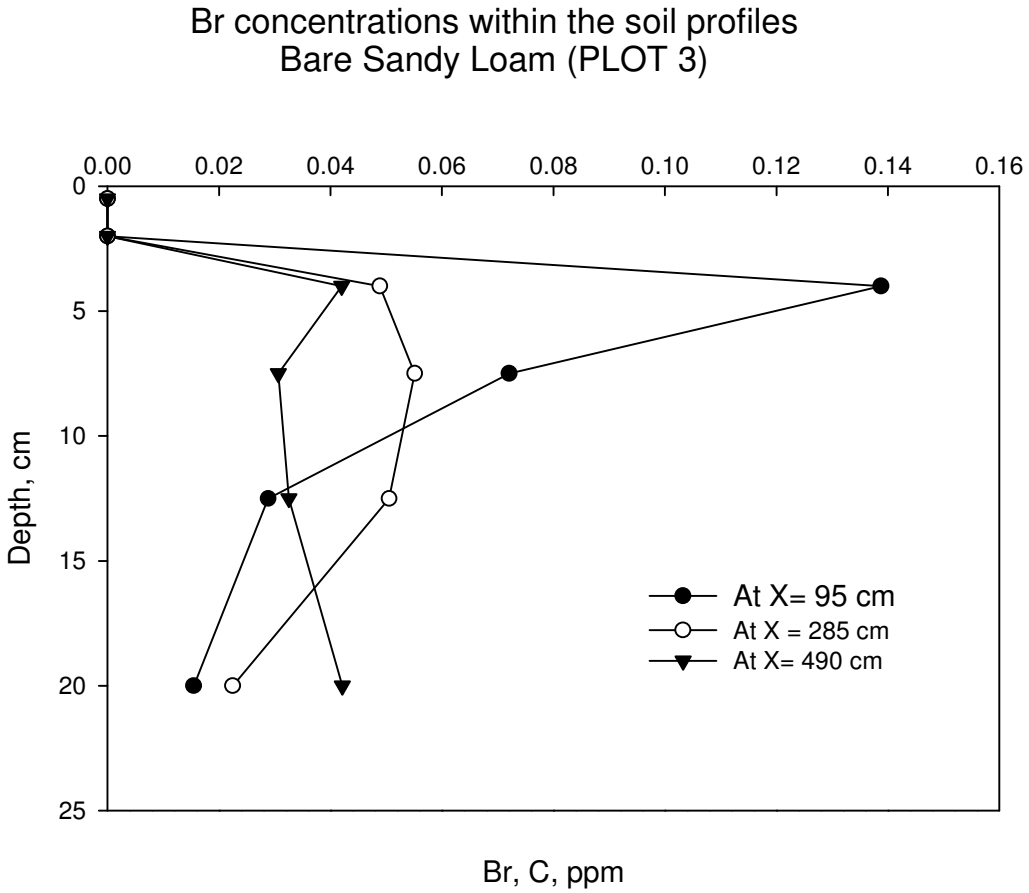

Figure 2.33. Concentrations of bromide after 24 hours in the soil profile at distances of 95, 285, and 490 cm from the ridge of the plot in the bare sandy loam (plot 3)

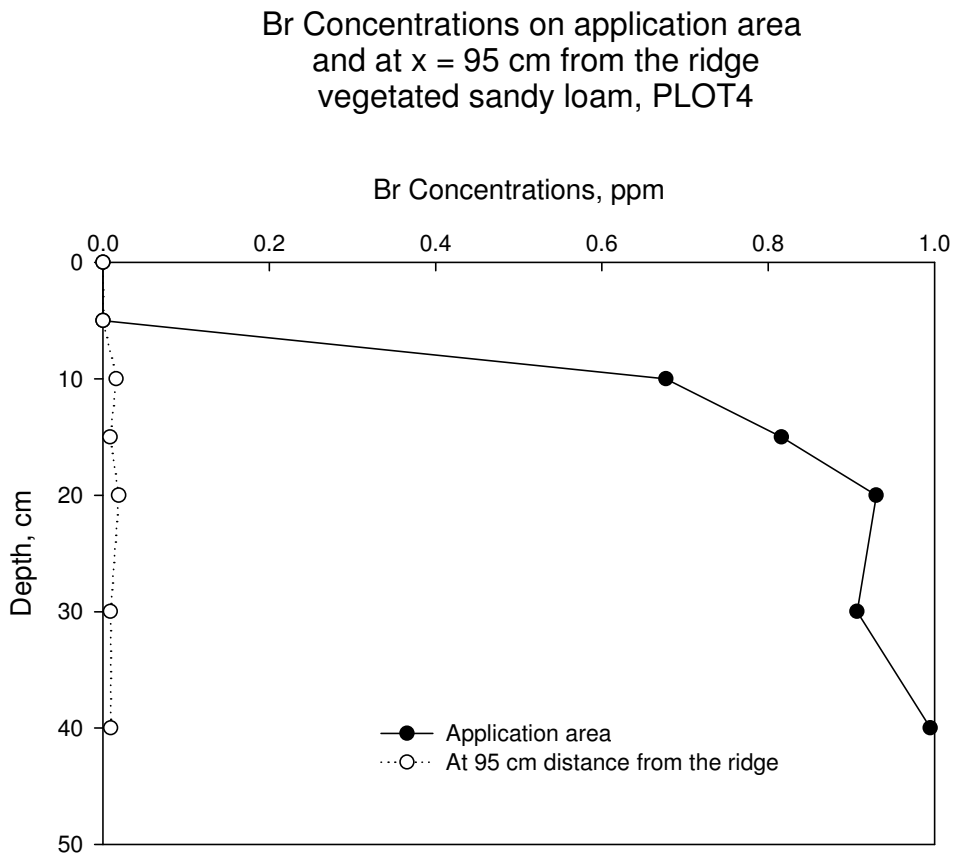

Figure 2.34 Concentrations of bromide within the soil profile in the vegetated sandy loam (plot 4) at the application area and at 95 cm distance from the ridge

Results also indicated that water movement on the bare sandy loam was slower in comparison to that of the bare clay loam (Figure 2.35 and 2.37). Therefore, FC and Br behaved more similarly in the bare sandy loam than in the bare clay loam. Contrary to the bare plots, only bromide maintained a unique transport pattern at different distances from the application area in the vegetated clay loam (Figure 2.36). Further indication of results in Figure 2.36 showed the complete distortion in the FC transport pattern by the soil surface vegetation, thus indicating the significance of VFS in attenuation of surface transport of FC.

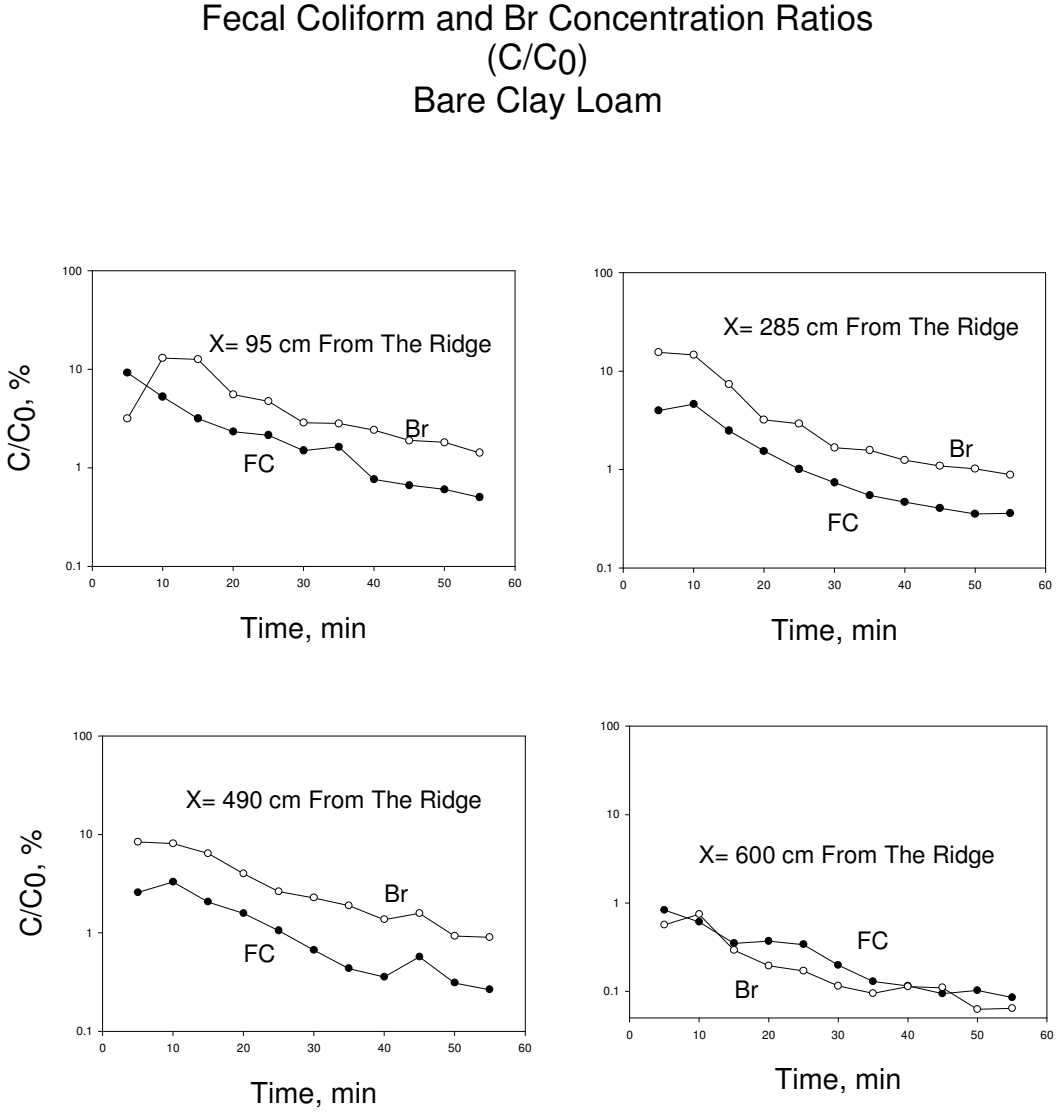

Figure 2.35. Fecal coliform and bromide concentrations in runoff, bare clay loam (plot 1)

Fecal Coliform and Br Concentration Ratios
(C/C_0)
Vegetated Clay Loam

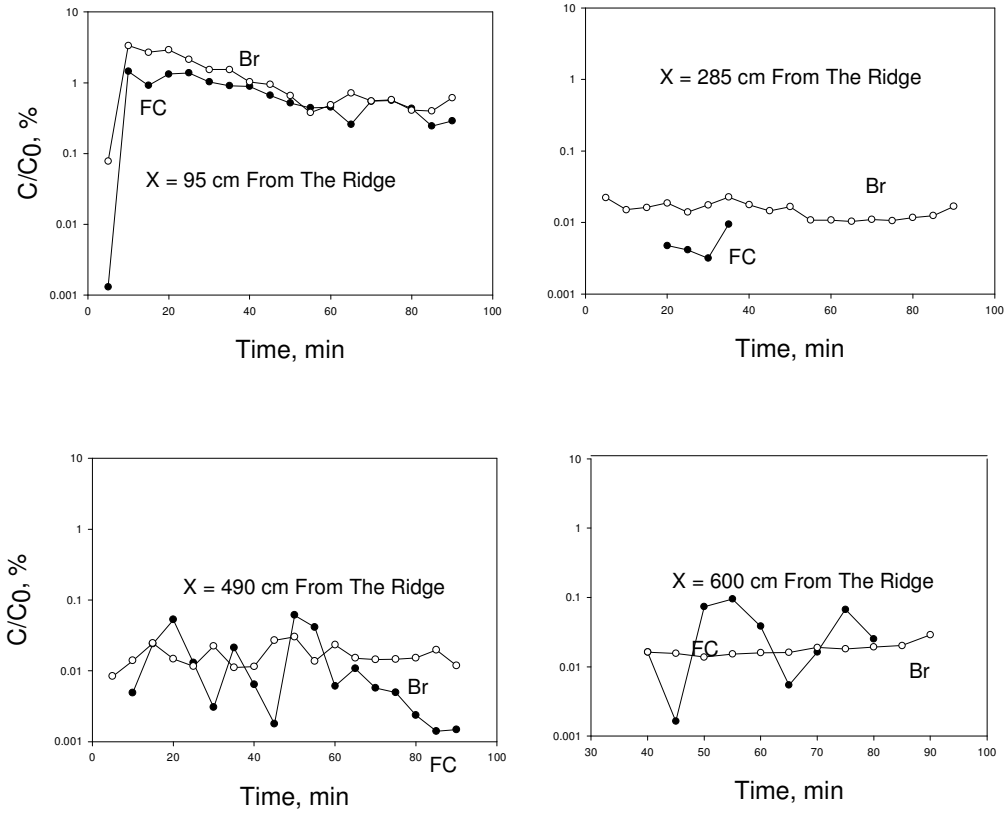

Figure 2.36. Fecal coliform and bromide concentrations in runoff, vegetated clay loam (plot 2)

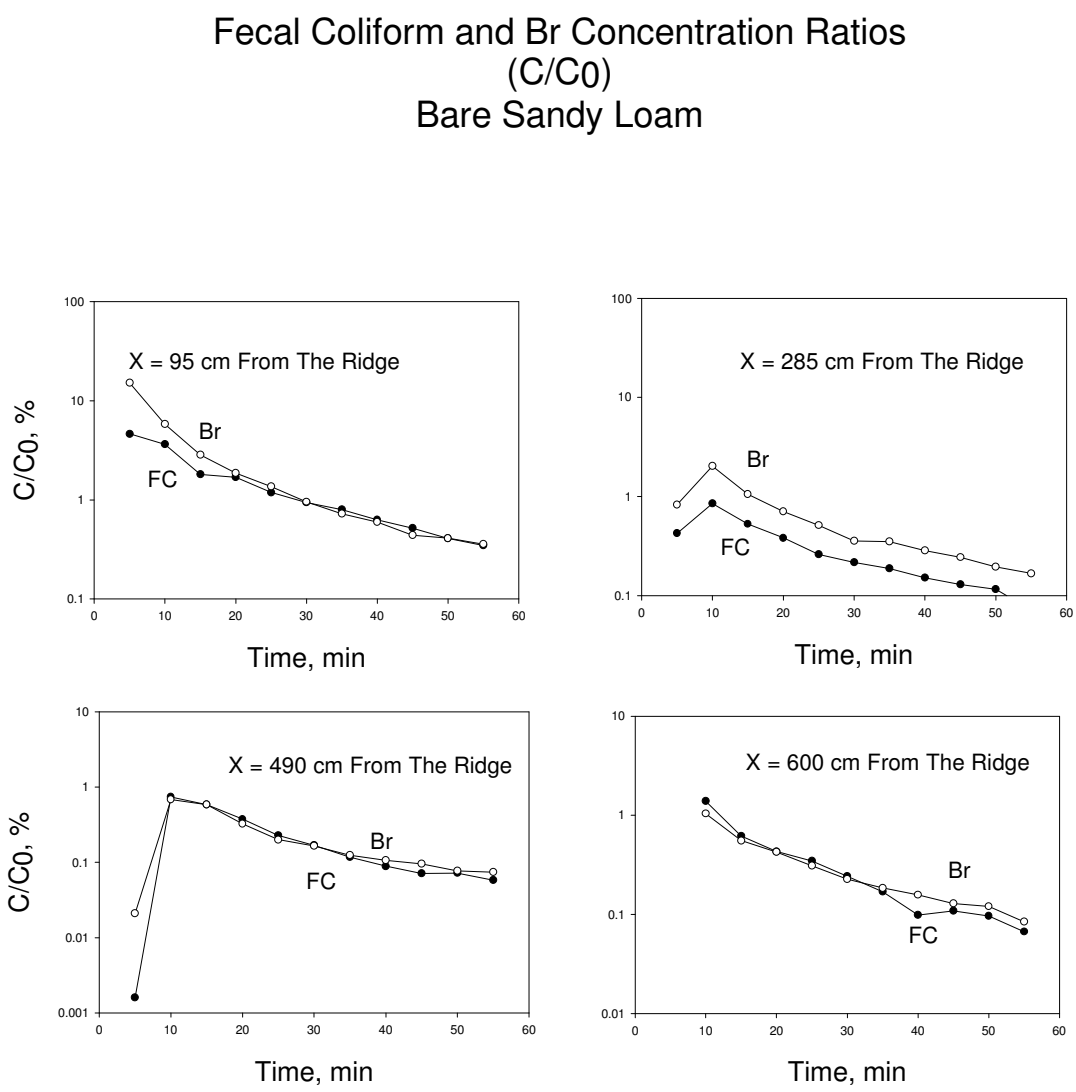

Figure 2.37. Fecal coliform and bromide concentrations in runoff, bare sandy loam (plot 3)

FC and bromide concentrations with regression equations, R^2 and r values for both bare clay loam and bare sandy loam are presented in Figure 2.38. The regression results indicated a high correlation between FC and Br and relatively similar transport patterns at 95, 285, 490, and 600 cm distances from the edge of the plot in both bare soils (Figure 2.38).

Accounting for a 25% of loss in FC population due to the adsorption of FC on the soil particles during the laboratory sampling procedures (refer to Section 2.4.2.4.9), results may be modified thus, a much clearer picture of the FC-Br transport pattern relationship on a one to one scale plot could be depicted (Figure 2.38). The similarity between the transport pattern of FC and Br concentrations provide relatively enough information for the future water budget problems and indicate the use of bromide as a tracer indicator to study fecal contamination of water bodies.

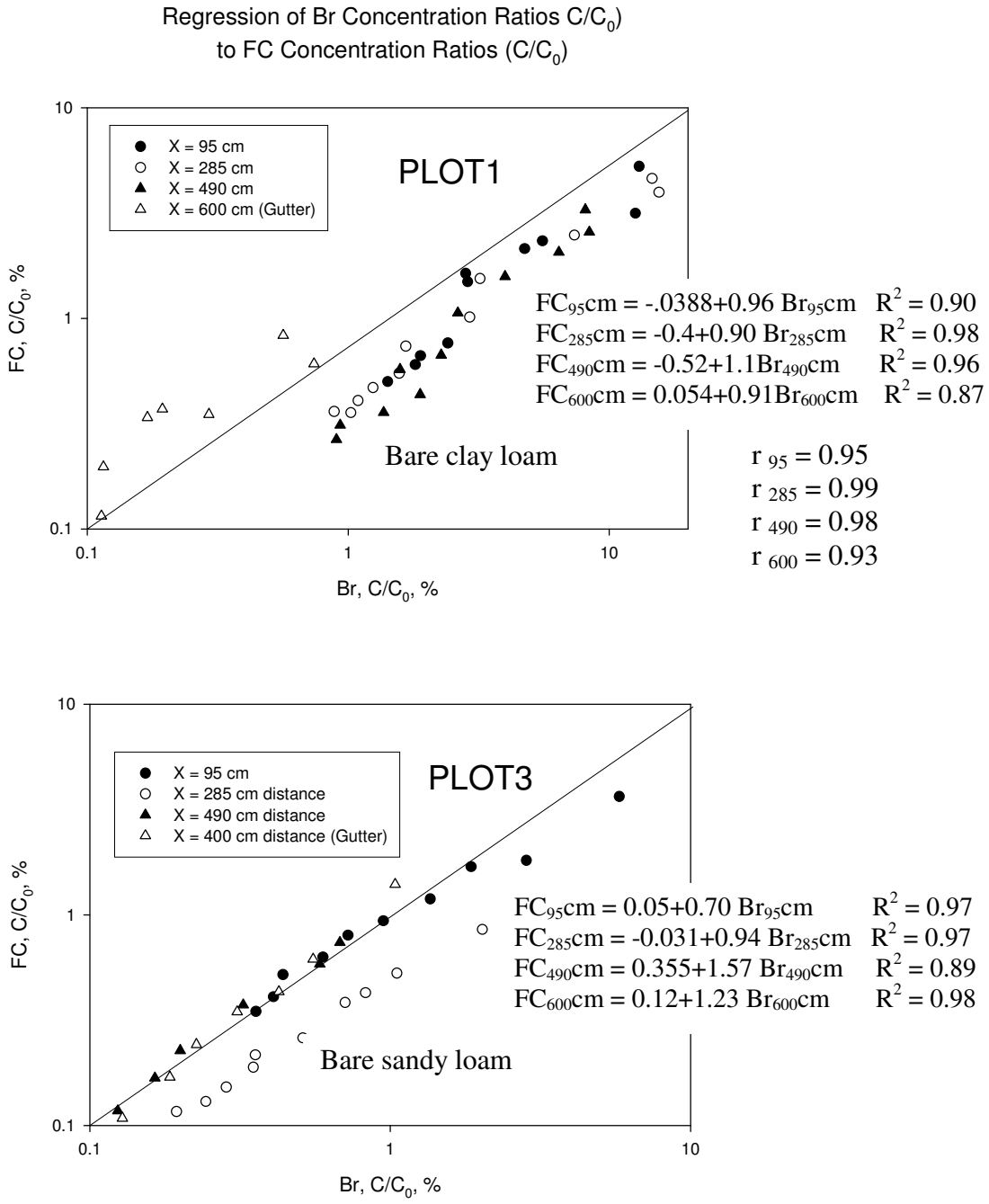

Figure 2.38. One to one base relationship between FC and Br

2.12.8. *E. coli* and *Salmonella cholerasuis* Concentrations

The results of *E.coli* concentrations in runoff from swine manure experiments are presented in Figures 2.39-2.42. Results indicate that *E.coli* and *Salmonella cholerasuis* behaved very similar in the bare soils (Figures 2.39, 2.40a, and 2.41). Results also showed that *E.coli* and *Salmonella cholerasuis* had relatively similar transport characteristics with exponential release rates (Figures 2.39 and 2.41). Results further indicated that both *E.coli* and *Salmonella cholerasuis* had fast release rates in the first ten minutes of the simulation and a slow release trend until the end of the simulation. Contrary to the bare soil plots, there was no significant difference in *E.coli* and *Salmonella cholerasuis* transport on the vegetated plots (Figures 2.40b and 2.42). Results of E.coli concentrations on both vegetated plots clearly exhibited the complete distortion of the flow pattern by the vegetated surface (Figure 2.40b and 2.42). However, vegetated clay loam seemed to adsorb more organisms (Figure 2.40b) than the vegetated sandy loam (Figure 2.42). This indicates that both *E.coli* and *Salmonella cholerasuis* had a higher tendency to attach to the clay particles than to the sand particles.

Results further showed that no significant concentrations of either organisms were recovered even at a distance of 95 cm from the manure application area in the vegetated plots (Figures 2.40b and 2.42). Results indicated that at 285 cm distance from the manure application area no *E.coli* was detected while at a further distance (at 490 cm distance), *E.coli* concentration has reached to a peak after 30 minutes of simulation. Possible cause may have been attributed to the surface channelization that has diverted the surface runoff from entering the funnels at 285 cm distance (Fig.

2.42). These results clearly reflect the significance of vegetated filter strips in attenuating the surface transport of microorganisms.

Due to the local difficulties of counting *Salmonella cholerasuis* in the samples collected from the vegetated plots, other laboratory methods were also employed. The results of Enterotubes showed no change in color in the glucose compartments, indicating that the organism was not a member of the Enterobacteriaceae and was not counted as *Salmonella cholerasuis* bacteria. Therefore, most organisms in the plates for vegetated plots were not considered as *Salmonella cholerasuis*. Culture samples of *E.coli* and *Salmonella cholerasuis* with random samples of each from runoff were also examined at 400 X with a Zeiss Axioskop epifluorescence microscope, equipped with a fluorescein isothiocyanate and Texas red dual wavelength filter. The results of this experiment and other physiological characteristic tests also indicated that those colonies were not *Salmonella cholerasuis*. However, based on the results of the bare soils and the laboratory experiments, it was then concluded that both *Salmonella cholerasuis* and *E.coli* had very similar release rates and transport pattern in all plots. Because *E.coli* and *Salmonella cholerasuis* have the same morphology, the final conclusion is that the transport dynamics of *E.coli* and *Salmonella cholerasuis* are expected to be similar.

Regression results of *Salmonella cholerasuis* vs. *E.coli* on both bare plots indicated a high correlation between *E.coli* and *Salmonella cholerasuis* (Figures 2.43 and 2.45). The one to one relationship with an R^2 value of 0.99 is indicative of similar transport patterns of *E.coli* and *Salmonella cholerasuis* (Figures 2.43, and 2.45). Results also indicated that *E.coli* concentrations were significantly different on

vegetated sandy loam and vegetated clay loam as they were compared to those of the bare sandy loam and the bare clay loam (Figures 2.44 and 2.46). Very low values of R^2 were obtained when *E.coli* concentrations in both vegetated soils were plotted against the *E.coli* concentrations in the bare soils (Figures 2.44 and 2.46). Results showed much lower concentrations of *E.coli* in the vegetated clay loam than in the bare clay loam when they were plotted on a one-to- one base scale (Figure 2.46). This again indicated the significance of VFS in both attenuation and distortion of surface flow transport patterns.

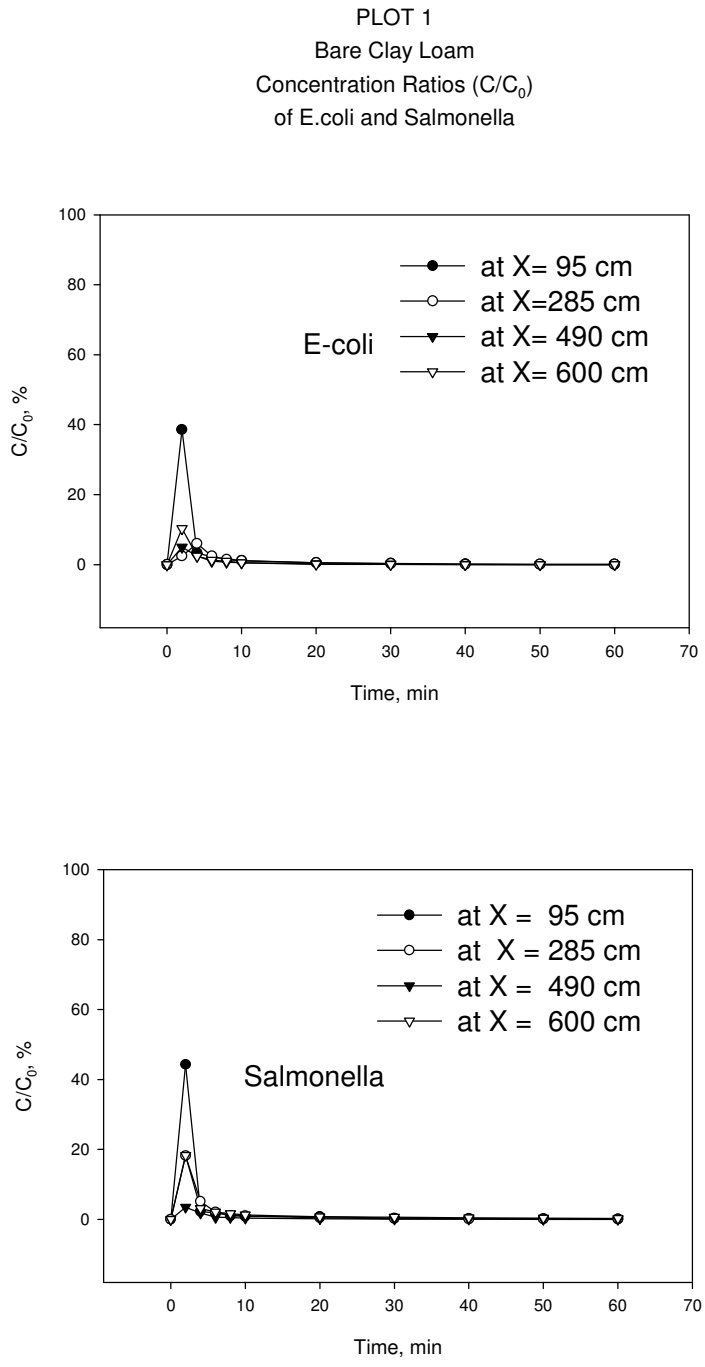

Figure 2.39. Relative concentration ratios of *E.coli* and *Salmonella cholerasuis* in runoff in the bare clay loam (plot 1)

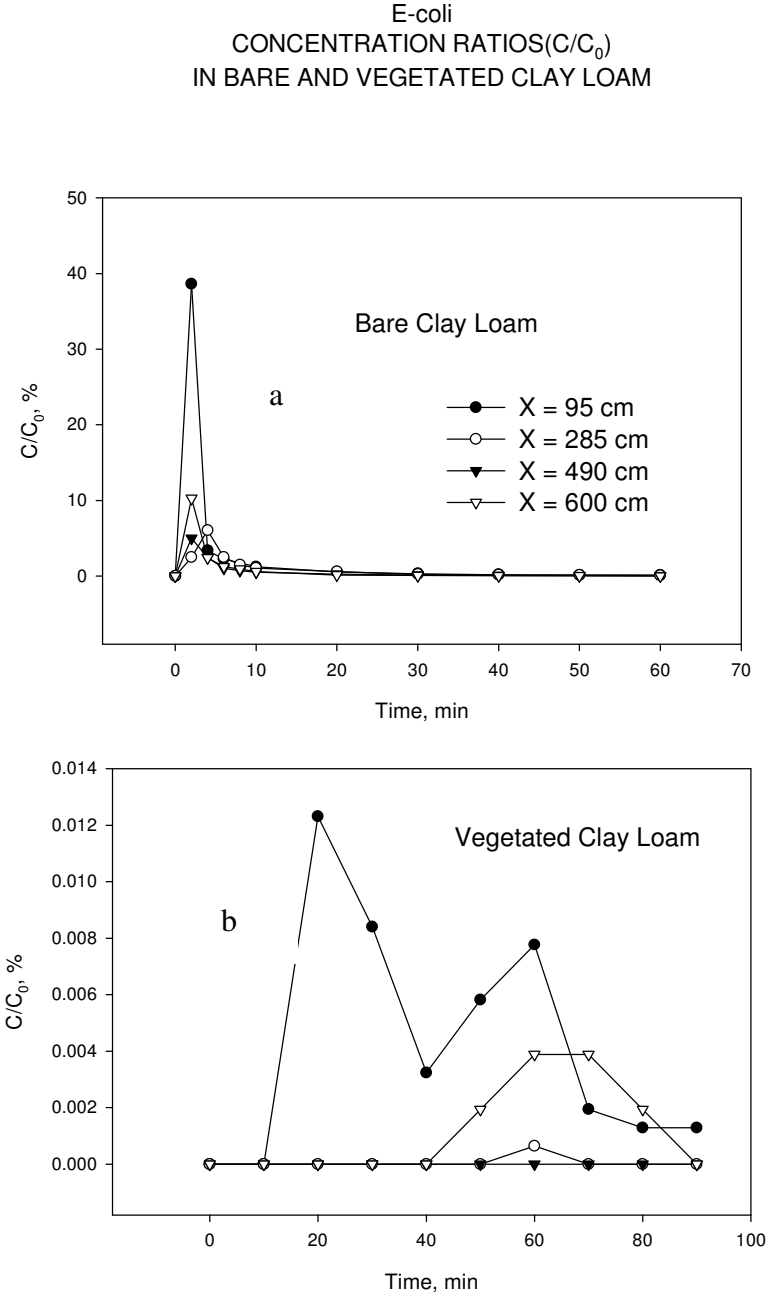

Figure 2.40. Relative concentration ratios in runoff of *E.coli* in the bare and vegetated clay loam (plots 1, and 2)

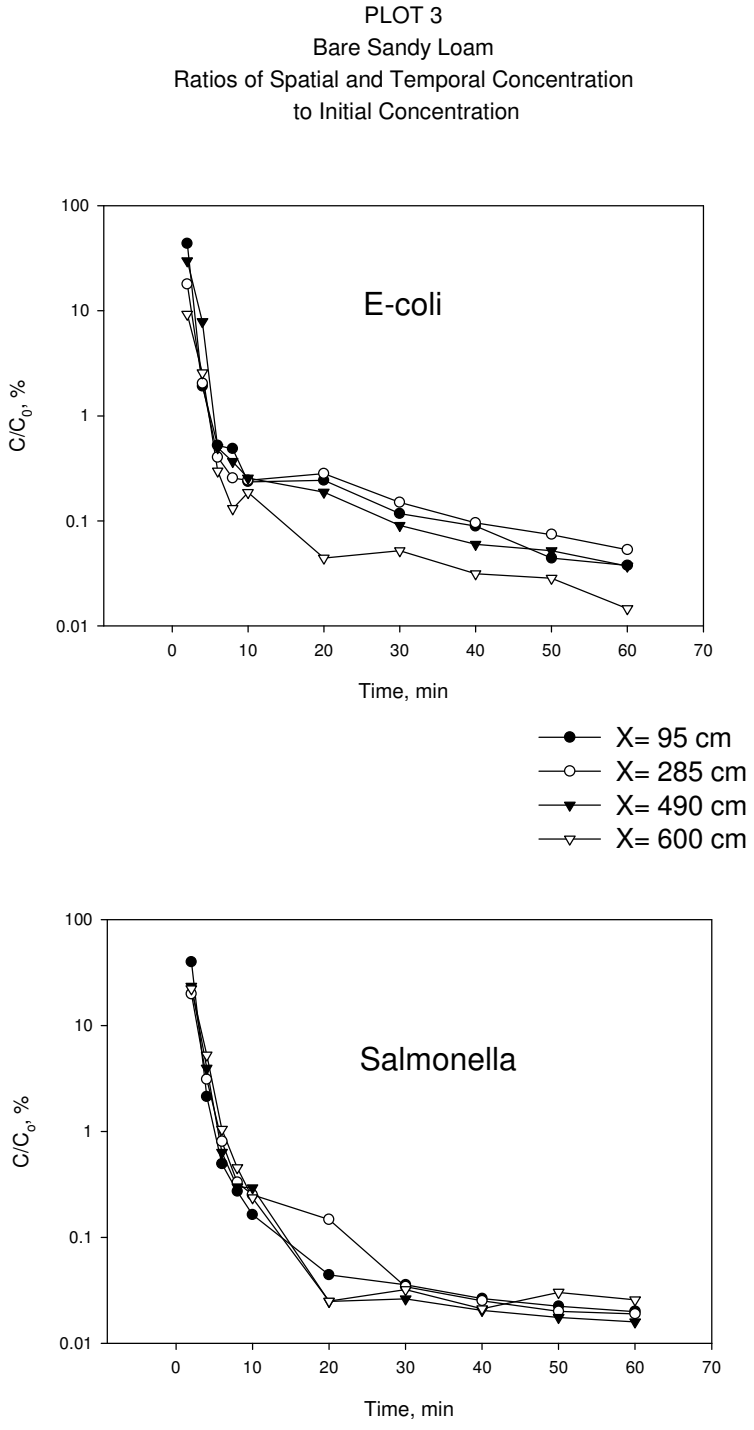

Figure 2.41. Relative concentration ratios of *E.coli and Salmonella cholerasuis* in the bare and sandy loam (plot 3)

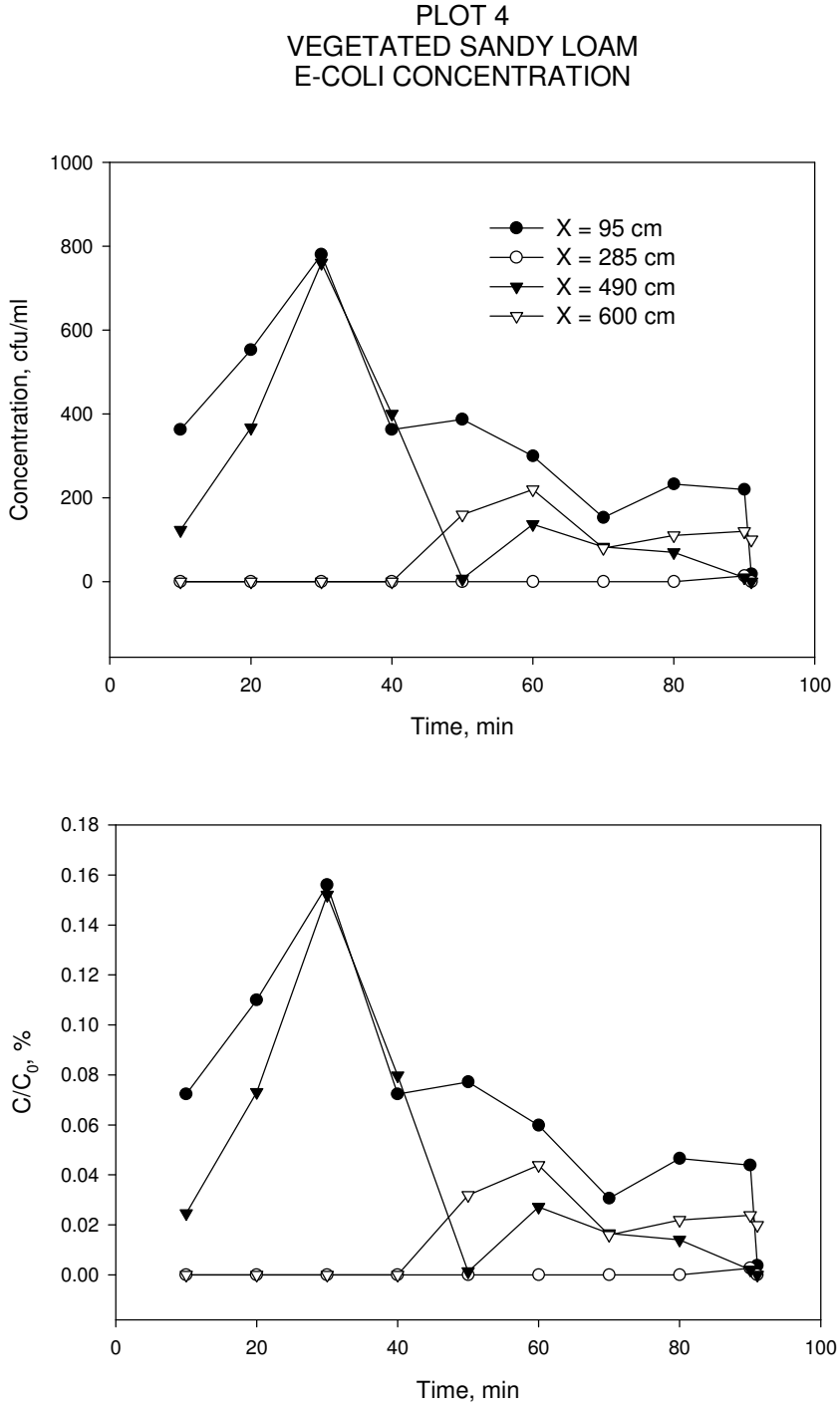

Figure 2.42. Relative concentration ratios of *E.coli* in runoff on vegetated sandy loam (plot 4)

PLOT 1
Bare Clay Loam
Regression of E-coli Concentration Ratios(C/C_0)
to Salmonella Concentration ratios(C/C_0)

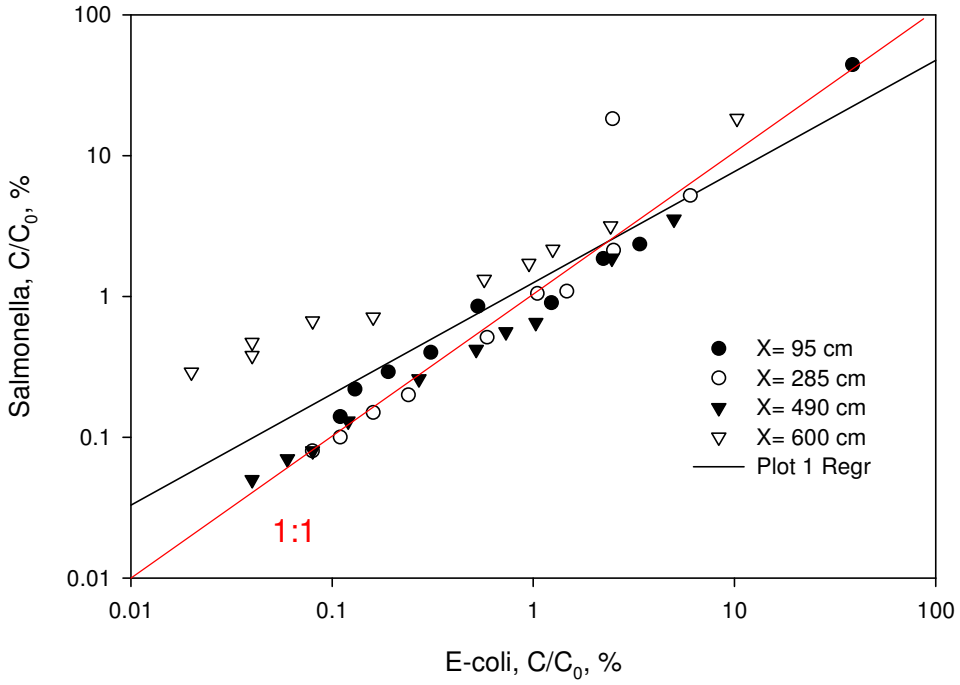

$S_{95\ cm}$=-0.24+1.15$E_{95\ cm}$ R^2=0.99

$S_{285\ cm}$=0.003 + 0.85$E_{285\ cm}$ R^2=0.99

$S_{490\ cm}$=0.03+ 0.71 $E_{490\ cm}$ R^2=0.99

$S_{600\ cm}$=0.16+1.74 $E_{600\ cm}$ R^2=0.99

Figure 2.43. Concentrations of *Salmonella cholerasuis* vs. *E.coli* in bare clay loam, (Plot 1)

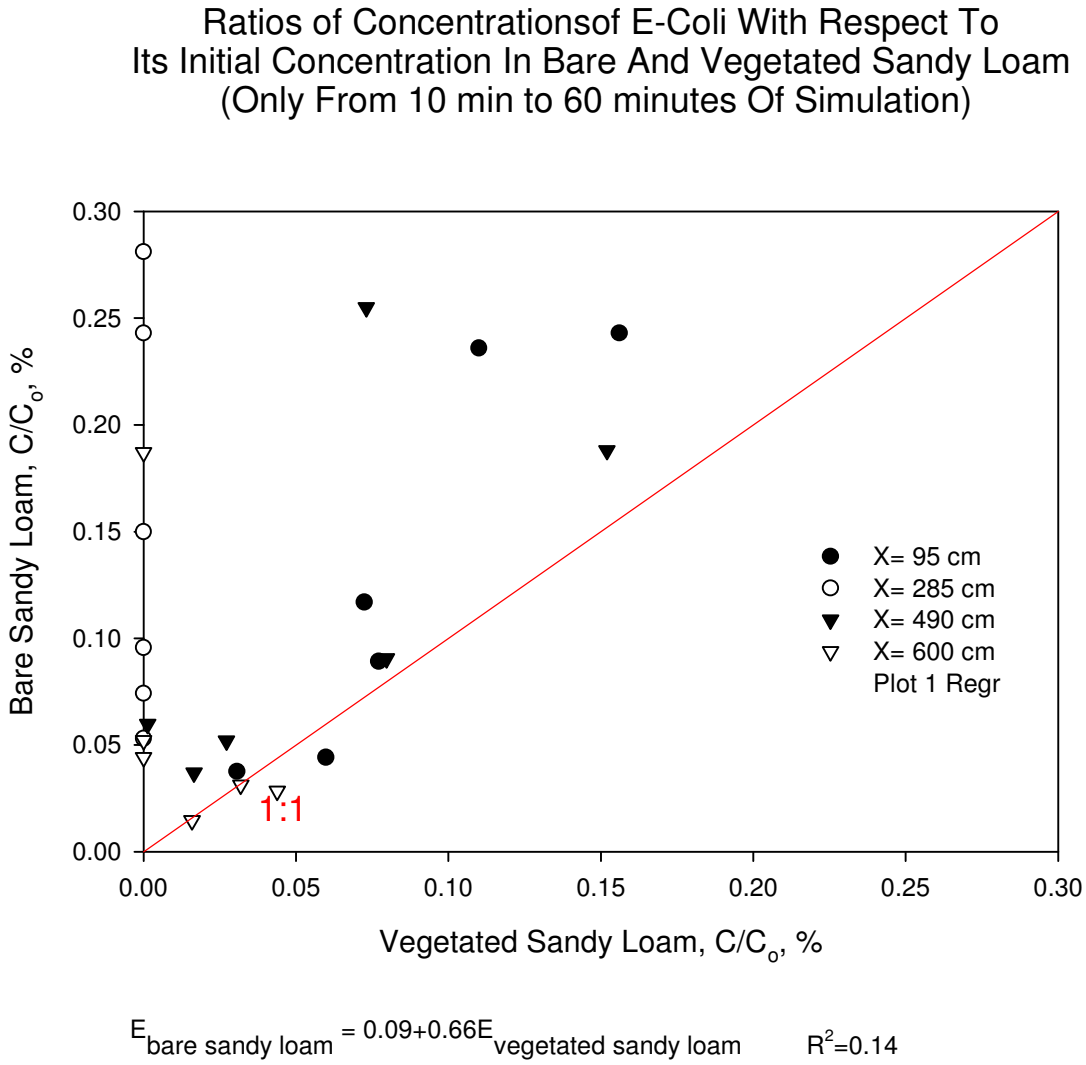

Figure 2.44. Concentration ratios of *E.coli* for bare sandy loam vs. the *E.coli* on vegetated sandy loam

PLOT 3
Bare Sandy Loam
Regression of Salmonella Concentration Ratio
to E-coli Concentration Ratio, (C/C_o)

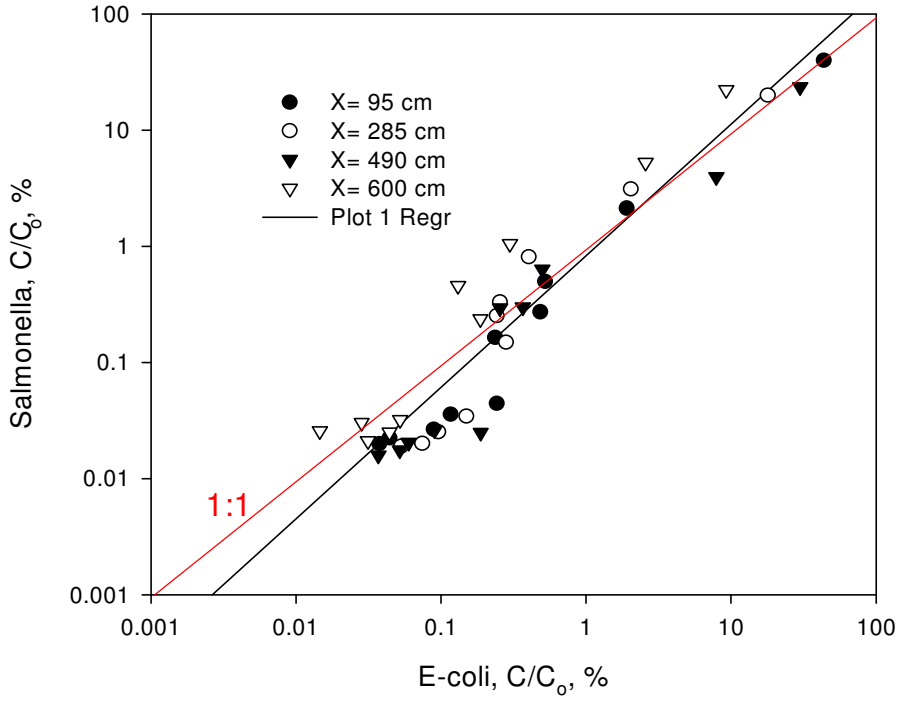

$S_{95\ cm}$= -0.02+0.91$E_{95\ cm}$ R^2=0.99

$S_{285\ cm}$ = 0.07+1.11 $E_{285\ cm}$ R^2=0.99

$S_{490\ cm}$ = -0.17+0.77E490 cm R2=0.99

$S_{600\ cm}$ = -0.07+2.38$E_{600\ cm}$ R^2=0.99

S_{overal} = -0.08+1.13E_{overal} R^2=0.90

Figure 2.45. Concentrations of *Salmonella cholerasuis* vs. *E.coli* concentrations in the bare sandy loam (plot 3) with regression results

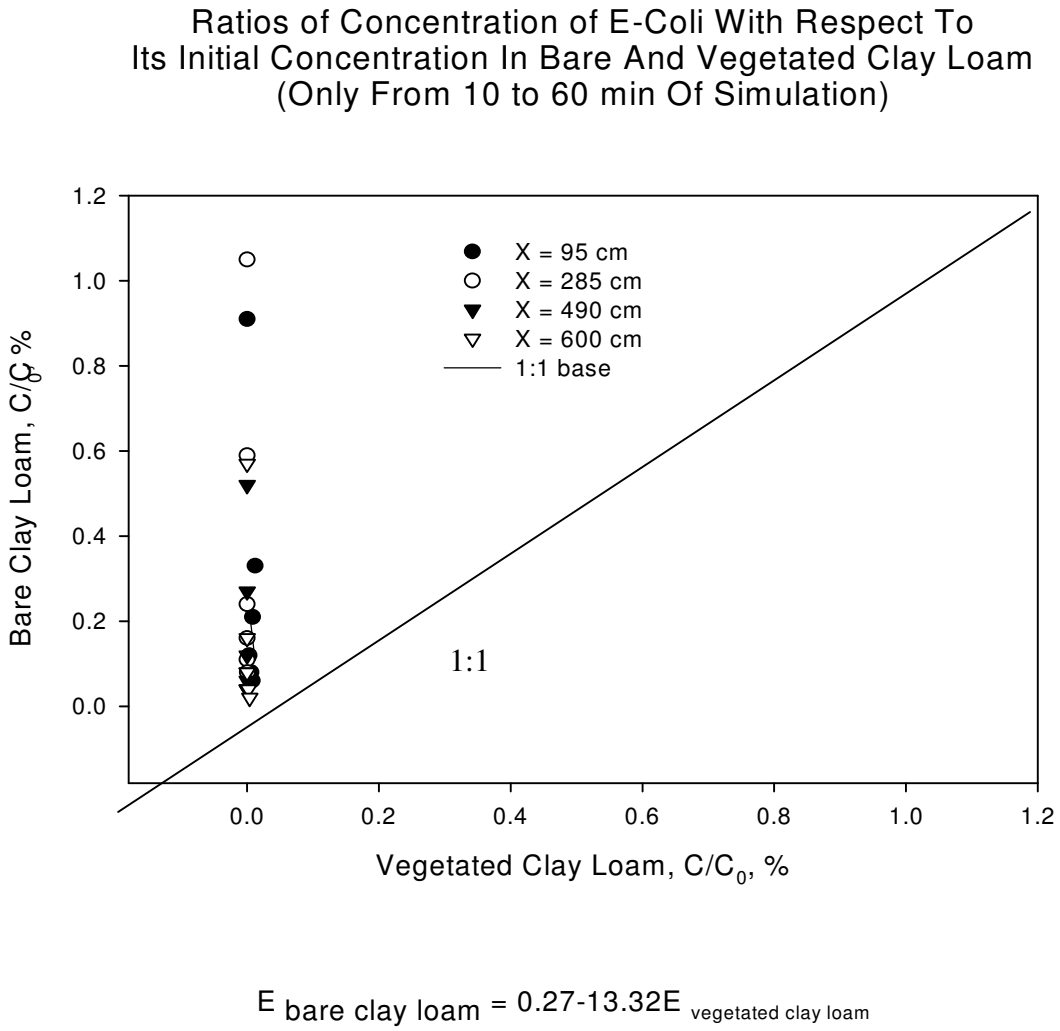

Figure 2.46. Comparison of concentrations of *E.coli* between bare clay loam (plot 1), and vegetated clay loam (plot 2) with regression results

2.12. 9. Sorption

The results of FC adsorption on the sediment particles for both bare plots (Plot 1 and Plot 3) are shown in Tables 1-2. The standard error was calculated as $\frac{\sigma}{\sqrt{n}}$ for both the bare clay loam and the bare sandy loam (n = 6 and 5 for Plot 3, and n=5 for Plot 1). Results of Table 2.1 indicate that an average value of 29.7% (average of 33.72, 31.31, 39.66, 24, 24, and 25%) of the total FC applied on the runoff samples were adsorbed by the sediment particles with a standard deviation of ± 6.4%, and a standard error of 2.61%. Results from Table 2.2 indicate that an average of 25.1% with a standard deviation of 6.27% and a standard error of 2.8% of the total FC applied on the runoff samples were adsorbed by the sediment particles after a period of six hours which reflects the approximate time that it took to process the field water samples after the simulations on the site were stopped. The slopes of the regressions of log-concentrations versus time were 0.023 ± 0.003 min^{-1} and 0.024 ± 0.002 min^{-1} for the bare clay loam and the bare sandy loam, respectively. It should be noted that in the vegetated clay loam, the slope of the regression (0.009 min^{-1}) of the log concentration versus time was much less than the slope of the bare clay loam soil (Table 2.3).

Standard errors for FC concentrations in runoff shown in Table 2.4 are relatively high. Possible sources of error may be attributed to the extraction efficiency of FC from the runoff samples during laboratory analysis. The extraction efficiency, in turn, depends on soil texture affecting textural composition of the sediment. Some sources of uncertainty (i.e., preferential flow in soil, and die-off and regeneration of

bacteria) remain uncertain. Such sources of uncertainty may explain more than 100% recovery of bacteria in runoff for the bare clay loam plot.

Table 2.1. Percentage of the total FC recovered in water samples for the bare sandy loam (Plot 3)

	PLOT 3 Experiment I	PLOT 3 Experiment I	PLOT 3 Experiment II	PLOT 3 Experiment II	PLOT3 (Repeated) I	PLOT3 (Repeated) I
Time, hr	%FC Recovered in Water (Static)	%FC Adsorbed On Sediment	%FC Recovered in Water (Static)	%FC Adsorbed On Sediment	%FC Recovered in Water (Static)	%FC Adsorbed On Sediment
2	43.81	56.19	66.28	33.72	76	24
4	40.17	59.83	66.69	31.31	76	24
6	43.64	56.36	60.34	39.66	75	25

Table 2.2. Percentage of the total FC recovered in water samples for the bare clay loam (Plot 1)

	PLOT 1 Experiment III	PLOT 1 Experiment III	PLOT 1 Experiment IV	PLOT 1 Experiment IV
Time, hr	%FC Recovered in Water (Static)	%FC Adsorbed On Sediment	%FC Recovered in Water (Static)	%FC Adsorbed On Sediment
2	79.25	20.75	77.20	22.80
4	66.81	33.19	70.40	29.60
6	81.79	18.21	Not Good	Not Good

Table 2.3. Regression equations of dependencies of relative FC concentrations in runoff C/C_0 on time *t*

Plot	Distance, cm	Equation, log (C/C_0) =	R^2
Bare Clay Loam	95	0.943 - 0.024 t	0.957
	285	0.712 - 0.024 t	0.930
	485	0.598 - 0.022 t	0.917
	600	0.051 - 0.020 t	0.944
Vegetated Clay Loam	95	0.235 –0.0094t	0.802
Bare Sandy Loam	95	0.689 - 0.022t	0.972
	285	0.033 - 0.021t	0.964
	485	0.068 - 0.026t	0.959
	600	0.235 - 0.027t	0.947

The FC recovered in runoff, in the soil profile, and on the soil surface of the manure application zone were 68, 5, and 44% of the initial population, respectively, for the bare clay loam soil (Table 2.4). For the vegetated clay loam soil, the values were 1, 90, and 0%, respectively, indicating the drastic impact of vegetation in retarding the FC transport on the surface. For the bare sandy loam plot, however, 23, 33, and 8% of the applied FC were recovered in runoff, in soil, and on the surface of manure application area, respectively. Likewise, for the vegetated sandy loam, 11% of the applied FC was recovered in the soil and none were detected in the runoff. This observation emphasizes that both vegetation and soil texture play a vital role in the overland pathogen transport processes.

Both soil texture and vegetation affected fecal coliform transport in runoff. Other factors such as rainfall intensity and duration, slope, manure consistency, source and age of manure were documented as well (Baxter, Potter, and Gilliland, 1988; Kres and Gifford, 1984). This may explain a wide range of filter strip efficiency values, from 10 to 75 %, which have been reported in the literature (i.e.,

Moore et al., 1983; Moore et al., 1988; Young et al., 1980; Coyne et al., 1995). Results of this study showed that vegetation filters reduced the FC transport in runoff from 68% (5.1×10^9 out of 7.5×10^9 FC) to 0.9% (0.1×10^9 to 11×10^9 FC) in clay loam and from 23% (12.8×10^9 out of 56×10^9 FC) to a non-detectable (ND) amount in sandy loam (Table 2.4). This study also showed that filter strips performed a complex rerouting and entrainment of bacteria, and efficiency of a particular strip could be evaluated when all aforementioned factors were taken into account.

Table 2.4. Components of mass balance of water and fecal coliform

Component of the balance	Clay loam		Sandy loam	
	Bare	Vegetated	Bare	Vegetated
Water, cm				
Rainfall	5.6	9.2	5.6	12.7
Runoff, cm Runoff, %	5.2 92.6	1.05 11.4	3.35 59.8	0.32 2.5
Bacteria, 10^9CFU				
Applied	7.5	11	56	32.3
Remained after rain	3.3	0	4.4	0
Runoff	5.1	0.1	12.8	ND
Soil	0.4	9.9	18.6	3.6
In runoff, %	121.4* (24.2)**	0.9(0.6)	24.8(19.2)	ND

* Based on # of participated bacteria (7.5-3.3), ** standard error in parentheses;
ND – Non-detectable
Infiltration = rainfall-runoff

The mass balance for water and FC are shown in Table 2.4. Data in Table 2.4 show that runoff decreased from 93% to 11% in the vegetated clay loam, and from 60% to 3% in the vegetated sandy loam soil, as compared to bare clay loam and bare sandy loam, respectively. Both vegetation and soil texture affected the water balance.

Much higher reductions of surface runoff were observed where vegetation was coupled with soil textures that favored infiltration. The percentage of total runoff for vegetated clay loam soil and vegetated sandy loam soil would have been 6.9% instead of 11.4% and 1.1% instead of 2.5% for clay loam soil and sandy loam soil respectively, if the duration of rainfall simulation for both vegetated plots was 55 minutes.

Results of the analysis of variance model for bromide concentrations after 20 minutes of rainfall simulation, and FC concentrations after 5, 10, and 20 minutes of simulation are presented in Tables 2.6 through 2.8. Results indicated that soil texture was the most significant parameter on Br concentration as compared to the soil surface condition and distances from the manure application area as well as the composite effect of surface-texture, row-texture, and row-texture-surface. Results from the analysis of variance (Tables 2.5 through 2.8) also showed that soil surface condition (vegetation) was the most significant parameter in FC transport after 5, 10, and 20 minutes of simulation as compared to the distances from the application area (rows), and the soil texture. This indicates the importance of vegetated buffer strips in the attenuation of FC transport.

The composite effects of surface-texture, row-texture, and row-texture-surface on Br and FC concentration were also analyzed. Results of the analysis of variance for Br concentration in runoff showed that soil surface condition with texture (surface-texture) was the most significant after 20 minutes of rainfall simulation (Table 2.5). Results for FC concentration after five minutes of simulation indicated that the row-texture-surface was the most significant as compared to surface* texture,

and row*texture after five minutes of rainfall simulation (Table 2.6). However, surface vegetation-soil texture (surface-texture) appeared to be the most significant after 10, and 20 minutes of rainfall simulation (Tables 2.7 and 2.8).

Table 2.5. Analysis of variance results for bromide concentrations after 20 minutes of simulation

	Df	∑ f	Mean Sq	F value	Pr (F)
Rows	2	7992.75	3996.37	5.194	0.0113
Surface Condition	1	11384.73	11384.73	14.79	0.0006
Soil Texture	1	13507.34	13507.34	17.55	0.0002
Surface*Texture	1	11721.31	11721.31	9.660	0.0039
Row*Texture	1	5562	5562	4.583	0.8554
Row*Tex.*Surface	1	1038.00	1038.00	0.855	0.3619

∑ f = sum of the square
Mean Sq = variance
Df = degrees of freedom
Rows: refers to distances from the ridge of the plot

Table 2.6. Analysis of variance results for FC concentrations after five minutes of simulation

	Df	∑ f	Mean Sq	F value	Pr (F)
Rows	2	4759334590	2379667295	3.169	0.056
Surface Condition	1	5813829508	5813829508	7.742	0.009
Soil Texture	1	607842998	607842998	0.809	0.375
Surface*Texture	1	5813829508	5813829508	9.297	0.004
Row*Texture	1	1725699318	1725699318	2.760	0.106
Row*Tex.*Surface	1	6908859854	6908859854	11.048	0.0022

Table 2.7. Analysis of variance model for FC concentrations after ten minutes of simulation

	Df	∑ f	Mean Sq	F value	Pr (F)
Rows	2	3079959106	1539979553	3.709	0.035
Surface Condition	1	8332654184	8332654184	20.068	0.0001
Soil Texture	1	2542028528	2542028528	6.122	0.019
Surface*Texture	1	8210051287	8210051287	19.51	0.00011
Row*Texture	1	1182212237	1182212237	2.808	0.1035
Row*Tex8Surface	1	3412589083	3412589083	8.106	0.00764

Table 2.8. Analysis of variance results for FC concentrations after 20 minutes of simulation

	Df	∑ f	Mean Sq	F value	Pr (F)
Rows	2	8.59e+14	4.29e+14	0.972	0.389
Surface Condition	1	2.25e+15	2.25e+15	5.099	0.031
Soil Texture	1	2.25e+15	2.25e+15	5.087	0.031
Surface*Texture	1	1023242807	1023242807	7.991	0.008
Row*Texture	1	268774335	268774335	2.100	0.157
Row*Tex*Surface	1	210132020	210132020	1.640	0.209

2.13. Conclusions

Results from vegetated plots showed that vegetation drastically attenuated the surface flow of water when compared to the bare plots. Runoff decreased from 93% to 11% in the vegetated clay loam, and from 60% to 3% in the vegetated sandy loam soil, when compared to the bare clay loam and the bare sandy loam, respectively. The reduced runoff on vegetated plots decreased the surface transport of FC while increasing its vertical transport because of increased infiltration.

Concentrations of FC in runoff decreased with time at various distances from the source of manure application on both bare clay loam and bare sandy loam. Unlike the bare soil, it was concluded that the vegetated soil surface created a much less uniform transport pattern for FC. Only at the distance of 95 cm from the edge of the manure application area did the pattern of FC transport have a steady decrease with time. Vegetation changed the transport patterns and levels of FC concentrations much more significantly than soil texture. In addition, vegetation promoted vertical FC transport close to the source, but did not seem to have much effect at distances away from the source of manure application.

Results of this study showed that vegetation filters reduced the FC transport in runoff from 68% to 0.9% in clay loam soil and from 23% to non-detectable in sandy loam soil. This study also showed that filter strips performed a complex rerouting and entrainment of bacteria, and the efficiency of a particular strip could be evaluated only when all aforementioned factors were taken into account.

Results of swine manure experiments showed that *E.coli* and *Salmonella cholerasuis* behaved very similarly and underwent similar transport patterns in both

bare plots. It was concluded that both organisms demonstrated a two-stages exponential release rate with a fast release rate in the first ten minutes of the rainfall simulation. Transport of both *E.coli* and *Salmonella cholerasuis* were completely attenuated by the soil surface vegetation on the vegetated plots (Plot 2 and Plot 4) and their flow patterns were significantly distorted. Even at 95 cm distance from the edge of the manure application area very low concentrations of these organisms were measured.

Despite the difficulties in quantifying the population of *Salmonella cholerasuis* from the sampling plates in the vegetated soils (*Salmonella cholerasuis* were suppressed by other local organisms living in the vegetated plots), it was concluded that *E.coli* and *Salmonella* exhibited relatively similar transport behavior based on the results obtained from the bare plots and the results from the physiological characteristics tests in the laboratory. These results demonstrated the significance of vegetated filter strips on microbial transport, and showed how drastically water flow could be attenuated even under a 20% slope. Therefore, this study concluded that vegetated filter strips are viable management practices to prevent pathogens from leaving plots of 20 % slope with both clay loam and sandy loam textures and reaching the surface bodies of water.

References

Abu-Ashour J., D.M. Joy, H. Lee, H.R. Whiteley, and S. Zelin. 1998. Movement of bacteria in unsaturated columns with macropores. Transactions of the ASAE 41:1043-1050.

Adler, J. 1969. Chemoreceptors in bacteria. Science. 166: 1588-1597.

Alexander, M. 1977. Introduction to soil microbiology, John Wiley and Sons, New York.

Andreini, M.S. and T.S. Steenhuis, 1990. Preferential paths of flow under conventional and conservation tillage. Geoderma 46: 85-102.

Atwill, E.R., R.A. Sweitzer, M. Das Graças C. Pereira, I.A. Gardner, D. Van Vuren, W.M. Boyce. 1997. Prevalence of and associated risk factors for shedding *Cryptosporidium parvum* and *Giardia* within feral pig populations in California. Applied and Environmental Microbiology 63(10): 3946-3949.

Baxter-Potter, W.R. and M.W. Gilliland. 1988. Bacterial pollution in runoff from agricultural lands. *J. Environ. Qual*. 17: 27-34.

Berg, H.C., and D.A. Brown, 1972. Chemotaxis in Escherichia coli analyzed by three-dimensional tracking. Nature. 239: 500-504.

Bitton, G., N. Lahav, and Y. Henis, 1974. Movement and retention of Klebsiella aerogenes in soil columns. Plant Soil. 42: 373-380.

Bitton, G., J.M. Davidson, and S.R. Farrah, 1979. On the value of soil columns for assessing the transport pattern of viruses through soils: a critical outlook. Water, Air, and Soil Pollution 12: 449-457.

Bitton, G., and R.W. Harvey, (1992). Transport of pathogens through soils and aquifers. In: Mitchell, R. (Ed) Environmental Microbiology (pp-103-124). Wiley-Liss, New York

Brock, T.D.1971. Biology of Microorganisms. Prentice-Hall, Inc., Englewood Cliffs, NJ.

Brooks, R.H., and A.T. Corey, 1964. Hydraulic properties of porous media. Hydrology paper Vol. 3, p. 27, Colorado State University, Fort Collins, Colorado.

Buss, P. 1993. The use of capacitance based measurements of real time soil water profile dynamics for irrigation scheduling, pp. 17-19. In: Proc. Natl. Conf.

Irrig. Assoc., Australia and Natl. Committee Irrig. Drain., Launceston, Tasmania. May 1993. Irrig. Assoc. of Aust., Homebush, NSW.

Butler, R.G., G.T. Orlob, and P.H. McGauhey, 1954. Underground movement of bacterial and chemical pollutants. J. Am. Water Works Assoc. 46: 97-11.

Campbell, G.S., 1974. A simple method for determining unsaturated conductivity from moisture retention data. Soil Sci. 117:311–314.

Chandler, D.S., J. Farran, and J.A. Graven. 1981. Persistence and distribution of pollution indicator bacteria on land used for disposal of piggery effluent. Applied Environmental Microbiology. 42:453-460.

Characklis, W.G., K.C. Marshall, 1990. Biofilms, pp. 110-112. John Wiley & Sons, New York, NY.

Chaubey, I., D.R. Edwards, T.C. Daniel, P.A. Moore, Jr. and D.J. Nichols. 1994. Effectiveness of vegetative filter strips in retaining surface-applied swine manure constituents. Transactions of the ASAE. 37(3): 845-850.

Corapcioglu Y. M., and A. Haridas. 1984. Transport and fate of microorganisms in Porous media: a theoretical investigation. Journal of Hydrology, 72:149-169

Corapcioglu Y. M., and A. Haridas, 1985. Microbial transport in soils and groundwater: a numerical model. Adv. Water Resour. 8: 188-200.

Coyne, M.S., R.A. Gilfillen, R.W. Rhodes, and R.L. Blevins. 1995. Soil and fecal coliform trapping by grass filter strips during simulated rain. J. Soil and Water Cons. 50(4): 405-408.

Crane, S.R., J.A. Moore, M.E. Grismer, and J.R. Miner. 1983. Bacterial pollution from agricultural sources: a review. Transactions of the ASAE. 26(3): 858-866.

Crane, S.R. and J.A. Moore. 1984. Modeling enteric bacteria die-off: a review. Paper No. 6699. Oregon Agricultural Experiment Station, Corvallis, OR.

Cunningham, A.B., W.G., Characklis, F. Abedeen, and D. Crawford, 1991. Influence of biofilm accumulation on pourous media hydrodynamics. Environ. Sci. Technol. 25: 1305-1310.

Dahlquist, F.W., P. Lovely, and D.E. Koshland, 1972. Quantitative analysis of bacterial migration in chemoxis. Nature New Biol. 236: 120-123.

Daniels, S.L. 1972. The adsorption of microorganisms onto surfaces: A review. Dev. Indus. Microbiol. 13:211-253.

Daniels, S.L. 1980. Mechanisms involved in sorption of microorganisms to solid surfaces. P 7-58. In: G. Bitton and K.C. Marshall (ed.) Adsorption of microorganisms to surfaces. Wiley - Interscience, New York.

Dickey, E. C. and D. H. Vanderholm. 1981. Vegetative filter treatment of livestock feedlot runoff. J. Envir. Qual. 10:279-284.

Dufour, A.P., 1977. Escherchia coli.: the fecal coliform, p. 48-58. In: A. W. Hoadley and B.J. Dutka (ed.), Bacterial Indicators/Health Hazards Associated with Water. ASTMSTP 635. American Society for Testing and Materials, Philadelphia, Pa.

Dunne, T., and R.D. Black 1970. An experimental investigation of runoff production in permeable soils. Water Resources Research 6(2):478-490.

Dutka, B.J., A.S.Y. Chau, and J. Coburn. 1974. Relationship between bacteria indicators of water pollution and fecal sterols. Water Res. 8:1047.1055.

Evans, M.R. and J.D. Owens. 1972. Factors affecting the concentration of fecal bacteria in land drainage water. J. Gen. Microbial. 71: 477-485.

Fajardo, J.J., J.W. Bauder, and S.D. Cash. 2001. Managing nitrate and bacteria in runoff from livestock contamination areas with vegetative filter strips. Journal of Soil and Water Conservation, 56(3): 185-191.

Fleming, R.J., D.M. Dean, and M.E. Foran. 1990. Effect of manure spreading on tile drainage water quality. P. 385. In: Proc. 6th Int'l Symp. Agricultural and Food Processing Wastes. St. Joseph, Mich: ASAE

Gagliardi, J.V., and J.S. Karns. 2000. Leaching of *Escherichia coli* O157:H7 in diverse soils under various agricultural management practices. Appl. Environ. Microbiol. 66:877–883.

Gannon, J.T., V.B. Manilal and M. Alexander. 1991a. Relationship between cell surface properties and transport of bacteria through soil. Appl. Environ. Microbiol. 57(1): 190-193.

Gannon, J.T., U. Mingelgrin, M. Alexander and Wagnet, R.T. 1991b. Bacteria transport through homogeneous soil. Soil Biol. Biochem. 23(12): 1155-1160.

Gerba, C.P., G. Bitton, 1984. Microbial pollutants: Their survival and transport pattern to groundwater. P. 65-88. IN Bitton, G. and Gerba, C.P. (ed). Groundwater pollution microbiology. Wiley- Interscience, New York.

Gerba, C.P., C. Wallis, and J.L Melnich, 1975. Fate of wastewater bactera and viruses in soil. J. Irrig. Drain. In: Proc. Am. Soc. Civ. Eng., 101 (IR3): 157-174.

Germann, P.E. and K. Beven, 1985. Kinematic wave approximation to infiltration into soils with sorbing macropores. Water Resources. Res. 21: 990-996.

Hagedorn, C., 1981. Transport and fate : Bacteria pathogens in groundwater. Pro. Con. On microbial health considerations of soil disposal of domestic wastewaters, Norman, Okla., pp. 84 -102.

Haggard, B.E., P.A., Moor, P.B. Delaune, D.R. Smith, S. Formica, P.J. Kleinman, and T.C. Daniel, 2002. Effect of slope, grazing and aeration on pasture hydrology. Transactions of the ASAE., paper number 022156, presented at 2002 ASAE Annual International Meeting at Chicago, July 28- July 31.

Heimovaara, T.J., and W. Bouten. 1990. A computer-controlled 36-channel time domain reflectometry system for monitoring soil water contents. Water Resour. Res. 26:2311-2316.

Hendricks, D.W., F.J. Post, and D.R. Khairnar, 1979. Adsorption of bacteria on soils: Experiments, thermodynamic rationale, and application. Water, Air and Soil Pollu. 12: 219-232.

Herkelrath, W.N., S.P. Hamburg, and F. Murphy. 1991. Automatic, real-time monitoring of soil moisture in a remote field area with time-domain reflectometry. Water Resour. Res. 27:857-864.

Herzig, J.P., D.M. Leclerc, and P. Le Golf, 1970. Flow of suspensions through porous media – Application to deep infiltration, pp. 129-157. In: Flow through porous media, Am. Chem. Soc., Washington, D.C.

Hunt, P.G., R.E. Peters, T.C. Sturgis, and C.R. Lee. 1979. Reliability problems with indicator organisms for monitoring overland flow treated wastewater effluent. J. Environ. Qual. 8(3): 301-304.

Huysman, F. and W. Verstraete, 1993. Water-facilitated transport of bacteria in unsaturated soil columns: Influence of inoculation and irrigation methods. Soil Biol. Biochem. 25: 91-97.

Iqbal, M.Z., N.C. Krothe, 1996. Transport of bromide and other inorganic ions by infiltrating storm water beneath a farm land plot: Ground Water, 34 (6): 972-978.

Isensee, A.R., and A.M. Sadeghi. 1999. Quantification of runoff in laboratory-scale chambers. Chemosphere 38:1733–1744.

Jabro, J.D., E.G. Lotse, K.E. Simmons, and D.E. Baker, 1991, A field study of macropore flow under saturated conditions using a bromide tracer: Journal of Soil and Water Conservation, 46 (5): 376-380.

Kao, T. Y. and B.J. Barfield. 1978. Prediction of flow hydraulics for vegetated channels, Transaction of ASAE 22:489-494

Kei, W., J. Yee-Chung, and T. Viraraghavan, 2002. Transport of bacteria in heterogeneous media under leaching conditions. J. Environ. Eng. Sci. 1:383-395.

Keller, E.F., and L.A. Segal, 1971. Model for chemotaxis. J. Theor. Biol. 30:225-234.

Khaleel, R., G.R. Foster, K.R. Reddy, M.R. Overcash, and P.W. Westerman. 1979. A nonpoint source model for land area receiving animal wastes. III A conceptual model for sediment and manure transport. Transaction of the ASAE 22:1353-1361.

Khaleel, R., R. Reddy, and M.R. Overcash, 1980. Transport of potential pollutants in runoff water. Water Research. 14: 421-436.

Kitahara, H., 1993. Characteristics of pipe flow in forested slopes. In: Bolle, H.J., R.A. Feddes, and J. Kalma. (Eds), Exchange Processes at the Land Surface for a Range of Space and Time Scales. Proc.Yokohama Symp., International Association of Hydrological Science Publ. No. 212. IAHS Press, Wallingford, UK. pp. 235-242.

Kres,M., and G. R. Gifford. 1984. Fecal coliform release from cattle fecal deposits. Water Resour. Bull., 20:61-66.

Lance, J.C., C.P. Gerba, and J.L. Melnick, 1976. Virus movement in soil columns flooded with secondary sewage effluent. Appli. Environ. Microbiol. 32: 520-526.

Lance, J. C., C. P. Gerha and S. S. Wang. 1982. Comparative movement of different enteroviruses in soil columns. J. Environ. Qual. 11:347-351.

Lance, S. C. and C. P. Gerba. 1984. Virus movement in soil during saturated and unsaturated flow. Appl. Environ. Microbiol. 47:335-337.

Li, R. M. and H. W. Shen. 1973. Effect of total vegetation on flow and sediment, J. Hyd. Div., Proceeding of ASCE, Vol. 99 (HY5) 793-814.

Lim, T. T., D. R. Edwards, S. R. Workman, and B. T. Larson. 1997. Vegetated filter strip length effects on quality of runoff from grazed pastures ASAE, Paper No.97- 2060. St. Joseph, Mich.: ASAE.

Loehr, R.C., 1979. Potential pollutants from agriculture—an assessment of the problem and possible control approaches. *Prog. Wat. Tech.* 11(6), 169-193.

Luxmoore, R.J.1981. Micro-, meso-, and maroporosity of soil. Soil Sci. Am. J. 45:671-72.

Ma, Q.L., R.D. Wauchope, J.E. Hook, A.W. Johnson, C.C. Dowler, G.J. Gascho, J.G. Davis, H.R. Summer, L.D. Chandler. 1998. GLEAMS, Opus, and PRZM-2 model predicted versus measured runoff from coastal plain loamy sand. Transactions of the ASAE 41(1):77-88.

Madsen, E.L., and M. Alexander, 1982. Transport of rhizobium and pseudomonas through soil. J. Environ. Qual. 46: 557-560.

Marshall, K.C. 1976. Interfaces in microbial ecology. Harvard University Press, Cambridge.

Matthess, G., and A. Pekdeger, 1981. Concepts of a survival and transport model of pathogenic bacteria and viruses in groundwater. Sci. Total Environ. 21: 149-159.

Mawdsley, J.L., A.E. Brooks, and R.J. Merry. 1996a. Movement of the protozoan pathogen Cryptosporidium parvum through three contrasting soil types. Biol. Fertil. Soils 21: 30-36.

Mawdsley, J.L., A.E. Brooks, R.J. Merry, and B.F. Pain. 1996b. Use of a novel soil-tilting table to demonstrate the horizontal and vertical movement of the protozoan pathogen Cryptosporidium parvum in soil. Biol. Fertil. Soils 23: 215-220.

McCarthy, J. F., and J. M. Zachara. 1989. Subsurface transport of contaminants: binding to mobile and immobile phases in groundwater aquifers. Environ. Sci. Technol. 23:496-504.

McDonald, A., D. Kay, and A. Jenkins. 1982. General fecal and total coliform surges by stream flow manipulation in the absence of normal hydrometerological stimuli. Applied and Environmental Microbiology 44, 292-300.

McDowell-Boyer, L.M., J.R. Hunt, and N. Sitar, 1986. Particle transport in porous media. Water Resour. Res. 22: 1901-1921.

McFeters, G.A., G.K. Bissonnette, J. J. Jezeski, C.A. Thomson, and D.G. Stuart, 1974. Comparative survival of indicator bacteria and enteric pathogens in well water Appl. Microbiol. May; 27 (5): 823–829.

McKensie, W.M. 1985. The design of a rotating nozzle rainfall simulator and the testing with selected nozzles. Bsc. thesis, Silsoe College, Cranfield Institute of Technology, UK.

McMurry, S.W., M.S. Coyne, and E. Perfect. 1998. Fecal coliform transport through intact soil blocks amended with poultry manure. J. Environ. Qual. 27: 86-92.

Miller, R.J., J.W. Bigger, and D.R. Nielsen, 1965. Chloride displacement in Panoche clay loam in relation to water movement and distribution. Water Resour. Res., 1(1): 63-73, 1965.

Miller, W.P. 1987. A solenoid-operated, variable intensity rainfall simulator. Soil Sci. Soc. Am. J. 51:832-834.

Monod, J. 1942. Recherches sur la Croissance des Cultures Bacteriennes. Hermann et Cie, Paris.

Moore, J.A., J.D. Smyth, E.S. Baker, and J.R. Miner. 1988. Evaluating coliform concentrations in runoff from various animal waste management systems. Special Report 817: Agricultural Experiment Station, Oregon State University, Corvallis, Oregan.

Moore, J.A., M.E. Grismer, S.R. Crane, and J.R. Miner. 1983. Modeling dairy waste management systems' in fluence on coliform concentration in runoff. Transactions of the ASAE 26(4): 1194-1200.

Mosley, M.P., 1979. Stream flow generation in a forested watershed, New Zealand. Water Resources. Res. 15: 795-806.

Nassif, S.H., and E.M. Wilson. 1975. The influence of slope and rain intensity on ranoff and infiltration. Hydrological Sciences Bulletin. 20:539-553.

O'Melia, C.R., and W. Stumn, 1967. Theory of water filtration. J. Am. Water Works Assoc. 59: 1393-1412.

Paltineanu, I.C., J.L. Starr. 1997. Real-time soil water dynamics using multisensor capacitance probes: Laboratory calibration. Soil Sci. Soc. Am. J. 61:1576-1585.

Parke, J.L., R. Moen, A.D. Rovira, and G.D. Bowen, 1986. Soil water flow affects the rhizosphere distribution of a seed-borne biological control agent, Pseudomonas fluorescence. Soil Biol. Biochem. 18:583-588.

Pasquarell, G.C., and D.G. Boyer**.** 1995. Agricultural impacts on bacterial water quality in karst groundwater. Journal of Environmental Quality 24:959-969.

Paterson, E., J.S. Kemp, S.M. Gammack, E. Fitz Patrick, C. Adisl, S. Malcom, C.E. Mullins, and K. Killham. 1992. Leaching of genetically modified pseudomonas fluorescents through intact soil microcosms: influence of soil type. Biol. Fertil. Soils 15: 308-314.

Patni, N.K., H.R. Toxepeus and P.Y. Jui. 1985. Bacterial quality of runoff from manure and non-manure cropland. Transactions of the ASAE 28:1871-1877.

Payment, P., L. Richardson, J. Siemiatycki, R. Dewar, M. Edwardes, end E. Franco. 1991. A randomized trial to evaluate the risk of gastrointestinal disease due to consumption of drinking water meeting current microbiological standards. Am. J. Public Health 81:703-708.

Pettygrove, G.S., and T. Asano, eds. 1985. Irrigation with reclaimed municipal wastewater- A Guidance Manual. Chelsea, Mich. Lewis Publishers.

Pourcher, A.M., L.A. Devriese, J.F. Hernandez, and J.M. Delattre. 1991. Enumeration by a miniaturized method of E. coli, S. bovis, and enterococci as indicators of

the origin of fecal pollution of waters. Journal of Applied Bacteriology. 70: 525-530.

Reddy, K.R., R. Khaleel, and M.R. Overcash. 1981. Behavior and transport of microbial pathogens and indicator organisms in soils treated with organic wastes. J.of Environ. Qual. 10(3): 2545-266.

Reed, S., R. Thomas, and N. Kowal, 1980. Long term land treatment, are there health or environmental risks? Proceedings of ASAE National Convention, Portland, OR.

Rice, R.C., D.B. Jaynes, and R.S. Bowman, 1991. Preferential flow of solute and herbicide under irrigated fields. Transactions of ASAE 34 (3): 914 -918.

Schaub, S. A., and C. A. Sorber. 1977. Virus and bacteria removal from wastewater by rapid infiltration though soil. Appl. Environ. Microbiol. 33:609-619.

Schellinger, G.R., and J.C. Clausen. 1992. Vegetated filter treatment of dairy barnyard runoff in cold regions. J. Environ. Qual. 21:40-45.

Smith, M.S., G.W. Thomas, R.E. White, and D. Ritonga, 1985. Transport of *Escherichia coli* through intact and disturbed soil columns. J. Environ. Qual. 14:87-91.

Srivastava, P., D.R. Edwards, T.C. Daniel, P.A. Moore, and T.A. Costello. 1996. Performance of vegetative filter strips with varying pollutant sources and filter strip length. Transactions of the ASAE 39(6): 2231-2239.

Starr, J.L., and I.C. Paltineanu. Soil water dynamics using multisensor capacitance probes in nontraffic interrows of corn. 1998. Soil Sci. Soc. Am. J. 62:114-122.

Steenhuis, T.S., W. Staubitz, Andreini, J. Surface, T.L. Richard, R. Paulson, N.B. Pickaering, J.R. Hagerman, and L.D. Geohring, 1990, Preferential movement of pesticides and tracers in agricultural soils, J. Irrigation and Drainage Engineering, v. 116, no. 1, p. 50.

Sykes, J.F., S. Soyupak, and G.J. Farquhar, 1982. Modeling of leached organic migration an attenuation in groundwater below sanitary landfills. Water Resour. Res., 18: 135-145.

Tan, Y., W.J. Bond, A.D. Rovira, P.G. Brisbane, and D.M. Griffin, 1991. Movement through soil of a biological control agent, Pseudomonas fluorescences. Soil Biol. Biochem. 23: 821-825.

Tan, Y., W.J. Bond, and D.M. Griffin, 1992. Transport of bacteria during unsteady unsaturated soil water flow. Soil Sci. Soc. Am. J. 56: 1331-1340.

Tan, Y., J.G. Gannon, P. Baveye, and M. Alexander.1994.Transport of bacteria in a saturated aquifer sand. Water Res. 30:3243-3252.

Tan, Y., W.J. Bond, 1995. Modeling subsurface transport of microorganisms. pp. 321-355. In: V.P. Singh (ed.), Environ. Hydro. Kluwer Academic Publishers, Netherland.

Tate, C.H., and K.F. Arnold. 1990. Health and a esthetic aspects of water quality. In American Water Works Association (Eds.), Water Quality and Treatment: A Handbook of Community Water Supplies. New York: McGraw Hill.

Taylor, S.W., P.C.D. Milly, and P. Jaffe, 1990. Biofilm growth and related changes in the physical properties of a porous medium. 2. Permeability. Wat. Resour. Res. 26(9), 2161-2169.

Taylor, S. W. and P. Jaffe, 1990a. Substrate and biomass transport in a porous medium. Water Resour. Res. 26:2181-2194.

Taylor, S. W. and P. Jaffe, 1990b. Biofilm growth and related changes in the physical properties of porous medium. 3. Dispersivity and model verification. Wat. Resour. Res. 26(9), 2171-2180.

Teutsch G., K. Herbold-Paschke, D. Tougianidou, T. Hanh, and K. Botzenhart. 1991. Water Science and Technology, 24 (2), 309.

Tindall, J.A., and W.K. Vencill, 1995. Preferential transport of atrazine in well structured soils. In Agricultural research to protect water quality (vol.I), 154-56. Proc. Conf., 21-24 February, Minneapolis, MN. Ankeny, IA: Soil and Water Conservation Society.

Toranzos, G.A., and G.A. McFeters. 1997. Detection of indicator microorganisms in environmental freshwaters and drinking waters. Manual of Environmental Microbiology, ASM PRESS, Washington, D.C.

Trevors, J.T., van Elsa, J.D., van Overbeek L.S., Starodub, M., 1990. Transport of a genetically engineered Pseudomamnas fluorescence strain through a soil microcosm. Appli. Environ. Microbiol. 56: 401-408.

Tsuboyama, Y., R.C. Sidle, S. Noguchi, and I. Hosoda, 1994. Flow and solute transport through the soil matrix and macropores of a hillslope segment. Water Resour. Res. 30, 879-890.

USEPA, 1994. National Water Quality Inventory: Report to Congress, USEPA, office of Water, Washington, D.C.

Van Elsa's, J.D., J.T. Trevors, and L.S. Van Overbeek. 1991. Influence of soil properties on the vertical movement of genetically –marked pseudomonas

fluorescents through large soil microorganisms. Biol. Fertil. Soils.10: 249-255.

Van Genuchten, M.Th., 1980. A closed-form equation for predicting the hydraulic conductivity of unsaturated soils. Soil Sci. Soc. Am. J. 44:892–898.

Van Wesenbeeck, I.J., and R.G. Kachanoski. 1988. Spatial and temporal distribution of soil water in the tilled layer under corn crop. Soil Sci. Soc. Am. J. 52:363-368.

Vilker, V.L., and W.D. Burge, 1980. Adsorption mass transfer model for virus transport in soils. Water Res. 14: 783-790.

Walch, M., and R.R. Colwell, 1994. Detection of non-culturable indicators and pathogens, p. 258-273. In: C.R. Hackney and M.D. Pierson 9ed.), Environmental Indicators and Shellfish Safety. Chapman and Hall, New York.

Walker, S.E., S. Mostaghimi, T.A. Dillaha, and F.E. Woeste. 1990. Modeling animal waste management practices: Impact on bacteria levels in runoff from agricultural lands. Trans. ASAE 33:807-817.

Weaver, R.W., 1981. Transport and fate of bacteria pathogens in soil. Proc. Conf. on microbial health considerations of soil disposal of domestic wastewaters, Norman, Okla., pp. 53-83.

Williams, A.G., J.F. Dowd, D. Scholeflield, N.M. Holden, and L.K. Deeks. 2003. Preferential flow variability in well-structured soil. Soil Sci. Soc. Am.J. 67:1272-1281.

William, E.J., and N.H. Kloot. 1953. Interpolation in a series of correlated observations. Austral. J. Appl. Sci., 4:1-17.

Wollum II, A.G. and Cassel, D.K., 1978. Transport of microorganisms in sand columns. Soil. Sci. Soc. Am. J., 42:72-76.

Wood, M, 1989. Soil Biology, Chapman & Hall, New York.

Yao, K., Habibian, M.T., and O'Melia, C.R. 1971. Water and wastewater filtration: Concepts and applications. Environ. Sci. Technol. 5:1105-1112.

Yates, M.V., and S.R. Yates. 1988. Modeling microbial fate in the subsurface environment. CRC Crit. Rev. Environ. Control. 17:307-344.

Young, R.A., T. Huntrods, and W. Anderson. 1980. Effectiveness of vegetated buffer strips in controlling pollution from feedlot runoff. J. Envir. Qual., 9:483-487.

Zacharias, S., and C.D. Heatwole. 1994. Evaluation of GLEAMS and PRZM for predicting pesticide leaching under field conditions. Transaction of ASAE. 37 (2): 439-51.

Zoldoske, D.F. 2003. Improving golf course irrigation uniformity: A California Case Study. The Center for irrigation technology. California State University, Fresno, CA, 2003.

Zyman, J., Sorber, C.A. (1988). Influence of simulated rainfall on the transport and survival of selected indicator organisms in sludge-amended soils. J. Water Pollut. Control Fed. 60: 2105-2110.

CHAPTER III. MODELING PATHOGEN TRANSPORT TROUGH VEGETATED WATERWAYS

3.1. Abstract

A one-dimensional (1-D) convective-dispersive model was implemented into an existing surface runoff model (KORMIL2), (Choi, 1992) to simulate the surface pathogen transport. The pathogen vertical transport was also simulated with a 1-D kinematic wave model. The explicit finite difference scheme and method of characteristics were used to solve transport equations of overland flow and subsurface flow transport of fecal coliform (FC), respectively. Green and Ampt, Philip, and Schmid (modified Green and Ampt) infiltration models were also applied to the vertical water flow movement. The Green and Ampt model appeared to produce satisfactory results when calibrated with the measured infiltration data. Calibrated parameters of this model were close to the values recommended for the soils of similar texture. Model simulations were compared to the experimental data collected from the field-based lysimeter (6.0 m $\times$ 6.4 m) site. Only low concentrations of FC were available when the runoff initiated in the vegetated plots. This was attributed to the adsorption of bacteria to soil and plant residue, and possible vertical migration into the soil profile in the vegetated plots. The model simulated the spatial and temporal distribution of FC in runoff assuming an exponential release of FC from the manure. Both flow and pathogen transport components performed satisfactorily. Simulations of the subsurface concentrations showed a delay, thus indicating a possible need for a two-dimensional description of the subsurface flow transport.

3.2. Introduction

The transmission of human pathogenic agents via water and treated water has been reported extensively in the literature (Barwick et al., 2000; Cruz et al., 1990). Nationally, an estimated 19,811 river miles, approximately 8% of the United States streams, are impaired by fecal coliform (FC) (USEPA, 1998). Organisms either live in association with various host organisms, or they live independently within the environment. Not all microorganisms are pathogenic; however, the presence of pathogenic bacteria in public and private water systems has become one of the main water quality problems.

Despite many potential sources that exist in the environment, agronomic practices appear to be the major contributors of most bio-contamination to water bodies (USEPA, 1998). Widespread public concerns may include septic tank effluent, sewage land application from municipal treatment centers, and land manure application through intensive livestock operations (Viraraghavan and Ionescu, 2002; Jenkins et al., 1994; Joy et al., 1998). The Animal Feeding Operations (AFOs) have been cited as the most important sources that can adversely impact the public and environmental health (USEPA, 1994). High rates of land-applied manure, particularly where rates exceed soil assimilative capacity, increase the risks for surface or groundwater contamination. Overland contamination from animal feedlots has been quantified in many studies, and was documented by Miner et al., (1966), Rhodes and Hrubant (1972) and Young et al. (1980).

Since microbes have intrinsic electronic charges, they adsorb to the surface of charged environmental particles (Grant et al., 1993; Moor et al., 1982). Adsorption to

the soil particles can enhance the surface transport of bacteria as particulates and increase their ability to survive in the environment (Hurst et al., 1980). In the subsurface, adsorption of organisms to the soil matrix will retard the movement of microorganisms (Powelson et al., 1994). The effects of other environmental factors such as soil pH, soil moisture, and sunlight on bacteria population have been investigated by Reddy et al. (1981) and Polprasert et al. (1983).

Mathematical modeling for hillslope flow involves simultaneously solving of governing equations of both surface and subsurface flow. Models are helpful to predict the bacteria concentration in runoff, the soil profile, and subsurface groundwater. Existing transport models mostly focus on nutrients, pesticides, and sediment transport from agricultural fields to surface waters. Despite numerous studies on surface flow and contaminant leaching, little effort has been devoted to combine the surface microbial transport models with subsurface contaminant models under field conditions. Although some of the existing models were developed to predict leaching of microorganisms through the soil profile, the modeling age of microbial transport on surface and subsurface flow in a field-scale is still in early stages.

The objective of this study was to develop a computer model to simulate the temporal and spatial concentrations of microorganisms in a field-based lysimeter from an applied bovine manure application area. Choi's runoff model (KORMIL2), (Choi, J., 1992) was modified by addition of a one dimensional (1-D) convective-dispersion model to simulate the surface pathogen transport. KORMIL2 is a numerical model, based on kinematic wave equations to simulate the overland runoff

in an intervening land system. A one-dimensional (1-D) kinematic wave model was also used to compute the vertical concentration of fecal coliforms within the soil profile.

3.3. Literature Review

Advection-dispersion equations are the dominant equations in almost all contaminant transport studies. The spatial and temporal effects of advection-dispersion of microbial transport can be presented using the fundamental law of conservation of mass. Conservation of mass states that a change in microbial mass with respect to time within a control volume is equal to the difference between the microbial mass flow rate into the control volume and microbial mass flow rate out of the control volume. The following schematic illustrates the law of conservation of mass in a control volume having a differential volume ΔV , inflow and outflow area dA, and a length of dx.

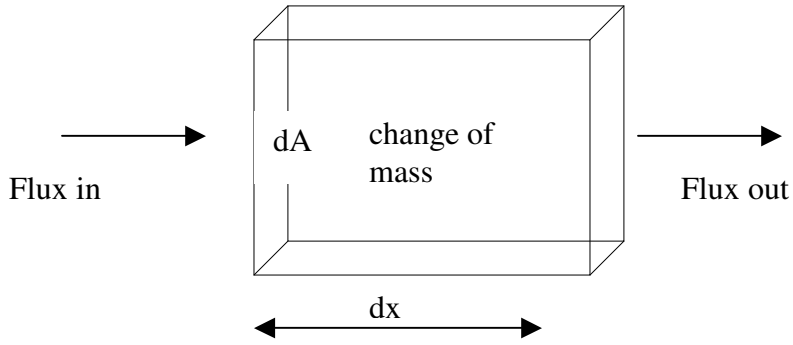

Flux is defined as the mass of microbial transport per unit area of flow (dA) per unit time. The conservation of mass states that rate of change mass in a unit

volume of water is equal to the difference between mass entering the volume and mass leaving the volume and may be presented as:

$$\frac{dm}{dt} = \{\text{Mass}\}_{\text{in}} - \{\text{Mass}\}_{\text{out}} \tag{3.1}$$

where mass (m) equals concentration times volume and $(\text{Mass})_{in}$ and $(\text{Mass})_{out}$ are defined as the mass of solute per unit time (flux of solute mass times the unit area) entering and leaving the control volume, respectively. The left side of Equation 3.1 may be written as:

$$\frac{dm}{dt} = \frac{d(\Delta V \times C\theta)}{dt} = \Delta V \frac{dC\theta}{dt} \tag{3.2}$$

where, C is the concentration (M/L^3), dA is the area of the control volume (L^2), θ is the volumetric water content (cm^3/cm^3), and ΔV is the volume (L^3). The combination of mass flow due to advection and dispersion are presented as:

$$\{\text{Mass}\}_{\text{in}} = \{\text{Mass}\}_{\text{adv}} + \{\text{Mass}\}_{\text{dis}} \tag{3.3}$$

$$\{\text{Mass}\}_{\text{out}} = \{\text{Mass}\}_{\text{adv}} + \{\text{Mass}\}_{\text{dis}} \tag{3.4}$$

where adv, and dis refer to advective and dispersive, respectively. The advective mass flow of bacteria into the control volume is due to the average flow velocity (advective velocity), and is presented as,

$$\{\text{Mass}_{\text{in}}\}_{\text{adv}} = \text{dA. advective flux} = \text{dA.U.C.}\theta \tag{3.5}$$

where U is the advective velocity (L/T). The dispersive mass flow is presented in Equation 3.6 and it is based on the Fick's law of diffusion as:

$$\{\text{Mass}_{\text{in}}\}_{\text{dis}} = \text{dA.dispersive flux} = \text{-dA.D.}\frac{\partial C\theta}{\partial x} \tag{3.6}$$

where D is the dispersion coefficient (L^2/T).

The advection and dispersion mass of bacteria out of the control volume can be then expressed as:

$$\{\text{Mass}_{\text{out}}\}_{\text{adv}} = \text{dA.U.C.}\theta + \text{dA. U.}\frac{\partial C\theta}{\partial x}dX \tag{3.7}$$

$$\{\text{Mass}_{\text{out}}\}_{\text{dis}} = \text{-dA.D.}\frac{\partial C\theta}{\partial x} - \text{dA.D.}\frac{\partial^2 C\theta}{\partial x^2}dX \tag{3.8}$$

where dx is the length of the control value (L).

By substituting Equation 3.2, and Equations 3.5–3.8 into Equation 3.1, the general transport equations becomes:

$$\Delta V\frac{dC\theta}{dt} = \{\text{dA.U.C.}\theta - \text{dA.D.}\frac{dC\theta}{dx}\}_{\text{in}} - \{\text{dA.U.C.}\theta + \text{dA. U.}\frac{\partial C\theta}{\partial x}dX +$$

$$(\text{-dA.D}\frac{dC\theta}{dx} - \text{dA.D.}\frac{\partial^2 C\theta}{\partial x^2}dX)\}_{\text{out}} \tag{3.9}$$

Using the relation $\Delta V = \text{dA.dx}$, and taking the limit as $\text{dx} \longrightarrow 0$ Equation 3.9 is simplified and yields the following equation for the microbial transport:

$$\frac{dC\theta}{dt} = -U\frac{dC\theta}{dx} + D\frac{d^2C\theta}{dx^2} \qquad (3.10)$$

Equation 3.10 assumes that the other fundamental factors such as attachment, detachment, and decay and growth rates of bacteria are neglected. If such factors are incorporated, then Equation 3.10 will get the following form:

$$\frac{dC\theta}{dt} = -U\theta\frac{dC}{dX} + D\theta\frac{d^2C}{dX^2} + B_g + B_{att} - B_{dec} - B_{det} \qquad (3.11)$$

where B is the rate of change of microbial mass per unit volume and time, and the subscripts g, att, dec, and det refer to growth, attachment, decay, and detachment, respectively.

Vilker and Burge (1980) and Matthess and Pekdeger (1981) were amongst the first to apply a transport equation to describe the distribution of bacteria and viruses in time and space. They presented the advection–dispersion equation for microbial transport. Most of today's existing models use numerical methods to approximate the exact solutions of the convective-dispersion equations with given boundary and initial conditions.

Few experimental studies have been performed to evaluate the transport of microorganisms in porous media and to test both specific mathematical models and conceptual approaches. Previous studies on bacterial transport focused mostly on saturated soil conditions (Reynolds et al., 1989). Recently there has been growing interest in evaluating bacterial transport under unsaturated soil conditions (Schafer et

al., 1998; Powelson and Mills, 1998). Preferential sorption and retention of bacteria tend to occur in the air-water interface in the unsaturated zone (Wan et al., 1994).

Tan et al. (1992) conducted experiments on columns of fine and coarse sand to measure the distribution of *Pseudomonas fluorescens* during unsteady and unsaturated flow conditions. Due to the short duration of experiments (less than one hour), no substrate was added. Therefore, the decay and growth rates were neglected and only adsorption of bacteria was considered in their experiments. Because their experiments were conducted on sandy soil, the water flow velocities were quite high and the d_m/ds ratio was very small (no straining of bacteria), the advection flow dominated the microbial transport and the chemotactic velocity was ignored (d_m and d_s were the average diameter of microorganisms and soil particles, respectively). The combination of the continuity equation (Equation 3.12), the combined flux of bacteria including advection flux (J_v), chemotactic flux (J_x), and the combination of dispersion, diffusion, and random motility (J_d) from Equation 3.13, and the rate of change of the attached biomass (Equation 3.14) resulted the Tan et al. (1992) model (Equation 3.15) to predict the concentration of bacteria.

$$\frac{d(\theta\, C)}{dt} + \frac{d(\rho_s\, C^a)}{dt} = -\nabla \cdot J + R_g - R_d \qquad (3.12)$$

where,

$\theta\, C$ = total biomass in the solution phase

$\rho_s C^a$ = total biomass in the attached phase

C^a = concentration of attached bacteria

$J = J_v + J_x + J_d$

J_v = advective flux of bacteria = $v_w \theta C$

J_x = chemotactic flux of bacteria = $v_x \theta C$

J_d = combined diffusion, dispersion and random motility flux of bacteria

$= \tau \theta D \nabla C$

v_w = velocity of flowing water

v_x = active chemotactic velocity of bacteria

D = diffusion coefficient (D_d) + hydrodynamic dispersion coefficient (D_h) + random motility coefficient (D_t).

τ = tortuosity (can be set to unity for solute transport (Bond, 1987))

R_g, R_d = growth and decay rates of the microorganisms combined for the water and attached biomass phases (mass of microorganisms per unit volume and time)

$$J = v_w \theta C + v_x \theta C - \tau \theta D \nabla C \tag{3.13}$$

$$\frac{d(\rho_s C^a)}{dt} = R_a - R_y + R_g^a - R_d^a \tag{3.14}$$

$$\frac{d(\theta C)}{dt} + \rho_s k_f N C^{N-1} \frac{dC}{dt} = \frac{d}{dx}(\theta D \frac{dC}{dx} - v_w \theta C) \tag{3.15}$$

where θ is the soil volumetric water content (L^3/L^3), C is the concentration of bacteria in solution (M/L^3), v_w is water velocity (L/T), D is the total diffusivity (the sum of diffusion, hydrodynamic dispersion, and the random motility coefficients), τ is the pore space tortuosity (assumed to equal to one for transport (Bond, 1987)), R_a, and R_y

are the rates of attachment and detachment of bacteria, respectively, and R_g^a, *and* R_d^a are the growth and decay rates of bacteria, respectively.

The Freundlich isotherm (Equation 3.16) was used to define the adsorbed mass of bacteria on the soil solid particles as:

$$C^a = k_f C^N \tag{3.16}$$

where C^a (a refers to adsorption) is the mass of microorganisms adsorbed per unit mass of solid particles, C is the concentration of microorganisms in solution, k_f and N are empirical constants and when N is equal to unity, the Freundlich isotherm becomes a linear isotherm.

Harvey and Garabedian (1991) developed an advection-dispersion model to include attachment and detachment of microorganisms. Their model assumed that growth and decay rates of bacteria were not important to bacteria transport through groundwater, thus they were neglected. Their model further assumed that adsorption of bacteria was at equilibrium and detachment was neglected. With respect to the movement mechanism of microorganisms, they further assumed that chemotactic movement of bacteria is not important, therefore, it was neglected. The model is presented in Equation 3.17 and it is in terms of only concentration, C.

$$\frac{d(\theta\, C)}{dt} + \rho_s k_f \frac{dC}{dt} = \theta\, D \frac{d^2C}{dx^2} - v_w \theta \frac{dC}{dx} - k_a \theta\, C \tag{3.17}$$

where k_a is the attachment coefficient. Although growth and decay terms were not included in the model, their predicted results appeared similar to their measured data.

Tan et al. (1994) studied another model on a column of packed coarse sand to evaluate the transport of bacteria. These experiments were conducted under three different bacteria concentrations (10^7, 10^8, 10^9 bacteria/liter of solution). The experiments were conducted under very low temperature conditions to limit the decay and growth activities of the bacteria. A Newton-Raphson iteration was coupled to the Crank-Nicolson scheme to solve the partial differential equations. They used a breakthrough curve obtained from a chloride tracer to estimate the dispersion coefficient, D. The soil water flow velocity, v_w, was calculated from the inflow and the average water content. The attachment coefficient, k_a, the detachment coefficient, k_y, and the maximum concentration of retained bacteria (maximum mass of bacteria retained by unit mass of soil particles), C_m^a, were estimated by an optimization technique to minimize the standard error. Their models are presented in Equations 3.18 and 3.19.

$$\theta \frac{dC}{dt} = \theta\ D \frac{d^2C}{dx^2} - v_w \theta \frac{dC}{dx} - k_a \frac{(C_m^a - C^a)}{C_m^a} \theta C + k_y \rho_s C^a \quad (3.18)$$

$$\rho_s \frac{dC^a}{dt} = k_a \frac{(C_m^a - C^a)}{C_m^a} \theta\ C - k_y \rho_s\ C^a \quad (3.19)$$

where m refers to the maximum and a is defined earlier.

These models also assumed that chemotactic movements of bacteria are not important and they were neglected. Equations 3.20 (Tan et al., 1994), and 3.21 (Corapcioglu and Harris, 1984) describe the rate of attachment and detachment of bacteria as:

$$R_a = k_a \ (1 - \frac{C^a}{C_m^a})\theta \ C \tag{3.20}$$

$$R_y = k_y \ \rho_b \ \sigma^h \tag{3.21}$$

where ρ_b is the mass density of bacteria, and σ is the volume of bacteria per unit volume of porous media, h is an empirical constant and assumed to be equal to one (Tan et al., 1994). After substituting $\rho_s \ C^a$ for $\rho_b \ \sigma$ in Equation 3.21, their model was finalized to Equations 3.18 and 3.19.

There are many computer models that simulate the contaminant transport in one, two, or three dimensions both in saturated and unsaturated zones. MWASTE is a model that was developed by Moor et al. (1988) to simulate waste generation and calculate the microbial concentrations in runoff from land-applied waste and management practices. The hydrological data to run the MWASTE model were obtained by a data file created by CREAMS (Thomas et al., 1989) non-point source pollution model. CREAMS is a field scale model developed to evaluate the runoff, chemicals, and erosion from agricultural management systems.

PRZM (Pesticide Root Zone Model) is a one-dimensional finite-difference model developed by Carsel et al. (1984) at the EPA Environmental Research Laboratory in Athens, Georgia. It consists of hydrologic (flow) and chemical transport components to simulate runoff, erosion, plant uptake, leaching, decay, and

volatilization. Pesticide transport and fate processes simulated in PRZM include advection, dispersion, molecular diffusion, and soil sorption. The model includes soil temperature effects, volatilization and vapor phase transport in soils, irrigation simulation and a method of characteristics algorithm to eliminate numerical dispersion. Predictions can be made for daily, monthly, or annual output. PRZM allows the user to perform dynamic simulations considering pulse loads, predicting peak events, and estimating time-varying emission or concentration profiles.

HYDRUS-2D (Simunek et al., 1999) is a Microsoft Windows based model that analyzes water flow and solute transport in unsaturated, partially saturated, or fully saturated porous media. This model was developed by the United States Department of Agriculture (USDA)/Agricultural Research Service (ARS) salinity laboratory, and uses finite elements techniques to solve the Richards' equation for saturated-unsaturated water flow. It is based on advection-dispersion equations for heat and solute transport. The model incorporates a sink term to account for water uptake by plant roots. This model may also be used to analyze water and solute movement in unsaturated, partially saturated, or fully saturated porous media.

GLEAMS (Leonard et al., 1987) is a continuous simulation model used to simulate processes affecting water quality events on an agricultural field using daily meteorological input such as precipitation and temperature. GLEAMS uses a storage routing technique to allow vertical movement of precipitation in excess of runoff through the root zone to the percolation depth. It includes pesticide degradation, convective transport, and loss via evapotranspiration and plant uptake. GLEAMS,

HYDRUS-2D, PRZM, and CREAMS models do not have a pathogen transport component.

Sadeghi and Arnold (2001) extended the Soil Water Assessment Tool (SWAT) capability by incorporating and validating a microbial sub-model component. The model contains functional relationships for both the die-off and re-growth rates, and an optional process that can easily be adapted to simulate both the release and transport of pathogenic organisms.

Regardless of the capabilities of some models to simulate pollutant transport, one has to keep in mind that different models have different constituents and limitations. Regardless of their types and applicability, they sometimes break down when used beyond their original scope of validity (Shirmohammadi et al., 2002). In another study, Shirmohammadi et al. (2001) used the GLEAMS model to simulate atrazine leaching through a coastal plain soil profile in the coastal plain of Maryland. Because GLEAMS is a Darcian-based model and does not consider the macropore effects, it failed to provide a proper trend in atrazine concentrations.

Sabu et al., (2002) used the "Better Assessment Science Integrating Point and Non-Point Sources (BASINS)" model to study its applicability as a prediction tool for uncertainty analysis for in-stream fecal coliform bacteria concentration. Their study showed that the major portion of the variance in simulated in-stream peak fecal coliform concentration was attributed to the maximum storage of fecal coliform on the pervious land surface.

MIKE SHE is an integrated, physically based, distributed model that simulates hydrological and water quality processes on a basin scale. The original MIKE SHE

(DHI, 1998) model was developed and became operational in 1982. The model was sponsored and developed by three European organizations: the Danish Hydraulic Institute (DHI), the British Institute of Hydrology, and the French consulting company SOGREAH.

MIKE SHE allows components to be used independently and customized to local needs. It is capable of simulating both surface and subsurface water flow. It models most major hydrological processes of water movement, including canopy and land surface interception after precipitation, snowmelt, evapotranspiration, overland flow, and saturated and unsaturated water flow. The MIKE SHE advection-dispersion module (MIKE SHE AD) simulates major solute transport under both saturated and unsaturated soil conditions. The MIKE SHE sorption/degradation module (MIKE SHE SD) simulates the sorption and attenuation of solute in both saturated and unsaturated soil conditions. It also evaluates the pollutant transport through soil macropores. The Biodegradation module (MIKE SHE BM) is aimed at simulating the growth and decay of the microbial population.

3.4. Theoretical Background On The Model Development

3.4.1. Surface Runoff Model

For concentration of FC in runoff, the KORMIL2 model (Choi, 1992) was selected for its relative simplicity and applicability and was modified to fit the objectives within the context of the lysimeter dimensions and characteristics. Choi's model is a numerical-based model using the kinematic wave equations for overland runoff simulations in an intervening land system. The kinematic wave in the KORMIL2 model is a simplified form of the full dynamic St. Venant equations, or

shallow water equations that comprise the continuity and momentum equations (Liggett and Woolhiser, 1976). It uses a depth-discharge relationship (Equation 3.22), and Manning's equation (Equation 3.23) with spacing hydraulic radius instead of flow depth.

$$\frac{dA_t}{dt} + \frac{dQ_t}{dx} = q_t - f_t \tag{3.22}$$

$$Q = \frac{1}{n} R^{\frac{2}{3}} S^{\frac{1}{2}} A \tag{3.23}$$

where A_t is the total cross-sectional flow area (m^2), x is the distance (m), Q_t is the total discharge (m^3/sec), q_t is the total lateral inflow (m^3/sec/m), f_t is the total lateral outflow (m^3/sec/m), R is the hydraulic radius (m), and S is the bed slope (m/m).

Since grass stem diameter and density affect the overland flow mechanism (Fenzl, 1962; Barfield et al., 1978), KORMIL2 uses the hydraulic radius in Manning's equation instead of mean flow depth to reflect the real flow dynamics in vegetated areas. The flow depth is corrected by a factor a to reflect the effects of media spacing and diameter on the flow depth. The continuity equation (Equation 3.22) is rewritten for unit width to yield (Miller, 1984; Huggins and Burney, 1982):

$$\frac{dA_n}{dt} + \frac{dQ}{dx} = qe \tag{3.24}$$

where A_n is the net flow cross sectional area (m^2), t is time (sec), Q is runoff rate (m^3/sec), x is distance along the flow path (m), and qe is the net lateral inflow per unit width (m^3/sec/m^2). The net flow area A_n is calculated by:

$$A_n = (1\text{-}NG_{ave}.d_{ave})\ y \tag{3.25}$$

where NG_{ave} is the average number of grass stalks per unit width, equal to $1/S_s$ where S_s is the mean media spacing (m), d_{ave} is the average diameter of grass stalks (m), and y is the mean flow depth (m). Both mean media spacing and average diameter of grass stems are input data. Considering the mean media spacing and average stem diameter, Equation 3.24 is rewritten to yield:

$$a\frac{dy}{dt} + \frac{dQ}{dx} = qe \tag{3.26}$$

where a is defined as:

$$a = 1\text{-}\left(\frac{1}{S_s}\right) d_{ave} \tag{3.27}$$

Equation 3.26 is a continuity equation for overland flow in a vegetated surface used in the simulation of surface concentration of fecal coliform. The hydraulic radius in Manning's Equation (3.23) was replaced with a new corrected defini tion to consider the effect of vegetated surface when computing the hydraulic radius. As a result, the hydraulic radius is defined as:

$$R = \frac{S_s * y}{2y + S_s} \tag{3.28}$$

Substituting R into Equation 3.23 yields the following:

$$Q = \frac{aS^{\frac{1}{2}}}{n}\left\{\frac{S_s\ y^{\frac{5}{2}}}{2y + S_s}\right\}^{\frac{2}{3}} \tag{3.29}$$

All of the parameters in Equation 3.29 are defined above. Equations 3.27 and 3.29 constitute the governing equations for determining the overland flow through vegetated surfaces. The finite difference method was used to solve Equations 3.27 and 3.29.

In constructing the finite difference formula for Equation 3.27, while Choi's (1992) KORMIL2 model uses the infiltration values computed by Horton's equation, the modified KORMIL2 model (MODCHOI in this study) uses the infiltration values obtained from both the measured data and the Green and Ampt infiltration model. To this effect, two separate polynomial models representing infiltration for bare and vegetated surfaces are obtained using the measured infiltration data. These models were used in the modified model (MODCHOI) to replace the Horton's model. The derivative of the infiltration function with respect to time then yielded the values for infiltration rate as:

$$f = \frac{dF}{dt}\Big|_{at\ every\ \min ute} \tag{3.30}$$

3.4.2. Infiltration Model

Infiltration may be predicted by existing models such as Green and Ampt (1911), Horton (1939), Philip (1957), and Schmid (1990). In choosing an appropriate model to predict a reasonable infiltration, one has to understand the input parameters required to simulate the model. Among the mentioned models, Green and Ampt, Philip, and Schmid models are more appropriate for optimization and prediction of infiltration when tested with the field measured infiltration data. Because Green and Ampt is a physically based model, this optimization lead the Green and Ampt infiltration model to be the appropriate model amongst others for prediction of

infiltration in this study. Therefore, modeling infiltration consists of two major parts. The first part is to choose the most applicable model to predict the infiltration, and the second part is to develop a computer model for the selected infiltration model. The aforementioned infiltration models are presented in Equations 3.31-3.38.

$$f = K_s + \frac{K_s(\theta_s - \theta_i)}{F} \times S_f \quad \text{(Green and Ampt)} \qquad (3.31)$$

$$F = (\theta_s - \theta_i) \times L_f \quad \text{(Green and Ampt)} \qquad (3.32)$$

Where f is the infiltration rate (L/T), K_s is the saturated hydraulic conductivity (L/T), θ_s and θ_i are the saturated and initial water content (L^3/L^3), S_f is the suction ahead of wetting front (L), and F is the total infiltration (L).

$$f = \tfrac{1}{2} S_p \times t^{-1/2} + K_p \quad \text{(Philip)} \qquad (3.33)$$

$$F = S_p \times t^{1/2} + K_p \times t \quad \text{(Philip)} \qquad (3.34)$$

where S_p is the sorptivity ($LT^{-1/2}$) and is approximately given by

$$S_p = (2K_s S_f)^{1/2} \qquad (3.35)$$

and K_p is often taken to equal K_s for a longer duration which is consistent with the Green and Ampt approach. However, for a shorter duration, K_p generally stays in the range of $K_s / 3 < K_p < 2K_s / 3$ (Sharma et al., 1980). Philip approach applies only after the time of ponding.

$$f = w\{1+2\frac{(w-K_s)^2}{K_s S_f (\theta_s-\theta_i)}\times t\}^{-1/2} \qquad \text{(Schmid)} \qquad (3.36)$$

$$F = K_s w\frac{S_f (\theta_s-\theta_i)}{(w-K_s)^2}\times\{[1+2\frac{(w-K_s)^2}{K_s S_f (\theta_s-\theta_i)}t]^{1/2}-1\}$$

$$\text{(Schmid)} \qquad (3.37)$$

where w is the rain intensity (L/T) and other parameters were defined earlier. Equations 3.36 and 3.37 are valid for the condition of X shown in the Equation 3.38.

$$X = \frac{F}{S_f (\theta_s-\theta_i)+wt_p} < 1 \qquad (3.38)$$

Where t_p is the time of ponding.

To compare the infiltration model performances using paired residuals, the Williams-Kloot (1953) criterion was applied. Green and Ampt, Philips, and Schmid infiltration models were fitted in pairs to measured infiltrations data and produced residuals $R_{i, G \& A}$, $R_{i, Philip}$, and $R_{i, Schmid}$. To apply the Williams-Kloot criterion, four auxiliary values ($M_i = R_{i, G \& A} - R_{i, Philip}$, $N_i = ½ (R_{i, G \&A} + R_{i, Philip})$, $T_i = R_{i, G \& A} - R_{i, Schmid}$, and $U_i = ½ (R_{i, G \& A} + R_{i, Schmid})$ were formed and slopes a and b of the regressions M = aN, and T = bU were estimated. The hypothesis of the models' performance could not be rejected if the values a and b did not differ significantly from zero. The Green and Ampt and Philip models performed a better fit when slopes a and b became significantly less than or greater than zero, respectively. The

following is the set of procedures for selecting the best model using Williams-Kloot criterion:

1. Residual I = Measured - Model I

2. Residual II = Measured - Model II

3. Residual I – Residual II

4. ½ (Residual I + Residual II)

5. Regression of Residual I – Residual II on ½ (Residual I + Residual II)

6. Find slope of the regression, and Std. Error of the slope

7. Calculate $\left| \frac{Slope}{Std.Error} \right|$

8. Assume level of confidence, α and find t from the table

9. $\left| \frac{Slope}{Std.Error} \right| < t_{critical}$ — Yes: Not comparable; No: slope < 0: Choose Model I; slope > 0: Choose Model II

3.4.3. Kinematic Wave Model (KINSUB)

To simulate the vertical movement of bacteria, a kinematic wave based equation was used. By definition, a kinematic wave equation is a convective-dispersive equation with no dispersion term. Elimination of the dispersion component was due to the fact that the main transport vector for bacteria is the advection process and not the dispersion process. Therefore, only the convective term was involved in

modeling the vertical transport of bacteria. The following one-dimensional equation was used for the vertical transport of bacteria in this study:

$$\frac{d(\theta\, c)}{dt} + \frac{d(q\, c)}{dz} + \mu c + \rho_b \frac{dS}{dt} = 0 \qquad (3.39)$$

where θ is the soil volumetric water content (cm^3/cm^3) and is assumed to be constant initially (based on the Green and Ampt model's assumption), c is the concentration of bacteria (g/cm^3), q is the soil water flux ($cm^3/cm^2/min.$), μ is the constant of entrapment-entrainment (1/min.), z is the vertical distance in the soil profile (cm), ρ_b is the soil bulk density (g/cm^3) and S is the concentration of the adsorbed fraction (mass of bacteria to mass of soil), which has a linear relationship to the solute concentration in pore water as;

$$S = K_d\, C \qquad (3.40)$$

where K_d is the distribution coefficient indicating the ratio between the adsorbed chemical concentration and dissolved chemical concentrations (cm^3/g of soil). Since θ is constant and there is a linear relationship between S and C, Equation 3.39 may be written as:

$$\frac{d(\theta\, c)}{dt} + \frac{d(q\, c)}{dz} + \mu c + \rho_b \frac{dK_d c}{dt} = 0 \qquad (3.41)$$

$$\theta\, \frac{dc}{dt} + \frac{d(q\, c)}{dz} + \mu c + \rho_b K_d \frac{dc}{dt} = 0 \qquad (3.42)$$

or

$$\frac{dc}{dt}(\theta + \rho_b K_d) + \frac{d(q\,c)}{dz} + \mu c = 0 \tag{3.43}$$

By rewriting Equation 3.43, the following equation may be obtained:

$$\theta\,(1+\frac{\rho_b K_d}{\theta})\frac{dc}{dt} = -\frac{d(qc)}{dz} - \mu c \tag{3.44}$$

$$\theta\,\mathrm{R}\frac{dc}{dt} = -\frac{d(qc)}{dz} - \mu c \tag{3.45}$$

where R is the total retardation coefficient and is related to the soil bulk density and soil water content θ, and is equal to:

$$\mathrm{R}=1+\frac{\rho_b K_d}{\theta} \tag{3.46}$$

Differentiating Equation 3.45 with the chain rule yields the following equation:

$$\theta\ R\ \frac{dc}{dt} = -q\frac{dc}{dz} - c\frac{dq}{dz} - \mu\ c \tag{3.47}$$

Assuming piston flow within the soil profile (based on Green and Ampt assumption) yields $\frac{dq}{dz} = 0$, and Equation 3.47 may be rewritten in the following form:

$$\theta\,\mathrm{R}\frac{dc}{dt} = -q\frac{dc}{dz} - \mu c \tag{3.48}$$

Equation 3.48 is the kinematic wave equation of solute transport with constant water content and an instantaneous linear adsorption.

Defining c = u exp $(-\frac{\mu}{R\theta}t)$, and using the Chain rule, Equation 3.48 becomes:

$$\theta R \frac{dc}{du}\frac{du}{dt} = -q\frac{dc}{dz} - \mu c \tag{3.49}$$

where u is the concentration at the surface.

Dividing Equation 3.49 by $\frac{dc}{du}$ yields:

$$\frac{\theta R \frac{dc}{du}\frac{du}{dt}}{\frac{dc}{du}} = \frac{-q\frac{dc}{dz} - \mu c}{\frac{dc}{du}} \tag{3.50}$$

$$\theta \mathrm{R}\frac{du}{dt} = -q\frac{du}{dz} - \mu \mathrm{c}\ \frac{du}{dc} \tag{3.51}$$

Because u is constant along the characteristic lines, $\frac{du}{dc} = 0$, and Equation 3.51 will be reduced into the following form:

$$\theta \mathrm{R}\ \frac{du}{dt} = -q\frac{du}{dz} \tag{3.52}$$

Dividing equation 3.52 by du, the following equation is formed:

$$\frac{dz}{dt} = -\frac{q}{\theta R} \tag{3.53}$$

Considering the Green and Ampt approximation in which q is the infiltration rate and it is a function of time alone, the equation of characteristic lines may be written as:

$$\mathrm{Z} = \frac{1}{R}\int_{tt}^{t} \frac{q(s)}{\theta} dt \tag{3.54}$$

$$Z = \frac{1}{R}\frac{Q(t) - Q(t_0)}{\theta} \tag{3.55}$$

where Q is the cumulative infiltration ($cm^3\ cm^{-2}$), and t_0 is the time when the characteristic line at point (z, t) crosses the axis at Z = 0.

Because u is constant along each of the characteristic lines, the following equation may be achieved:

$$C(t) = C_s(t_0) \exp\left[-\frac{\mu}{R\theta}(t - t_0)\right] \tag{3.56}$$

Equation 3.56 indicates that the concentration along each characteristic line exponentially decreases from its initial concentration at the surface (C_s) as time progresses.

Overall the modeling effort in this study produced three different modules as indicated in Figure 3.3 and listed below:

1. MODCHOI: This component uses the continuity equation for overland flow and the convective-dispersive equation for the surface concentration of FC.
2. Green and Ampt infiltration model: This model computes infiltration for the time interval of interest, which is used as input into both KINSUB and MODCHOI (modified KORMIL2) models.
3. KINSUB: This model uses the 1-D kinematic wave form of the convective-dispersive equation and computes the vertical migration of FC.

3.5. Model Calibration

To get the optimal solution that best fits the models, input parameters were adjusted either manually or by formal mathematical procedures. Zheng and Bennet (1995) suggested that these procedures be continued until the best agreement between the model output and the observed field data was achieved. The field-observed data used in this calibration came directly from the actual experiments conducted at the lysimeter site in Greenbelt, Maryland.

Two approaches may be used to perform model calibration: (1) manual trial and error approach to select parameter values; and (2) automated selection of parameter values. In the trial and error approach, values are initially assigned and then they are arbitrarily adjusted based on the experience of the modeler within a reasonable range in a series of runs to match the measured data. This method of model calibration does not have a unique solution because different combinations of parameter values may lead to the same results. The automated calibration process is an inverse modeling where the relationships between the parameters, model predictions, and the observed data are mathematically quantified by least-squares regression to provide the best-fit estimates for the model (Scott et al., 2003). The range of parameter values for this method is unlimited and may not be subjective and is not influenced by the modeler. However, it may suffer from complication and computer execution time and the same non-uniqueness issues. In this method, an objective function will be minimized by multiple weighted parameter values to incorporate the uncertainty in the calibration process.

In either case, the results of calibration should be compared with the measured field data both quantitatively and qualitatively. For the qualitative evaluation of the calibration, the overall trend of the calibrated data is compared to the trend of the measured values by visual inspection. The quantitative evaluation of the calibration considers the direct comparison of predicted values relative to the measured values, and determines the degree of agreement by appropriate statistics.

3.6. Model Input Parameters

The parameter values for simulation of models may be obtained by three distinct methods: direct measurements, available literature and the modeler's experience, and the process of model calibration itself. Due to experimental difficulties, parameter estimation often becomes an iterative or fine tuning process (Hutson and Wagenet, 1991).

Infiltration parameter values determined from the measured data included initial and saturated soil water contents, saturated hydraulic conductivity, moisture deficit, and the suction ahead of the wetting front. These values were then modified within reasonable range to best fit the measured infiltration data. Modifications were necessary because measured parameter values in the laboratory do not consider field variability due to heterogeneity, scale differences, etc. Parameters were also compared with data provided by Rawls et al. (1998).

Cumulative infiltration (F) was calculated at every five-minute interval using a simple mass balance equation (infiltration = rainfall - runoff). Then, a cubic polynomial was fitted to represent cumulative infiltration versus time. Finally, the

infiltration rate (f) versus time was computed by determining the derivative of the function F versus time at every one-minute interval for the 60 minutes duration.

Cumulative infiltration, and surface concentration of FC (C_s) were provided as input data files to solve Equations 3.47 and 3.48. The retardation coefficient (R) in Equations 3.47 and 3.48, the soil water content (θ), and the entrapment-entrainment constant (μ) were defined with appropriate input values. The depth increment selected for the model simulation was similar to the analysis of FC.

Table 3.1. Estimated parameters to simulate the models

β	Proportionality factor (percentage of manure contributed in runoff)
μ	Constant of entrapment-entrainment
R	Retardation factor
n	Manning's roughness coefficient
k_f	Fast release rate coefficient
k_s	Slow release rate coefficient

3.7. Model Sensitivity Analysis

Sensitivity analysis should be considered as an essential step in mathematical modeling. Evaluating a model's response to any alteration in input parameters is the most important aspect of any sensitivity analysis. In the process of modeling, sensitivity analysis can be utilized for a better identification of a set of the specific input parameters to which the model is most sensitive. Once the analysis identifies the

most important input parameters, field sampling may be used to obtain the most accurate values for such parameters. In addition, the modeler may concentrate on assigning proper values for such sensitive parameters during the calibration stage of the model.

If results indicate model sensitivity to a certain parameter, the uncertainty associated with that parameter may significantly affect the model predictions. Cases where results do not reflect any sort of sensitivity with respect to a given parameter cause little impact on the model's prediction due to the uncertainty associated with that particular parameter (Zheng and Bennett, 1995). The main advantage of a sensitivity analysis in evaluating uncertainty is its simplicity, flexibility, and versatility (Uhl and Sullivan, 1982).

3.8. Sensitivity Coefficient

Sensitivity is a measure of the impact of change in one input parameter on the output results. The coefficient of sensitivity can be defined as the ratio of the change in the dependent variable to the change in the input parameter. Two types of sensitivity coefficients, absolute sensitivity and relative sensitivity can be calculated (Haan, 1995). The absolute sensitivity, S is calculated as:

$$S = \frac{\partial y}{\partial x} \tag{3.57}$$

where S is the sensitivity coefficient, y is the dependent variable, and x is the independent input parameter. The relative sensitivity, S_r is calculated as:

$$S_r = \frac{\partial y}{\partial x} * \frac{x}{y} \qquad (3.58)$$

The relative sensitivity is the percent change in the output for a unit change in input.

3.9. Approaches to Compute Sensitivity Coefficient

There are different methods to determine the sensitivity coefficients. They include the adjoin, perturbation, and direct methods (Skaggs and Barry, 1996). The perturbation method is known as the divided difference method. It is the simplest of the sensitivity methods to determine the dominant parameters. It computes a numerical approximation for the sensitivity coefficient for the model input parameters. The direct method analytically computes the sensitivity coefficient by differentiating the governing equations of sensitivity under specific boundary and initial conditions with respect to the model input parameters. The adjoin method uses similar sensitivity equations, and gets the sensitivities by solving the adjoin problems. In this method, the dependent variables are formulated and their sensitivities are computed directly without evaluating the sensitivities of independent variables (Skaggs and Barry, 1996). Skaggs and Barry (1996) used a series of reasonable parameter values of soil moisture deficits (θ_{sat} - θ_i) and soil saturated hydraulic conductivities (K_s) to measure the impact of change in these parameters on infiltration.

3.10. Model Layout and Numerical Solution Techniques

A finite difference approach was used to solve kinematic wave equations in the modified Choi's model (MODCHOI) . Figure 3.1 shows the schematic diagram for node generation. Every six centimeters of flow path was considered to be a nodal point. The large filled-circles on each row indicate the positions of runoff sampling funnels relative to the ridge of the lysimeter.

Method of characteristics (MOC) was used to simulate the vertical transport of FC concentration by solving the one dimensional kinematic wave model (Equation 3.48). The schematic diagram of characteristics lines is shown in Figure 3.2.

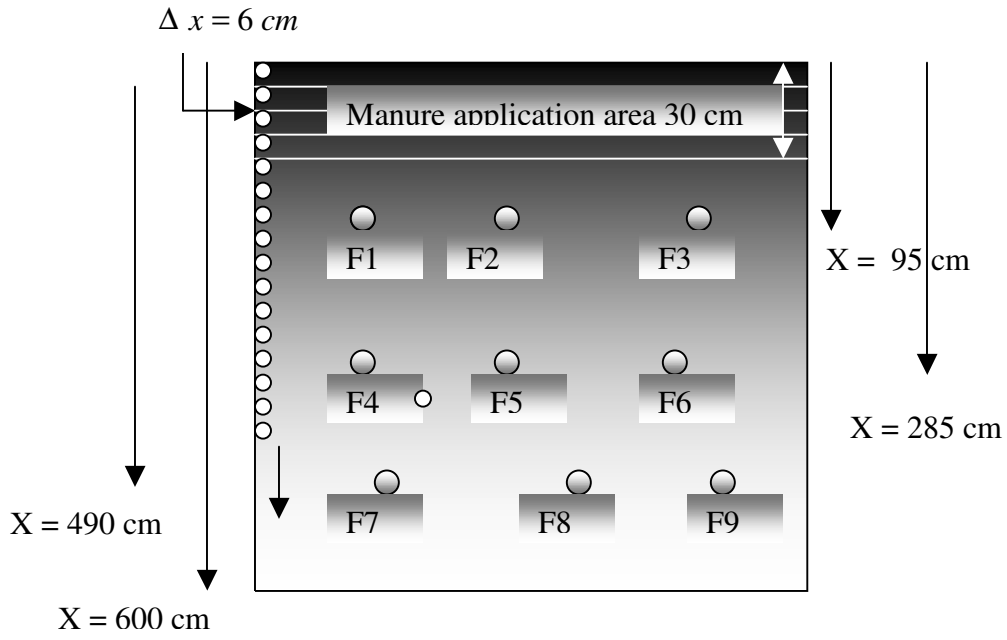

Figure 3.1 Schematic diagrams of the nodes orientation for the experimental site (not to scale).

The MOC was developed by Garder et al. in 1964 mainly to overcome the numerical dispersion problem resulting from solving the advection-dispersion equation with conventional finite-difference techniques. Having "tabs.txt" (data file that contains total infiltration (Q, cm) and the surface FC concentration (Cs (t_0), cfu/cm^3) at one-minute time interval) as an input data file to the KINSUB, the following steps were incorporated in the KINSUB model to simulate the concentration of FC within the soil profile by the MOC.

1. Assume Q (t) be the total infiltration at the end of rainfall simulation
2. Read the first sampling depth (z) from the input data (ztab.txt which contains depths for soil samples);

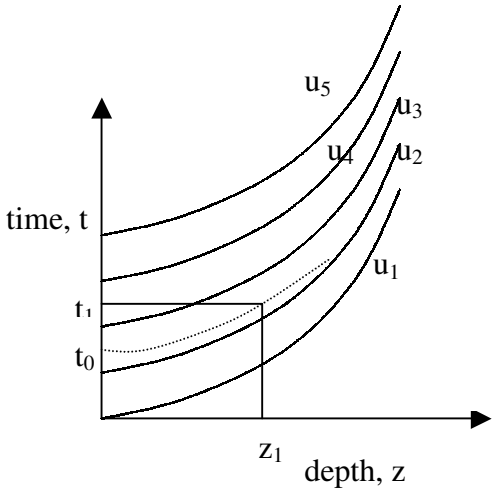

Figure 3.2. Characteristic curves provided to KINSUB model to simulate the vertical transport of FC within the soil profile.

3. Assume a value of R, the retardation factor, and the water content, θ, the Q (t_0) may be calculated using Equation 3.55;

4. Knowing Q (t_0) (from step 3), the corresponding time (t_0) and its surface concentration (Cs (t_0)) may be solved from data file tabs.txt.
5. Assume a value for constant of entrapment-entrainment, μ , solve for the concentration of FC for the selected depth using Equation 3.56 since Cs (t_0), R, θ , t (time at the end of the rainfall simulation), t_o (corresponding time for Cs (t_0)) are known; and
6. Use the same steps to determine the FC concentration for the remaining depths.

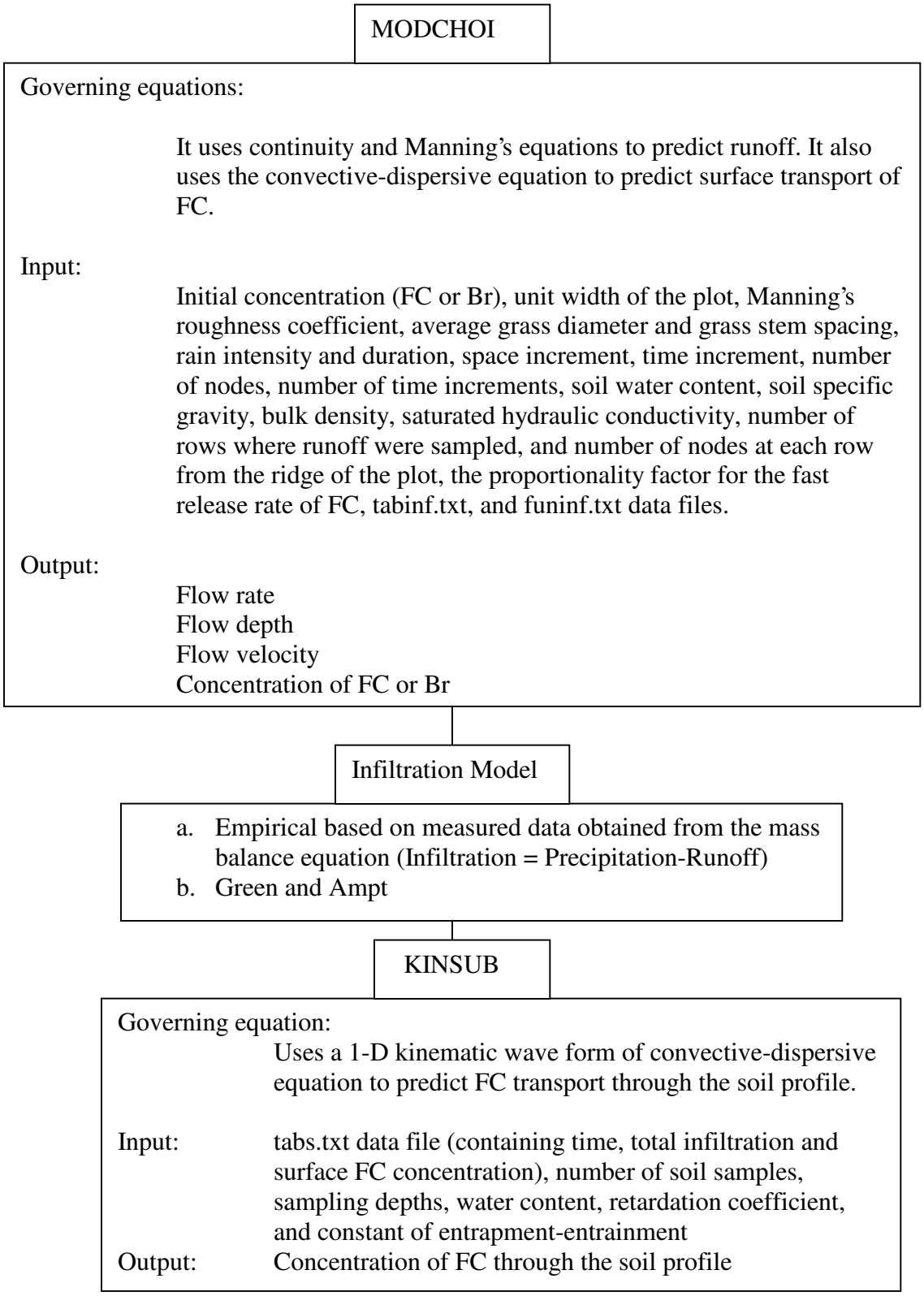

Figure 3.3. Schematic chart showing different modules of the models used in this study.

3.11. Results and Discussion

The results of sensitivity analysis presented in Figures 3.4 and 3.5 indicate the sensitivity of infiltration to both soil moisture deficit and saturated hydraulic conductivity. However, the graphs clearly indicate that the saturated moisture content had a higher influence on total infiltration. Sensitivity analysis also indicated that infiltration is sensitive to slope and the surface condition. The results of simulated infiltration (Figures 3.6 and 3.7) indicate that the Green and Ampt infiltration model more closely predicted infiltration than the Philip and the Schmid (Modified Green and Ampt) model when compared to the measured data. Based on these results, the simulated infiltrations from the Green and Ampt model were used with the kinematic wave model to simulate the FC concentrations within the soil profile. Comparison of simulated infiltration using the Green and Ampt model and the measured data are presented in Figures 3.6-3.8.

The trend of simulated results from all infiltration models seems to suggest that all of the models performed reasonably well compared to the measured infiltration data in the bare clay loam plot (Figure 3.6). However, observations of model performance on the bare sandy loam soil showed that the Green and Ampt infiltration model predicted a better infiltration than the Philip and the Schmid models (Figure 3.7). This may be attributed to the fact that Green and Ampt model is developed based on the concept of the piston flow, which is inherent in sandy loam soils. Figure 3.8 shows the graphical comparison of the Green and Ampt model's simulation with the measured infiltration data for all four plots. Plots 1, 2, 3, and 4 represent bare clay loam, vegetated clay loam, bare sandy loam, and vegetated sandy

loam, respectively. Results indicate that the Green and Ampt model performed well regardless of soils and surface conditions. Such results were not too surprising for the sandy loam soil, but were contrary to the literature findings regarding the clay loam soil (Shirmohammadi and Skaggs, 1985; Bergstrom and Shirmohammadi, 1999). Steep slope (20%) in this experiment may be the culprit regarding the low infiltration amounts, thus not showing a drastic difference between measured and simulated values.

Statistical results of the William–Kloot Criterion for comparing infiltration models are presented in Table 3.2. Results show that the Green and Ampt infiltration model predicted a better infiltration than the Philip and the Schmid infiltration models as it was compared to that of the calculated infiltration from measured hydrologic data. Results of model performance using paired residuals showed greater t-statistics than the $t_{critical}$ values in bare clay loam and bare sandy loam plots ($T_{0.95}$ = 6.536, and 3.734 for Green and Ampt and Philip pair, $T_{0.95}$= 4.3271, and 4.04 for the Green and Ampt and Schmid pair, in bare clay loam and bare sandy loam, respectively) indicating significant difference in models prediction at a level of confidence of α = 0.05 (Table 3.1). Negative slopes in both cases indicated better prediction of the Green and Ampt model over the Philip and Schmid models when compared to the measured infiltration data (slope= -1.897, -0.6197, -0.9, and –0.7381, in bare clay loam and bare sandy loam soils, respectively). Although the $T_{0.95}$ values for both vegetated plots showed no significant difference between the model's performance ($T_{0.95} < t_{critical}$), negative values of slopes indicated a better prediction of the Green and Ampt model over the Philip and Schmid models (Table 3.2). Results only showed a

positive slope when Green and Ampt and Schmid were compared against the measured infiltration data (slope = 0.483), indicating a better performance of the Schmid model over the Green and Ampt model. However, the t-statistic result ($T_{0.95}$ = 2.1586 < $t_{critical}$ = 2.45) indicated no significant difference in their prediction. Procedures for William-Kloot Criterion are presented in section 2.11.

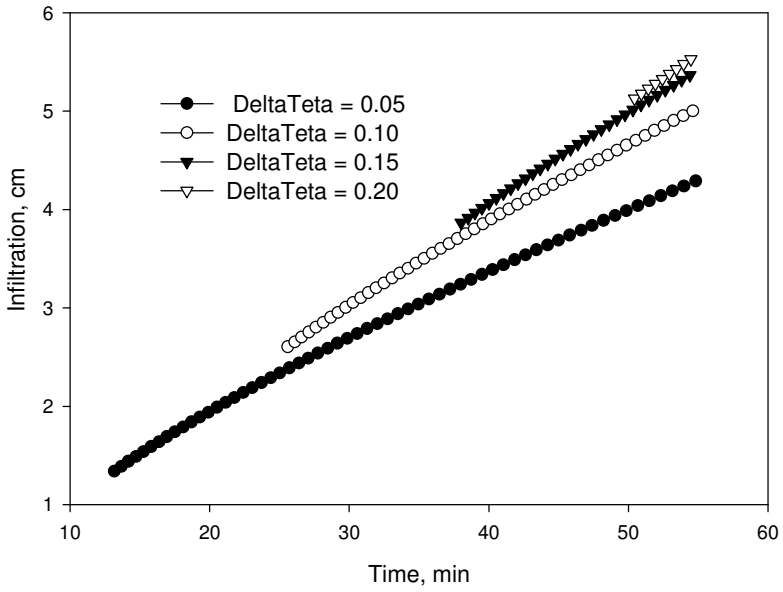

Figure 3.4. Sensitivity of infiltration to the moisture deficit (θ_s-θ_i), (bare clay loam)

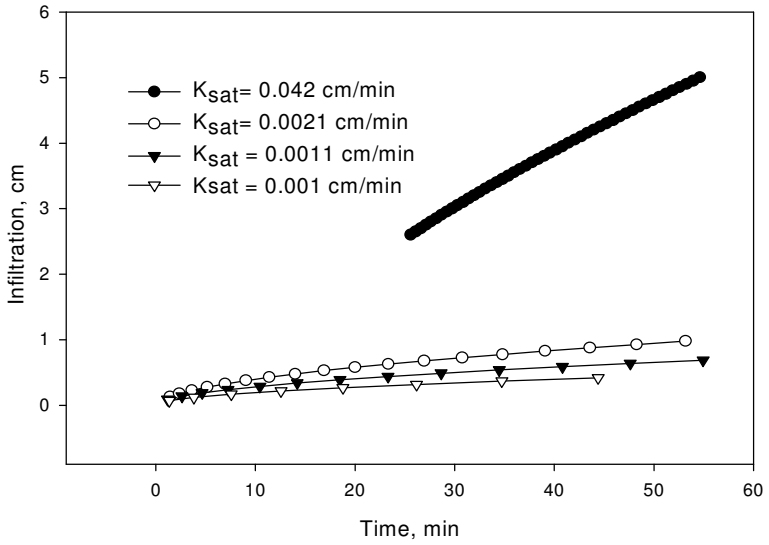

Figure 3.5. Sensitivity of infiltration to the saturated hydraulic conductivity (K_{sat}), (bare clay loam)

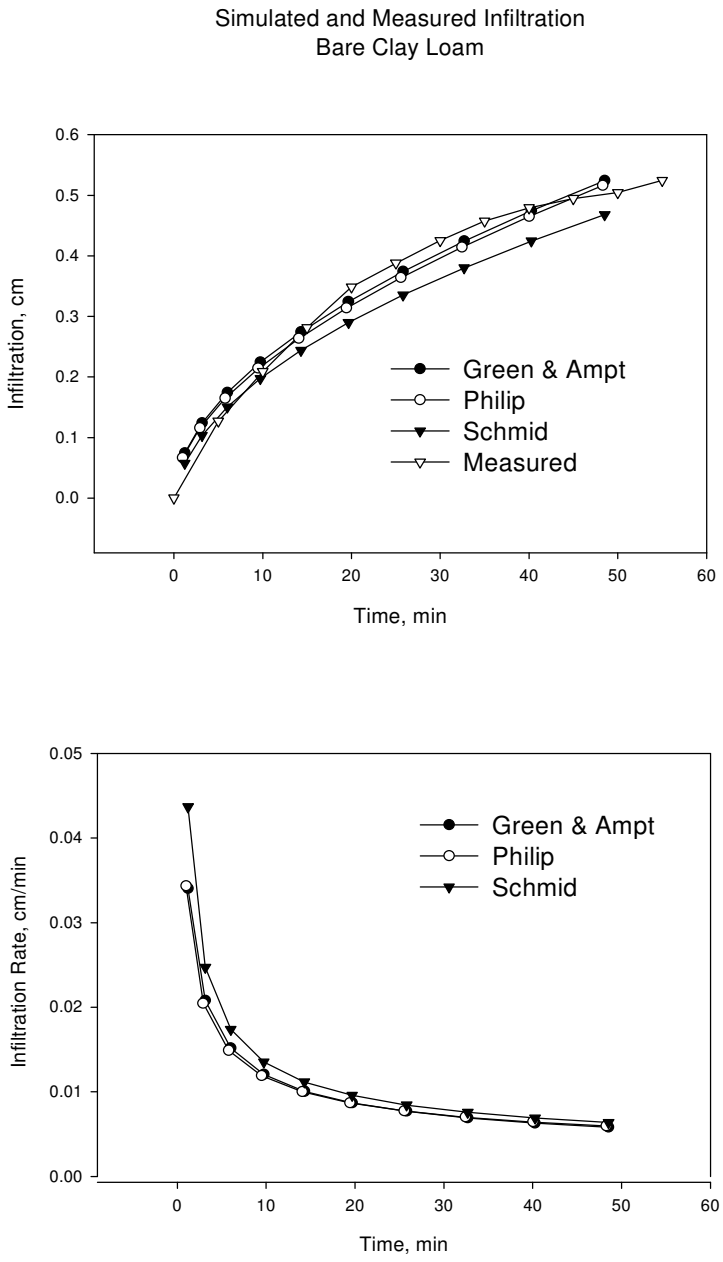

Figure 3.6. Simulation of infiltration and infiltration rates for the bare clay loam.

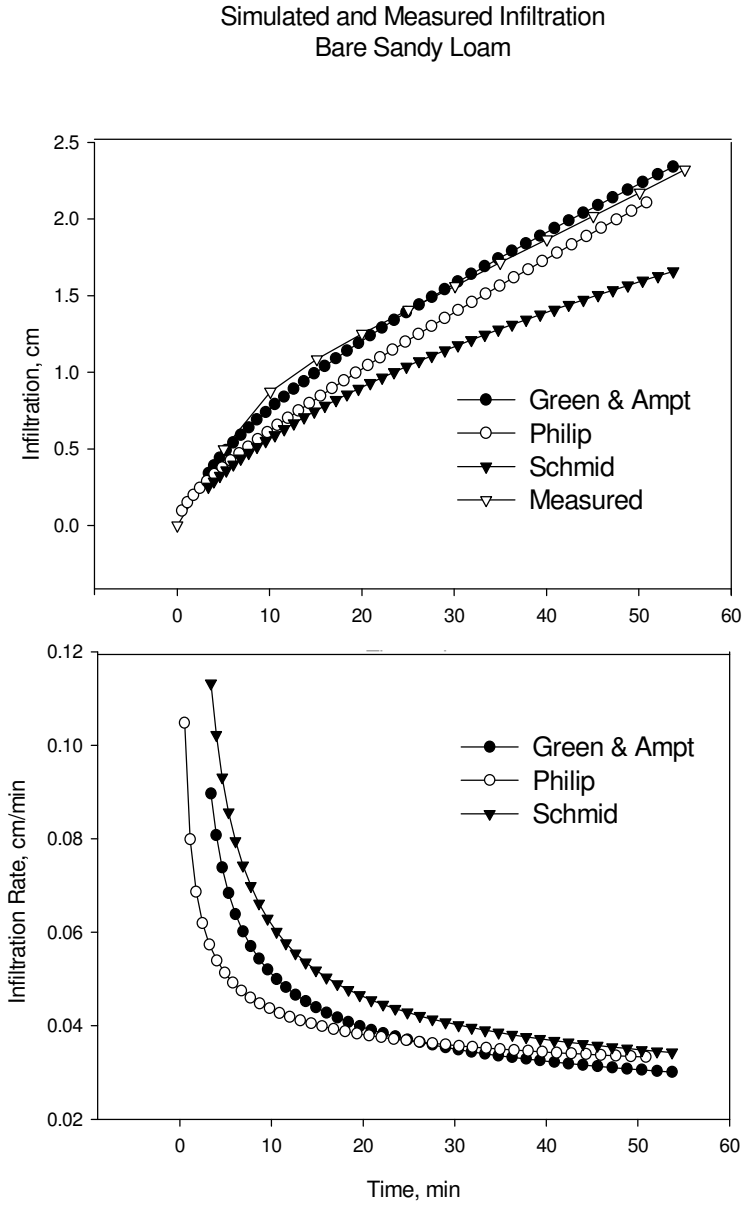

Figure 3.7. Simulation of infiltration and the infiltration rates for the bare sandy loam.

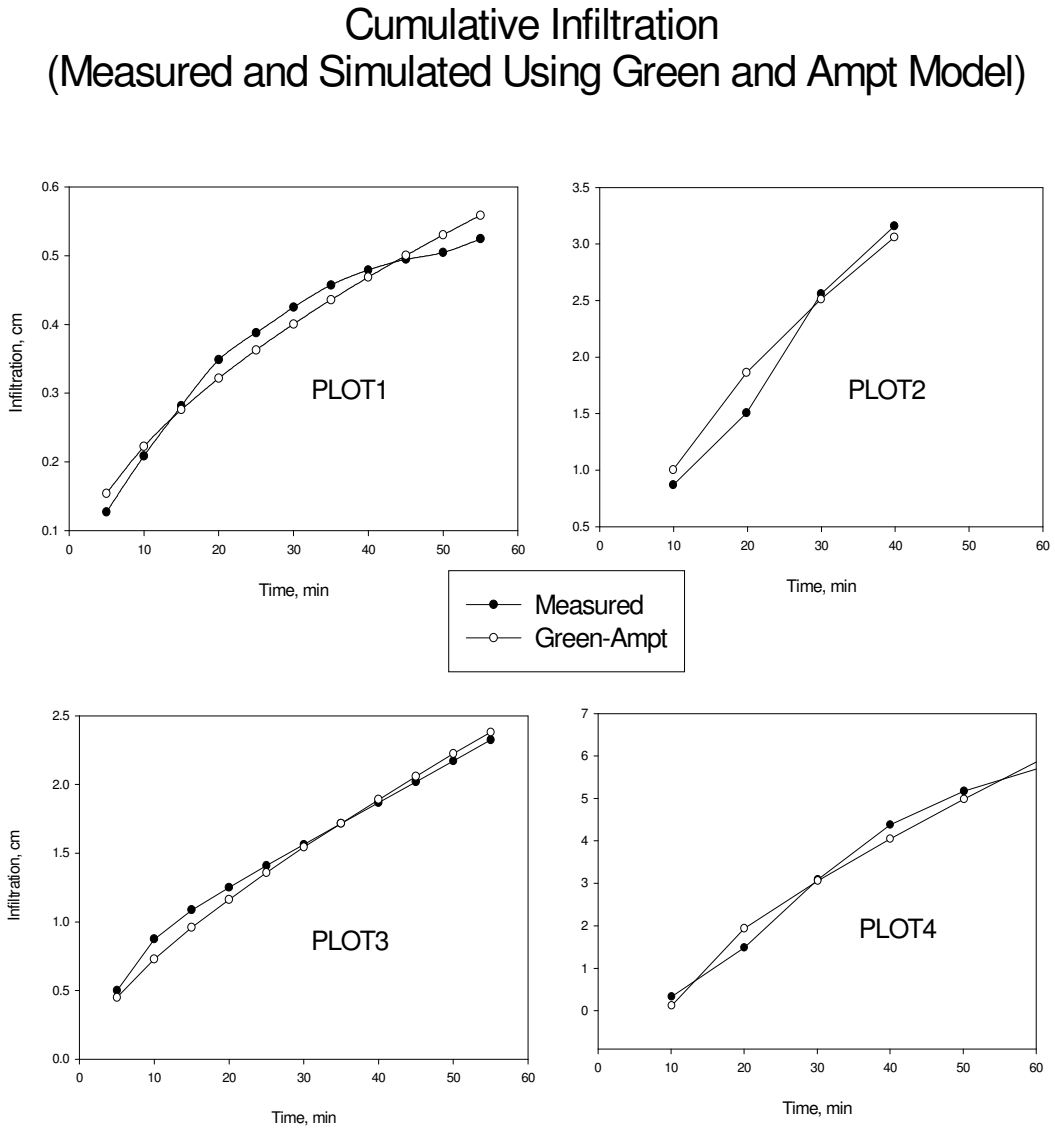

Figure 3.8. Simulated infiltration using Green and Ampt model as compared to the measured infiltration for plots 1(bare clay loam), 2 (vegetated clay loam), 3 (bare sandy loam), and 4 (vegetated sandy loam).

Table 3.2. Williams-Kloot criterion statistics for comparison of the Green-Ampt , Philip and Schmid infiltration models to the measured infiltrations using a level of confidence of $\alpha = 0.05$.

	PLOT1		PLOT2		PLOT3		PLOT4	
	G &A P	G &A S	G &A P	G &A S	G &A P	G &A S	G &A P	G &A S
Slope	-1.897	-0.61971	-0.43121	-0.68087	-0.90	-0.7381	-0.4451	0.483
Standard Error of Slope	0.29	0.143	0.2628	0.8556	0.2410	0.18270	0.4034	0.223
Degree of Freedom	10	10	7	7	11	11	6	6
$T_{0.95} = \left\| \frac{slope}{Std.Error} \right\|$	6.54	4.32	1.641	0.796	3.734	4.040	1.1035	2.2
$T_{Critical}$	2.23	2.23	2.36	2.36	2.22	2.22	2.45	2.45

G & A = Green and Ampt
S = Schmid
P = Philip

Figures 3.9 and 3.10 show the graphical comparison of the simulated runoff and the measured data in both bare clay loam and bare sandy loam soils. Results indicate satisfactory prediction of surface runoff by the MODCHOI model at 600 cm from the ridge of the plot during the 60 minute rainfall simulation. These results indicate that the kinematic wave approach in the KORMIL2 model performed well in predicting the overland runoff. This may be due to the fact that the model was comprehensive enough to consider the surface conditions such as the surface roughness, vegetation density, etc.

Exponential decrease in FC concentration with respect to time reflects the exponential kinetics of the bacteria release (Figure 3.11). The exponential decrease in FC population indicates a much faster release of bacteria from the source for the first

15 minutes of simulation, and a lower release rate thereafter. The simulation trend of FC concentration in surface runoff seems to match the measured data for the bare clay loam plot (Figure 3.11). However, the results of standard error of measured FC concentrations reflect a higher variability at 450 cm distance from the edge of the manure application area (Figure 3.11). Possible sources of error may be attributed to the non-uniform dispersion of FC due to surface heterogeneity, surface micro depressions and possible non-uniform hydrology due to macropores. Such factors seem to be magnifying the impact with distance from the manure application area.

Results of simulated FC concentrations within the soil profile (Figure 3.12) indicate that the one-dimensional kinematic wave model predicted the concentration of FC within an acceptable range. Observations of model predictions showed similar FC concentration trends within the 20 cm depth of soil profile for both the Green-Ampt simulated and the measured infiltration (Figure 3.12). However, higher standard error of the measured FC concentration within the first five centimeters depth of soil indicated high variability in FC concentration closer to the soil surface. A possible source of error could be that bacteria closer to the soil surface were more capable of being affected by the topsoil organic matter and exposure to the light. However, the measured runoff data reflected a poor concentration trend of FC in vegetated clay loam, indicating a possible source of sampling error (Figure 3.13).

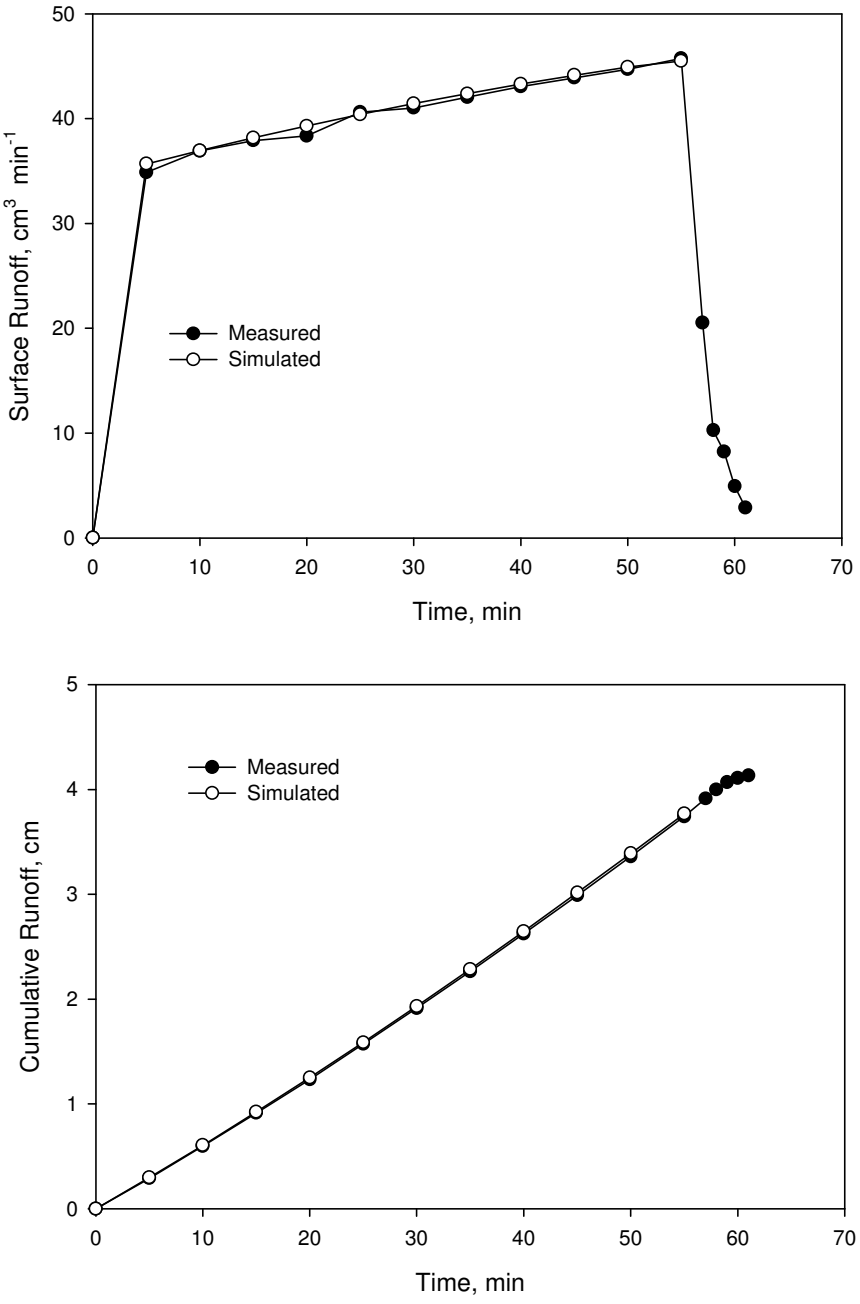

Figure 3.9. Simulated and measured surface runoff at 600 cm from the top edge of the manure application area in bare clay loam.

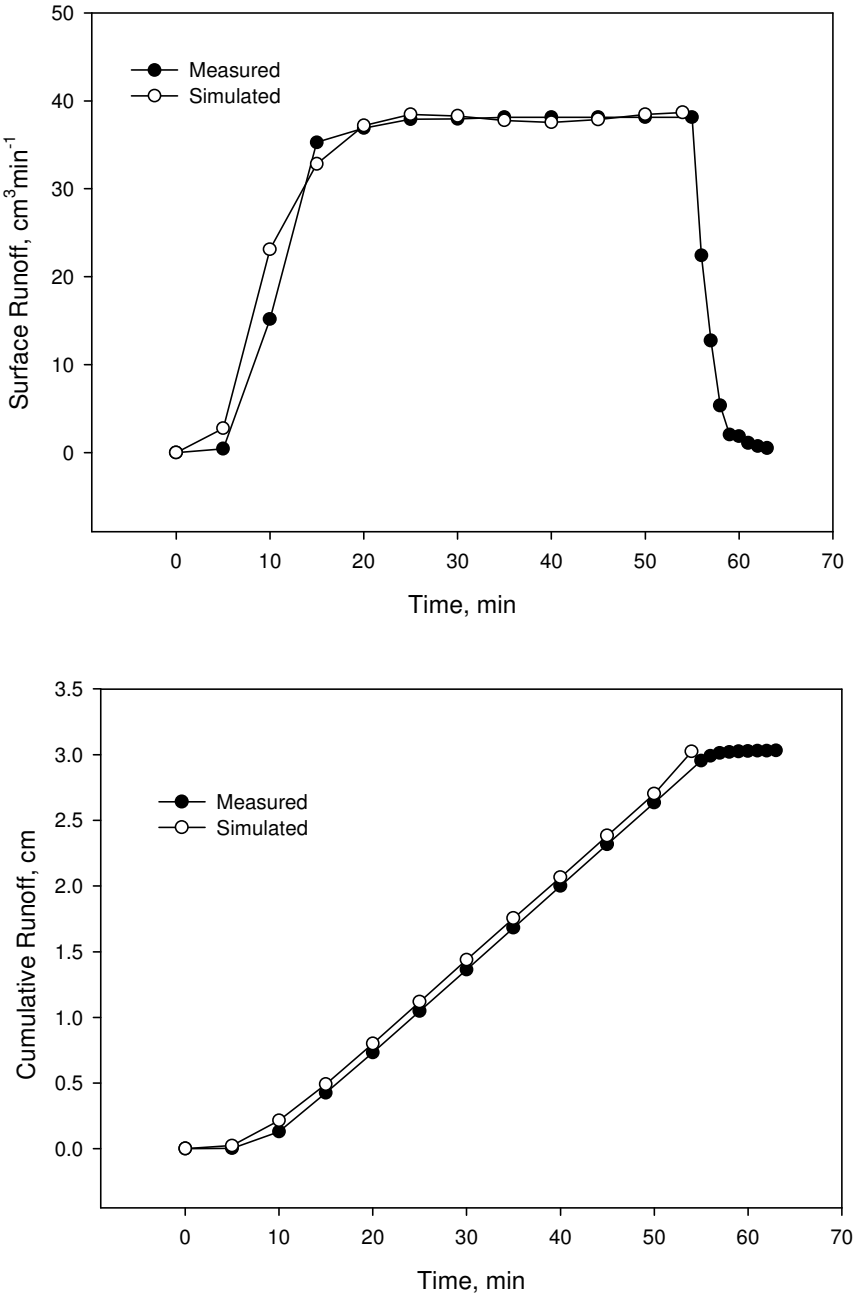

Figure 3.10. Simulated and measured surface runoff at 600 cm from the top edge of the manure application area in bare sandy loam.

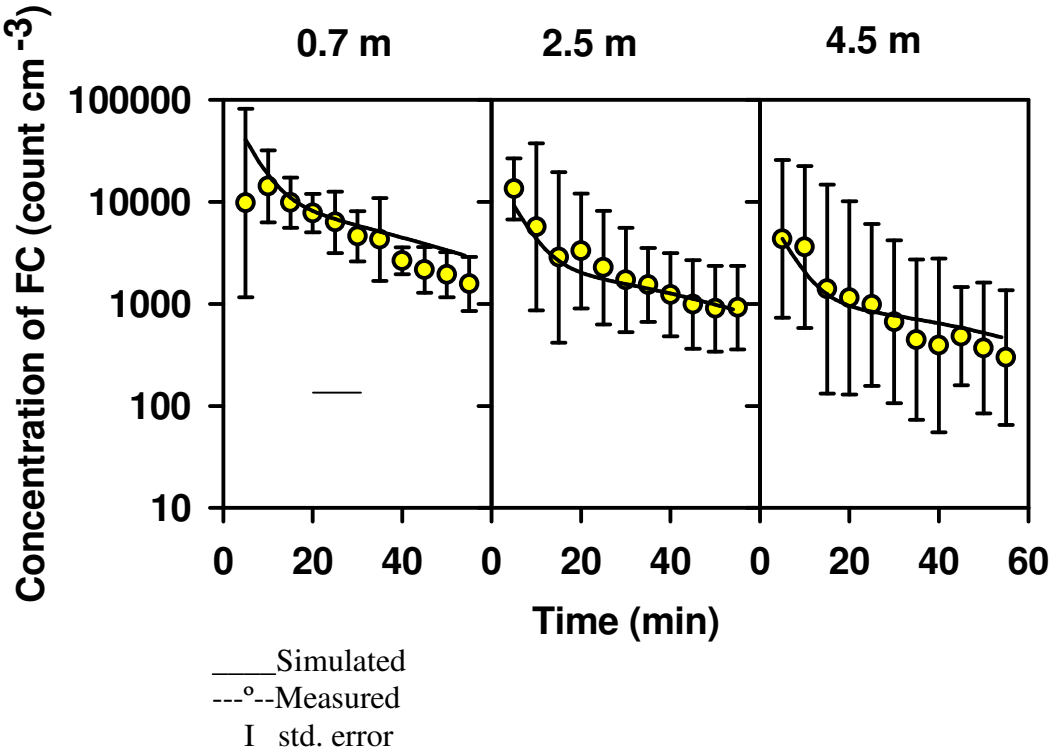

Figure 3.11. Simulated and measured FC concentrations for runoff in bare clay loam.

The results also showed an excellent FC concentration trend within the soil profile in the vegetated clay loam (Figure 3.13). The statistical results showing the performance capability of the kinematic wave model (KINSUB) in predicting FC concentration are presented in Table 3.3. The results support the graphical comparison of the model predictions with the measured data. The coefficient of determination value (R^2) indicates that 94% of total variations in measured data were captured by the model simulations regardless of the source of infiltration input into the model in both bare sandy loam soil and vegetated clay loam soil. The r value of 0.97 in both plots indicated a significant relationship between the model predictions and the measured FC concentrations within the soil profile. Similar statistical results for the FC concentrations in the vegetated clay loam indicated a significant relationship between the model predictions and the measured data. The R^2 value of 0.94 also indicated that the model was able to predict 94% of variability in FC concentrations at 95 cm from the manure application area in the vegetated clay loam plot.

Results indicated that the one-dimensional kinematics wave model performed well in predicting the FC transport through the soil profile even with the vegetation on the surface. Results such as these provide great promise for the MODCHOI model and the kinematics wave model of the convective-dispersive equation (KINSUB). However, the model needs further testing with field data as the data become available through future research.

Table 3.3 Statistical results comparing measured and simulated FC concentrations within the soil profile for the bare sandy loam plot, and vegetated clay loam plot

	Bare sandy loam		Vegetated clay loam
	With measured infiltration	With simulated infiltration	With measured Infiltration
b	342.41	385.81	46.50
slope	0.46	0.46	0.97
r	0.97	0.97	0.97
R^2	0.94	0.94	0.94

R2: coefficient of determination
r: correlation coefficient

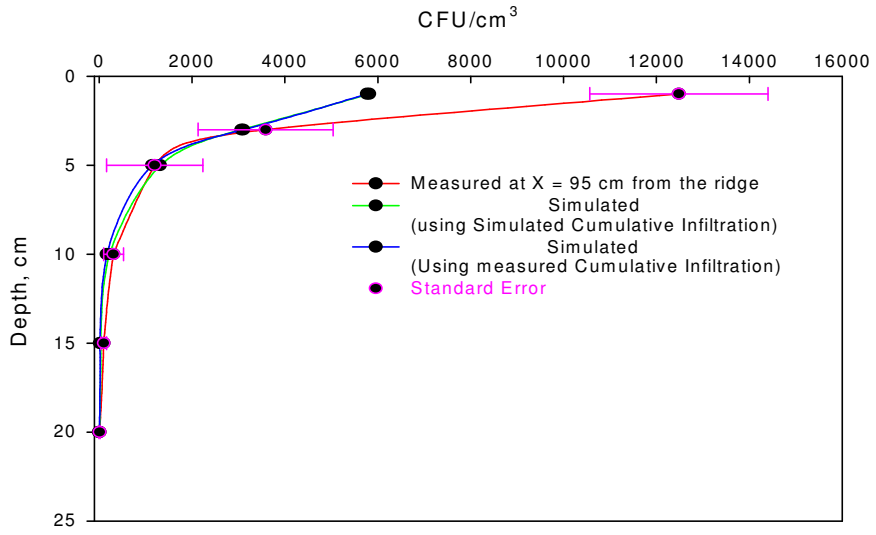

Figure 3.12. Simulated FC concentration in the soil profile at 95 cm distance from the manure application area (bare sandy loam).

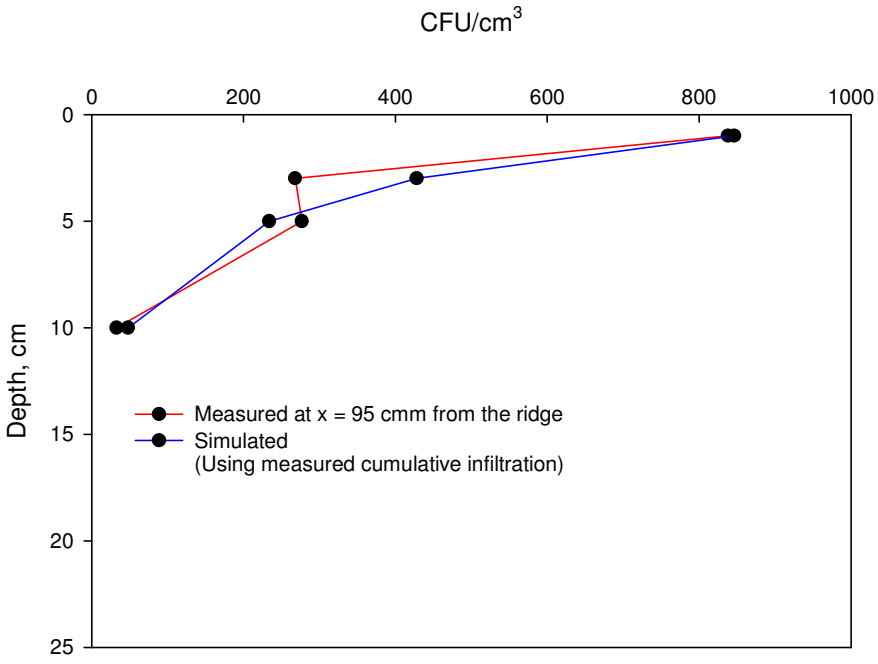

Figure 3.13. Simulated FC concentration in the soil profile at 95 cm distance from the manure application area (Vegetated Clay Loam)

3.12. Summary and Conclusions

A convective-dispersive model was implemented to an existing overland flow model (Choi, 1992) to simulate FC surface transport. This model was a numerical-based model using the kinematic wave equations for overland runoff simulations in an intervening land system. The model's prediction of surface runoff fit the measured data very well at 600 cm distance from the ridge of the plot in both bare clay loam and bare sandy loam soils. Despite the high variability that was observed in the measured FC concentration data at 285 cm and 490 cm, the model reflected relatively similar transport pattern at different distances from the edge of the manure application area.

It was concluded that the Green and Ampt infiltration model fit the measured infiltration data better than the Philip and the Schmid infiltration models. The kinematic wave model (KINSUB) developed in this study proved to be capable of simulating FC concentrations within the soil profiles regardless of the surface cover. The statistical results supported the graphical goodness of fit between the model simulations and the measured data for both hydrology and the FC concentrations.

Future model development is required to integrate all three modules developed in this study to predict the microbial transport. It is obvious that by integrating these models, the degree of uncertainty in model's input parameters may increase, thus making predictions less stable.

References

Barfield, B.J., E.W. Tollner, and J.C. Hayes. 1978. Prediction of sediment transport in grassed media. ASAE Paper No. 77-2023. American Society of Agricultural Engineers, St. Joseph, Michigan 49085.

Barwick, R.S., D.A. Levy, G.F. Craun, M.J. Beach, and R.L. Calderon. 2000. Surveillance for waterborne-disease outbreaks-United States. 1997-1998. Morbidity and Mortality Wkly. Report. 49 (SS04): 1-35.

Bergstrom, L.F. and A. Shirmohammadi: 1999. A real extent of preferential flow with depth in sand and clay Monoliths. J. of Soil. Contamination 8(6): 637-651.

Bond, W.J. 1987. Solute transport during unsteady, unsaturated soil water flow: The pulse impute. Aust. J. Soil Res. 25: 223-241.

Carsel, R.F., C.N. Smith, L.A. Mulkey, J.D. Dean and P. Jowise. 1984. Users Manual for the Pesticide Root Zone Model (PRZM) Release 1. EPA-600/3-84-109. U.S. EPA, Athens, GA.

Choi, J. 1992. Effect of intervening land use on runoff quality. PhD. dissertation, University of Maryland, College Park, MD.

Corapcioglu, M.Y., and D. Haridas. 1984.Transport and fate of microorganisms in porous media: A theoretical investigation J. Hydro. 72:149-169.

Cruz, J.R., P. Caceres, F. Cano, 1990. Adenovirus types 40 and 41 and rotaviruses associated with diarrhea in children from Guatemala. J. Clin. Microbiol. 28:1780-1784.

Danish Hydraulic Institute (DHI). 1998. MIKE SHE Water Movement – User Guide and Technical Reference Manual, Edition 1.1

Fenzl, R.N. 1962. Hydraulic resistance of broad shallow vegetated channels. Ph.D. Thesis, University of California at Berkley. Berkley, California.

Garder, A.O., D. W. Peaceman and A.L. Pozzi, 1964. Jr., Numerical Calculation of Multidimensional Miscible Displacement by the Method of Characteristics, Soc. Pet. Eng. J. 4(1), 26-36.

Grant, S.B., E.J. List, and M.E. Lidstrom. 1993. Kinetic analysis of virus adsorption and inactivation in bath experiments. Water Resource. Res. 29: 2067-2085.

Green, W.H., and G.A. Ampt. 1911. Studies on soil physics, 1: The flow of air and water through soils. Journal of Agricultural Science 4(1): 1-24.

Haan, C. T., B. Allred, D. E. Storm, G. J. Sabbagh, and S. Prabhu. 1995. Statistical procedure for evaluating hydrologic/water quality models. transaction ASAE 38(3):725-733.

Harvey, R. W., and S. P. Garabedian. 1991. Use of colloid filtration theory in modeling movement of bacteria through a contaminated sandy aquifer. Environ. Sci. Technol. 25:178-185.

Horton, R.E. 1939. Analysis of runoff-plot experiments with varying infiltration-capacity. Transactions American Geophysical Union 20: 693-711.

Huggins, L.F. and J.R. Burney. 1982. Surface runoff, storage and routing. In: C.T. Haan, H.P. Johnson and D.L. Brakensiek, Eds. Hydrologic modeling of small watersheds. ASAE Monograph No. 5. American Society of Agricultural Engineers, St. Joseph, Michigan.

Hurts, C.J., C.P. Gerba, I. Cech. 1980. Effects of environmental variables and soil characteristics on virus survival in soil. Appl. Environ. Microbiol. 40: 1067-1079.

Hutson, J.L. and R.J. Wagenet. 1991. Simulating nitrogen dynamic in soils using a deterministic model. Soil Use and Management 7: 74-78.

Jenkins, M.B., J.H., Chen, D.J. Kadner, and L.W. Lion. 1994. Methanotrophic bacteria and facilitated transport of pollutants in aquifer material. Appl. Environ. Microbiol. 60: 3491-3498.

Joy, D.M., H. Lee, C. Reaume, H.R. Whiteley, and S. Zelin. 1998. Microbial contamination of subsurface tile drainage water from field applications of liquid manure. J. Can. Soc. Agric. Eng. 40: 153-160.

Leonard, R.A., W.G. Knisel, and D.A. Still. 1987. GLEAMS: Groundwater Loading Effects of Agricultural Management Systems. Trans. ASAE 30: 14031418.

Liggett, J.A., Woolhiser, D.A. 1976. Different solutions of the Shallow-Water Equation. J. Eng. Mech. Div., Proceeding of ASCE, 93 (EM2): 39-71.

Matthess, G., and A. Pekdeger. 1981. Concepts of a survival and transport model of pathogenic bacteria and viruses in groundwater. Sci. Total Environ. 21:149-159.

Miller, J.E. 1984. Basic concepts of kinematic-wave models. U.S. Geological Survey Professional Paper 1302. U.S. Government Printing Office, Washington D.C. for sale by distribution branch, U.S. Geological Survey, 604 South Pickett, Alexandria, Virginia 22304.

Miner, J.R., L.R. Bernard, L.R. Fina, G.H. Larson and R.I. Lipper. 1966. Cattle feedlot runoff nature and behavior. Proc. 21st Ind. Waste Conf. Purdue Univer. pp. 834-847.

Moore, R.S., D.H. Taylor, M.M. Eddy, and L.S. Sturman. 1982. Adsorption of reovirus by minerals and soils. Appl. Environ. Microbiol. 44: 852-859.

Moor, J.A., Smyth, E.S. Baker, and J.R. Miner. 1988. Evaluating coliform concentrations in runoff from various animal waste management systems. Special Report 817: Agricultural Experiment Stations, Oregon State University, Corvallis, Oregon.

Philip, J.R. 1957. The theory of infiltration, the infiltration equation and its solution. Soil Science 83: 345-57

Polprasert, C., Dissanayake, M.G., and Thanh, N.C. 1983. Bacteria die-off kinetics in waste stabilization pont. J. Water Pollut. Control Fed. 55(3): 285-296.

Powelson, D.K., and C.P. Gerba. 1994. Virus removal from sewage effluent during saturated and unsaturated flow through soil columns. Water Res. 28: 2175-2181.

Powelson, D.K., and A.L. Mills, 1998. Water saturation and surfactant effects on bacteria transport in sand columns. Soil Sci. 163: 694-707.

Rawls, W.J., Gimenez, D., and R. Grossman, 1998. Use of soil texture, bulk density, and slope of the water retention curve to predict saturated hydraulic conductivity, Transactions of ASAE, Vol. 41(4): 983-988.

Reddy, K.R., R. Khaleel, M.R. Overcash, 1981. Behavior and transport of microbial pathogens and indicator organisms in soils treated with organic wastes. J.of Environ. Qual. 10(3): 2545-266.

Reynolds, P.J., P. Sharma, G.E. Henneman, and M.J. McInerney. 1989. Mechanisms of microbial movement in subsurface materials. Appl. Environ. Microbio. 55: 2280- 2286.

Rhodes, R.A. and C.R. Hrubant. 1972. Microbial. Population of feedlot waste and associated sites. Appli. Microbial. 24(3): 269-337.

Sabu, P., M. Matlock, P. Haan, S. Mukhtar ans S. Pillai. 2002. Uncertainty analysis as a first step of developing a risk-based approach to nonpoint source modeling of fecal coliform pollution for total maximum daily load estimates. Texas A & M University.

Sadeghi, A.M. and J.G. Arnold, 2001. A SWAT microbial sub-model for predicting pathogen loadings in surface and groundwater at watershed and basin scales. Proceeding of TMDL. Environmental Regulations, Fort Worth, TX. Marsh 11-13, 2002; A. Saleh., Eds., ASAE 2002; 56-63.

Schafer, A., H. Harms, A.J.B. Zehnder. 1998. Bacterial accumulation at the air-water interface. Environ. Sci. Technol. 32: 3704-3712.

Schmid, B. 1990. Derivation of an explicit equation for infiltration on the basis of the Mein-Larson model. Hydrological Sciences Journal. 35: 197-208.

Scott, D.T., M.N. Gooseff, K.E. Bencala, and R.L. Runkel. 2003. A automated calibration of a stream solute transport model: implications for interpretation of biogeochemical parameters. J. N. Am. Benthol. Soc., 22(4): 492-510.

Sharma, M.L., G.A. Gander, and G.C. Hunt. 1980. Spatial variability of infiltration in a watershed. Journal of Hydrology 45:101-122.

Shirmohammadi, A., H.J. Montas, L.F. Bergstrom, and W.G. Knisel. 2001. Water Quality Models, pp. 233-256. In: Agricultural nonpoint source pollution-watershed management and hydrology: Ritter. W.F. and A. Shirmohammadi, (eds.); Lewis Publishers, Washington, D.C.

Shirmohammadi, A., H. Montas, A. Sadeghi, and L. Bergstrom. 2002. Using hydrologic and water quality models beyond their boundaries. ASAE paper Number 022090, Chicago, IL.

Shirmohammadi, A. and R.W. Skaggs. 1985. Predicting infiltration for shallow water table soils with different surface cover. Transactions of ASAE 28(6): 1829-1837.

Simunek, J., K. Huang, M. Sejna, and M.T. Van Genuchten. HYDRUS-2D, 1999. U.S. Salinity Laboratory, USDA/ARS, Riverside, California

Skaggs, T. H. and D. A. Barry, 1996. Sensitivity methods for time-continuous, spatially discrete groundwater contaminant transport models. Water Resources Research 32(8): 2409-2420.

Tan, Y., Bond, W.J., and Griffin, D.M. 1992. Transport of bacteria during unsteady unsaturated soil water flow. Soil Sci. Soc. Am. J. 56: 1331-1340.

Tan, Y., J.G. Gannon, P. Baveye, and M. Alexander.1994.Transport of bacteria in a saturated aquifer sand. Water Res. 30:3243-3252.

Thomas, D.L., K.L. Campbell, and R.L. Bengtson. 1989. CREAMS, pp 14-20.

In: application of water quality models for agricultural and forested watersheds, D.B. Beasley and D.L. Thomas, editors. So. Coop. Ser. Bul. No. 388.

Uhal, V.W., and S.T. Sullivan, 1982. Uncertainty analysis in the appraisal of capital investment project. Uncertainty analysis for engineers. V.W. Uhal and W.E. Lowthian eds. AICHE Symposium Series, vol. 78, no. 220, American Institute of Chemical Engineers, New York, pp.10-22.

USEPA,1998. 1998 TMDL Tracking system data version 1.0. Total maximum daily load program. USEPA office of Water, Washington, D.C.

USEPA, 1994. National Water Quality Inventory: Report to Congress, USEPA, office of water, Washington, D.C.

Vilker, V.L., and W.D. Burge. 1980.Adsorption mass transfer model for virus transport in soils. Water Res. 14:783-790.

Viraraghavan, T., and M. Ionescu. 2002. Land application of phosphorus-laden sludge: a feasibility analysis. J. Environ. Manage. 64: 171-177.

Wan, J., J.L. Wilson, and T.L. Kieft, 1994.Influence of the gas-water interface on transport of microorganisms through unsaturated porous media. Appli. Environ. Microbio. 60: 509-516.

Yates, M.V., and S.R. Yates. 1988. Modeling microbial fate in the subsurface environment. CRC Crit. Rev. Environ. Control. 17:307-344.

Young, R.A., T. Untrods, and W. Anderson. 1980. Effectiveness of vegetated buffer strips in controlling pollution from feedlot runoff. J. Environ. Qual. 9(3): 483-487.

Zheng, C. and G.D. Bennett. 1995. Applied Contaminant Transport Model, Theory and Practice. John Wiley and Sons, New York, NY.

APPENDICES

Appendix A

Input Data For The Kinematic Wave Model (MODCHOI)

A1. MODCHOI input data parameters

itinput
coo beta
wids cm ss so cn agd
drain dsra dera
dsyin dssy desy
delx delt nnod ntime ey
wc
sg bd
df1 df2 df3 cd1 cd2 cd3
fs si
su fts
ck
nln
ln1 ln2 ln3 ln4
ct1 ct2

A2. Parameter definition

wids = unit width (m) of each of the four plots, 1 cm = 0.01 m

cm = coefficient "a" in the $Q = a\,\alpha\,(\frac{SS\,h^{5/2}}{SS + 2\,h})$, and assumed to be equal to 0.667

ss = average grass stem spacing (m), fixed value of 0.0283 m

cn = Manning's roughness coefficient

agd = average diameter of grass stems (m), fixed to 0.00261 m

drain = dry run rainfall intensity (mm/hr), 6.1 cm/hr = 61 mm/hr

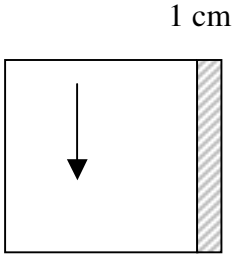

dsra = starting time for dry run, 0 minute

dera = ending time for dry run, 55 minutes

dsyin = dry run synthetic runoff input rate (l/min)

dssy = dry run synthetic runoff starting time, min

desy = dry run synthetic runoff ending time, min

delx = space increment (m), 6 cm=0.06 m (fixed)

delt = time increment (sec), fixed for 10 sec.

nnod = number of nodes, 101 (600 cm of flow path with an $\Delta x = 6\ cm$)

ntim = number of time increments, 330 (55*60=3300 sec /10 = 330)

ey = estimated flow depth (m), of synthetic input runoff assumed to be 0.0 (no input runoff)

wc = weigh based average water contents of the top layer, %

sg = specific gravity, fixed value of 2.62 was used

bdu = bulk density, (g/cm^3)

df1, df2, df3 = sediment deposition fronts (space node numbers) from the top of the plots for high, moderate, and low deposition, respectively (10, 20, and 40, with respect to df1, df2, df3, referred to Choi's model)

cd1,cd2, cd3 = infiltration reduction coefficients due to the sediment deposition corresponding to df1, df2, df3, assumed to be 1.

fs, si = saturated hydraulic conductivity, and infiltration rates in mm/h

su = assumed degree of saturation

ck = constant for Horton's model, fixed value of 0.105 was used by Choi's

nln = number of rows where samples were taken

ln1, ln2, ln3, ln4 = node numbers at 95, 285, 290, and 600 cm of sampling locations

ct1, ct2 = end of infiltration index at the end of run, assumed to be 1 m (KORMIL2)

A3. MODCHOI input data files (hyd08.dat) for bare clay loam

```
1
1          0.7
0.01  0.667  0.0283  0.06  0.042  0.00261
61.0   0.0     55.00
0.0     0.0   0.00
0.06    10      101       330  0.000
13  0.3
2.62 1.47
10      20     40     1      1      1
1  1.0
30.0    1.0
0.105
4
16   48   82   100
0.1  0.1
```

A4. Input data for MODCHOI (tabinf.txt) for bare clay loam

t(min.)	f(mm/hr)
0	0.00
1	14.63
2	14.07
3	13.55
4	13.03
5	15.53
6	12.04
7	11.56
8	11.09
9	10.63
10	10.18
11	9.75
12	9.33
13	8.92
14	8.52
15	8.13
16	7.75
17	7.39
18	7.03
19	6.69
20	6.36
21	6.04
22	5.74
23	5.44
24	5.16
25	4.89

A4. Continued

26	4.63
27	4.38
28	4.14
29	3.92
30	3.70
31	3.50
32	3.31
33	3.13
34	2.96
35	2.81
36	2.66
37	2.53
38	2.41
39	2.30
40	2.20
41	2.11
42	2.04
43	1.98
44	1.92
45	1.88
46	1.86
47	1.84
48	1.83
49	1.84
50	1.86
51	1.89
52	1.93
53	1.98
54	2.05
55	2.21

A5. Sample computation of Infiltration data (tabinf.txt) as an input to MODCHOI model.

Computation of infiltration data (tabinf.txt) used for simulating the MODCHOI model. Sigma Plot was used to determine cubic regression parameters based on the computed data. Infiltration data was computed using mass balance equation (Infiltration = rain-runoff). The following equation was obtained by the regression and was used to compute infiltration rate data for MODCHOI model.

$R = 15.186t-16.7675t^2+7.03368t^3$

$f = dR/dt=15.186-2*16.7675t+3*7.03368t^2$ (With no interception, $y_0 = 0$)

Table A1. Computed infiltration data (tabinf.txt) as an input for MODCHI model for bare clay loam (F is cumulative infiltration, P is precipitation and R is runoff)

Time min	Time hr	P mm	R mm	F mm	Time min	Time hr	f mm/hr	Time min	Time hr	f mm/hr
0.000	0.000	0	0.00	0.00	0	0	0.00	28	0.467	4.13
5.000	0.083	5.10	3.81	1.27	1	0.017	14.63	29	0.483	3.91
10.000	0.167	10.2	8.08	2.09	2	0.033	14.09	30	0.5	3.69
15.000	0.250	15.25	12.44	2.81	3	0.05	13.56	31	0.517	3.49
20.000	0.333	20.33	16.85	3.48	4	0.067	13.04	32	0.533	3.30
25.000	0.417	25.42	21.54	3.88	5	0.083	12.54	33	0.55	3.13
30.000	0.500	30.50	26.25	4.25	6	0.1	12.04	34	0.567	2.96
35.000	0.583	35.58	31.01	4.57	7	0.117	11.56	35	0.583	2.80
40.000	0.667	40.67	35.87	4.79	8	0.133	11.09	36	0.6	2.66
45.000	0.750	45.75	40.80	4.95	9	0.15	10.63	37	0.617	2.53
50.000	0.833	50.83	45.79	5.05	10	0.167	10.18	38	0.633	2.41
55.000	0.917	55.92	50.67	5.25	11	0.183	9.75	39	0.65	2.30
					12	0.2	9.32	40	0.667	2.21
					13	0.217	8.91	41	0.683	2.12
					14	0.233	8.51	42	0.7	2.05
					15	0.25	8.12	43	0.717	1.99
					16	0.267	7.74	44	0.733	1.94
					17	0.283	7.38	45	0.75	1.90
					18	0.3	7.03	46	0.767	1.88
					19	0.317	6.68	47	0.783	1.87
					20	0.333	6.35	48	0.8	1.86
					21	0.35	6.03	49	0.817	1.87
					22	0.367	5.73	50	0.833	1.89
					23	0.383	5.43	51	0.85	1.93
					24	0.4	5.15	52	0.867	1.97
					25	0.417	4.88	53	0.883	2.03
					26	0.433	4.62	54	0.9	2.10

A6. MODCHOI funinf.txt data file for bare clay loam

Column 1, 2, and 3 are the total flow rates at row 1, 2, and 3, respectively

0.00	0.00	0.00
0.94	2.80	7.85
0.95	2.94	7.97
0.96	3.08	8.08
0.96	3.21	8.20
0.97	3.34	8.30
0.98	3.46	8.41
0.98	3.58	8.51
0.99	3.69	8.60
0.99	3.80	8.69
1.00	3.90	8.78
1.00	4.01	8.86
1.01	4.10	8.93
1.01	4.19	9.00
1.01	4.28	9.07
1.02	4.37	9.13
1.02	4.45	9.19
1.02	4.52	9.24
1.03	4.59	9.29
1.03	4.66	9.34
1.03	4.72	9.37
1.03	4.78	9.41
1.04	4.83	9.44
1.04	4.88	9.46
1.04	4.93	9.49
1.04	4.97	9.50
1.04	5.01	9.51
1.04	5.04	9.52
1.04	5.07	9.52
1.04	5.09	9.52
1.04	5.11	9.51
1.04	5.12	9.50
1.04	5.14	9.49
1.04	5.14	9.47
1.04	5.14	9.44

A.6 Continued

1.03	5.14	9.41
1.03	5.14	9.38
1.03	5.13	9.34
1.03	5.11	9.29
1.02	5.09	9.25
1.02	5.07	9.19
1.02	5.04	9.14
1.02	5.01	9.07
1.01	4.97	9.01
1.01	4.93	8.94
1.00	4.89	8.86
1.00	4.84	8.78
0.99	4.79	8.70
0.99	4.73	8.61
0.98	4.67	8.51
0.98	4.60	8.41
0.97	4.53	8.31
0.97	4.45	8.20
0.96	4.38	8.09
0.95	4.29	7.97
0.95	4.20	7.85

A7. Sample computation of data file ”funinf.txt” as an input to MODCHOI model for bare clay loam

Computation of flow rate at funnels in mm/hr for funinf.txt as an input to simulate the MODCHOI model. Sigma Plot was used to determine cubic regression parameters based on the computed total funnel flow on each row.

Table A2 Calculated data for data file funinf.txt, first row (95 cm from the ridge of the plot) bare clay loam

T, MIN	F1, ml	F2, ml	F3, ml	Sum, ml	R1, mm	T,hr	Cumulative[1] Inf., mm
0	0	0	0	0	0.00	0.000	0.00
5	1240	540	1140	2920	45.63	0.083	0.08
10	1560	640	1100	3300	51.56	0.167	0.16
15	1300	680	1280	3260	50.94	0.250	0.25
20	1320	680	1100	3100	48.44	0.333	0.33
25	1500	720	1320	3540	55.31	0.417	0.42
30	1560	680	1120	3360	52.50	0.500	0.51
35	1420	660	1140	3220	50.31	0.583	0.59
40	1390	700	1160	3250	50.78	0.667	0.68
45	1380	680	1080	3140	49.06	0.750	0.76
50	1390	680	1220	3290	51.41	0.833	0.84
55	1380	700	1060	3140	49.06	0.917	0.93

Table A2. (Continued), second row, 285 cm from the ridge of the plot.

T, MIN	F4	F5	F6	Sum, ml	R2, mm	T,hr	Cumulative Inf., mm
0	0	0	0	0	0.00	0.000	0.00
5	1100	2900	5300	9300	145.31	0.083	0.24
10	5300	440	6800	12540	195.94	0.167	0.57
15	4900	340	6400	11640	181.88	0.250	0.87
20	5000	4100	6100	15200	237.50	0.333	1.27
25	5600	4700	6200	16500	257.81	0.417	1.70
30	5700	4500	6000	16200	253.13	0.500	2.12
35	5800	4400	6000	16200	253.13	0.583	2.54
40	5700	4200	5900	15800	246.88	0.667	2.95
45	5900	4000	5800	15700	245.31	0.750	3.36
50	5500	3600	5800	14900	232.81	0.833	3.75
55	5800	3900	5800	15500	242.19	0.917	4.15

[1] Flow through funnels at each row were considered as macropore in MODCHOI's model when the runoff was simulated.

For cumulative (last column), the R1 (sixth colun) values were divided by 600 (the length of the plot)

Table A2. (Continued), third row, 490 cm from the ridge of the plot.

T, MIN	F7	F8	F9	Sum, ml	R3, mm	Time,hr	Cumulative, mm
0	0	0	0	0	0.00	0.000	0.00
5	13200	1600	7900	22700	354.69	0.083	0.59
10	13500	2280	14050	29830	466.09	0.167	1.37
15	14550	2430	14050	31030	484.84	0.250	2.18
20	13000	2300	13150	28450	444.53	0.333	2.92
25	13580	2300	14150	30030	469.22	0.417	3.70
30	13800	2400	13950	30150	471.09	0.500	4.48
35	12400	2500	13950	28850	450.78	0.583	5.24
40	13500	2600	13850	29950	467.97	0.667	6.02
45	13550	2400	14050	30000	468.75	0.750	6.80
50	14000	2400	13750	30150	471.09	0.833	7.58
55	6600	2300	13650	22550	352.34	0.917	8.17

Cubic Polynomials were fitted to all three rows and their equations of best fit for bare clay loam

Equations

Row1
$R=562.511t+132.103t^2-94.124t^3$
$dR/dt = 562.511+2*132.103t-3*94.124t^2$

Row2
$R=1596.1t+2626.2t^2-1542.27t^3$
$dR/dt=1596.1+5252.4t-4626.81t^2$

Row3
$R=4631.25t+2316.67t^2-1653.05t^3$
$dR/dt=4631.25+2*2316.67t-3*1653.05t^2$

Row1, Row2 and Row3 are 95 cm, 285 cm and 490 cm distance from the ridge of the plot.

Appendix B

Input Data For The Kinematic Wave Model (KINSUB)

B.1. Input data file (ztab.txt) for KINSUB model

9 (number of sampling depths)

2 4 6 8 10 12 14 16 18 (sampling depths, cm)

B.2. Input data file (tabs.txt) to simulate KINSUB model

Data in columns 1, 2, and 3 represent the time, total infiltration, and surface concentration of FC, respectively. This is an input data file to KINSUM model. The infiltration values (cm) are computed from the measured data using mass balance equation [Infiltration (F) = Rainfall (P)-Runoff (R)]; FC concentrations (cfu/g) are computed using MODCHOI model. In other words, one has to use infiltration data and FC concentrations at the boundary as input into the KINSUB model in order to produce FC concentrations at different desired depths in the soil profile.

0	0	0.000
1	0.14	0.000
2	0.22	0.000
3	0.31	0.000
4	0.39	0.000
5	0.47	0.000
6	0.54	0.002
7	0.61	0.006
8	0.68	0.010
9	0.74	0.014
10	0.80	0.018
11	0.86	0.021
12	0.92	0.025
13	0.97	0.027
14	1.02	0.029
15	1.07	0.030
16	1.11	0.031
17	1.16	0.032
18	1.20	0.033
19	1.24	0.033
20	1.28	0.033
21	1.32	0.033
22	1.35	0.033
23	1.38	0.032
24	1.42	0.032
25	1.45	0.031

26	1.48	0.030
27	1.51	0.030
28	1.54	0.029
29	1.57	0.028
30	1.60	0.027
31	1.62	0.026
32	1.65	0.026
33	1.68	0.025
34	1.70	0.024
35	1.73	0.023
36	1.76	0.022
37	1.79	0.022
38	1.81	0.021
39	1.84	0.020
40	1.87	0.020
41	1.90	0.019
42	1.93	0.018
43	1.97	0.018
44	2.00	0.017
45	2.03	0.017
46	2.07	0.016
47	2.11	0.016
48	2.15	0.015
49	2.19	0.015
50	2.23	0.015
51	2.27	0.014
52	2.32	0.014
53	2.37	0.014
54	2.42	0.013

Appendix C

Measuring Rainfall Uniformity Coefficient

Calibration of Rainfall Simulator and The V-notched Weir

To maintain a reasonable uniformity of synthetic rain, the rainfall simulator had to be calibrated. To achieve this goal, the rainfall simulator was adjusted back and fort, and up and down for the best position. After the final position of rainfall simulator was fixed for each subplot, the nozzles were adjusted horizontally and circularly one at a time in the right position. The generator and the pump were turned on, and the pressure of individual pressure gauge located on the rainfall simulator was tested for our desire rainfall intensity. Many experiments were conducted for duration of fifteen minutes after each adjustment on each nozzle, and samples were taken to achieve the most reasonable rainfall uniformity coefficient. The following tables and formula show the procedures for calculation of uniformity coefficient.

Christiansen's uniformity equatio n was used to calculate the uniformity coefficient (C_u).

$$C_u = 100(1-\frac{SUM(ABS(x_i - Mean))}{Mean \times n})$$

Where Cu is the uniformity coefficient, x_i is volume of collected rainfall, and n is number of replications.

The uniformity coefficient was obtained under 20 PSI pressure on each nozzle for an intensity of 6.1 cm/hr throughout the entire experiment. Figure C.1 shows the rainfall uniformity coefficient obtained for different simulation trials. The final trial (specific setting and nozzle location) produced C_u value of about 94%, which is way above the recommended 80% value (Zoldoske et al., 1994).

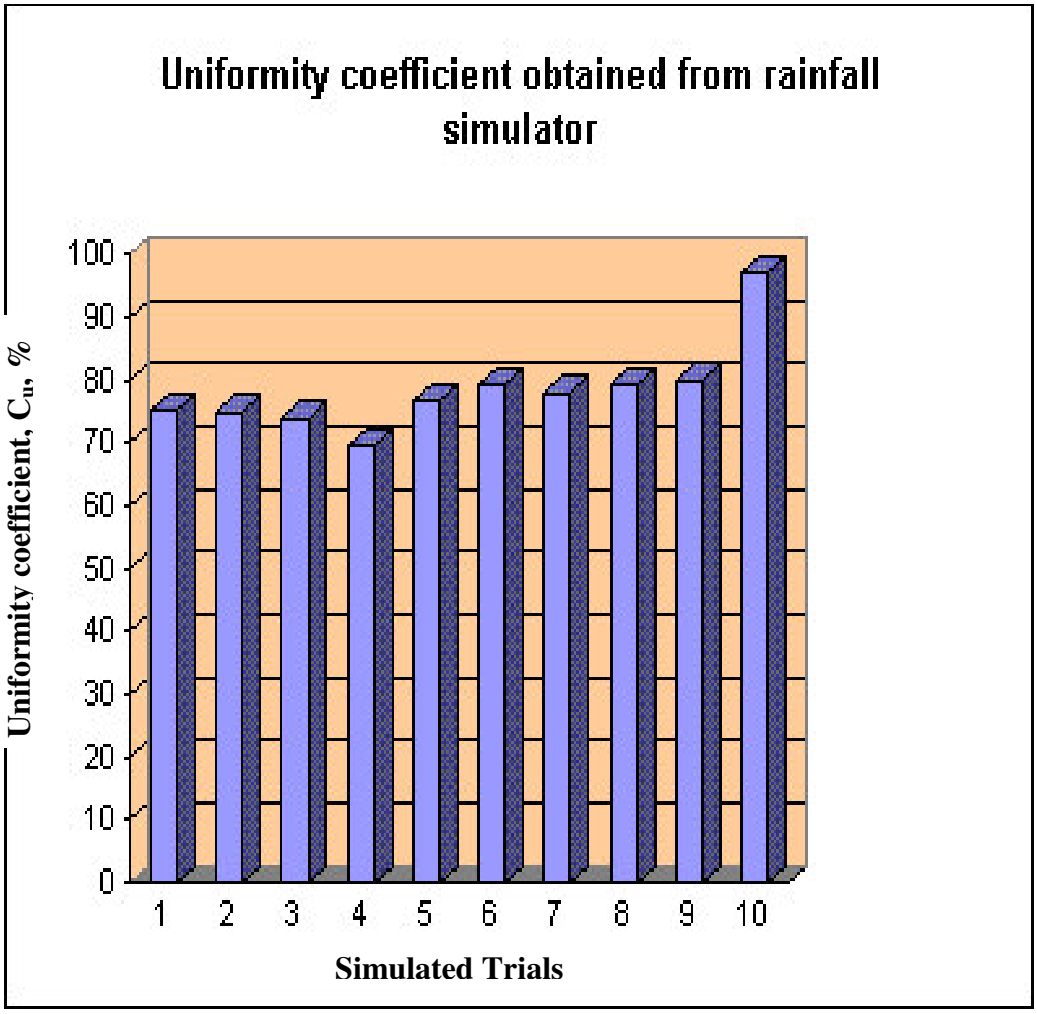

Figure C.1 Uniformity Coefficient (C_u) obtained by Christiansen's formula

Reference

Zoldoske, D.F., K.H. Solomon and E.M. Norum. 1994. Uniformity measurement for turfgrass: What's best? Center for Irrigation Technology, California State University, Fresno, CA.

Table C1. Measured data at the lysimeter to calibrate the v-notched weir

1 gpd = 0.046297 ml/sec

Reading from the weir

Trial	Time(sec)	V(ml)	Q(ml/sec)	Q, (gpd)	Q, (ml/sec)
1	20	675			
	20	660			
	20	660			
	Average	665	33.25	1064	46.68
2	8	1420			
	8	1500			
	8	1480			
	Average	1466.66	183.375	4690	205.20
3	10	4010			
	10	4500			
	10	4010			
	10	3790			
	Average	4077.5	407.75	11290	494
4	10	5720			
	10	6000			
	10	5680			
		5800	580	16000	700

Summary

Actual	Weir	Weir
Q, (ml/sec)	Q, (gpd)	Q, (ml/sec)
33.25	1064	46.68
183.37	4690	205.20
407.75	11290	494
580	16000	700

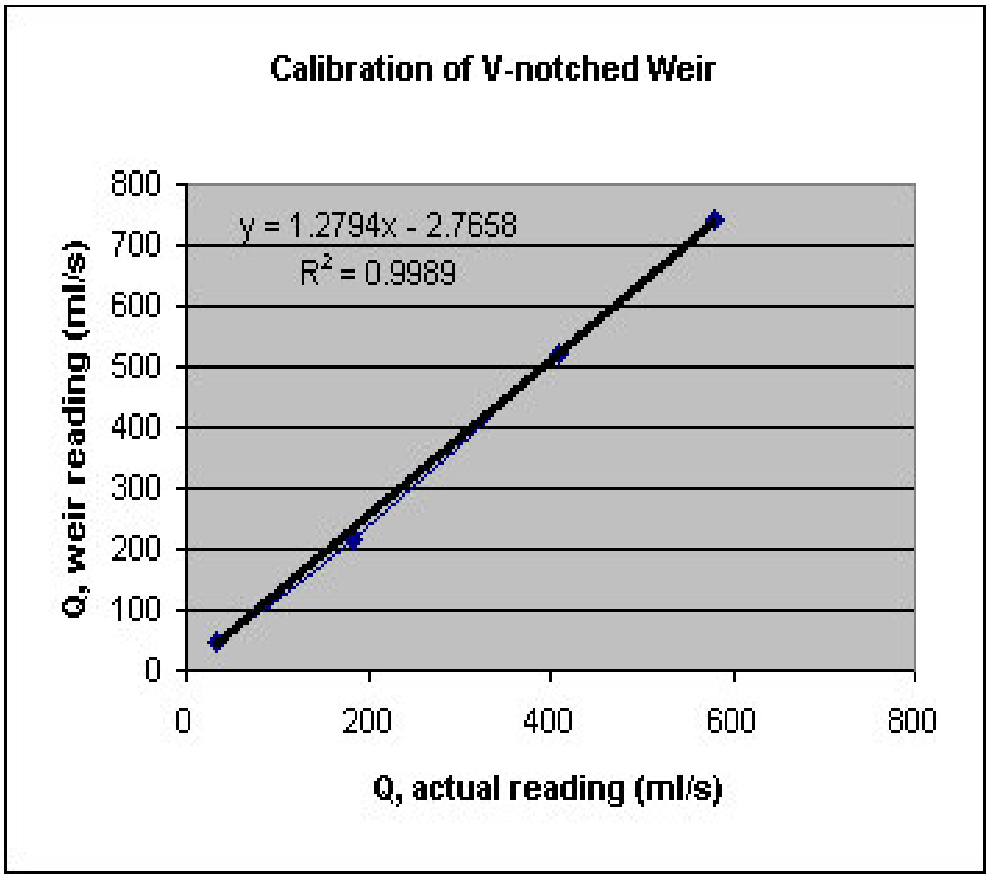

Figure C. 2. Calibration of the v-notched weir

Appendix D

Site Physical Characterization Data With Procedures

D.1. Soil Textural Analysis using Standard Method (Paul et al., 1974)

Texture is one of the most important physical properties of soil and is one of the major features distinguishing different soil types. To evaluate the soil types used at the site, four locations in each plot were selected for texture analysis. Eight soil samples at the top and at the bottom of each subplot were taken for analysis. These samples were taken at 0-10 cm, 10-20 cm, 20-30 cm, 30-40 cm, 40-50 cm, 50-60 cm, 60-70 cm, and 70-80 cm depth. Laboratory analysis included both the sample preparation and the use of the hydrometer method.

Fifty grams of oven-dried soil was placed into a dispersion cup and was filled 2/3 full by distilled water. Fifty ml of 10% metaphosphate solution then was added and was mixed on a disperser for 5 minutes. Quantitatively, the soil suspension was poured into a 1000 mL graduated cylinder and distilled water was added to bring the suspension to 1000 mL. The content of the graduated cylinder was vigorously stirred with a plunger. The plunger then was removed from the cylinder and a hydrometer was placed carefully in suspension. The time was recorded right after the plunger was removed and 40 seconds after the hydrometer was placed into the cylinder. A thermometer was also used to record the suspension temperature.

Exactly two hours after the plunger was removed, hydrometer reading was recorded again without any disturbance to the suspension cylinder. The hydrometer readings were corrected by adding 0.2 for each degree above 68 ˚F and by subtracting 0.2 for each degree below 68 ˚F (Paul et al., 1974). Whenever the surface of the suspended solution was covered with foam, one drop of amyl alcohol was added in order to take a hydrometer reading.

Table D.1. Soil texture analysis for bare clay loam and vegetated clay loam soils

Sample ID	% Silt + % Clay	% Clay	% Silt	% Sand	Texture
ST P2 TL 0-10	77.1	38.2	38.9	22.9	clay loam
ST P2 TL 10-20	64.5	34.7	29.9	35.5	clay loam
ST P2 TL 20-30	69.5	36.2	33.3	30.5	clay loam
ST P2 TL 30-40	75.1	38.2	36.9	24.9	clay loam
ST P2 TL 40-55	30.6	17.0	13.6	69.4	sandy loam
ST P2 TL 55-70	30.4	16.6	13.8	69.6	sandy loam
ST P2 TL 70-85	32.8	18.8	14.0	67.2	sandy loam
ST P2 TL 85-100	32.9	18.9	14.0	67.1	sandy loam
ST P2 TR 0-10	81.5	40.3	41.2	18.5	silty clay
ST P2 TR 10-20	80.2	37.6	42.7	19.8	silty clay loam
ST P2 TR 20-30	43.8	24.4	19.4	56.2	sandy clay loam
ST P2 TR 30-40	39.3	22.2	17.1	60.7	sandy clay loam
ST P2 TR 40-55	32.9	20.9	12.0	67.1	sandy clay loam
ST P2 TR 55-70					
ST P2 TR 70-85					
ST P2 TR 85-100					
ST P1 TL 0-10	79.8	42.6	37.2	20.2	clay
ST P1 TL 10-20	80.0	43.0	37.0	20.0	clay
ST P1 TL 20-30	95.6	51.7	43.8	4.4	silty clay
ST P1 TL 30-40	40.6	25.5	15.2	59.4	sandy clay loam
ST P1 TL 40-55	35.7	19.9	15.8	64.3	Sandy loam
ST P1 TL 55-70					
ST P1 TL 70-85					
ST P1 TL 85-100					
ST P1 TR 0-10	84.1	40.7	43.4	15.9	silty clay
ST P1 TR 10-20	79.8	40.8	39.1	20.2	clay
ST P1 TR 20-30	76.5	41.1	35.4	23.5	clay
ST P1 TR 30-40	41.1	22.5	18.6	58.9	sandy clay loam
ST P1 TR 40-55	31.8	16.0	15.8	68.2	sandy loam
ST P1 TR 55-70	33.7	17.9	15.8	66.3	sandy loam
ST P1 TR 70-85	31.8	18.0	13.9	68.2	sandy loam
ST P1 TR 85-100					
ST P1 BL 0-10	78.3	38.1	40.2	21.7	clay loam
ST P1 BL 10-20	79.7	38.9	40.8	20.3	clay loam
ST P1 BL 20-30	83.8	41.0	42.8	16.2	silty clay
ST P1 BL 30-40	37.3	18.7	18.6	62.7	sandy loam
ST P1 BL 40-55	33.5	15.9	17.7	66.5	sandy loam
ST P1 BL 55-70	29.3	15.7	13.6	70.7	sandy loam
ST P1 BL 70-85	39.3	21.1	18.3	60.7	sandy clay loam
ST P1 BL 85-100					unknown texture
ST P1 BR 0-10	78.4	35.3	43.2	21.6	clay loam
ST P1 BR 10-20	38.5	6.1	32.4	61.5	sandy loam
ST P1 BR 20-30	40.3	21.4	18.9	59.7	sandy clay loam

Table D.1. (Continued)

Sample ID	% Silt + % Clay	% Clay	% Silt	% Sand	Texture
ST P1 BR 30-40	42.0	27.7	14.3	58.0	sandy clay loam
ST P1 BR 40-55	32.4	18.6	13.8	67.6	sandy loam
ST P1 BR 55-70	31.5	16.2	15.2	68.5	Sandy loam
ST P1 BR 70-85	51.1	34.8	16.2	48.9	sandy clay loam
ST P1 BR 85-100	32.8	25.0	7.8	67.2	sandy clay loam
ST P2 BL 0-10	60.8	37.3	23.5	39.2	clay loam
ST P2 BL 10-20	74.3	40.4	33.9	25.7	clay
ST P2 BL 20-30	64.2	33.0	31.2	35.8	clay loam
ST P2 BL 30-40	33.2	17.6	15.5	66.8	sandy loam
ST P2 BL 40-55	39.9	23.5	16.3	60.1	sandy clay loam
ST P2 BL 55-70	49.8	42.2	7.6	50.2	sandy clay
ST P2 BL 70-85	38.7	22.7	16.0	61.3	sandy clay loam
ST P2 BL 85-100					
ST P2 BR 0-10	61.1	40.8	20.3	38.9	clay
ST P2 BR 10-20	62.9	33.1	29.8	37.1	clay loam
ST P2 BR 20-30	74.0	34.3	39.7	26.0	clay loam
ST P2 BR 30-40	46.6	26.0	20.6	53.4	sandy clay loam
ST P2 BR 40-55	29.7	15.9	13.8	70.3	sandy loam
ST P2 BR 55-70	29.6	15.8	13.7	70.4	sandy loam
ST P2 BR 70-85	31.7	17.9	13.8	68.3	sandy loam
ST P2 BR 85-100					

Table D.2. Soil texture analysis for bare and vegetated sandy loams

Sample ID	Dry wt., gr	Temp C	40 sec reading	2 hour reading	Hydrometer calibration	Corrected 40 sec reading	Corrected 2 hr reading
P3P4-CL 0-10	36.63	21	18	9.5	3	15.36	6.86
P3P4-CL 10-30	50.01	21	21	11.5	3	18.36	8.86
P3P4-CL 30-55	50.01	21	21	11.5	3	18.36	8.86
P3P4-CL 55-60	16.11	21	11	8	3	8.36	5.36
P3P4-CFL 0-10	36.13	23	18.5	10	3	16.58	8.08
P3P4-CFL 10-30	50.00	23	21	11.5	3	19.08	9.58
P3P4-CFL 30-55	50.00	23	19	11	3	17.08	9.08
P3P4-CFL 55-64	49.49	23	20	11	3	18.08	9.08
P3P4-BL 0-10	35.67	23	19	10	5.5	14.58	5.58
P3P4-BL 10-30	49.00	23	23	13	5.5	18.58	8.58
P3P4-BL 30-55	50.00	23	17	5.5	5.5	12.58	1.08
P3P4-CR 0-10	35.29	23	16	9	5.5	11.58	4.58
P3P4-CR 10-30	50.00	23	21	12	5.5	16.58	7.58
PP3P4-CR 30-55	50.00	23	19	11	5.5	14.58	6.58
P3P4-CR 55-61	36.11	23	17	10	5.5	12.58	5.58
P3P4-BR 0-10	37.77	22	19	9	5	14.72	4.72
P3P4-BR 10-30	50.00	22	21	11.5	5	16.72	7.22
P3P4-BR 30-53	50.00	22	21	11.5	5	16.72	7.22
P3P4-TR 0-10	34.94	22	20.6	9	5	16.32	4.72
P3P4-TR 10-30	50.00	22	19	11	5	14.72	6.72
P3P4-TR 30-55	50.00	22	18	11	5	13.72	6.72
P3P4-TR 55-70	50.00	22	18	10.5	5	13.72	6.22
P3P4-TL 0-10	40.31	22	19.5	10.5	5	15.22	6.22
P3P4-TL 10-30	50.00	22	22	12	5	17.72	7.72
P3P4-TL 30-48	50.00	22	21.5	12	5	17.22	7.72

Table D.2. (Continued)

Sample ID	% Silt + % Clay	% Clay	% Silt	% Sand	Texture
P2P3-CL 0-10	41.9	18.7	23.2	58.1	sandy loam
P2P3-CL 10-30	36.7	17.7	19.0	63.3	sandy loam
P2P3-CL 30-55	36.7	17.7	19.0	63.3	sandy loam
P2P3-CL 55-60	51.9	33.3	18.6	48.1	sandy clay loam
P2P3-CFL 0-10	45.9	22.4	23.5	54.1	sandy clay loam
P2P3-CFL 10-30	38.2	19.2	19.0	61.8	sandy loam
P2P3-CFL 30-55	34.2	18.2	16.0	65.8	sandy loam
P2P3-CFL 55-64	36.5	18.3	18.2	63.5	sandy loam
P2P3-BL 0-10	40.9	15.6	25.2	59.1	sandy loam
P2P3-BL 10-30	37.9	17.5	20.4	62.1	sandy loam
P2P3-BL 30-55	25.2	2.2	23.0	74.8	loamy sand
P2P3-CR 0-10	32.8	13.0	19.8	67.2	sandy loam
P2P3-CR 10-30	33.2	15.2	18.0	66.8	sandy loam
P2P3-CR 30-55	29.2	13.2	16.0	70.8	sandy loam
P2P3-CR 55-61	34.8	15.5	19.4	65.2	sandy loam
P2P3-BR 0-10	39.0	12.5	26.5	61.0	sandy loam
P2P3-BR 10-30	33.4	14.4	19.0	66.6	sandy loam
P2P3-BR 30-53	33.4	14.4	19.0	66.6	sandy loam
P2P3-TR 0-10	46.7	13.5	33.2	53.3	sandy loam
P2P3-TR 10-30	29.4	13.4	16.0	70.6	sandy loam
P2P3-TR 30-55	27.4	13.4	14.0	72.6	sandy loam
P2P3-TR 55-70	27.4	12.4	15.0	72.6	sandy loam
P2P3-TL 0-10	37.8	15.4	22.3	62.2	sandy loam
P2P3-TL 10-30	35.4	15.4	20.0	64.6	sandy loam
P2P3-TL 30-48	34.4	15.4	19.0	65.6	sandy loam

D.2. Soil Water Characteristics

The soil water characteristics describes the soil's ability to store and release water. It is a nonlinear relationship between soil water content and the soil matric potential. The models most frequently used to describe the relationship between soil water content and the soil matric potential are those proposed by Brooks and Corey (1964), Campbell (1974) and Van Genuchten (1980). Experiences indicate that soil texture predominately determine the water-holding characteristics.

For this research, on the sandy loam plots, four spots (two at the top and two at the bottom) were sampled for water retention purposes. On each designated spot, four samples were taken at 0-10 cm, 10-20 cm, 20-30 cm, 30-40 cm depth. On the clay loam side the same procedures were followed except for an additional soil sample taken from 40 cm to 50 cm (Fig. D.2). Figure D.2 shows the soil water characteristics curve ($\theta - h$) for both clay loam and sandy loam soils (θ is volumetric water content (L^3L^{-3}) and h is the pressure (L).

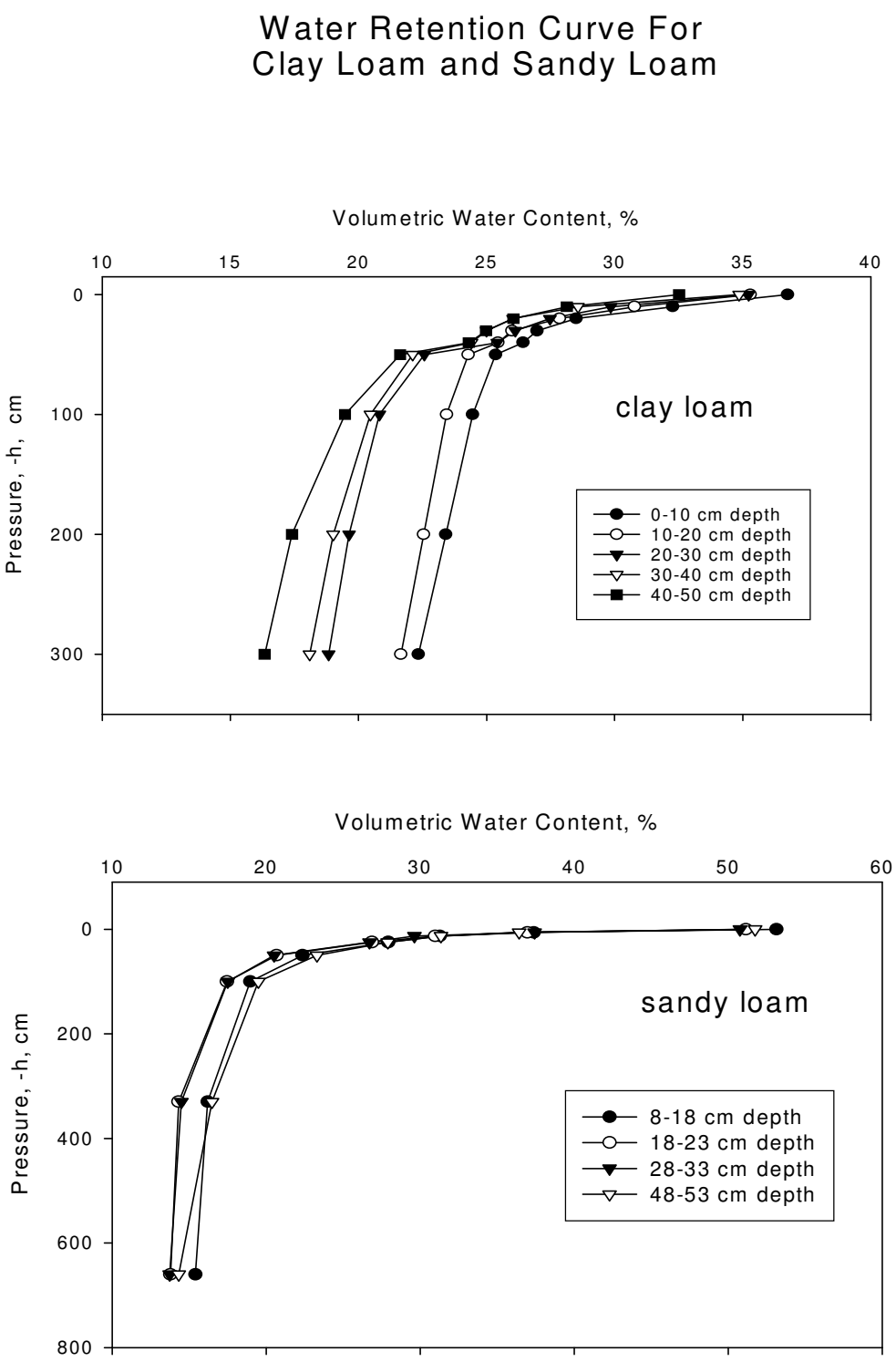

Figure D.2 Soil Water Characteristics for clay loam and sandy loam soils.

D.3. Soil Organic Matter

To determine the soil organic matter, samples of soils were taken from four locations in both clay loam and sandy loam plots. These locations were at the top left, top right, bottom left, and bottom right of the plot. For clay loam soil, two more samples were also taken at the center of the plot. Results are shown in the following table.

Table D.3 Soil organic matter for clay loam and for sandy loam soils

Sample ID	Texture	pH	Mg index	P index	K	O.M. %
1A	Clay Loam	6	87	103	109	2.88
1B	Clay Loam	5.7	93	305	141	3.57
1C	Clay Loam	5.1	81	372	119	1.05
1D	Clay Loam	5.7	73	131	48	3.11
1E	Clay Loam	5.7	86	134	111	3.04
1F	Clay Loam	6.9	79	139	54	2.73
2A	Sandy Loam	5.9	82	170	84	1.13
2B	Sandy Loam	5.9	94	165	61	1.51
2C	Sandy Loam	6.1	86	162	92	1.14
2D	Sandy Loam	6.7	115	150	54	1.71
2E	Sandy Loam	6.2	87	54	87	3.12

Where Mg is the magnesium, P is phosphorous, and K is the potassium. They considered as macronutrients in soil.

The average soil organic matter content and pH of the top 10 cm from five random samples were 2.7±0.9% & 5.9±0.6 and 1.7±0.9% & 6.2±0.3 for the clay loam and sandy loam soils, respectively

D.4. Determination of Soil Saturated Hydraulic Conductivity (K_s)

Soil samples in standard 7.62 cm (3 inch) diameter cores with a length of 7.62 cm (3 inch) were taken from the lysimeter to the soil and water laboratory at the University of Maryland to measure the soil saturated hydraulic conductivity. The constant head method was used with Darcy's Equation for determination of the saturated hydraulic conductivity. Figure D.3 shows the schematic of the constant head procedure in obtaining the saturated hydraulic conductivity (K_s).

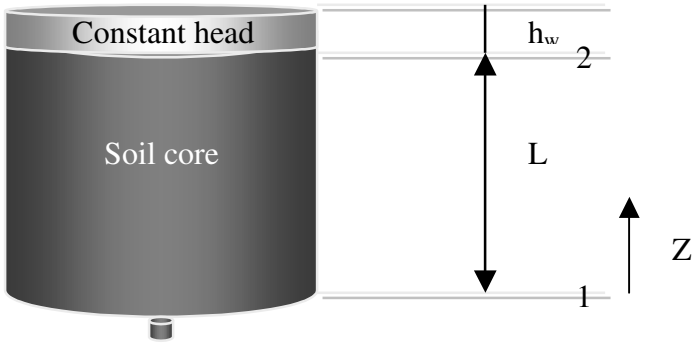

Figure D.3. Schematic of soil core used to calculate the saturated hydraulic conductivity

The soil was completely saturated from the bottom and then was placed in a small flume. Water was slowly added from the top of the core until a constant head (pounded water) was maintained. Volume of water was collected for series of

different time. Darcy's equation was then used to determine the soil saturated hydraulic conductivity.

$$Q = K_s . A. \frac{\Delta H}{\Delta Z} = \frac{\Delta H}{L}$$

$$\Delta H = H_2 - H_1$$

$$H_2 = Z_2 + h_2 = L + h_2 = L + h_w$$

$$H1 = Z_1 + h_1 = 0 + 0 = 0$$

where Q is the flow rate (cm^3/min.), A is soil cross-sectional area of the core, Z1 and Z2 are the elevation head, h1 and h2 are the pressure head, and ΔH is difference in total hydraulic head between points 1 and 2. The K_s values were found to be close to the K_s values obtained by Rawls et al. (1998) for soil of similar texture. The following table indicates the results of constant head procedures to calculate K_s.

Table D.4. Data obtained in the laboratory to calculate the K_s for clay loam and sandy loam plots.

	Clay Loam			Sandy Loam			Sandy Loam	
Time, min.	Q, ml.	Ks, cm/min	Time, min.	Q, ml.	Ks, cm/min	Time, sec.	Q, ml.	Ks, cm/min
12	39.5	0.054	1	62	1.02	30	42	1.38
12	36	0.049	1	56.1	0.92	30	43	1.41
12	34.5	0.047	1	57.5	0.95	30	43	1.41
12	41	0.056	1	56	0.92	30	43.5	1.43
			1	55	0.9	30	43	1.41
Average		0.052			0.94			1.41

Reference

Paul, R. Day, C.H.M. von Bavel, V.C. Jamison, H. Konke, J.F. Lutz, R.D. Miller, J,B. Page, and T.C. Peele. 1974. Vol. 20, S.S.S.A. Proc. Pages 167-169.

Appendix E

Soil physical and hydrological Data

E.1. Average Suction Ahead of wetting Front

Pore-size distribution index (λ) and $\eta = 2+3\lambda$ were determined using Brooks and Corey (1964) method. The results are shown on Table E.1, and Presented on Figures E.1 and E.2. The bubbling pressure (P_b) was found using Table E.1. The saturation $S = \frac{\theta}{\theta_s}$, *and the residual saturation*, $Sr = \frac{\theta_{residual}}{\theta_{sat}}$ were also calculated and tabulated (Table E.1). Then, the effective saturation, S_e, was calculated using Se $= \frac{S - S_r}{1 - S_r}$. Finally, S_e versus log (-h) was plotted on the log-log scale (Figures E.1, and E.2.). The value of P_b was determined at the intersection of the best-fit line of S_e verses –h. Then, the value of S_{av} (average suction ahead of wetting front) was estimated using equation $S_{av} = \frac{1}{2} P_b \frac{\eta}{\eta - 1}$ (Brooks and Corey, 1964). $S_{av,}$ was also calculated by Brakensiek (1977) as shown in the following:

$S_{av} = 0.76\ P_b = 0.76 * 50 = 38$ cm for clay loam

$S_{av} = 0.76\ P_b = 0.76 * 30 = 22.8$ cm for sandy loam

Table E.1. Effective saturation and pressure head values for clay and sandy loam within the top 30 cm depth.

Pressure, cm	Average θ	Clay Loam S	Clay Loam S_e	Pressure, cm	Average θ	Sandy Loam S	Sandy loam S_e
0	0.35	1	1	0	0.54	1	1
10	0.30	0.857	0.668	0.1	0.52	0.963	0.948
20	0.27	0.771	0.468	6	0.37	0.685	0.557
30	0.26	0.743	0.402	13	0.31	0.574	0.400
40	0.25	0.714	0.336	25	0.27	0.500	0.296
50	0.23	0.657	0.203	50	0.22	0.407	0.165
100	0.22	0.629	0.136	100	0.18	0.333	0.061
200	0.20	0.571	0.003	330	0.15	0.278	-0.017
300	0.20	0.571	0.003	660	0.14	0.259	-0.043

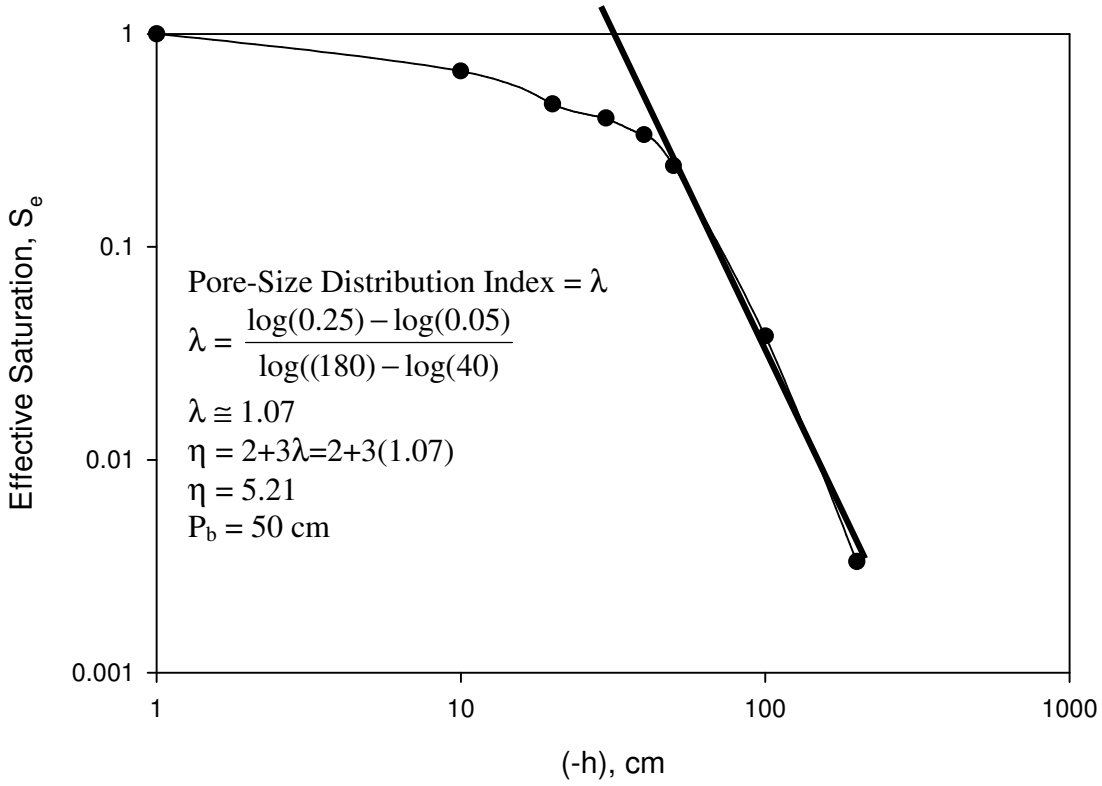

Figure E.1. Determination of bubbling pressures for clay loam

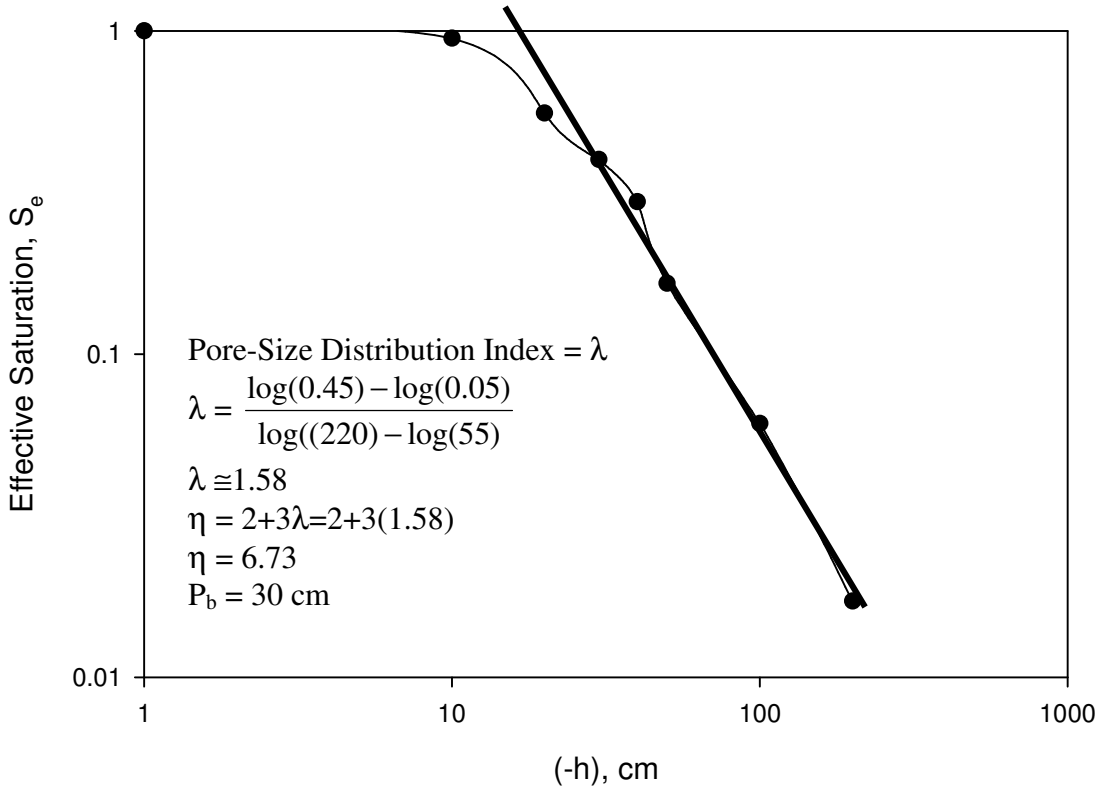

Figure E.2. Determination of bubbling pressures for sandy loam

Appendix F

Data and Procedures To Calculate the Total Runoff and The Infiltration on Each PLOT

F1. Procedures to determine total runoff and infiltration

Total runoff discharging through funnels and the gutter on each plot were determined according to the following procedures:

Funnels:

$$R_F = \left(\frac{(\Sigma\,(V1 \cdots V9)}{(Area) \times T} * 10\right.$$

Gutter:

$$R_G = \left(R_{gutter} \times \frac{3780}{(24 \times 60)(Area)}\right) \times 10$$

Where, R_F is the funnels total runoff rates in mm/min at every time step, V1…V9 are the total runoff volume at each time step (ml), Area is the area of each plot and is equal to $600 \times 640\,\text{cm}^2$, T is the time increment in minutes, RG is the gutter runoff rate in mm/min, and R_{gutter} is the gutter runoff in gpd at each time interval.

Example computations for vegetated clay loamPLOT2, FC Experiments

Time, min	F1, ml	F2, ml	F3, ml	F4, ml	F5, ml	F6, ml	F7, ml	F8, ml	F9, ml	Time, min	Gutter, gpd
40	13	270	580	40	80	60	4	120	80	40	60
45	40	285	610	100	60	50	13	410	120	44	735

$$\sum (V1 \cdots V9) = 1688 \text{ ml at 45 minutes}$$

$$R_F = \left(\frac{1688\ ml}{(640 \times 600\ cm^2) \times 5\ \text{min}}\right) \times 10 = 0.00879 \text{ mm/min}$$

$$R_G = \frac{900\ gallons}{\min ute} \times \frac{3780\ cm3}{(24\ hours \times 60\ \min utes)(600 \times 640\ cm2)}) \times 10 = 0.062\ \text{mm/min}$$

Total runoff rate = 0.00879+0.0615 = 0.070 mm/min after 45 minutes of simulation.

The infiltration of water on each plot was measured based on a simple mass balance equation as shown in the following;

$$F=P-R-E-I$$

Where,

F= Total infiltration, cm

P= Total precipitation, cm

R= Total measured runoff at the gutter during the experiment, cm

E= Total evaporation, cm

I= Total interception either by depression or by surface cover, cm

Since the experiments were conducted on early mornings, and the vegetated plots could only intercept 1 mm of total rainfall, both evaporation (E), and surface intercepts (I) were neglected during the 55 minutes and 90 minutes of simulation for the two bare and the vegetated plots respectively.

The intensity of the synthetic rain was selected based on the local meteorological information for the Prince George's County in the State of Maryland (area where the experiments were conducted) provided by NOAA on a 10-year return period. During the entire simulation of all experiments, intensity was maintained at a constant rate of 6.1 cm/h. The surface runoff from each plot was measured at the end of each time increment (five minutes intervals) in the gutter directly from a V-notch

Weir and later added to the total water volume collected through the entire funnels on each plot at the same time increments to obtain the corresponding total surface runoff of each plot. The measured total runoff on each time increment then was divided to one unit flow area (1 cm by 600 cm) to get the total incremental surface runoff. The total infiltrations on each time increment (5 minutes) for each plot then, was calculated by subtracting the incremental runoff from the incremental precipitation.

Table F.1 Total measured runoff for bare clay loam

T, min	F1, ml	F2, ml	F3, ml	F4, ml	F5, ml	F6, ml	F7, ml	F8, ml	F9, ml	Sum F1-F9 ml
0	0	0	0	0	0	0	0	0	0	0
5	1240	540	1140	1100	2900	5300	13000	1600	7900	34720
10	1560	640	1100	5300	440	6800	13350	2280	14050	45520
15	1300	680	1280	4900	340	6400	14400	2430	14050	45780
20	1320	680	1100	5000	4100	6100	13300	2300	13150	47050
25	1500	720	1320	5600	4700	6200	13650	2300	14150	50140
30	1560	680	1120	5700	4500	6000	13830	2400	13950	49740
35	1420	660	1140	5800	4400	6000	12000	2500	13950	47870
40	1390	700	1160	5700	4200	5900	13900	2600	13850	49400
45	1380	680	1080	5900	4000	5800	1390	2400	14050	36680
50	1390	680	1220	5500	3600	5800	14000	2400	13750	48340
55	1380	700	1060	5800	3900	5800	6550	2300	13650	41140
57										
58.5										
59										
59.5										
60										

F1, F2 and F3 are the funnels at Row 1 (95 cm distance from the ridge of the plot)
F4, F5 and F6 are the funnels at Row 2 (285 cm distance from the ridge of the plot)
F7, F8 and F9 are the funnels at Row 3 (490 cm distance from the ridge of the plot)

Table F.1 (Continued)

T, min	Funnels Total Runoff Rate mm/min	Gutter, gpd	Gutter Total Runoff Rate mm/min	Total Runoff Rate mm/min
0	0.00	0	0.00	0.00
5	0.18	8500	0.58	0.76
10	0.24	9000	0.62	0.85
15	0.24	9243	0.63	0.87
20	0.25	9350	0.64	0.88
25	0.26	9900	0.68	0.94
30	0.26	10000	0.68	0.94
35	0.25	10250	0.70	0.95
40	0.26	10500	0.72	0.98
45	0.19	10700	0.73	0.92
50	0.25	10900	0.75	1.00
55	0.21	11150	0.76	0.98
57		5000	0.34	0.34
58.5		2500	0.17	0.17
59		2000	0.14	0.14
59.5		1200	0.08	0.08
60		700	0.05	0.05

Table F.2 Total measured runoff for vegetated clay loam

T, min	F1, ml	F2, ml	F3, ml	F4, ml	F5, ml	F6, ml	F7, ml	F8, ml	F9, ml	Sum F1-F9 ml
0	0	0	0	0	0	0	0	0	0	0
5	15	104	65	68	68	40	0	0	47	407
10	27	225	200	91	67	62	5	30	88	795
15	70	310	350	93	77	63	16	58	83	1120
20	33	250	465	78	98	125	4	30	71	1154
25	14	250	600	83	90	85	5	39	89	1255
30	58	310	620	82	87	93	8	82	96	1436
35	21	260	660	97	93	120	4	131	110	1496
40	13	270	580	40	80	60	4	120	80	1247
45	40	285	610	100	60	50	13	410	120	1688
50	40	90	355	90	50	50	9	583	130	1397
55	20	280	650	60	90	50	5	620	170	1945
60	80	340	610	70	85	30	30	900	190	2335
65	360	450	630	135	105	25	60	1620	220	3605
70	160	260	400	70	60	25	35	850	130	1990
75	220	360	570	100	60	25	40	1430	220	3025
80	215	330	500	100	70	25	30	1380	200	2850

Table F.2 (Continued)

T, min	Funnels Total Runoff Rate mm/min	Gutter, gpd	Gutter Total Runoff Rate mm/min	Total Runoff Rate mm/min
0	0.00	0	0.00	0.00
5	0.00	0	0.00	0.00
10	0.00	0	0.00	0.00
15	0.01	0	0.00	0.01
20	0.01	0	0.00	0.01
25	0.01	0	0.00	0.01
30	0.01	0	0.00	0.01
35	0.01	0	0.00	0.01
40	0.01	60	0.00	0.01
45	0.01	900	0.06	0.07
50	0.01	1300	0.09	0.10
55	0.01	1550	0.11	0.12
60	0.01	1950	0.13	0.15
65	0.02	2410	0.16	0.18
70	0.01	3000	0.21	0.22
75	0.02	4100	0.28	0.30
80	0.01	4300	0.29	0.31
85	0.02	4300	0.29	0.31
90	0.02	4300	0.29	0.31
95		2900	0.20	0.20
96		2500	0.17	0.17
97		2000	0.14	0.14
98		1600	0.11	0.11
100		1200	0.08	0.08

Table F.3 Total measured runoff for bare sandy loam

T, min	F1, ml	F2, ml	F3, ml	F4, ml	F5, ml	F6, ml	F7, ml	F8, ml	F9, ml	Sum F1-F9 ml
0	0	0	0	0	0	0	0	0	0	0
5	930	175	240	175	270	400	71	0	60	2321
10	1880	510	810	510	2200	2100	1200	680	780	10670
15	1960	540	920	540	2500	2100	1800	780	1740	12880
20	1860	480	1240	480	3100	2500	1660	860	1700	13880
25	1910	750	1040	750	2900	2700	1500	720	2100	14370
30	2350	710	910	710	3000	2500	1760	640	2200	14780
35	2400	760	820	760	3400	2500	1760	700	2100	15200
40	2800	810	860	810	3500	2600	1440	660	2000	15480
45	2600	890	930	890	3000	2800	1300	850	2200	15460
50	2500	920	880	920	3000	2700	1360	880	2400	15560
55	2150	920	820	920	3000	3000	1300	1160	2700	15970

Table F.3 (Continued)

T, min	Funnels Total Runoff Rate mm/min	Gutter, gpd	Gutter Total Runoff Rate mm/min	Total Runoff Rate mm/min
0	0.00	0	0.00	0.00
5	0.01	100	0.01	0.02
10	0.06	3700	0.25	0.31
15	0.07	8600	0.59	0.66
20	0.07	9000	0.62	0.69
25	0.07	9240	0.63	0.71
30	0.08	9250	0.63	0.71
35	0.08	9300	0.64	0.72
40	0.08	9300	0.64	0.72
45	0.08	9300	0.64	0.72
50	0.08	9300	0.64	0.72
55	0.08	9300	0.64	0.72
56		5470	0.37	0.37
57		3100	0.21	0.21
58		1300	0.09	0.09
59		500	0.03	0.03
60		450	0.03	0.03
61		260	0.02	0.02
62		180	0.01	0.01
63		120	0.01	0.01

Table F.4 Total measured runoff for vegetated sandy loam

T, min	F1, ml	F2, ml	F3, ml	F4, ml	F5, ml	F6, ml	F7, ml	F8, ml	F9, ml	Sum F1-F9 ml
0	0	0	0	0	0	0	0	0	0	0
10	87.4	173.25	283.83	180.88	213.01	90.68	173.35	119.66	137.41	1459.47
20	99.6	181.16	233.11	180.79	196.72	84.94	196.47	166.91	173.33	1513.03
30	107.92	176.29	208.84	174.37	176.34	89.89	204.92	178.9	160.11	1477.58
40	68.67	189.89	192.71	156.36	158.84	41.49	157.5	160.41	159.37	1285.24
50	75.12	189.15	196.72	168.47	159.44	74.08	165.63	165.44	151.04	1345.09
60	67.9	216.23	184.2	164.47	148.56	72.67	166.97	156.19	139.99	1317.18
70	44.01	194.19	181.97	145.9	179.21	97.34	165.69	145.48	152.66	1306.45
80	65.97	188.72	175.67	146.65	167.86	122.08	148.25	162.43	144.62	1322.25
90	74.58	188.65	182.56	176.36	160.58	81.89	166.72	171.16	143.88	1346.38
100	85.59	195.31	180.69	179.32	141.96	88.85	185.37	165.02	145.44	1367.55
110	88.85	187.2	172.4	180.54	169.78	84.69	174.96	161.9	161.09	1381.41
120	86.33	194.15	187.88	184.46	188.06	87.68	200.79	180.52	160.15	1470.02
130	79.51	191.77	196.31	166.51	200.55	94.62	174.61	172.51	159.4	1435.79
140	59.38	154.44	139.02	132.37	139.63	62.54	116.17	123.11	123.27	1049.93
150	22.32	30.92	26.89	20.16	0.27	16.27	21.57	24.97	12.87	176.24

Table F.4 (Continued)

T, min	Funnels Total Runoff, mm/min	Gutter, gpd	Gutter Total Runoff Rate, mm/min	Total Runoff Rate mm/min
0	0.000	0	0.000	0.00
10	0.008	0	0.000	0.008
20	0.008	0	0.000	0.008
30	0.008	0	0.000	0.008
40	0.007	0	0.000	0.007
50	0.007	200	0.014	0.021
60	0.007	400	0.027	0.034
70	0.007	470	0.032	0.039
80	0.007	500	0.034	0.041
90	0.007	500	0.034	0.041
100	0.007	500	0.034	0.041
110	0.007	500	0.034	0.041
120	0.008	500	0.034	0.042
130	0.007	410	0.028	0.036
140	0.005	150	0.010	0.016
150	0.001	50	0.003	0.004

Table F.5 Total infiltration obtained from mass balance equation (F = Precipitation-Runoff), bare clay loam

Time, min	Cumulative Rain cm	Cumulative Runoff @ Gutter, cm	Cumulative Runoff @ Funnels, cm	Total Infiltration cm
0	0.00	0.00	0.00	0.00
5	0.51	0.29	0.09	0.13
10	1.02	0.60	0.21	0.21
15	1.53	0.91	0.33	0.28
20	2.03	1.23	0.45	0.35
25	2.54	1.57	0.58	0.39
30	3.05	1.91	0.71	0.43
35	3.56	2.26	0.84	0.46
40	4.07	2.62	0.96	0.48
45	4.58	2.99	1.09	0.49
50	5.08	3.36	1.22	0.50
55	5.59	3.74	1.32	0.52

Table F.6 Total infiltration obtained from mass balance equation (F= Precipitation-Runoff), vegetated clay loam

Time, min	Cumulative Rain cm	Cumulative Runoff @ Gutter, cm	Cumulative Runoff @ Funnels, cm	Total Infiltration cm
0	0.00	0.00	0.00	0.00
5	0.51	0.00	0.00	0.51
10	1.02	0.00	0.00	1.01
15	1.53	0.00	0.01	1.52
20	2.03	0.00	0.01	2.02
25	2.54	0.00	0.01	2.53
30	3.05	0.00	0.02	3.03
35	3.56	0.00	0.02	3.54
40	4.07	0.00	0.02	4.04
45	4.58	0.03	0.03	4.52
50	5.08	0.07	0.03	4.98
55	5.59	0.12	0.04	5.43
60	6.10	0.19	0.04	5.87
65	6.61	0.27	0.05	6.28
70	7.12	0.37	0.06	6.69
75	7.63	0.51	0.06	7.05
80	8.13	0.66	0.07	7.40
85	8.64	0.81	0.08	7.75
90	9.15	0.95	0.09	8.11

Table F.7 Total infiltration obtained from mass balance equation (F= Precipitation-Runoff), bare sandy loam

Time, min	Cumulative Rain cm	Cumulative Runoff @ Gutter, cm	Cumulative Runoff @ Funnels, cm	Total Infiltration cm
0	0.00	0.00	0.00	0.00
5	0.51	0.00	0.01	0.50
10	1.02	0.11	0.03	0.87
15	1.53	0.37	0.06	1.09
20	2.03	0.68	0.10	1.25
25	2.54	1.00	0.14	1.41
30	3.05	1.31	0.17	1.56
35	3.56	1.63	0.21	1.72
40	4.07	1.95	0.25	1.87
45	4.58	2.27	0.29	2.02
50	5.08	2.59	0.33	2.17
55	5.59	2.90	0.37	2.32

Table F.8 Total infiltration obtained from mass balance equation (F= Precipitation-Runoff), vegetated sandy loam

Time, min	Cumulative Rain cm	Cumulative Runoff @ Gutter, cm	Cumulative Runoff @ Funnels, cm	Total Infiltration cm
0	0.00	0.00	0.00	0.00
10	1.02	0.00	0.00	1.01
20	2.03	0.00	0.01	2.03
30	3.05	0.00	0.01	3.04
40	4.07	0.00	0.01	4.05
50	5.08	0.00	0.02	5.06
60	6.10	0.02	0.02	6.05
70	7.12	0.06	0.03	7.04
80	8.13	0.09	0.03	8.01
90	9.15	0.12	0.03	8.99
100	10.17	0.16	0.04	9.97
110	11.18	0.19	0.04	10.95
120	12.20	0.23	0.04	11.93

Appendix G

Determination of Volumetric and Relative Concentrations

The concentrations were calculated based on arithmetic, geometric, and volumetric mean however, volumetric concentrations of FC, *E.coli*, and *Salmonella* were closer to simulated results. Following equation was deployed to calculate the volumetric concentrations of FC, *E.coli*, and *Salmonella*.

$$C_{row\ 1} = \frac{[C_1V_1]\ F_1 \times [C_2V_2]F_2 \times [C_3V_3]F_3}{V_1 + V_2 + V_3}$$

$$C_{row\ 2} = \frac{[C_4V_4]\ F_4 \times [C_5V_5]F_5 \times [C_6V_6]F_6}{V_4 + V_5 + V_6}$$

$$C_{row\ 3} = \frac{[C_7V_7\ ]\ F_7 \times [C_8V_8]F_8 \times [C_9V_9]F_9}{V_7 + V_8 + V_9}$$

Where,

C = Total concentrations in each row (95, 285, and 490 cm from the ridge), CFU/ml

$C_1 \ldots C_9$ = the concentrations on each funnel, CFU/ml at every time step

$V_1 \ldots V_9$ = runoff at each funnel at each time step, ml

The initial concentrations of FC, *E.coli*, and *Salmonella* were determined right before each experiment. After the concentrations of each organism were quantified in the laboratory at every funnel, the relative concentration then were determined by

dividing them to the initial concentrations to get the relative concentrations on each funnel and the gutter at every time interval.

Appendix H

Sorption Data

Experiments for sorption were conducted in laboratory under static and dynamics conditions using the actual runoff samples from the lysimeter.

Table H.1. Presence of FC colonies in water and soil samples, bare clay loam, (PLOT1), Experiment I

Time Hr	Water Ave. FC cfu/ml	Water Stdev	Sediment Ave. FC cfu/ml	Sed. stdev	Static Ave. FC cfu/ml	Static Stdev	Dynam. Ave. FC cfu/ml	Dynam. Stdev
0	1.06E+03	5.30E+01	8.85E+02	1.06E+02				
2	**9.93E+02**	2.02E+01	5.68E+02	1.31E+02	**7.87E+02**	8.10E+01	8.78E+02	7.65E+01
4	**9.10E+02**	1.81E+02	3.42E+02	9.80E+01	**6.08E+02**	2.01E+02	8.13E+02	1.58E+02
6	**8.13E+02**	1.27E+02	4.03E+02	1.40E+02	**6.65E+02**	1.75E+02	7.30E+02	2.27E+02

Solid Liquid ratio = 1.93%

I = refers to Experiment one.

Table H.2. Presence of FC colonies in water and soil samples, bare clay loam (PLOT1), experiment II

Time Hr	Water Ave. FC cfu/ml	Water Stdev	Sediment Ave. FC cfu/ml	Sed. stdev	Static Ave. FC cfu/ml	Static Stdev	Dynam. Ave. FC cfu/ml	Dynam. Stdev
0	6.17e+2	6.75e+1	4.38e+2	1.04e+1				
2	**6.93e+2**	3.33e+1	4.92e+2	2.84e+1	**5.35e+2**	1.39e+2	5.57e+2	4.25e+1
4	**5.00e+2**	1.15e+2	4.18e+2	6.53e+1	**3.47e+2**	1.77e+2	4.08e+2	1.53e+2
6	**4.28e+2**	1.30e+2	4.58e+2	1.23e+2	**4.00e+2**	1.41e+2	4.50e+2	1.08e+2

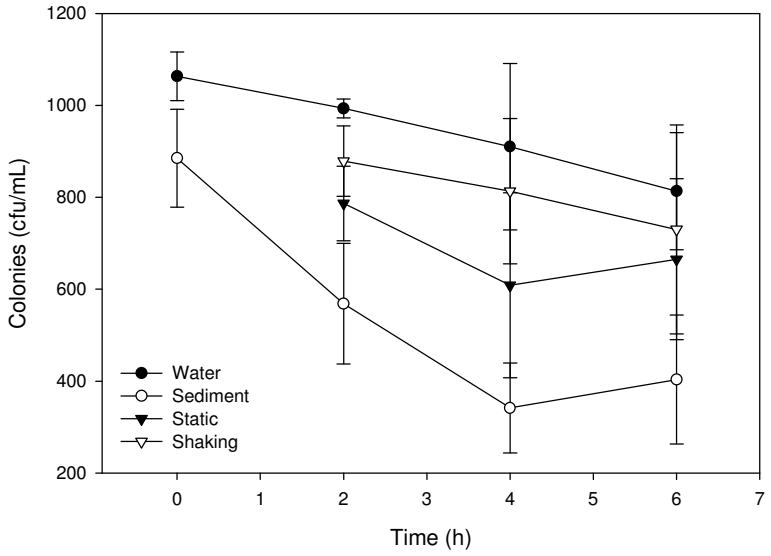

Figure H.1. Presence of Fecal coliform colonies in water and soil sediment samples, Experiment I using bare clay loam runoff sample (PLOT1)

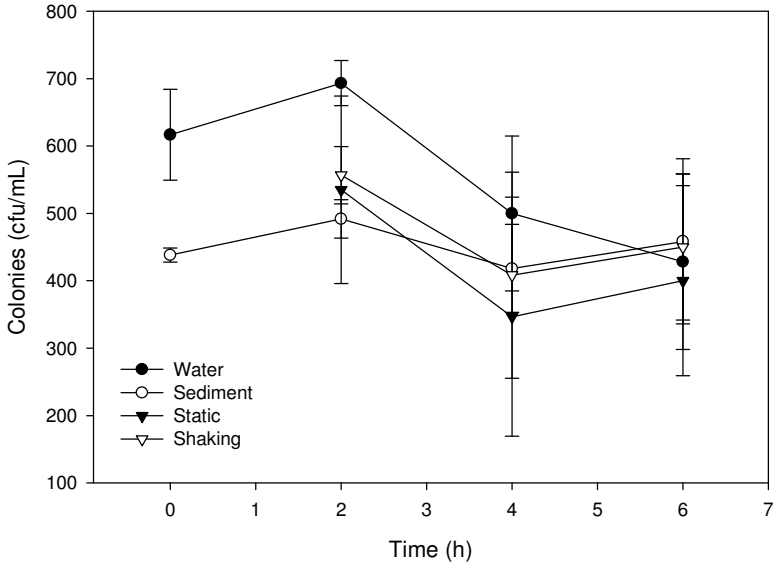

Figure H.2. Presence of fecal coliform colonies in water and soil sediment samples, Experiment II using bare clay loam runoff samples (PLOT1)

% FC remained in water	% of FC attached on sediments
$\frac{7.87E2}{9.93E2} * 100$=79.25 (2 hrs, I)	20.75
66.81 (4 hrs, I)	33.19
81.79 (6 hrs, I)	18.21
77.20 (2 hrs, II)	22.80
70.40 (4 hrs, II)	29.90
Not good(6 hrs)	

Average% FC remained in water and on the sediments are 74.9%, and 25.1%, respectively.
Standard deviation = +/-6.27%
Standard error = 6.27/$\sqrt{5}$ =2.80%

Table H.3. Presence of FC colonies in water and soil samples, bare sandy loam, (PLOT3), I

Time Hr	Water Ave. FC	Water stdev	Sediment Ave. FC	Sed. stdev	Static Ave. FC	Static Stdev	Dynam. Ave. FC	Dynam. Stdev
0	1.27E+03	7.57E+01	6.12E+02	4.07E+01				
2	**1.18E+03**	6.50E+01	3.92E+02	5.06E+01	**5.17E+02**	7.29E+01	5.22E+02	5.51E+01
4	**1.19E+03**	9.80E+01	2.95E+02	7.55E+01	**4.78E+02**	5.58E+01	4.55E+02	3.28E+01
6	**1.07E+03**	1.16E+02	2.43E+02	2.08E+01	**4.67E+02**	3.25E+01	4.13E+02	4.65E+01

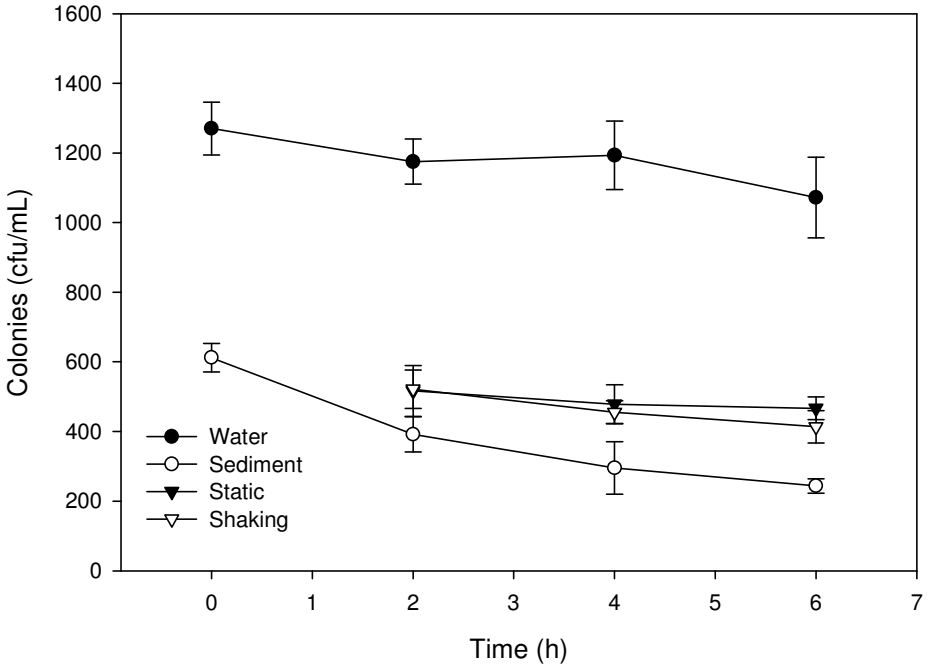

Figure H.3. Presence of fecal coliform colonies in water and soil sediment samples, Experiment I, using runoff sample from bare sandy loam (PLOT3)

Table H.4. Presence of FC colonies in water and soil samples, bare sandy loam, (PLOT3), II

Time hr	Water Ave	Water stdev	Sed. Ave.	Sed. stdev	Static Ave.	Static Stdev	Dynam. Ave.	Dynam. Stdev
0	7.60e+2	7.00e+1	5.53e+2	3.18e+1				
2	**7.80e+2**	1.26e+2	3.67e+2	2.75e+1	**5.17e+2**	3.79e+1	3.62e+2	5.62e+1
4	**6.77e+2**	7.29e+1	3.32e+2	6.21e+1	**4.65e+2**	1.02e+2	3.48e+2	1.46e+2
6	**6.43e+2**	1.60e+2	2.57e+2	5.01e+1	**3.88e+2**	1.01e+2	3.40e+2	8.18e+1

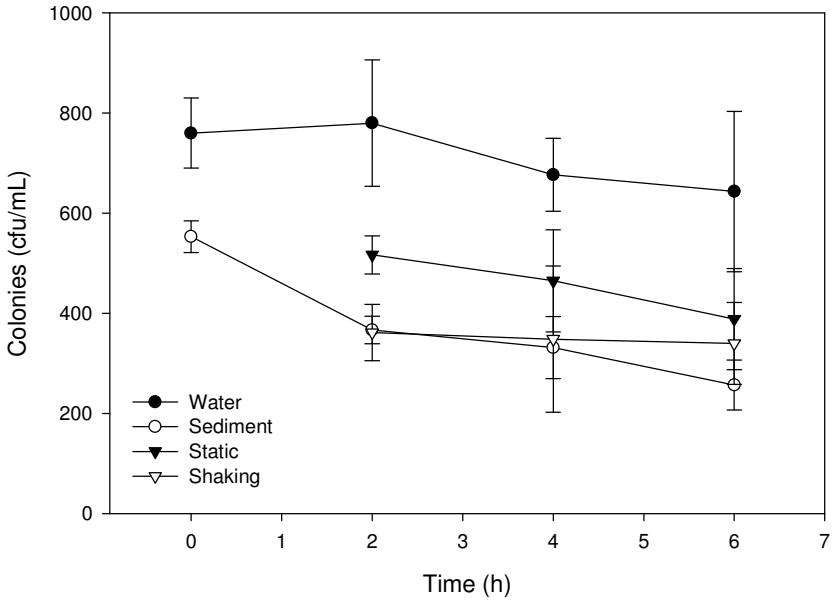

Figure H.4. Presence of fecal coliform colonies in water and soil sediment samples, Experiment II using runoff samples from bare sandy loam (PLOT3)

Results of Experiment I on PLOT 3 was quite high relative to Experiment II,

therefore, another experiment was conducted for PLOT 3.

Table H.5. Presence of FC colonies in water and soil samples, bare sandy loam, (PLOT3), III (Only static condition is concerned)

Time Hr	Water Ave. FC	Water stdev	Static Ave. FC	Static Stdev		
0	1.40E+03	1.18E+03	9.08E+01	8.07E+01		
2	**1.44E+03**	1.33E+02	**1.09E+03**	1.03E+02		
4	**1.44E+03**	8.47E+01	**1.10E+03**	7.92E+01		
6	**1.36E+03**	8.45E+01	**1.02E+03**	7.20E+01		

% FC remained in water	% of FC attached on sediments
$\frac{1.09e3}{1.44e3}\times 100 = 76\%$ (2hrs, III)	24%
$\frac{1.1e3}{1.44e3}\times 100 = 76\%$ (4hrs, III)	24%
$\frac{1.02e3}{1.44e3}\times 100 = 75\%$ (6hrs, III)	25%
66.3%(2 hrs, II)	33.72%
66.7%(4 hrs, II)	33.30%
60.3%(6 hrs, II)	39.66%

Total average = 29.7% with a standard deviation of 6.4%, and a standard error of $6.4/\sqrt{6} = 2.61\%$.

Appendix I

Source Code for MODCHOI
Simulation of Surface Runoff and FC Transport

```
* Overland Runoff
c
      IMPLICIT DOUBLE PRECISION (A-H,O-Z)
c Double precision introduced
c Parameters of the sediment model removed
  **************************** MODCHOI **********************
c==============================
c  ft = infiltration rate (mm/h)
c  sft = infiltration rate (m/s)
c  cft = cumulative infiltration (m)
c  rrt = a global coeficient ???
c  fh = average flow depth (m)
c  fq = flow volume (m^3/sec).
c  tabinf = ft tabulated each minute
c==============================
      Dimension lnn(10)
      Dimension tabinf(101,2), funinf(101,2,3)
      common /a1/ft(110,2) /a2/sft(110,2) /a3/cft(110,2)
     A       /a4/fh(110,2) /a5/fq(110,2) /a6/fv(110,2)
/a7/shr(110,2)
      Dimension conc(110,2)
      open(21, file='hyd08.dat',status='OLD')
      Write(*,*) 'itinput (1 - exp, 2 -step, 3 - lin)'
      read(*,*) itinput
      Write(*,*) 'C00, beta'
      read(*,*) C00, beta
      Read(21,*)
      read(21,*) wids, cm, ss, so, cn, agd
      Read(21,*)
      read(21,*) drain, dsra, dera
      Read(21,*)
      read(21,*) dsyin, dssy, desy
      Read(21,*)
      read(21,*) delx, delt, nnod, ntim, ey
      Read(21,*)
      read(21,*) wc
      Read(21,*)
      read(21,*) sg, bd
      Read(21,*)
      read(21,*) df1, df2, df3, cd1, cd2, cd3
      Read(21,*)
      read(21,*) fs, si
      Read(21,*)
      read(21,*) su, fts
      Read(21,*)
      read(21,*) ck
      Read(21,*)
      read(21,*) nln
      Read(21,*)
      read(21,*) (lnn(j),j=1,4)
      Read(21,*)
      Read(21,*) ct1,ct2
      close(21)
      Open(22,file='tabinf.txt')
      Read(22,*)
      Read(22,*) ninfdata
      Read(22,*)
```

```
      Do i=1,ninfdata
        Read(22,*) (tabinf(i,j),j=1,2)
      Enddo
      Close(22)
      Open(22,file='funinf.txt')
      Read(22,*)
      Read(22,*) ninfdata
      Read(22,*)
      Do i=1,ninfdata
        Read(22,*) ((funinf(i,j,k),j=1,2),k=1,3)
      Enddo
      Close(22)

c
c============================
c  Open hydrology output files
c============================
16    open(5, file='pa08.prn')
      open(6, file='fq08.prn')
      open(7, file='fh08.prn')
      open(8, file='fv08.prn')
      open(9, file='ft08.prn')
      open(l0, file='shr08.prn')
      open(12, file='cnc08.prn')
      solin =  0.0D+00
      solout = 0.0D+00
      open(11,file='infout.txt')

      write(6,510) ((lnn(j))*delx,j=1,4)
510   format(2x,'Overland Runoff Simulation - fiow rate (L/min)',/
     */4x,'min',7x,F3.1,' m',9x, F3.1,' m',9x,F3.1,' m',8x,F3.1,'
m')
      write(7,520) ((lnn(j))*delx,j=1,4)
520   format(2x,'Overland Runoff Simulation - flow depth (mm)',/
     */4x,'min',7x,F3.1,' m',9x, F3.1,' m',9x,F3.1,' m',8x,F3.1,'
m')
      write(8,530) ((lnn(j))*delx,j=1,4)
530   format(2x,'Overland Runoff Simulation - flow velocity (m/sec)'
     *//4x,'min',9x,F3.1,' m',9x,F3.1,' m',9x,F3.1,' m',8x,F3.1,'
m')
      write(9,540) ((lnn(j))*delx,j=1,4)
540   format(2x,'Overland Runoff Simulation - infiltration', //4x,
     * 'Units ; ft = mm/h'/
     */4x,'min',7x,F3.1,' m',9x, F3.1,' m',9x,F3.1,' m',8x,F3.1,'
m')
c=================================================================
c Data conversion and coefficient calculation (all units are
converted to m, m2, m3, sec,
c m/sec, m2/sec, and m3/sec umess otherwise specified)
c=================================================================
17    drain = drain/3600000.0D+00
      dera = dera*60.0D+00
      dsra = dsra*60.0D+00
      dsyin = dsyin/(60000.0D+00*wids)
      dssy = dssy*60.0D+00
      desy = desy*60.0D+00
      theta = delx/delt
```

```
      a = 1.0D+00 - (1.0D+00/ss*agd)
      cs = ss / ey
      alpha = so**0.5D+00/cn
c=============================================================
c Calculation of the soil parameters for both dry and wet runs
c total porosity of the soil (%)
c=============================================================
      tp=(1.0D+00-bd/sg)*100.0D+00
c=========================
c  degree of saturation (%)
c=========================
      ds = sg*wc/(sg/bd-1.0D+00)
c====================
c max. infilt (mm/hr)
c====================
      ek = 1.0D+00/(100.0D+00-su)*dlog(fts/fs)
      cf = fs / dexp(-100.0D+00*ek)
      fm = cf * dexp(-ek*ds)

18    write(5,500)
500   format(2x,'Overland Runoff Simulation - constants computed'/)
      write(5,400) tpu, tpl
400   format(2x,'Total porosity of the soil (%)',/
     *4x,'Upper area (tpu)= ',f8.2,4x,'Lower area (tpl)= ',f8.2,/)
      write(5,410) ddsu,ddsl,wdsu,wdsl
410   format(2x,'Degree of saturation (%)',/
     *4x,'Dry run, Upper area(ddsu)=',f8.2,4x,'Lower (ddsl)=',f8.2,/
     *4x,'Wet run, Upper area(wdsu)=',f8.2,4x,'Lower (wdsl)='f8.2/)
      write(5,470) dfmu,dfml,wfmu,wfml
470   format(2x,'Maximum infiltration rate under given soil ',
     A'moisture content (mm/hr)'/
     *4x,'Dry run, Upper area(dfmu)=',f8.2,4x,'Lower (dfml)=',f8.2/
     *4x,'Wet run, Upper area(wfmu)=',f8.2,4x,'Lower (wfml)=',f8.2/)
c=====================================================
c  k = an iteration index for time.
c  kkl = an index to check whether an iteration converges or not.
c  ntm = number of iteration per minute.
c=====================================
19    ntm = 60.0D+00/delt
      k = 0
20    k = k+1
      itim = dfloat(k)*delt-delt
      ttim = dfloat(itim)/60.0D+00
      call rn(rain,itim,dera,drain)
      if (k.ge.2) goto 40
c=====================================================
c Assign initial values for (i,1) when time is zero (k=1)
c=====================================================
      do 30 i=1,nnod,1
        fq(i,1)=0.0D+00
        fh(i,1)=0.0D+00
        fv(i,1)=0.0D+00
        shr(i,1) = 0.0D+00
        rain = drain
        ft(i,1) = drain*3600000.0D+00
        sft(i,1) = drain
        cft(i,1) = 0.0D+00
```

```
30    continue

      goto 83
c=============================================================
c  Start of a loop to compute unknown fh(i,2) and other parameters
c  kk1=iteration index for initial guess of ro
c=============================================================
40    kk1 =0
      do 80 i=1,nnod,1
      if (i.ge.2) goto 50
c=================================================
c Assign boundary values for fh,fq,fv and shr at (1,2)
c=================================================
      if (itim.lt.dssy) then
        fq(1,2) = 0.0D+00
      else if (itim.ge.dssy.and.itim.le.desy) then
        fq(1,2) = dsyin
      else if (itim.gt.desy) then
        fq(1,2) = 0.0D+00
      endif
c
      if (fq(1,2) .gt. 0.0D+00) then
        qt = (cn*fq(1,2) / (a*so**0.5D+00))**1.5D+00 /ss
        tol1 = qt/100.0D+00
        call bound(cs,ss,a,so,tol1,qt,cn)
        if (fh(1,2).eq.9999.0D+00) go to 1000
        shr(1,2) = ss*fh(1,2) / (ss+2.0D+00*fh(1,2))
        fv(1,2) = alpha * shr(1,2)**cm
      else
        fh(1,2) = 0.0D+00
        shr(1,2) = 0.0D+00
        fv(1,2) = 0.0D+00
      endif
c==============================
c   Infiltration rates for (1,2)
c==============================
      call
inf(ninfdata,tabinf,funinf,lnn,ttim,delt,delx,1,ft,sft,cft)
      goto 80
c=======================================
c Compute infiltration for (i,2), i=2,3,4...
c=======================================
50    call
inf(ninfdata,tabinf,funinf,lnn,ttim,delt,delx,i,ft,sft,cft)
c=============================================================
=
c  Net lateral inflow (qe ;cu.m/sec per 1 m width and per 1 m
length)
c=============================================================
=
      qe1 = 4.0D+00*rain
      qe2 = 2.0D+00*sft(i,2) + sft(i-1,2) + sft(i,1)
      qe = (qe1-qe2)/4.0D+00
c================================================
c Known value (ohm) to compute unknown (fh(i) ; m)
c================================================
      oh1 = a*theta*fh(i,1)
```

```
      oh2 = a*alpha*(ss*fh(i-1,2)**2.5D+00/(ss+2.0D+00*fh(i-1,2)))
     A                            **(2.0D+00/3.0D+00)
      ohm = oh1 + oh2 + delx*qe
c
      if (ohm.le.0.0D+00) then
        ohm = 0.0D+00
        shr(i,2) = 0.0D+00
        fq(i,2)=0.0D+00
        fh(i,2)=0.0D+00
        fv(i,2)=0.0D+00
        goto 80
      endif
      tol = ohm/100.0D+00
c============================
c  Initial guess of fh(i,2)=ro
c============================
      if (fh(i-1,2).le.0.0D+00 .and. fh(i,1).le.0.0D+00) then
        ro = ohm/(a*theta)
      else
        tr = (fh(i-1,2)+fh(i,1))/2.0D+00
        tr1 = 5.0D+00*a*alpha/3.0D+00*(ss*tr/(ss+2.0D+00*tr))
     A              **(2.0D+00/3.0D+00)
        tr2 = 4.0D+00*a*alpha/3.0D+00*ss**(2.0D+00/3.0D+00)
     A              *(tr/(ss+2.0D+00*tr))**(5.0D+00/3.0D+00)
        tr3 = tr1 - tr2
        tr4 = a*fh(i,1)/delt + fh(i-1,2)/delx*tr3 + qe
        tr5 = a/delt + tr3/delx
        ro = tr4/tr5
      endif
c
91    if (ro.le.0.0D+00) then
        ro = 0.0D+00
        shr(i,2) = 0.0D+00
        fq(i,2)=0.0D+00
        fh(i,2)=0.0D+00
        fv(i,2)=0.0D+00
        goto 80
      endif
c=========================================================
c  Iteration for a new fh(i,2) with the initial guess ro
c=========================================================
      kk1=kk1+1
c     if (kk1.GT.400) then
c       pause
c     endif
      if (kk1.gt.500) then
c        print '(a30)', 'check ro loop to find fh(i,2)'
c        goto 1000
         kk1 = 0
         print *,itim,i
      else
        fr = a*theta*ro + a*alpha*(ss*ro**2.5D+00/(ss+2.0D+00*ro))
     A                    **(2.0D+00/3.0D+00)
        fr1 = ro/(ss+2.0D+00*ro)
        fr2 = 5.0D+00*fr1**(2.0D+00/3.0D+00) + 4.0D+00*fr1
     A                    **(5.0D+00/3.0D+00)
        dfr = a*theta + a*alpha*ss**(2.0D+00/3.0D+00)*fr2/3.0D+00
```

```
        fr3 =
10.0D+00/(3.0D+00*ro**(1.0D+00/3.0D+00)*(ss+2.0D+00*ro)
     A                      **(2.0D+00/3.0D+00))
        fr4 = 20.0D+00*(ro**(5.0D+00/3.0D+00)-ro**(2.0D+00/3.0D+00))
     A             /(3.0D+00*(ss+2.0D+00*ro)**(5.0D+00/3.0D+00))
        fr5 =
40.0D+00*ro**(5.0D+00/3.0D+00)/(3.0D+00*(ss+2.0D+00*ro)
     A                **(8.0D+00/3.0D+00))
        ddfr = a*alpha*ss**(2.0D+00/3.0D+00)/(fr3-fr4-fr5)/3.0D+00

        fr6 = ((dfr/ddfr)**2.0D+00 - 2.0D+00*(fr-ohm)/ddfr)**0.5D+00
        rnew1 = ro - dfr/ddfr + fr6
        rnew2 = ro - dfr/ddfr - fr6
CYAP
        if(rnew1. LT.0.0D+00. AND. rnew2.GT.0.0D+00) rnew1=rnew2
        if(rnew1. GT.0.0D+00. AND. rnew2.LT.0.0D+00) rnew2=rnew1

        if (rnew1.lt.0.0D+00) rnew1 = 0.0D+00
        if (rnew2.lt.0.0D+00) rnew2 = 0.0D+00
        if (rnew1.EQ.0.0D+00.AND.rnew2.EQ.0.0D+00) then
          shr(i,2) = 0.0D+00
          fq(i,2)=0.0D+00
          fh(i,2)=0.0D+00
          fv(i,2)=0.0D+00
          goto 80
        endif


fr7=a*theta*rnew1+a*alpha*(ss*rnew1**2.5D+00/(ss+2.0D+00*rnew1))
     A         **(2.0D+00/3.0D+00)

fr8=a*theta*rnew2+a*alpha*(ss*rnew2**2.5D+00/(ss+2.0D+00*rnew2))
     A         **(2.0D+00/3.0D+00)

        diff1 = dabs(ohm-fr7)
        diff2 = dabs(ohm-fr8)
        small = diff1
        if (small.gt.diff2) small=diff2
c
        if (small.eq.diff1) then
          ro = rnew1
        else
          ro = rnew2
        endif

        if (small.gt.tol) then
          goto 91
        else
          kk1 = 0
          fh(i,2) = ro
        endif
      endif
c=============================================================
c  Flow depth adjustment for recession hydrograph.
c  This part should be replaced after
c  return flow is consideted in the infiltration subroutines.
c=============================================================
```

```
79    if (itim.gt.dera.and.fh(i,2).gt.fh(i,1)) then
        fh(i,2) = fh(i,1)
      endif
c=======================
c  Compute flow parameters
c=======================
      shr(i,2) = ss*fh(i,2)/(ss+2.0D+00*fh(i,2))
      fv(i,2) = alpha * shr(i,2)**cm
      fq(i,2) = fv(i,2)*a*fh(i,2)

80    continue
c====================================
c
c====================================

83    continue

c=================
c  Solute transport
c=================
      if(k. le. 2) goto 270
c================================================
c Define time step to satisfy Courant's condition
c================================================
      print *, ttim
      vmax=0.0
      D = 1.0D-02
      Do j=1,nnod
        vmax=dmax1(vmax,fv(j,1),fv(j,2))
      Enddo
      dtmin1=0.5*delx/vmax
c     dtmin2 = 0.5*delx*delx/D
c     dtmin = dmin1(dtmin1,dtmin2)
      dtmin=dtmin1
      NTMIN = ifix(sngl(delt)/sngl(dtmin))+1
      dtsol = delt/dfloat(NTMIN)
      B=D*dtsol/delx/delx
C!!!!!!!!!!!!!!!!!!!!!!!!!!!!!!!!!!!!!!!!
c      if (ttim.LE.10.) then
c     conc(2,1)=dmax1(0.0D+00,1.0D+00 - ttim/10.0D+00)
c      conc(2,2)=dmax1(0.0D+00,1.0D+00 - ttim/10.0D+00)
c     else
c     conc(2,1)=0.0D+00
c      conc(2,2)=0.0D+00
c      Endif
c      conc(2,1)=dexp(-(ttim/20D+00)**2.0D+00)
c      conc(1,1)=dexp(-(ttim/20D+00)**2.0D+00)
c      conc(2,1)=2000.0D+00/(1+(ttim/10.0D+00)**3)**1.2D+00
c      conc(2,2)=2000.0D+00/(1+(ttim/10.0D+00)**3)**1.2D+00
      Do j=1,6
        goto (701,702,703),itinput
c exponential
701     aux1=
     A  C00*(beta*dexp(-0.25D+00*ttim)+
     B  (1.00D+00 - beta)*dexp(-0.03D+00*ttim))
        conc(j,1)=aux1
        conc(j,2)=aux1
```

```
        goto 704
c step-wise
702     if(ttim.LE.10.0D+00) then
          conc(j,1)=C00
          conc(j,2)=C00
        else
          conc(j,1)=C00
          conc(j,2)=C00
        endif
        goto 704
c linear
703        if(ttim.LE.10.0D+00) then
          conc(j,1)=C00*(1.0D+00 - ttim/10.0D+00)
          conc(j,2)=C00*(1.0D+00 - ttim/10.0D+00)
        else
          conc(j,1)=0.0D+00
          conc(j,2)=0.0D+00
        endif
        goto 704
704     continue
      Enddo
      do m=2,NTMIN
        Do j=7,nnod
           aux1 = - sft(j,1)*conc(j,1)
           aux2 = - (fq(j,1)*conc(j,1) - fq(j-1,1)*conc(j-1,1))/delx
c          aux3 = 0.0D+00
c          if (j.NE.nnod) aux3=B*
c     A                     (conc(j+1,1)-2.0D+00*conc(j,1)+conc(j-
1,1))
           if (fh(j,2). GT. 0) then
               conc(j,2) = (conc(j,1)*fh(j,1) + dtsol*(aux1 + aux2))
     A  /fh(j,2)
           else
             conc(j,2)=conc(j,1)
           endif
        Enddo
      if(ttim.LE.55.) then
        solin = solin   + conc(6,1)     *fq(6,1)     *1.D-04*dtsol
        solout = solout + conc(nnod-1,1)*fq(nnod-1,1)*1.D-04*dtsol
        Write(11,'(5E14.4)') ttim,solin,conc(6,1),solout,conc(nnod-
1,1)
      Endif
        Do j=2,nnod
           conc(j,1) = conc(j,2)
        Enddo
      Enddo
c=============================================================
c Write the runoff model results on output files every minute.
c=============================================================
270   nk = k-1
      if (MOD(nk,ntm) .eq. 0) then
        write( 6,600) ttim,
(fq(lnn(j)+1,2)*60000.0D+00*wids,j=1,nln)
        write( 7,600) ttim, (fh(lnn(j),2)*1000.0D+00,j=1,nln)
        write( 8,600) ttim, (fv(lnn(j),2),j=1,nln)
        write( 9,600) ttim, (ft(lnn(j),2),j=1,nln)
        write(10,600) ttim, (shr(lnn(j),2)*1000.0D+00,j=1,nln)
```

```
        write(12,600) ttim, (conc(lnn(j),2),j=1,nln)
600   format(2x,f5.1,4e14.6)
      endif
c      if (MOD(nk,5*ntm) .eq. 0) then
c       Do j=1,nnod
c         write(11,'(3F10.3,5E14.4)') ttim,
c     A           delx*(j-1),ft(j,2),fq(j,2),fh(j,2)
c       Enddo
c      endif

c=====================================
c Check the end of the whole iteration.
c=====================================
350   if (k.eq.ntim) goto 1000
c=====================================================================
======
c Replace values of (i,2) to (i,l) for the next time step runoff
iteration
c=====================================================================
======
      if (k .eq. 1) then
        goto 380
      else
        do 370 i = 1,nnod
          ft(i,1) = ft(i,2)
          sft(i,1) = sft(i,2)
          cft(i,1) = cft(i,2)
          fq(i,1) = fq(i,2)
          fh(i,1) = fh(i,2)
          fv(i,1) = fv(i,2)
          shr(i,1) = shr(i,2)
370     continue
      endif
c==========================
c Move to the new iteration.
c==========================
380   goto 20
c================================
c Procedures to end the simulation.
c================================
1000        write(11,*) solin,solout
      close(5)
      close(6)
      close(7)
      close(8)
      close(9)
      close(10)
c
      stop
      end
C
C
C

      Subroutine rn(rain,itim,dera,drain)
c
      IMPLICIT DOUBLE PRECISION (A-H,O-Z)
```

```
      if (itim.le.dera) then
        rain = drain
      else
        rain = 0.0D+00
      endif
c
      return
      end
C
C
C
      Subroutine
     A
inf(ninfdata,tabinf,funinf,lnn,ttim,delt,delx,i,ft,sft,cft)
      IMPLICIT DOUBLE PRECISION (A-H,O-Z)
c Unit of ft is mm/hr.
c
      Dimension ft(110,2),sft(110,2),cft(110,2)
      Dimension tabinf(101,2),funinf(101,2,3),lnn(10)
      L = ifix(sngl(ttim))+1
      ft(i,2)=tabinf(L,2)+
     C     (tabinf(L+1,2)-tabinf(L,2))*(ttim-tabinf(L,1))
      do j=1,3
        if(i.EQ.lnn(j)+1) then
           ft(i,2)=ft(i,2)+funinf(L,2,j)*(0.01/delx)
        endif
      Enddo
      sft(i,2) = ft(i,2)/3600000.0D+00
      cft(i,2) = cft(i,1)+sft(i,2)*delt
      return
      end
      subroutine bound(cs, ss, a, so, tol1, qt, cn)
      IMPLICIT DOUBLE PRECISION (A-H,O-Z)
c=================================================================
================
C This subroutine is to convert volumetric synthetic runoff input to
flow depth input
c (boundary condition). Tayler series expansion and an iteration
scheme are used.

      common /a5/fq(110,2) /a4/fh(110,2)
      save  /a5/, /a4/
c================
c  Initial guess y
c=================
      y1 = ((2.0D+00 + cs) / ss)**(2.0D+00/3.0D+00)
      y2 = cn*fq(1,2) / (a*so**0.5D+00)
      y = y1 * y2
      if (y.le.0.0D+00) then
        fh(1,2) = 0.0D+00
        go to 1000
      endif
c
      k2 = 0
100   k2 = k2+1
      if (k2.gt.1000) then
        fh(1,2) = 9999.0D+00
```

```
        print '(a30)', 'check y loop for fh(1,2)'
        go to 1000
      endif
c=========================
c Function and derivatives
c=========================
      fy = y**2.5D+00 / (ss+2.0D+00*y)
      cy = y / (ss+2.0D+00*y)
      dy = y**1.5D+00/(ss+2.0D+00*y) * (2.5D+00 - 2.0D+00*cy)
      ddy = y**0.5D+00/(ss+2.0D+00*y) * (15.0D+00/4.0D+00 - cy *
     A         (10.0D+00 - 8.0D+00 *cy))
c============================
c Compute new y, yn1 and yn2
c============================
      y3 = ((dy/ddy)**2.0D+00 - 2.0D+00*(fy - qt)/ddy)**0.5D+00
      yn1 = y - dy/ddy + y3
      yn2 = y - dy/ddy - y3
c=================
c Check yn1 and yn2
c=================
      if (yn1.le.0.0D+00 .and. yn2.gt.0.0D+00) then
        yn1 = yn2
      else if (yn2.le.0.0D+00 .and. yn1.gt.0.0D+00) then
        yn2 = yn1
      else if (yn1.le.0.0D+00 .and. yn2.le.0.0D+00) then
        fh(1,2) = 0.0
        go to 1000
      endif
      fy1 = yn1**2.5D+00/(ss+2.0D+00*yn1)
      fy2 = yn2**2.5D+00/(ss+2.0D+00*yn2)
      diff1 = dabs(fy1-qt)
      diff2 = dabs(fy2-qt)
      small = diff1
      if (small.gt.diff2) small=dim
      if (small.eq.diff1) then
        y = yn1
      else
      y = yn2
      endif
      if (small.gt.tol1) then
        go to 100
      else
        fh(1,2) = y
        k2 = 0
      endif
1000  return
      end
```

Appendix J

Source Code for INFSELECT

(Infiltration Models Including Green and Ampt, Philips, and Schmid)

```
      PROGRAM INFILTRATION1
C     TT=CALCULATED TIME FOR EACH CALCULATION STEP OF
INFILTRATION,MIN.
C     SMALLFT1=INFILTRATION RATE
C     BIGFT1=TOTAL INFILTRATION
C     ZWET1=DEPTH OF WETTING FRONT
C     TPHILIP=TOTAL INFILTRATION IN PHILIP MODEL,CM.
C     KSAT=SOIL SATURATED HYDRAULIC CONDUCTIVITY,CM/MIN.
C     KPHILIP=HYDRAULIC CONDUCTIVITY IN PHILIP'S MODEL
C     SP=SORPTIVITY IN PHILIP APPROACH,(LT**(-0.5))
C     SCSTINF=TOTAL INFILTRATION IN SCS CURVE METHOD
C     CN=CURVE NUMBER IN SCS METHOD
C     W=INTENSITY OF SIMULATED RAINFALL,CM/HR
C     D=DURATION OF SIMULATED RAINFALL,MIN
C     TETAI=INITIAL SOIL WATER CONTENT,%
C     TETASAT=SOIL SATURATED WATER CONTENT,%
C     CMD=SOIL MOISTURE DEFICIT
C     SAAYF=EFFECTIVE TENSION OF WETTING FRONT,CM
C     SAAYS=THE AIR-ENTRY TENSION
C     TP=TIME OF PONDING,MIN.
C     FTP=CUMULATIVE INFILTRATION AT THE TIME OF PONDING,CM.
C     ZWETEXP=DEPTH OF WETTING FRONT IN EXPLICIT MODIFIED GREEN AND
AMPT
C     MODEL(SCHMID)
C     S=CONSTANT IN SCS METHOD
C     PHINFR=PHILIP'S INFILTRATION RATE (cm/m)
C     PHTINF= PHILIP'S TOTAL INFILTRATION (cm)
C     EXPLICIT FORM OF GREEN-AND -AMPT EQUATION
C     EXPTINF=EXPLICIT GREEN AND AMPT MODEL TOTAL INFILTRATION (cm)
C     EXPINFR=EXPLICIT GREEN AND AMPT MODEL INFILTRATION RATE
(cm/min)
C     ZWETEXP=DEPTH OF WETTING FRONT IN EXPLICIT MODIFIED GREEN-AND-
      AMPT MODEL
C     PHINFR=(Sp/2)*(TPHILIP(I))**(-0.5)+Kp

      IMPLICIT REAL*8 (A-H,O-Z)

C     IMPLICIT DOUBLE PRECISION:(A-H,O-Z)

      DIMENSION TT(100),SMALLFT1(100),BIGFT1(100),ZWET1(100)

      DIMENSION TPHILIP(100),PHTINF(100),PHINFR(100)

      DIMENSION EXPTINF(100),EXPINFR(100),ZWETEXP(100)

      INTEGER I,N


      REAL*8 KSAT,KPHILIP,SP,X
      REAL*8 SUM1,SUM2,SUM3,SUM4
      REAL*8 RUNOFF,SCSTINF,CN,W,S

            SUM1=0.0
            SUM2=0.0
            SUM3=0.0
            SUM4=0.0
```

```
c     REAL W,CMD,D,TETAI,TETASAT,KSAT,SAAYS,SAAYF,TP,FTP
c     REAL T(100),SMALLFT(100),BIGFT(100),ZWET(100)

      WRITE(* , *)'ENTER THE INTENSITY OF RAIN IN cm/h .'
      READ(*,*)W
      WRITE(*,*)'ENTER RAIN DURATION IN MINUTES.'
      READ(*,*)D
      WRITE(*,*)'ENTER THE INITIAL WATER CONTENT.'
      READ(*,*)TETAI
      WRITE(*,*)'ENTER SOIL SATURATED WATER CONTENT.'
      READ(*,*)TETASAT
      WRITE(*,*)'ENTER SOIL SATURATED HYDRAULIC CONDUCTIVITY IN
      cm/min.'
      READ(*,*)KSAT
      WRITE(*,*)'ENTER SATURATED PRESURE HEAD IN cm.'
      READ(*,*)SAAYS
C     WRITE(*,*)'ENTER THE CURVE NUMBER FOR THIS PLOT'
C     READ(*,*)CN
C     CONVERSION OF RAIN INTENSITY TO 'cm/min'.

            W=W/60

C     MOISTURE DEFICIT

            CMD= TETASAT-TETAI

C     EFFECTIVE TENSION OF WETTING FRONT

            SAAYF=0.76*SAAYS

             I=1

      IF (D == 0.0) THEN


            BIGFT1(I)=0.0

      ELSE

C     CALCULATION FOR TIME OF PONDING

            TP=KSAT*SAAYF*CMD/(W*(W-KSAT))

      IF (TP<0.0 .OR. TP>D ) THEN

            BIGFT1(I)=W*D

      ELSE  IF (TP==0.0 .AND. W>KSAT) THEN

                  BIGFT1(I)=KSAT*D

      ELSE  IF (TP==0.0 .AND. W<=KSAT) THEN

            BIGFT1(I)=W*D

      ELSE
```

```
C     CUMULATIVE INFILTRATION AT THE TIME OF PONDING

            FTP=W*TP
      END IF
      END IF

      WRITE(*,*)'TIME FOR PONDING IS', TP, 'MINUTES.'

C     NOW, SERIES OF CUMULATIVE INFILTRATION VALUES
      (FTP<ASSUMPTION<TOTALRAIN)
C     ARE SELECTED TO CALCULATE TIME, INFILTRATION RATE, AND THE
      WETTING FRONT DEPTH.

C           I=0

            BIGFT1(I)=FTP+0.05

      WRITE(*,*) '  T (min.)  SMALLFT(cm/min)  BIGFT(cm)   ZWET(cm)'

 20         T1=(BIGFT1(I)-FTP)/KSAT

      TT(I)=T1+SAAYF*CMD/KSAT*LOG((FTP+SAAYF*CMD)/
     &(BIGFT1(I)+SAAYF*CMD))+TP

C       IMPLEMENTING THE PHILIP'S PARAMETERS FOR PHILIP'S
INFILTRATION
C      APPROXIMATELY, Kp AND Sp ARE CALCULATED BY THE FOLLOWING
      EQUATIONS.



C            KPHILIP=KSAT

C            SP=(2*KPHILIP*SAAYF)**0.5

C     USING LEAST SQUARES METHOD TO CALCULATE Sp,AND Kp FOR PHILIP'S
      MODEL



           TPHILIP(I)=TT(I)-TP

             SUM1=SUM1+1/TPHILIP(I)
             SUM2=SUM2+1/(TPHILIP(I)**0.5)
             SUM3=SUM3+ KSAT*(1+SAAYF*CMD/BIGFT1(I))

SUM4=SUM4+(KSAT*(1+SAAYF*CMD/BIGFT1(I)))/(TPHILIP(I)**0.5)


C     PHTINF(I)=SP*(TPHILIP(I))**0.5+KPHILIP*TPHILIP(I)

C     PHINFR(I)=(SP/2)*(TPHILIP(I))**(-0.5)+KPHILIP


C     SCHMID (EXPLICIT GREEN AND AMPT MODEL
```

```
      EXPTINF(I)=(KSAT*W*SAAYF*CMD/(W-KSAT)**2)*
     &((1+2*((W-KSAT)**2/(KSAT*SAAYF*CMD))*TT(I))**0.5-1)

C     X=EXPTINF(I)/(SAAYF*CMD+W*TP)

C     VALIDITY CONDITION FOR GREEN AMPT EXPLICIT MODEL

C     IF(X>1) THEN

C     WRITE (*,*)'EXPLICIT MODIFIED GREEN-AND-AMPT MODEL NOT
      APPLICABLE'

C     ENDIF

C           I=I+1

C     INFILTRATION RATE, f(t) ( tp <= t <= tw )

          EXPINFR(I)=KSAT*(1+SAAYF*CMD/EXPTINF(I))


            SMALLFT1(I)=KSAT*(1+SAAYF*CMD/BIGFT1(I))

C     DEPTH OF WETTING FRONT

            ZWETEXP(I)=EXPTINF(I)/CMD

          X=EXPTINF(I)/(ZWETEXP(I)*CMD+W*TP)

      IF(X>1) THEN

      WRITE (*,*)'EXPLICIT MODIFIED GREEN-AND-AMPT MODEL NOT
      APPLICABLE'

      ENDIF

            ZWET1(I)=BIGFT1(I)/CMD

C     CHECKING TO SEE IF THE CONDITION IS VALID

      WRITE(*,*)


            DO WHILE (TT(I)<D)


      WRITE(*,*) TT(I),SMALLFT1(I),BIGFT1(I),ZWET1(I)

            I=I+1

            BIGFT1(I)=BIGFT1(I-1)+0.05

C     IF (I==5) THEN
C           STOP

C     ELSE
```

```
            GO TO 20

      END DO

C     END IF



C     END DO

      N=1

      OPEN(UNIT=150,FILE= 'GREEN&PHILIP.OUT', STATUS= 'NEW')

C     OPEN(UNIT=60,FILE= 'NEWINFILRATE.OUT', STATUS= 'NEW')

C     OPEN(UNIT=70,FILE= 'NEWTOTALINFIL.OUT', STATUS= 'NEW')

C     OPEN(UNIT=80,FILE= 'NEWWETTINGFRONT.OUT', STATUS= 'NEW')


CC    WRITE(*,*) 'N  T (min.)  SMALLFT(cm/min)  BIGFT(cm)
ZWET(cm)'

C     WRITE(50,*) T(1:100)
C     WRITE(60,*) SMALLFT(1:100)
C     WRITE(70,*) BIGFT(1:100)
C     WRITE(80,*) ZWET(1:100)

C     CLOSE(UNIT=50)
C     CLOSE(UNIT=60)
C     CLOSE(UNIT=70)
C     CLOSE(UNIT=80)



 120  DO WHILE (TT(N)<D)

      N=N+1

      GO TO 120

      END DO

      SP=(2*N*SUM4-2*SUM3*SUM2)/(N*SUM1-SUM2**2)

      KPHILIP=(2*SUM3-SP*SUM2)/(2*N)

      WRITE(*,*)SP,KPHILIP

      J=1

 160  DO WHILE (TT(J)<D)

      PHTINF(J)=SP*(TPHILIP(J))**0.5+KPHILIP*TPHILIP(J)
```

```
      PHINFR(J)=(SP/2)*(TPHILIP(J))**(-0.5)+KPHILIP
      J=J+1

      GO TO 160

      END DO

      K=1

 30   DO WHILE (TT(K)<D)

      WRITE(150,22) K,TT(K),BIGFT1(K),SMALLFT1(K),ZWET1(K),

&TPHILIP(K),PHTINF(K),PHINFR(K),EXPTINF(K),EXPINFR(K),ZWETEXP(K)
 22   FORMAT(I3,3X,10D12.5)

      K=K+1

      GO TO 30

      END DO

C     WRITE(50,*) T(1:100),SMALLFT(1:100),BIGFT(1:100),ZWET(1:100)
C     DO I=1,100
C     WRITE(50,*) T(I),SMALLFT(I),BIGFT(I),ZWET(I)

C     END DO
      CLOSE(UNIT=150)

      CALL SCS(W,CN)
C     CONVERSION OFTOTAL RUNOFF AND TOTAL INFILTRATION INTO cm

      SCSTINF=SCSTINF*2.54
      RUNOFF=RUNOFF*2.54

C     WRITE(*,*)' TOTAL INFILTRATION FROME SCS =', SCSTINF,'CM'
C     WRITE(*,95)SCSTINF
C 95  FORMAT(2X,D5.3)
C     WRITE(*,*)' TOTAL RUNOFF FROME SCS =', RUNOFF,'CM'
      END
      SUBROUTINE SCS(W,CN)
C     THIS SUBROUTINE CALCULATES TOTAL RUNOFF USING SCS CURVE NUMBER
      METHOD.
C     IT IS NOT AN EXPLICIT INFILTRATION MODEL. HOWEVER, WHEN W
      EXCEEDS THE
C     SATURATED HYDRAULIC CONDUCT, K_SAT, IT CAN BE USED TO MODEL TOTAL
      INFITRATION

      IMPLICIT REAL*8 (A-H,O-Z)
      REAL*8 RUNOFF,SCSTINF,CN,W,S
C     REAL CN
      W=W*60/2.54
      S=1000/CN-10
      RUNOFF=((W-0.2*S)**2)/(W+0.8*S)
      SCSTINF=W-RUNOFF
      END
```

Appendix K

Source Code for GAPINFIL

(Green and Ampt Infiltration Model)

```
C     This Program uses the Green and Ampt infiltration model to
      simulate the
C     predicted total infiltration.(The Green and Ampt model was
      chosen after
C     a clear investigation to compare to two other models; Philip
      and Schmid
C     using a different model named; NewInfilGreenAmpt. (The
Simulated   infiltration
C     from this late model indicated a better picture to the
measured    infiltration).
C     W=The rain intensity, cm/hr
C     Delta=The moisture deficit (Teta(S)-Teta(I))
      COMMON /R/W,DELTA
      DIMENSION X(20), Y(20), F(20), R(20),
     +         B(10), E(10), ST(10),
     +         D(10,10)
C+1   The genparplot...dat, is the data file for measured
      infiltration of a       specific
C     Plot.Therefore, when running this Model for Plot1, the Open
      file would be     as
C     Open(10,file='genparplot1.dat and so on)
      Open(10,file='genparplot1.dat')
      READ(10,*) W,DELTA
      W=W/60.
        READ(10,*) NOB
      DO J=1,NOB
        READ(10,*) X(J),Y(J)
      ENDDO
      CLOSE(10)
      OPEN(20,file='GENPARX.par')
      READ(20,*) NP
      DO K=1,NP
        READ(20,*) B(K)
      ENDDO
      CLOSE(20)
C+2   The GENPARplotX1.TXT, is the output for cumulative simulated
      infiltration      of a specific
C     Plot.Therefore, when running this Model for Plot1, the Open
      file would be     as
C     Open(11,file='GENPARplotX1.TXT and so on)

      OPEN(11,FILE='GENPARplotX1.TXT')
      call marqu(np,nob,b,x,y,f,r,sumb,sdev,e,d,st,100,IER)
      write(11,100)
      write(11,1010) b(1),st(1)
      write(11,1011) b(2),st(2)
      write(11,102)
      do i=1,nob
        write(11,103) i,x(i),y(i),f(i),r(i)
      end do
100   format(45('-'),/'Parameter # | Estimated Mean | Stand. Error|'
     +                /,45('-'))
1010  format('KSAT         ',E12.4,3x,e12.4)
1011  format('G            ',E12.4,3x,e12.4)
```

```
102   format(54('-'),/,
     +'Point # | Time     | Measured | Estimated | Residual |'/
     +'        |          | cumul    | cumul     |  value   |'/
     +'        |          | inf      | inf       |          |'/
     +54('-'))
103   format(i3,3x,4e12.4)
105   close(11)
      stop
      end
c
      subroutine marqu(np,nob,b,x,y,f,r,sumb,sdev,e,d,st,mit,IER)
*
      dimension y(nob),x(nob),f(nob),r(nob),st(np),b(np),e(np),
     .          c(10), p(10), q(10), a(10,10), d(10,10),
     .          delz(200,10),dz(200)
*
      data eps /0.0005/
*
      IER=0
      ga = 0.02
      sumb = 0.0
      call model(b,np,f,nob,x)
      do 10 k = 1,nob
      z = y(k) - f(k)
      r(k) = z
      if(abs(z) .gt. 1.0e-37) sumb = sumb + z * z
 10   continue
*
      do 200 nit = 1,mit
*      print *,b
      ssq = sumb
      if(b(1).LT.1.E-05) then
        IER=1
        Goto 500
      Endif
      ga = 0.1 * ga
      do 30 j = 1,np
      temp = b(j)
      b(j) = 1.01 * b(j)
      call model(b,np,dz,nob,x)
      do 15 i = 1,nob
      delz(i,j) = dz(i)
 15   continue
      sum = 0.0
      do 20 k = 1,nob
      delz(k,j) = 100.0 * (delz(k,j) - f(k))
      tmp = delz(k,j) * r(k)
      sum = sum + tmp
 20   continue
      q(j) = sum / b(j)
      b(j) = temp
      c(j) = temp
 30   continue
      sum3 = 0.0
      do 60 i = 1,np
      do 50 j = 1,i
      sum = 0.0
```

```
      do 40 k = 1,nob
      temp = delz(k,i) * delz(k,j)
      sum = sum + temp
40    continue
      d(j,i) = sum / (b(j) * b(i))
      d(i,j) = d(j,i)
50    continue
      e(i) = sqrt(d(i,i))
      If(e(i).LE.0.) then
        IER=1
        Goto 500
      Endif
      q(i) = q(i) / e(i)
      if(abs(q(i)) .gt. 1.0e-37) sum3 = sum3 + q(i) * q(i)
60    continue
70    do 90 i = 1,np
      do 80 j = 1,i
      a(j,i) = d(j,i) / e(j) / e(i)
      a(i,j) = a(j,i)
80    continue
90    continue
      do 100 i = 1,np
      p(i) = q(i)
100   a(i,i) = a(i,i) + ga
      call matinv(a,np,p)
      sum1 = 0.0
      sum2 = 0.0
      do 110 i = 1,np
      temp = p(i) * q(i)
      sum1 = sum1 + temp
      temp = p(i) * p(i)
      sum2 = sum2 + temp
110   continue
      an = sqrt((sum1/sum2)*(sum1/sum3))
      angle = 57.2958 * atan((sqrt(abs(1-an**2)))/an)
      step = 1.0
120   do 130 i = 1,np
130   b(i) = p(i) * step / e(i) + c(i)
      do 140 i = 1,np
      if(c(i)*b(i) .le. 0.0) go to 160
140   continue
      sumb = 0.0
      call model(b,np,f,nob,x)
      do 150 k = 1,nob
      z = y(k) - f(k)
      r(k) = z
      if(abs(z) .gt. 1.0e-37) sumb = sumb + z*z
150   continue
      if(sumb-ssq .lt. 1.0e-8) go to 180
160   if(angle .gt. 30.0) go to 170
      step = 0.5 * step
      go to 120
170   ga = 10.0 * ga
      go to 70
180   do 190 i = 1,np
      if(abs(c(i)-b(i)) .gt. eps*abs(b(i))) go to 200
190   continue
```

```
      go to 210
 200  continue
 210  call matinv(d,np,p)
      sdev = sqrt(sumb/float(nob-np))
      do 220 i = 1,np
      e(i) = sqrt(amax1(d(i,i),1.0e-20))
      st(i) = e(i) * sdev
 220  continue
*
 500  return
      end
*
      subroutine matinv(a,np,b)
*
      dimension a(10,10),b(np),indx1(10),indx2(10)
*
      do 10 j = 1,np
 10   indx1(j) = 0
      i = 0
 20   amax = -1.0
      do 40 j = 1,np
      if(indx1(j) .ne. 0) go to 40
      do 30 k = 1,np
      if(indx1(k) .ne. 0) go to 30
      p = abs(a(j,k))
      if(p .le. amax) go to 30
      ir = j
      ic = k
      amax = p
 30   continue
 40   continue
      if(amax .le. 0.0) go to 120
      indx1(ic) = ir
      if(ir .eq. ic) go to 60
      do 50 l = 1,np
      p = a(ir,l)
      a(ir,l) = a(ic,l)
      a(ic,l) = p
 50   continue
      p = b(ir)
      b(ir) = b(ic)
      b(ic) = p
      i = i + 1
      indx2(i) = ic
 60   p = 1.0 / a(ic,ic)
      a(ic,ic) = 1.0
      do 70 l = 1,np
      a(ic,l) = a(ic,l) * p
 70   continue
      b(ic) = b(ic) * p
      do 90 k = 1,np
      if(k .eq. ic) go to 90
      p = a(k,ic)
      a(k,ic) = 0.0
      do 80 l = 1,np
      a(k,l) = a(k,l) - a(ic,l) * p
 80   continue
```

```
      b(k) = b(k) - b(ic) * p
 90   continue
      go to 20
 100  ic = indx2(i)
      ir = indx1(ic)
      do 110 k = 1,np
      p = a(k,ir)
      a(k,ir) = a(k,ic)
      a(k,ic) = p
 110  continue
      i = i - 1
 120  if(i .gt. 0) go to 100
*
      return
      end
*
      SUBROUTINE MODEL(B,NP,ABIGFT,NOB,TIMES)
      COMMON /R/W,DELTA
      DIMENSION TIMES(100),ABIGFT(100),B(10)
      REAL*4 KSAT
      KSAT=B(1)
c     G=B(2)
C+3
C     G is the value of suction ahead of wetting front(cm). The
      value of G has    to alter for
C     runnig this model for different PLOTS(it gets diiferent
      values). For      example when we are
C     running this model for Bare Clay Loam(PLOT1), G would be equal
      to 40 cm (Walter Raws)
      G=40
      TP=G*DELTA*KSAT/(W-KSAT)/W
      FTP=TP*W
      T2=TP
      BIGFT=FTP
      DO J=1,NOB
        T1=T2
        T2=TIMES(J)
        DT=(T2-T1)/100.
        BIGFT01=BIGFT
        BIGFT02=BIGFT
        DO K=1,100
          DO M=1,10
            BIGFT02=BIGFT01+
     # KSAT*DT*(G*DELTA*0.5D+0*(1D+0/BIGFT01 + 1D+0/BIGFT02) + 1D+0)
          ENDDO
          BIGFT01=BIGFT02
        ENDDO
        BIGFT=BIGFT02
        ABIGFT(J)=BIGFT
      ENDDO
      RETURN
      END
```

Appendix L

Source Code for KINSUB

```
Dimension ttab(100),Q(100),cs(100)
```

```
      Dimension Ztab(10)
      Open(10,file='tabs.txt')
      Read(10,*)
      Do i=1,41
        read(10,*) ttab(i),Q(i),cs(i)
      Enddo
      Close(10)
      Open(20,file='params.txt')
      Read(20,*)
      Read(20,*) theta,R,amu
      Close(20)
      Open(30,file='ztab.txt')
      Read(30,*)
      Read(30,*) nztab
      Read(30,*)
      Read(30,*) (ztab(j),j=1,nztab)
      Write(*,*) 'time, min'
      Read(*,*) t
      open(11,file='kwres.txt')
      Do j=1,nztab
      z=ztab(j)
C=======================================
C Interpolating in the table to find Q(t)
C=======================================
      i=1
10    tL=ttab(i)
      tR=ttab(i+1)
      If((tL-t)*(tr-t).GT.0.0) then
        i=i+1
        if(i. GT. 40) goto 500
        goto 10
      Endif
      Qt=Q(i)+(t-tL)*(Q(i+1)-Q(i))/(tr-tL)
C=======================================
C Interpolating in the table to find t0
C=======================================
      Qt0=Qt-z*R*theta
      i=1
20    QL=Q(i)
      QR=Q(i+1)
      if((QL-Qt0)*(QR-Qt0).GT.0.0) then
        i=i+1
        if(i. GT. 40) goto 500
        goto 20
      Endif
      t0=ttab(i)+(Qt0-QL)*(ttab(i+1)-ttab(i))/(QR-QL)
C=======================================
C Interpolating in the table to find cst0
C=======================================
      i=1
30    tL=ttab(i)
      tR=ttab(i+1)
      IF((tL-t0)*(tr-t0).GT.0.0) then
        i=i+1
        if(i. GT. 40) goto 500
        goto 30
      Endif
```

```
      cst0=cs(i)+(t0-tL)*(cs(i+1)-cs(i))/(tr-tL)
C=======================
C Computing concentration
C=======================
      c=cst0*exp(-amu*(t-t0)/theta/R)
      Print *,c
      write(11,*) z,c
      goto 501
500   Print *,'out of limits'
501   Continue
      Enddo
      close(11)
      Stop
      End
```

References

Abu-Ashour J., D.M. Joy, H. Lee, H.R. Whiteley, and S. Zelin. 1998. Movement of bacteria in unsaturated columns with macropores. Transactions of the ASAE 41:1043-1050.

Addiscott, T.M., and A.P. Whitemore, 1991. Simulation of solute leaching in soils of differing permeabilities. Soil Use Manag. 7, 97-102.

Addiscott, T.M., and R.J. Wagenet. 1986. Concepts of solute leaching in soils: A review of modeling approaches. J. Soil Sci. 36:411-424.

Adler, J. 1969. Chemoreceptors in bacteria. Science. 166: 1588-1597.

Alexander, M. 1977. Introduction to soil microbiology, John Wiley and Sons, New York.

Andreini, M.S. and T.S. Steenhuis, 1990. Preferential paths of flow under conventional and conservation tillage. Geoderma 46: 85-102.

Atwill, E.R., R.A. Sweitzer, M. Das Graças C. Pereira, I.A. Gardner, D. Van Vuren, W.M. Boyce. 1997. Prevalence of and associated risk factors for shedding *Cryptosporidium parvum* and *Giardia* within feral pig populations in

Barfield, B.J., E.W. Tollner, and J.C. Hayes. 1978. Prediction of sediment transport in grassed media. ASAE Paper No. 77-2023. American Society of Agricultural Engineers, St. Joseph, Michigan 49085.

Barraclough, P.B., H. Kuhlmann, and A.H. Weir. 1989. The effects of prolonged drought and nitrogen fertilizer on root and shoot growth and water uptake by winter wheat. Journal of Agronomy and Crop Science 163, 352-360.

Barwick, R.S., D.A. Levy, G.F. Craun, M.J. Beach, and R.L. Calderon. 2000. Surveillance for waterborne-disease outbreaks-United States. 1997-1998. Morbidity and Mortality Wkly. Report. 49 (SS04): 1-35.

Baxter-Potter, W.R. and M.W. Gilliland. 1988. Bacterial pollution in runoff from agricultural lands. *J. Environ. Qual*. 17: 27-34.

Beasley, D.B. and L.F. Huggins. 1981. A real Nonpoint Source Watershed Environment Response Simulation (ANSWERS). User Manual. EPA-905/9-82-001. U.S. EPA, Region V. Chicago, IL.

Berg, H.C., and D.A. Brown, 1972. Chemotaxis in Escherichia coli analyzed by three-dimensional tracking. Nature. 239: 500-504.

Bergstrom, L., A. McGibbon, S. Day, and M. Snel. 1991. Leaching potential and decomposition of clopyralid in Swedish soils under field conditions. Environ. Toxicol. Chem. 10:563–571.

Bergstrom, L.F. and A. Shirmohammadi: 1999. A real extent of preferential flow with depth in sand and clay Monoliths. J. of Soil. Contamination 8(6): 637-651.

Bitton, G., and R.W. Harvey, (1992) Transport of pathogens through soils and aquifers. In: Mitchell R (Ed) Environmental Microbiology (pp-103-124). Wiley- Liss, New York.

Bitton, G., and R.W. Harvey, (1992). Transport of pathogens through soils and aquifers. In: Mitchell, R. (Ed) Environmental Microbiology (pp-103-124). Wiley-Liss, New York

Bitton, G., J.M. Davidson, and S.R. Farrah, 1979. On the value of soil columns for assessing the transport pattern of viruses through soils: a critical outlook. Water, Air, and Soil Pollution 12: 449-457.

Bitton, G., N. Lahav, and Y. Henis, 1974. Movement and retention of Klebsiella aerogenes in soil columns. Plant Soil. 42: 373-380.

Bond, W.J. 1987. Solute transport during unsteady, unsaturated soil water flow: The pulse impute. Aust. J. Soil Res. 25: 223-241.

Brock, T.D.1971. Biology of Microorganisms. Prentice-Hall, Inc., Englewood Cliffs, NJ.

Brooks, R.H., and A.T. Corey, 1964. Hydraulic properties of porous media. Hydrology paper Vol. 3, p. 27, Colorado State University, Fort Collins, Colorado.

Buss, P. 1993. The use of capacitance based measurements of real time soil water profile dynamics for irrigation scheduling, pp. 17-19. In: Proc. Natl. Conf. Irrig. Assoc., Australia and Natl. Committee Irrig. Drain., Launceston, Tasmania. May 1993. Irrig. Assoc. of Aust., Homebush, NSW.

Butler, R.G., G.T. Orlob, and P.H. McGauhey, 1954. Underground movement of bacterial and chemical pollutants. J. Am. Water Works Assoc. 46: 97-11. California. Applied and Environmental Microbiology 63(10): 3946-3949.

Campbell, G.S., 1974. A simple method for determining unsaturated conductivity from moisture retention data. Soil Sci. 117:311–314.

Carsel, R.F., C.N. Smith, L.A. Mulkey, J.D. Dean and P. Jowise. 1984. Users Manual for the Pesticide Root Zone Model (PRZM) Release 1. EPA-600/3-84-109. U.S. EPA, Athens, GA.

Carsel, R.F., C.N. Smith, L.A. Mulkey, J.D. Dean and P. Jowise. 1984. Users Manual for the Pesticide Root Zone Model (PRZM) Release 1. EPA-600/3-84-109. U.S. EPA, Athens, GA.

Chandler, D.S., J. Farran and J.A. Craven. 1981. Persistence and distribution of pollution indicator bacteria on land used for disposal of piggery effluent. Applied and Environmental Microbiology 42:453-460.

Characklis, W.G., K.C. Marshall, 1990. Biofilms, pp. 110-112. John Wiley & Sons, New York, NY.

Chaubey, I., D.R. Edwards, T.C. Daniel, P.A. Moore, Jr. and D.J. Nichols. 1994. Effectiveness of vegetative filter strips in retaining surface-applied swine manure constituents. Transactions of the ASAE. 37(3): 845-850.

Choi, J. 1992. Effect of intervening land use on runoff quality. PhD. dissertation, University of Maryland, College Park, MD.

Corapcioglu Y. M., and A. Haridas, 1985. Microbial transport in soils and groundwater: a numerical model. Adv. Water Resour. 8: 188-200.

Corapcioglu, M.Y., and D. Haridas. 1984.Transport and fate of microorganisms in porous media: A theoretical investigation J. Hydro. 72:149-169.

Coyne, M.S., R.A. Gilfillen, R.W. Rhodes, and R.L. Blevins. 1995. Soil and fecal coliform trapping by grass filter strips during simulated rain. J. Soil and Water Cons. 50(4): 405-408.

Coyne, M.S., R.A. Gilfillen, R.W. Rhodes, and R.L. Blevins. 1995. Soil and fecal coliform trapping by grass filter strips during simulated rain. J. Soil and Water Cons. 50(4): 405-408.

Crane, S.R. and J.A. Moore. 1984. Modeling enteric bacteria die-off: a review. Paper No. 6699. Oregon Agricultural Experiment Station, Corvallis, OR.

Crane, S.R., J.A. Moore, M.E. Grismer, and J.R. Miner. 1983. Bacterial pollution from agricultural sources: a review. Transactions of the ASAE. 26(3): 858-866.

Cruz, J.R., P. Caceres, F. Cano, 1990. Adenovirus types 40 and 41 and rotaviruses associated with diarrhea in children from Guatemala. J. Clin. Microbiol. 28:1780-1784.

Cunningham, A.B., W.G., Characklis, F. Abedeen, and D. Crawford, 1991. Influence of biofilm accumulation on pourous media hydrodynamics. Environ. Sci. Technol. 25: 1305-1310.

Dahlquist, F.W., P. Lovely, and D.E. Koshland, 1972. Quantitative analysis of bacterial migration in chemoxis. Nature New Biol. 236: 120-123.

Daniels, S.L. 1972. The adsorption of microorganisms onto surfaces: A review. Dev. Indus. Microbiol. 13:211-253.

Daniels, S.L. 1980. Mechanisms involved in sorption of microorganisms to solid surfaces. P 7-58. In: G. Bitton and K.C. Marshall (ed.) Adsorption of microorganisms to surfaces. Wiley - Interscience, New York.

Danish Hydraulic Institute (DHI). 1998. MIKE SHE Water Movement – User Guide and Technical Reference Manual, Edition 1.1

Dickey, E. C. and D. H. Vanderholm. 1981. Vegetative filter treatment of livestock feedlot runoff. J. Envir. Qual., 10:279-284.

Donigian, A.S. Jr., Baker, D.A. Haith and M.F. Walter. 1983. HSPF Parameter Adjustments to Evaluate the Effects of Agricultural Best Management Practices, EPA Contract No. 68-03-2895, U.S. EPA Environmental Research Laboratory, Athens, GA, (PB-83-247171).

Dufour, A.P., 1977. Escherchia coli.: the fecal coliform, p. 48-58. In: A. W. Hoadley and B.J. Dutka (ed.), Bacterial Indicators/Health Hazards Associated with Water. ASTMSTP 635. American Society for Testing and Materials, Philadelphia, Pa.

Dunne, T., and R.D. Black 1970. An experimental investigation of runoff production in permeable soils. Water Resources Research 6(2):478-490.

Dutka, B.J., A.S.Y. Chau, and J. Coburn. 1974. Relationship between bacteria indicators of water pollution and fecal sterols. Water Res. 8:1047.1055.

Elder, R.O., J.L. Keen. G.R. Siragusa, G.A. Barkocy-Gallagher, M. Koohmaraie, and W.W. Laegreid. 2000. Correlation of enterohemorrhagic Escherichia coli O157 prevalence in feces, hides, and carcasses of beef cattle during processing. Proc. Natl. Acad. Sci. USA 97:2999-3003.

Evans, M.R. and J.D. Owens. 1972. Factors affecting the concentration of fecal bacteria in land drainage water. J. Gen. Microbial. 71: 477-485.

Fajardo, J.J., J.W. Bauder, and S.D. Cash. 2001. Managing nitrate and bacteria in runoff from livestock contamination areas with vegetative filter strips. Journal of Soil and Water Conservation, 56(3): 185-191.

Fenzl, R.N. 1962. Hydraulic resistance of broad shallow vegetated channels. Ph.D. Thesis, University of California at Berkley. Berkley, California.

Fleming, R.J., D.M. Dean, and M.E. Foran. 1990. Effect of manure spreading on tile drainage water quality. P. 385. In: Proc. 6th Int'l Symp. Agricultural and Food Processing Wastes. St. Joseph, Mich: ASAE

Gagliardi, J.V., and J.S. Karns. 2000. Leaching of *Escherichia coli* O157:H7 in diverse soils under various agricultural management practices. Appl. Environ. Microbiol. 66:877–883.

Gannon, J.T., U. Mingelgrin, M. Alexander and R.T. Wagnet, 1991b. Bacteria transport through homogeneous soil. Soil Biol. Biochem. 23(12): 1155-1160

Gannon, J.T., V.B. Manilal and M. Alexander. 1991a. Relationship between cell surface properties and transport of bacteria through soil. Appl. Environ. Microbiol. 57(1): 190-193.

Gannon, J.T., V.B. Manilal and M. Alexander. 1991a. Relationship between cell surface properties and transport of bacteria through soil. Appl. Environ. Microbiol. 57(1): 190-193.

Garder, A.O., D. W. Peaceman and A.L. Pozzi, 1964. Jr., Numerical Calculation of Multidimensional Miscible Displacement by the Method of Characteristics, Soc. Pet. Eng. J. 4(1), 26-36.

Gerba, C.P., C. Wallis, and J.L Melnich, 1975. Fate of wastewater bactera and viruses in soil. J. Irrig. Drain. In: Proc. Am. Soc. Civ. Eng., 101 (IR3): 157-174.

Gerba, C.P., G. Bitton, 1984. Microbial pollutants: Their survival and transport pattern to groundwater. P. 65-88. IN Bitton, G. and Gerba, C.P. (ed). Groundwater pollution microbiology. Wiley- Interscience, New York.

Germann, P.E. and K. Beven, 1985. Kinematic wave approximation to infiltration into soils with sorbing macropores. Water Resources. Res. 21: 990-996.

Grant, S.B., E.J. List, and M.E. Lidstrom. 1993. Kinetic analysis of virus adsorption and inactivation in bath experiments. Water Resource. Res. 29: 2067-2085.

Green, W.H., and G.A. Ampt. 1911. Studies on soil physics, 1: The flow of air and water through soils. Journal of Agricultural Science 4(1): 1-24.

Haan, C. T., B. Allred, D. E. Storm, G. J. Sabbagh, and S. Prabhu. 1995. Statistical procedure for evaluating hydrologic/water quality models. transaction ASAE 38(3):725-733.

Hagedorn, C., 1981. Transport and fate : Bacteria pathogens in groundwater. Pro.Con. on microbial health considerations of soil disposal of domestic wastewaters, Norman, Okla., pp. 84 -102.

Hagedorn, C., 1981. Transport and fate : Bacteria pathogens in groundwater. Pro. Con. On microbial health considerations of soil disposal of domestic wastewaters, Norman, Okla., pp. 84 -102.

Haggard, B.E., P.A. Moor, P.B. Delaune, D.R. Smith, S. Formica, P.J. Kleinman, amd T.C. Daniel, 2002. Effect of slope, grazing and aeration on pasture hydrology. Transactions of the ASAE., paper number 022156, presented at ASAE Annual International Meeting at Chicago, July 28- July 31.

Haggard, B.E., P.A., Moor, P.B. Delaune, D.R. Smith, S. Formica, P.J. Kleinman, and T.C. Daniel, 2002. Effect of slope, grazing and aeration on pasture hydrology. Transactions of the ASAE., paper number 022156, presented at 2002 ASAE Annual International Meeting at Chicago, July 28- July 31.

Hancock, D.D., T.E. Besser, D.H. Rice, E.D. Ebel, D.E. Herriott, and L.V. Carpenter. 1998. Multiple sources of Escherichia coli O157 in feedlots and dairy farms in the Northwestern USA. Prev. Vet. Med. 35:11-19.

Harvey, R. W., and S. P. Garabedian. 1991. Use of colloid filtration theory in modeling movement of bacteria through a contaminated sandy aquifer. Environ. Sci. Technol. 25:178-185.

Heimovaara, T.J., and W. Bouten. 1990. A computer-controlled 36-channel time domain reflectometry system for monitoring soil water contents. Water Resour. Res. 26:2311-2316.

Hendricks, D.W., F.J. Post, and D.R. Khairnar, 1979. Adsorption of bacteria on soils: Experiments, thermodynamic rationale, and application. Water, Air and Soil Pollu. 12: 219-232.

Herkelrath, W.N., S.P. Hamburg, and F. Murphy. 1991. Automatic, real-time monitoring of soil moisture in a remote field area with time-domain reflectometry. Water Resour. Res. 27:857-864.

Herzig, J.P., D.M. Leclerc, and P. Le Golf, 1970. Flow of suspensions through porous media – Application to deep infiltration, pp. 129-157. In: Flow through porous media, Am. Chem. Soc., Washington, D.C.

Hirsch, R.M., W.M. Alley, and W.G. Wilber. 1988. Concepts for a National-Water Quality Assessment Program. U.S. Geol. Surv. Circ. 1021.

Horton, R.E. 1939. Analysis of runoff-plot experiments with varying infiltration-capacity. Transactions American Geophysical Union 20: 693-711.

Huggins, L.F. and J.R. Burney. 1982. Surface runoff, storage and routing. In: C.T. Haan, H.P. Johnson and D.L. Brakensiek, Eds. Hydrologic modeling of small watersheds. ASAE Monograph No. 5. American Society of Agricultural Engineers, St. Joseph, Michigan.

Hunt, P.G., R.E. Peters, T.C. Sturgis, and C.R. Lee. 1979. Reliability problems with indicator organisms for monitoring overland flow treated wastewater effluent. J. Environ. Qual. 8(3): 301-304.

Hurts, C.J., C.P. Gerba, I. Cech. 1980. Effects of environmental variables and soil characteristics on virus survival in soil. Appl. Environ. Microbiol. 40: 1067-1079.

Hutson, J.L. and R.J. Wagenet. 1991. Simulating nitrogen dynamic in soils using a deterministic model. Soil Use and Management 7: 74-78.

Huysman, F. and W. Verstraete, 1993. Water-facilitated transport of bacteria in unsaturated soil columns: Influence of inoculation and irrigation methods. Soil Biol. Biochem. 25: 91-97.

Iqbal, M.Z., N.C. Krothe, 1996. Transport of bromide and other inorganic ions by infiltrating storm water beneath a farm land plot: Ground Water, 34 (6): 972-978.

Isensee, A.R., and A.M. Sadeghi. 1999. Quantification of runoff in laboratory-scale chambers. Chemosphere 38:1733–1744.

Jabro, J.D., E.G. Lotse, K.E. Simmons, and D.E. Baker, 1991, A field study of macropore flow under saturated conditions using a bromide tracer: Journal of Soil and Water Conservation, 46 (5): 376-380.

Jarvis, N.J., L. Bergström, and P.E. Dik, 1991. Modeling water and solute movement in macroporous soil. II. Chloride leaching under non-steady flow. Journal of Soil Science 42, 71-81.

Jarvis, N.J., L.F. Bergstrom, and C.D. Brown. 1995. Pesticiae leaching model and their use for management purposes. In: T.R. Robert and P.C. Kearney (ed.), Environmental Behavior of Agrochemicals, 185.

Jenkins, M.B., J.H., Chen, D.J. Kadner, and L.W. Lion. 1994. Methanotrophic bacteria and facilitated transport of pollutants in aquifer material. Appl. Environ. Microbiol. 60: 3491-3498.

Joy, D.M., H. Lee, C. Reaume, H.R. Whiteley, and S. Zelin. 1998. Microbial contamination of subsurface tile drainage water from field applications of liquid manure. J. Can. Soc. Agric. Eng. 40: 153-160.

Kao, T. Y. and B.J. Barfield. 1978. Prediction of flow hydraulics for vegetated channels, Transaction of ASAE. 22:489-494.

Kei, W., J. Yee-Chung, and T. Viraraghavan, 2002. Transport of bacteria in heterogeneous media under leaching conditions. J. Environ. Eng. Sci. 1:383-395.

Keller, E.F., and L.A. Segal, 1971. Model for chemotaxis. J. Theor. Biol. 30:225-234.

Khaleel, R., G.R. Foster, K.R. Reddy, M.R. Overcash, and P.W. Westerman. 1979. A nonpoint source model for land area receiving animal wastes. III conceptual model for sediment and manure transport. Transaction of the ASAE 22:1353-1361.

Khaleel, R., R. Reddy, and M.R. Overcash, 1980. Transport of potential pollutants in runoff water. Water Research. 14: 421-436.

Kitahara, H., 1993. Characteristics of pipe flow in forested slopes. In: Bolle, H.J., R.A. Feddes, and J. Kalma. (Eds), Exchange Processes at the Land Surface for a Range of Space and Time Scales. Proc.Yokohama Symp., International Association of Hydrological Science Publ. No. 212. IAHS Press, Wallingford, UK. pp. 235-242.

Knisel, W.G. 1980. CREAMS: a field scale model for Chemicals, Runoff, and Erosion for Agricultural Management Sysytems. USDA Cnservation Research Report No. 26.640 pp.

Knisel, W.G., F.M. Davis, R.A. Leonard, 1993. GLEAMS version 2.10. Part I: Nutrient Component Documentation. USDA-ARS, Coastel Plain. Experiment Station. Southeast Watershed Research Laboratory. Tifton, Georgia, 31793. 81 p.

Kres,M., and G. R. Gifford. 1984. Fecal coliform release from cattle fecal deposits. Water Resour. Bull., 20:61-66.

Lance, J. C., C. P. Gerha and S. S. Wang. 1982. Comparative movement of different enteroviruses in soil columns. J. Environ. Qual. 11:347-351.

Lance, J.C., C.P. Gerba, and J.L. Melnick, 1976. Virus movement in soil columns flooded with secondary sewage effluent. Appli. Environ. Microbiol. 32: 520-526.

Lance, S. C. and C. P. Gerba. 1984. Virus movement in soil during saturated and unsaturated flow. Appl. Environ. Microbiol. 47:335-337.

Leonard, R.A., W.G. Knisel, and D.A. Still. 1987. GLEAMS: Groundwater Loading Effects of Agricultural Management Systems. Trans. ASAE 30: 14031418.

Li, R. M. and H. W. Shen. 1973. Effect of total vegetation on flow and sediment, J. Hyd. Div., Proceeding of ASCE, Vol. 99 (HY5) 793-814.

Liggett, J.A., Woolhiser, D.A. 1976. Different solutions of the Shallow-Water Equation. J. Eng. Mech. Div., Proceeding of ASCE, 93 (EM2): 39-71.

Lim, T. T., D. R. Edwards, S. R. Workman, and B. T. Larson. 1997. Vegetated filter strip length effects on quality of runoff from grazed pastures ASAE, Paper No.97- 2060. St. Joseph, Mich.: ASAE.

Lim, T.T., D.R. Edwards, S.R. Workman, and B.T. Larson, 1997. Vegetated filter strip length effects on quality of runoff from grazed pastures. Transactions of the ASAE, 41 (5).
load program. USEPA office of Water, Washington, D.C.

Loehr, R.C., 1979. Potential pollutants from agriculture—an assessment of the problem and possible control approaches. *Prog. Wat. Tech.* 11(6), 169-193.

Luxmoore, R.J.1981. Micro-, meso-, and maroporosity of soil. Soil Sci. Am. J. 45:671-72.

Ma, Q.L., R.D. Wauchope, J.E. Hook, A.W. Johnson, C.C. Dowler, G.J. Gascho, J.G. Davis, H.R. Summer, L.D. Chandler. 1998. GLEAMS, Opus, and PRZM-2 model predicted versus measured runoff from coastal plain loamy sand. Transactions of the ASAE 41(1):77-88.

Madsen, E.L., and M. Alexander, 1982. Transport of rhizobium and pseudomonas through soil. J. Environ. Qual. 46: 557-560.

Marshall, K.C. 1976. Interfaces in microbial ecology. Harvard University Press, Cambridge.

Matthess, G., and A. Pekdeger, 1981. Concepts of a survival and transport model of pathogenic bacteria and viruses in groundwater. Sci. Total Environ. 21: 149-159.

Mawdsley, J.L., A.E. Brooks, and R.J. Merry. 1996a. Movement of the protozoan pathogen Cryptosporidium parvum through three contrasting soil types. Biol. Fertil. Soils 21: 30-36.

Mawdsley, J.L., A.E. Brooks, R.J. Merry, and B.F. Pain. 1996b. Use of a novel soil-tilting table to demonstrate the horizontal and vertical movement of the protozoan pathogen Cryptosporidium parvum in soil. Biol. Fertil. Soils 23: 215-220.

McCarthy, J. F., and J. M. Zachara. 1989. Subsurface transport of contaminants: binding to mobile and immobile phases in groundwater aquifers. Environ. Sci. Technol. 23:496-504.

McDonald, A., D. Kay, and A. Jenkins. 1982. General fecal and total coliform surges by stream flow manipulation in the absence of normal hydrometerological stimuli. Applied and Environmental Microbiology 44, 292-300.

McDowell-Boyer, L.M., J.R. Hunt, and N. Sitar, 1986. Particle transport in porous media. Water Resour. Res. 22: 1901-1921.

McFeters, G.A., G.K. Bissonnette, J. J. Jezeski, C.A. Thomson, and D.G. Stuart, 1974. Comparative survival of indicator bacteria and enteric pathogens in well water Appl. Microbiol. May; 27 (5): 823–829.

McKensie, W.M. 1985. The design of a rotating nozzle rainfall simulator and the testing with selected nozzles. Bsc. thesis, Silsoe College, Cranfield Institute of Technology, UK.

McMurry, S.W., M.S. Coyne, and E. Perfect. 1998. Fecal coliform transport through intact soil blocks amended with poultry manure. J. Environ. Qual. 27: 86-92.

McMurry, S.W., M.S. Coyne, and E. Perfect. 1998. Fecal coliform transport through intact soil blocks amended with poultry manure. J. Environ. Qual. 27: 86-92.

Miller, J.E. 1984. Basic concepts of kinematic-wave models. U.S. Geological Survey Professional Paper 1302. U.S. Government Printing Office, Washington D.C. for sale by distribution branch, U.S. Geological Survey, 604 South Pickett, Alexandria, Virginia 22304.

Miller, R.J., J.W. Bigger, and D.R. Nielsen, 1965. Chloride displacement in Panoche clay loam in relation to water movement and distribution. Water Resour. Res., 1(1): 63-73, 1965.

Miller, W.P. 1987. A solenoid-operated, variable intensity rainfall simulator. Soil Sci. Soc. Am. J. 51:832-834.

Miner, J.R., L.R. Bernard, L.R. Fina, G.H. Larson and R.I. Lipper. 1966. Cattle feedlot runoff nature and behavior. Proc. 21st Ind. Waste Conf. Purdue Univer. pp. 834-847.

Monod, J. 1942. Recherches sur la Croissance des Cultures Bacteriennes. Hermann et Cie, Paris.

Moor, J.A., Smyth, E.S. Baker, and J.R. Miner. 1988. Evaluating coliform concentrations in runoff from various animal waste management systems. Special Report 817: Agricultural Experiment Stations, Oregon State University, Corvallis, Oregon.

Moore, J.A., J.D. Smyth, E.S. Baker, and J.R. Miner. 1988. Evaluating coliform concentrations in runoff from various animal waste management systems.

Special Report 817: Agricultural Experiment Station, Oregon State University, Corvallis, Oregan.

Moore, J.A., M.E. Grismer, S.R. Crane, and J.R. Miner. 1983. Modeling dairy waste management systems' influence on coliform concentration in runoff. Transactions of the ASAE 26(4): 1194-1200.

Moore, R.S., D.H. Taylor, M.M. Eddy, and L.S. Sturman. 1982. Adsorption of reovirus by minerals and soils. Appl. Environ. Microbiol. 44: 852-859.

Mosley, M.P., 1979. Stream flow generation in a forested watershed, New Zealand. Water Resources. Res. 15: 795-806.

Nassif, S.H., and E.M. Wilson. 1975. The influence of slope and rain intensity on ranoff and infiltration. Hydrological Sciences Bulletin. 20:539-553.

O'Melia, C.R., and W. Stumn, 1967. Theory of water filtration. J. Am. Water Works Assoc. 59: 1393-1412.

Paltineanu, I.C., J.L. Starr. 1997. Real-time soil water dynamics using multisensor capacitance probes: Laboratory calibration. Soil Sci. Soc. Am. J. 61:1576-1585.

Parke, J.L., R. Moen, A.D. Rovira, and G.D. Bowen, 1986. Soil water flow affects the rhizosphere distribution of a seed-borne biological control agent, Pseudomonas fluorescence. Soil Biol. Biochem. 18:583-588.

Pasquarell, G.C., and D.G. Boyer**.** 1995. Agricultural impacts on bacterial water quality in karst groundwater. Journal of Environmental Quality 24:959-969.

Paterson, E., J.S. Kemp, S.M. Gammack, E. Fitz Patrick, C. Adisl, S. Malcom, C.E. Mullins, and K. Killham. 1992. Leaching of genetically modified pseudomonas fluorescents through intact soil microcosms: influence of soil type. Biol. Fertil. Soils. 15: 308-314.

Patni, N.K., H.R. Toxepeus and P.Y. Jui. 1985. Bacterial quality of runoff from manure and non-manure cropland. Transactions of the ASAE 28:1871-1877.

Payment, P., L. Richardson, J. Siemiatycki, R. Dewar, M. Edwardes, end E. Franco. 1991. A randomized trial to evaluate the risk of gastrointestinal disease due to consumption of drinking water meeting current microbiological standards. Am. J. Public Health 81:703-708.

Pettygrove, G.S., and T. Asano, eds. 1985. Irrigation with reclaimed municipal wastewater- A Guidance Manual. Chelsea, Mich. Lewis Publishers.

Philip, J.R. 1957. The theory of infiltration, the infiltration equation and its solution. Soil Science 83: 345-57

Pickaering, J.R. Hagerman, and L.D. Geohring, 1990, Preferential movement of pesticides and tracers in agricultural soils, J. Irrigation and Drainage Engineering, v. 116, no. 1, p. 50.

Polprasert, C., Dissanayake, M.G., and Thanh, N.C. 1983. Bacteria die-off kinetics in waste stabilization pont. J. Water Pollut. Control Fed. 55(3): 285-296.

Porter, J., K. Moobs, C.A. Hart, J.R. Saunders, R.W. Pickup, and C. Edwards. 1997. Detection, distribution and probable fate of Escherichia coli O157 from asymptomatic cattle on a dairy farm. J. Appl. Microbio. 83:297-306.

Pourcher, A.M., L.A. Devriese, J.F. Hernandez, and J.M. Delattre. 1991. Enumeration by a miniaturized method of E. coli, S. bovis, and enterococci as indicators of the origin of fecal pollution of waters. Journal of Applied Bacteriology. 70: 525-530.

Powelson, D.K., and A.L. Mills, 1998. Water saturation and surfactant effects on bacteria transport in sand columns. Soil Sci. 163: 694-707.

Powelson, D.K., and C.P. Gerba. 1994. Virus removal from sewage effluent during saturated and unsaturated flow through soil columns. Water Res. 28: 2175-2181.

Rawls, W.J., Gimenez, D., and R. Grossman, 1998. Use of soil texture, bulk density, and slope of the water retention curve to predict saturated hydraulic conductivity, Transactions of ASAE, Vol. 41(4): 983-988.

Reddy, K.R., R. Khaleel, and M.R. Overcash. 1981. Behavior and transport of microbial pathogens and indicator organisms in soils treated with organic wastes. J.of Environ. Qual. 10(3): 2545-266.

Reed, S., R. Thomas, and N. Kowal, 1980. Long term land treatment, are there health or environmental risks? Proceedings of ASAE National Convention, Portland, OR.

Reynolds, P.J., P. Sharma, G.E. Henneman, and M.J. McInerney. 1989. Mechanisms of microbial movement in subsurface materials. Appl. Environ. Microbio. 55: 2280- 2286.

Rhodes, R.A. and C.R. Hrubant. 1972. Microbial. Population of feedlot waste and associated sites. Appli. Microbial. 24(3): 269-337.

Rice, R.C., D.B. Jaynes, and R.S. Bowman, 1991. Preferential flow of solute and herbicide under irrigated fields. Transactions of ASAE 34 (3): 914 -918.

Sabu, P., M. Matlock, P. Haan, S. Mukhtar ans S. Pillai. 2002. Uncertainty analysis as a first step of developing a risk-based approach to nonpoint source modeling of fecal coliform pollution for total maximum daily load estimates. Texas A & M University.

Sadeghi, A.M. and J.G. Arnold, 2001. A SWAT microbial sub-model for predicting pathogen loadings in surface and groundwater at watershed and basin scales. Proceeding of TMDL. Environmental Regulations, Fort Worth, TX. Marsh 11-13, 2002; A. Saleh., Eds., ASAE 2002; 56-63.

Schafer, A., H. Harms, A.J.B. Zehnder. 1998. Bacterial accumulation at the air-water interface. Environ. Sci. Technol. 32: 3704-3712.

Schaub, S. A., and C. A. Sorber. 1977. Virus and bacteria removal from wastewater by rapid infiltration though soil. Appl. Environ. Microbiol. 33:609-619.

Schellinger, G.R., and J.C. Clausen. 1992. Vegetated filter treatment of dairy barnyard runoff in cold regions. J. Environ. Qual. 21:40-45.

Schmid, B. 1990. Derivation of an explicit equation for infiltration on the basis of the Mein-Larson model. Hydrological Sciences Journal. 35: 197-208.

Scott, D.T., M.N. Gooseff, K.E. Bencala, and R.L. Runkel. 2003. A automated calibration of a stream solute transport model: implications for interpretation of biogeochemical parameters. J. N. Am. Benthol. Soc., 22(4): 492-510.

Sharma, M.L., G.A. Gander, and G.C. Hunt. 1980. Spatial variability of infiltration in a watershed. Journal of Hydrology 45:101-122.

Shirmohammadi, A. and R.W. Skaggs. 1985. Predicting infiltration for shallow water table soils with different surface cover. Transactions of ASAE 28(6): 1829-1837.

Shirmohammadi, A., H. Montas, A. Sadeghi, and L. Bergstrom. 2002. Using hydrologic and water quality models beyond their boundaries. ASAE paper Number 022090, Chicago, IL.

Shirmohammadi, A., H.J. Montas, L.F. Bergstrom, and W.G. Knisel. 2001. Water Quality Models. In: Agricultural Nonpoint Source Pollution-Watershed Management and Hydrology: Ritter. W.F. and A. Shirmohammadi, (eds.); Lewis Publishers Washington, D.C., pp. 233-256.

Shirmohammadi, A., H.J. Montas, L.F. Bergstrom, and W.G. Knisel. 2001. Water Quality Models, pp. 233-256. In: Agricultural nonpoint source pollution-watershed management and hydrology: Ritter. W.F. and A. Shirmohammadi, (eds.); Lewis Publishers, Washington, D.C.

Simunek, J., K. Huang, M. Sejna, and M.T. Van Genuchten. HYDRUS-2D, 1999. U.S. Salinity Laboratory, USDA/ARS, Riverside, California

Skaggs, T. H. and D. A. Barry, 1996. Sensitivity methods for time-continuous, spatially discrete groundwater contaminant transport models. Water Resources Research 32(8): 2409-2420.

Smith, M.S., G.W. Thomas, R.E. White, and D. Ritonga, 1985. Transport of *Escherichia coli* through intact and disturbed soil columns. J. Environ. Qual. 14:87-91.

Smith, M.S., Thomas, G.W., White, R.E., Ritonga, D. 1985. Transport of *Escherichia coli* through intact and disturbed soil columns. J. Environ. Qual. 14:87-91.

Srivastava, P., D.R. Edwards, T.C. Daniel, P.A. Moore, and T.A. Costello. 1996. Performance of vegetative filter strips with varying pollutant sources and filter strip length. Transactions of the ASAE 39(6): 2231-2239.

Starr, J.L., and I.C. Paltineanu. Soil water dynamics using multisensor capacitance probes in nontraffic interrows of corn. 1998. Soil Sci. Soc. Am. J. 62:114-122.

Steenhuis, T.S., W. Staubitz, Andreini, J. Surface, T.L. Richard, R. Paulson, N.B. Sykes, J.F., S. Soyupak, and G.J. Farquhar, 1982. Modeling of leached organic migration an attenuation in groundwater below sanitary landfills. Water Resour. Res., 18: 135-145.

Tan, Y., Bond, W.J., and Griffin, D.M. 1992. Transport of bacteria during unsteady unsaturated soil water flow. Soil Sci. Soc. Am. J. 56: 1331-1340.

Tan, Y., Bond, W.J., Rovira, A.D. Brisbane, P.G., and Griffin, D.M. 1991. Movement through soil of a biological control agent, Pseudomonas fluorescences. Soil Biol. Biochem. 23: 821-825.

Tan, Y., J.G. Gannon, P. Baveye, and M. Alexander.1994.Transport of bacteria in a saturated aquifer sand. Water Res. 30:3243-3252.

Tan, Y., W.J. Bond, 1995. Modeling subsurface transport of microorganisms. pp. 321-355. In: V.P. Singh (ed.), Environ. Hydro. Kluwer Academic Publishers, Netherland.

Tan, Y., W.J. Bond, A.D. Rovira, P.G. Brisbane, and D.M. Griffin, 1991. Movement through soil of a biological control agent, Pseudomonas fluorescences. Soil Biol. Biochem. 23: 821-825.

Tan, Y., W.J. Bond, and D.M. Griffin, 1992. Transport of bacteria during unsteady unsaturated soil water flow. Soil Sci. Soc. Am. J. 56: 1331-1340.

Tate, C.H., and K.F. Arnold. 1990. Health and a esthetic aspects of water quality. In American Water Works Association (Eds.), Water Quality and Treatment: A Handbook of Community Water Supplies. New York: McGraw Hill.

Taylor, S. W. and P. Jaffe, 1990a. Substrate and biomass transport in a porous medium. Water Resour. Res. 26:2181-2194.

Taylor, S. W. and P. Jaffe, 1990b. Biofilm growth and related changes in the physical properties of porous medium. 3. Dispersivity and model verification. Wat. Resour. Res. 26(9), 2171-2180.

Taylor, S.W., P.C.D. Milly, and P. Jaffe, 1990. Biofilm growth and related changes in the physical properties of a porous medium. 2. Permeability. Wat. Resour. Res. 26(9), 2161-2169.

Teutsch G., K. Herbold-Paschke, D. Tougianidou, T. Hanh, and K. Botzenhart. 1991. Water Science and Technology, 24 (2), 309.

Thomas, D.L., K.L. Campbell, and R.L. Bengtson. 1989. CREAMS, pp 14-20. In: application of water quality models for agricultural and forested watersheds, D.B. Beasley and D.L. Thomas, editors. So. Coop. Ser. Bul. No. 388.

Tindall, J.A., and W.K. Vencill, 1995. Preferential transport of atrazine in well structured soils. In Agricultural research to protect water quality (vol.I), 154-56. Proc. Conf., 21-24 February, Minneapolis, MN. Ankeny, IA: Soil and Water Conservation Society.

Toranzos, G.A., and G.A. McFeters. 1997. Detection of indicator microorganisms in environmental freshwaters and drinking waters. Manual of Environmental Microbiology, ASM PRESS, Washington, D.C.

Trevors, J.T., van Elsa, J.D., van Overbeek L.S., Starodub, M., 1990. Transport of a genetically engineered Pseudomamnas fluorescence strain through a soil microcosm. Appli. Environ. Microbiol. 56: 401-408.

Tsuboyama, Y., R.C. Sidle, S. Noguchi, and I. Hosoda, 1994. Flow and solute transport through the soil matrix and macropores of a hillslope segment. Water Resour. Res. 30, 879-890.

Uhal, V.W., and S.T. Sullivan, 1982. Uncertainty analysis in the appraisal of capital investment project. Uncertainty analysis for engineers. V.W. Uhal and W.E. Lowthian eds. AICHE Symposium Series, vol. 78, no. 220, American Institute of Chemical Engineers, New York, pp.10-22.

USEPA, 1994. National Water Quality Inventory: Report to Congress, USEPA, office of water, Washington, D.C.

USEPA,1998. 1998 TMDL Tracking system data version 1.0. Total maximum daily load program. USEPA office of Water, Washington, D.C.

Van Elsa's, J.D., J.T. Trevors, and L .S. Van Overbeek. 1991. Influence of soil properties on the vertical movement of genetically –marked pseudomonas fluorescents through large soil microorganisms. Biol. Fertil. Soils.10: 249-255.

Van Genuchten, M.Th., 1980. A closed-form equation for predicting the hydraulic conductivity of unsaturated soils. Soil Sci. Soc. Am. J. 44:892–898.

Van Wesenbeeck, I.J., and R.G. Kachanoski. 1988. Spatial and temporal distribution of soil water in the tilled layer under corn crop. Soil Sci. Soc. Am. J. 52:363-368.

Vilker, V.L., and W.D. Burge, 1980. Adsorption mass transfer model for virus transport in soils. Water Res. 14: 783-790.

Viraraghavan, T., and M. Ionescu. 2002. Land application of phosphorus-laden sludge: a feasibility analysis. J. Environ. Manage. 64: 171-177.

Walch, M., and R.R. Colwell, 1994. Detection of non-culturable indicators and pathogens, p. 258-273. In: C.R. Hackney and M.D. Pierson 9ed.), Environmental Indicators and Shellfish Safety. Chapman and Hall, New York.

Walker, S.E., S. Mostaghimi, T.A. Dillaha, and F.E. Woeste. 1990. Modeling animal waste management practices: Impacts on bacteria levels in runoff from agricultural lands. Trans. of the ASAE 33(3): 807-817.

Wan, J., J.L. Wilson, and T.L. Kieft, 1994.Influence of the gas-water interface on transport of microorganisms through unsaturated porous media. Appli. Environ. Microbio. 60: 509-516.

Weaver, R.W., 1981. Transport and fate of bacteria pathogens in soil. Proc. Conf. on microbial health considerations of soil disposal of domestic wastewaters, Norman, Okla., pp. 53-83.

William, E.J., and N.H. Kloot. 1953. Interpolation in a series of correlated observations. Austral. J. Appl. Sci., 4:1-17.

Williams, A.G., J.F. Dowd, D. Scholeflield, N.M. Holden, and L.K. Deeks. 2003. Preferential flow variability in well-structured soil. Soil Sci. Soc. Am.J. 67:1272-1281.

Wilson, L.G. 1967. Sediment removal from flood water, Transaction of ASAE, 10 (1): 35 -37

Wollum II, A.G. and Cassel, D.K., 1978. Transport of microorganisms in sand columns. Soil. Sci. Soc. Am. J., 42:72-76.

Wood, M, 1989. Soil Biology, Chapman & Hall, New York.

Yao, K., Habibian, M.T., and O'Melia, C.R. 1971. Water and wastewater filtration: Concepts and applications. Environ. Sci. Technol. 5:1105-1112.

Yates, M.V., and S.R. Yates. 1988. Modeling microbial fate in the subsurface environment. CRC Crit. Rev. Environ. Control. 17:307-344.

Young, R.A., T. Huntrods, and W. Anderson. 1980. Effectiveness of vegetated buffer strips in controlling pollution from feedlot runoff. J. Envir. Qual., 9:483-487.

Zacharias, S., and C.D. Heatwole. 1994. Evaluation of GLEAMS and PRZM for predicting pesticide leaching under field conditions. Transaction of ASAE. 37 (2): 439-51.

Zheng, C. and G.D. Bennett. 1995. Applied Contaminant Transport Model, Theory and Practice. John Wiley and Sons, New York, NY.

Zoldoske, D.F. 2003. Improving golf course irrigation uniformity: A California Case Study. The Center for irrigation technology. California State University, Fresno, CA, 2003.

Zyman, J., Sorber, C.A. (1988). Influence of simulated rainfall on the transport and survival of selected indicator organisms in sludge-amended soils. J. Water Pollut. Control Fed. 60: 2105-2110.